Department of Chemical Engineering

Engineering bacteriophage encapsulation processes to improve stability and controlled release using pH responsive formulations

Doctoral Thesis

Submitted by

©Gurinder Kaur Vinner BSc MSc

Supervised by

Dr D. J. Malik and Dr Goran Vladisavljević

A Doctoral Thesis submitted in fulfilment of the requirements for the award of the degree of Doctor of Philosophy in Chemical Engineering from Loughborough University

Abstract

Enteric pathogens form a large part of infectious diseases which contribute to a bulk of the healthcare costs. Enteric infections are usually contracted via the faecal-oral route or through contact with contaminated surfaces. Treatment by antibiotics is becoming increasingly ineffective due to the growing number of antibiotic resistant strains. Anti-microbial resistance poses a serious threat to the future of healthcare worldwide and necessitates the search for alternate forms of therapy. Bacteriophages (phages), are viruses which specifically infect and lyse bacteria. To introduce phages as a viable form of therapy, route of administration needs to be considered carefully. Model phages with broad host ranges are ideal for therapy however oral delivery to the lower gastro-intestinal (GI) poses several challenges. The acidic stomach environment can be detrimental to phages, rendering them inactive during passage. To overcome this challenge and improve the stability of phage during encapsulation and storage, this PhD research has been conducted. pH responsive polymers, Eudragit and alginate were used to develop composite microparticles which protected phage from acidic pH (pH 1-3). A novel method of acidifying oil was developed for crosslinking droplets *in vitro* to avoid the use of harsh solvent systems that can cause phage inactivation. Platform microfluidic technology was employed for phage encapsulation for the first time. Monodispersed droplets and particles were produced, offering fine-tuning of droplet diameter to tailor the release and pH protection of encapsulated phage. Process scale-up was attempted using membrane emulsification (ME) to produce larger volumes of encapsulated phage. *In vitro* and *in-situ* models investigated the efficacy of encapsulated phage-bacterial killing. Industrial scale method of spray drying, and electrospinning were also used to demonstrate the versatility of the formulation. Tableting dry powder phage, showed an effective method for producing solid dosage forms for therapy. Additionally, electrospun phage fibres also showed the potential use of pH responsive formulations in addressing wound infections. Improvement in encapsulated phage storage stability was observed with the addition of trehalose in

the formulation. This research underpins the need for testing phage encapsulation for site-specific delivery and offers insight into the potential use of commercially available technologies.

Acknowledgments

I would like to start by saying that these 3 years have been life-changing. I have learnt so much and I wouldn't change a thing! Yes, not even the things that didn't work!

I would like to especially thank my supervisor Dr D. J. Malik for all his help, support and encouragement throughout my PhD. I'm grateful to my second supervisor Dr Goran Vladisavljević for his guidance and Professor Martha Clokie who has always shared words of wisdom and gave me this opportunity.

A massive thank you to my parents for their encouragement and support in helping me achieve more than I ever thought I could. I hope I have made you proud by becoming the first Doctor in the Vinner family! A special thanks to my sister, Harmeet for making me delicious lunches and dinners to keep me going after long days. Thank you to my husband Jas, who listened to my endless moans about how the world is going to end if one experiment doesn't work, but your words gave me comfort and I have come a long way.

I would like to thank Deep and Gurjeet for everything that we've been through it only made me stronger. Also, my nephews and niece Gurjot, Amitoj, Jodh and little Miss Harneet for making me feel like a kid when I needed it the most! Also, a special thanks to my in-laws and Mandy for all their support! Now this journey wouldn't have been possible without a few inspirational people, so I would like to thank Anisha for here continued support and guidance. Monalie for being a dear friend throughout. My friends, Chandni, Mital, Jay, Purvi, Amna for being there to give me encouragement when I needed it the most.

A big thank you to the 3 musketeers, Andrea, Francesco and Salvo without whom this PhD wouldn't have been as fun and enjoyable. Thank you for teaching me Italian and feeding me lots of yummy food! 'When the water is not enough the duck cannot float' 😉 a lesson learnt!

A special thanks to the staff of Chemical Engineering department for all the training and support.

Publications

1. Microencapsulation using glass microcapillary devices of clostridium difficile specific bacteriophages in pH responsive Eudragit S 100 for colon targeted delivery. *Soc. Chem. Ind.* 2016:0-2.

2. Rashid S, Barylski J, Hargreaves K, Millard A, Vinner G, Clokie M. Two Novel Myoviruses from the North of Iraq Reveal Insights into Clostridium difficile Phage Diversity and Biology. *Viruses* 2016;8(11):310. doi:10.3390/v8110310.

3. Gurinder K. Vinner, Goran T. Vladisavljević, Martha R.J. Clokie, Danish J. Malik Microencapsulation of *Clostridium difficile* specific bacteriophages using microfluidic glass capillary devices for colon delivery using pH triggered release. (12th October 2017)

4. Danish J. Malik, Ilya J. Sokolov, Gurinder V. Vinner, Francesco Mancuso, Salvatore Cinquerrui, Goran T. Vladisavljevic, Martha R.J. Clokie, Natalie J. Garton, Andrew G.F. Stapley, Anna Kirpichnikova. Formulation, Stabilisation and Encapsulation of Bacteriophage for Phage therapy. Advances in Colloid and Interface Science (May 2017)

5. Gurinder K. Vinner, Danish J. Malik High precision microfluidic microencapsulation of bacteriophages for enteric delivery. Research Methods in Microbiology (Submitted March 2018)

Conferences and presentations

Vinner, G. K., Vladisavljevic, G. T., Clokie, M. R. J., & Malik, D. J. (2017). Formulation and encapsulation of bacteriophages in pH responsive microparticles for gastrointestinal delivery. In *Book of Abstracts* (pp. 134-135). Institut Pasteur, Paris, France.

Vinner, G. K., Vladisavljevic, G. T., Clokie, M. R. J., & Malik, D. J. (2016). Clostridium difficile specific bacteriophage microencapsulation within porous Eudragit particles and pH dependent controlled release for colon targeted delivery. In *2nd Annual InterPore UK Chapter Conference, Particle Characterisation Interest Group, Royal Society of Chemistry* (pp. 40). Loughborough.

Vinner, G. K., Vladisavljevic, G. T., Clokie, M. R. J., & Malik, D. (2016). Microencapsulation using glass microcapillary devices of clostridium difficile specific bacteriophages in pH responsive Eudragit® S 100 for colon targeted delivery. In M. Cox (Ed.), *IEX 2016 Ion Exchange - a continuing success story* (pp. 119-120). Cambridge.

Vinner, G. K., Vladisavljevic, G. T., Clokie, M. R. J., & Malik, D. J. (2016). Microencapsulation of Clostridium difficile specific bacteriophage using glass microcapillary devices and pH dependent controlled release for colon targeted delivery. In *4th World Congress on Infectious Diseases – Phage Therapy 2016*. Paris, France.

List of Figures

List of Tables

Abbreviations

ATCC American Type Culture Collection

BHI Brain Heart Infusion

CCEY Cefoxitin Cycloserine Egg-Yolk

CDI *Clostridium difficile* Infection

CFU/ml Colony Forming Units per ml

DNA Deoxyribonucleic Acid

dsDNA Double Stranded DNA

dsRNA Double Stranded RNA

Ephage Encapsulated Phage

ES100 Eudragit S100

FAB Fastidious Anaerobic Broth

FBS Foetal Bovine Serum

FDA US Food and Administration

HLB Hydrophilic-Lipophilic Balance

IBD Inflammatory Bowel Disease

IPTG Isopropyl β-D-1-thiogalactopyranoside

kJ Kilojoule

kN Kilonewton

kV Kilovolts

LB Luria Broth

ME Membrane Emulsification

M:C Miglyol 840 : Castor oil

MOI Multiplicity Of Infection

mPa Millipascal

MRSA *Multiplicity-resistant staphylococcus aureus*

ms^{-1}	Meter per second
NHS	National Health Service
OD	Optical Density
PFU/ml	Plaque-Forming Unites per ml
PGPR	Polyglycerol Polyricinoleate
PHE	Public Health England
PLGA	Poly Lactic-co-Glycolic Acid
PVA	Polyvinyl Alcohol
RFP	Red Fluorescent Protein
RPM	Rotations per minute
SEM	Scanning Electron Microscope
SGF	Simulated Gastric Fluid
SIF	Simulated Intestinal Fluid
SPAN 80	Sorbitan mobooleate 8-0
SPG	Shiras-Porous Glass
TEM	Transmission Electron Microscope
Tg	Glass Transition Temperture
v/v	Volume per Volume
w/v	Weight per volume

Table of Contents

Chapter 1: Introduction

Research exploiting bacteriophages (phages) which are viruses that infect bacteria, as alternatives to antibiotics has risen in the past decade as the use of antibiotics as a conventional method to treat infectious diseases has reached a plateau with increased antibiotic resistance. Pathogens associated with enteric infections and diseases have all been reported to develop some degree of antibiotic resistance (Holmes et al., 2016). Phage are self-amplifying and specifically lyse their host bacterial strains without harming the natural gut flora. Unlike antibiotics, phages can target bacteria by penetrating through biofilms and attack strains which have evolved antibiotic resistance. Combining phage and antibiotics may be an effective treatment for infection (Lu & Koeris, 2011). Phages are largely composed of nuclei acids occur naturally rendering them relatively low in toxicity (Loc-Carrillo & Abedon, 2011). Phages being the next generation for treatment (Housby & Mann, 2009) it is important to address their site specific delivery in order for the phages to work at their optimum.

Studies have already been undertaken to encapsulate drugs and other active agents for colon targeted delivery. The significance of this lies in the complex and harsh environment instigated by the gastro-intestinal tract. The ability of the GI tract acid and enzymes to inactivate microbes and chemical agents reduces the ability of the active agent to reach the site of infection and provide curative processes (McConnell *et al*., 2008). With this in mind many methods have been developed and are commercially used for encapsulating drugs and active agents to improve their viability (Amidon *et al.*, 2015). As well the healthcare industry, encapsulation for controlled release is also an important part of the food, cosmetic and pharmaceutical industries.

Control over size of microparticles has been a highlight in the encapsulation discipline and has encouraged the diversity in the techniques for production of these products. The properties of the active agent such as its water solubility, chemical topology etc. poses a challenge in encapsulation process. Modifications and variation in encapsulation techniques serve to improve the stability, safety and controlled release of the encapsulated agent (S. Zhang et al., 2011). In addition to that the uniformity of droplets on a micro or nano scale has also led improvements and development in the methods for product production.

So far, phage encapsulation has not been investigated extensively, limited studies on encapsulation discuss techniques and formulations (Colom *et al*., 2017b; Dini *et al*., 2012; S. S. Y. Leung *et al*., 2016;

S. S. Y. Leung *et al*., 2017; Yongsheng Ma *et al*., 2008, 2012; Stanford *et al*., 2010b; Tang *et al*., 2013; Tang *et al.*, 2015). Phage encapsulation for enteric delivery specifically, poses challenges, especially since the acidic environment of the stomach can render many phages inactive (Yongsheng Ma *et al*., 2008, 2012; Stanford *et al.*, 2010b). This impacts the dose of the phage delivered to the site of infection, which is crucial in arresting bacterial growth.

Modern techniques such as microfluidics are platform technologies for the development of novel formulations and applications. Precision control over process parameters provide a useful tool when developing encapsulated biologics. Versatility of polymers such as Eudragit can be tested on different techniques including membrane emulsification which offers a useful platform for scaling up microfluidic formulations. Spray drying, and electrospinning are both contrasting techniques which may be employed to test polymer applications in hosting phages for therapy further.

Aims and Objectives

This report will look at different methods and techniques available for microencapsulation of phages, with emphasis on improving stability of phages. It will assess the various parameters that contribute to successful encapsulation of phages. An optimised encapsulation formulation will be developed, which will protect the phages against changes in gastrointestinal pH. Encapsulation will be optimised to produce uniform sized droplets and particles using a glass capillary microfluidic device. The process will then be translated to a commercially available microfluidic chip pushing the boundaries of the formulation. This will then be upscaled for bulk production using membrane emulsification technology once again investigating the optimising process parameters. In contrast, dry powder phage will be produced using spray drying to demonstrate the efficacy of the formulation. The formulation will be further probed by producing encapsulated phage in electrospun fibres for wound dressing application.

This research will aim to formulate and develop a viable encapsulation system intended to delivery bacteriophages to the colon. The components for encapsulation will be studied to produce a robust shell to protect the bacteriophage from hostile environments. The formulation for encapsulation will be subjected to a technique for producing monodispersed droplets and particles which enable control over release kinetics. Downstream processes (after encapsulation) will be used to confirm the efficiency of the encapsulation system.

To synthesise microparticles a glass microfluidic device with two different geometrical variations will be used. This will enable the study of size of variation of droplets and particles with its subsequent effect on encapsulation efficiency. The performance of the flow-focussing microfluidic device will be observed in its ability to produce microparticles and determine the optimum device conditions for microparticle synthesis. This technique will be studied for its ability as a proficient system to produce microdroplets/particles. Mathematical analysis will determine the amount of phage captured in each particle.

The effect of each element of the emulsion on the viability of bacteriophage will be carried out. Survival of the bacteriophage in each of the encapsulation elements will determine the suitability of the polymer to encapsulate the bacteriophage adequately. The bacteriophage survival will be observed over a period and reduction in titre recorded. With statistical analysis, it will be possible to conclude the suitability of the system before it is run via microfluidic device to produce droplets and particles.

Stability of the microfluidic device on producing monodispersed droplets over an extended period will be studied. Droplet size analysis over the period of 6 hours of droplet production will be analysed to determined coefficient of variance. This analysis will determine the stability and robustness of the device over a period. Droplet to particle transition will be observed by processing particles through isolation, rinsing and drying. SEM analysis will be used to study the morphology of the particles. The process will be replicated in a commercial chip, with a different geometry. Probing the formulation to push the efficacy of encapsulation and protection against SGF will be investigated. Impact of particle size on acid protection will be examined.

The process will be up-scaled using membrane emulsification technology, highlighting the challenges encountered during scale-up. The process parameters will be studied and optimised to produced particles encapsulating phage providing SGF protection. Efficacy of the formulation will be further probed by using conventional spray drying method to produce dry powder encapsulated phage. Here, emphasis will be on the long-term storage stability of phage under different conditions. Further investigation into the production of tablets from dry powder will be studied. The ability of these tablets to conform to pharmaceutical standards will be examined. To further investigate the formulation, electrospinning phage into fibres will be performed to produce a novel matt of fibres for wound dressing applications.

Multiple phages with varying hosts will be studied in the encapsulation system to conclude the suitability of the formulation and production. This will confirm the novel approach to producing microparticles containing phages produced via multiple devices. Downstream processes will be improved for better retention and purification of product. Modification to the formulation and the geometry will be analysed for enhancing production rate, stability and efficiency of the microparticles.

Particles will be exposed to simulated gastric and intestinal fluids to observe the release of bacteriophages over a period of 6 hours. The particles will be analysed for their ability to protect and deliver the bacteriophage to a pH simulated colon environment. Differences in phage titre will represent the survival of phage in each simulated environment. The ability of release phages on arresting bacterial growth will also be analysed to determine the efficacy of the encapsulation. Further analysis will involve *in-situ* experiments to observe the three-way interaction of phage infection (released from a particle) of *C. difficile* in the presence of human epithelial cells.

Research Novelty

Microfluidics has been used extensively over the past few decades to produce emulsion droplets and has been exploited for lab-on-chip research. There have been studies into using microfluidics for discovery and drug delivery however the use of microfluidics for bacteriophage encapsulation has never been exploited before. Encapsulation of bacteriophage has been studied very little; literature search has revealed only a handful of studies into the formulation for encapsulation and the use of spray drying as a method for producing particles encapsulating phage. There is a lot of research that is still required in this field due to the promise of using phages as alternative therapeutics.

There are also no reports of phage encapsulation where scale-up, on a commercial scale has been reported. Here, up-scaling the phage encapsulation process has been investigated for the first time. Spray drying of phage in sugars has previously been reported with only one paper showing the use of polymer for site specific delivery. This project reports the encapsulation of phage in a pH responsive polymer using spray drying with subsequent tableting for the first time. Electrospinning phage in nanofibers has also been reported however, this work shows a novel formulation for the production nano and micro fibres carrying phage with a pH triggered release.

Overall, this study provides a one-stop platform exploiting the use of multiple technologies for phage encapsulation. Advantages and limitations are addressed for phage encapsulation and impact on stability. A further emphasis on the use of encapsulated phage *in situ* is also addressed providing useful

insight into the efficiency of the system. Phage encapsulation processes have been optimised with the importance of dosage and site-specific delivery in mind. Work has been performed in different phages against various pathogens to show the transferable nature of the encapsulation process.

The novel formulation and approaches taken for phage encapsulation fill many gaps in literature such as the need for sufficient acid protection from pH 2. This work is one of the first to provide a useful insight into the little explored world of phage application for therapy. This work provides a starting point for exploring avenues and pushing boundaries for phage encapsulation.

Thesis structure

Chapter 1 Introduction. The first chapter of the thesis explains the overall aims and objectives of the research. It includes discussing and reasoning the use of multiple techniques for phage encapsulation. It further elaborates on the research novelty and purpose.

Chapter 2 Literature review. Discusses the problem of enteric infections and associated pathogens. Introduction to phage, properties, life cycle and their potential as alternative form of therapy is given. A literature review on the different encapsulation technologies present and their mode of action in producing encapsulated active agents is included. Focussing on their potential use for phage encapsulation and possible advantages and shortfalls. A further insight into the pH of human gastrointestinal tract, and potential polymers for phage encapsulation is discussed.

Chapter 3 Clostridium difficile specific bacteriophage encapsulation using microfluidic glass capillary devices for colon delivery. Introduces the use of in-house made glass microcapillary device for producing tuneable microparticles carrying *C. difficile* phage CDKM9. Developing a formulation with phage CDKM9 that causes minimal impact on phage viability for a stimulus triggered function and protection against stomach acid pH 2

Chapter 4 Microfluidic encapsulation of bacteriophages in a commercial chip with high precision control. The use of commercial microfluidic chips to produce high precision phage encapsulated particles with focus on process parameters, acid protection at pH 1, arresting bacterial growth and storage stability.

Chapter 5 Scaling-up bacteriophage microencapsulation using membrane emulsification technology in a pH responsive polymer. Purposing the use membrane emulsification technology to scale up the

process of phage encapsulation. Investigating the influence of experimental parameters on the production of microparticles. Following the stability of encapsulated phage and analysing the three-way interaction of phage, bacteria and mammalian cells.

Chapter 6 Microencapsulation of Felix O1 in pH responsive polymers using spray drying for tableting and improved storage. Demonstrating the use of a well-established technique; spray drying for phage encapsulation. Using Eudragit and trehalose to produce pH responsive dry powder particles. Producing tablets from powder for ease of use, storage and manufacture. Investigating the storage stability in powder and tablet form under different conditions.

Chapter 7 Electrospun pH responsive nano and micro fibres for bacteriophage encapsulation. Demonstrating the versatility of Eudragit in delivering phage at site of infection by electrospinning in fibres ranging from nano to micron size. Showing a novel technique to produce phage encapsulated fibres to be used for wound dressing or oral delivery.

Chapter 8 Overall conclusion of the research carried out in each chapter. Focussing on the key findings and its impact on phage research to the scientific community. Recommendations and plans for future work is discussed.

Chapter 2: Literature review

2.1 Enteric pathogens

Gastrointestinal infection is an umbrella term covering various pathogen related to illnesses starting from the stomach all the way to the colon. This covers infections caused through food poisoning, poor hygiene related transmission and opportunistic pathogens (Wikswo et al., 2015). Due to the vast array of bacterial species involved, it is difficult to target just one since all pathogens have shown anti-microbial resistance which poses a serious healthcare challenge. Some clinically relevant pathogens that cause gastrointestinal infections include: *Clostridium difficile*, *Clostridium perfringens*, *Helicobacter pylori*, *Bacillus cereus*, *Yersinia*, *Salmonella* spp., *Staphylococcus* spp (Wikswo *et al*., 2015).

Mechanism of action and transmission of infections differs for each pathogen and usually are indicative of the possible route of transmission. A key symptom common for all gastrointestinal infections is the onset of diarrhoea, which may be short lived or in severe cases lead to dysentery (Viswanathan *et al.*, 2009). Usually pathogens related to food contamination can follow one of two routes in being ingested, one, high dose of the microbial agent is taken in with food or secondly, the toxins are produced in the food prior to ingestion. Once the contaminated food is ingested, damage to the lining of gastrointestinal tract begins leading to the onset of symptoms (Wikswo *et al*., 2015).

Poor hygiene when handling food can increase risk of contamination, which includes poor hand washing practice and non-sanitised work surfaces. Awareness about heating food is a crucial factor, cooked foods are recommended to be heated to 60°C and raw meats should be heated at much higher temperatures to avoid growth of bacteria and toxins. *Staphylococcus aureus* food poisoning occurs due to malpractice of food handling, which leads to *S. aureus* producing enterotoxins which are then ingested via food. There are up to 21 enterotoxins associated with *Staphylococcus* known to cause food poisoning (Loir Yves Le, 2003). These toxins are pH and heat resistant proteins which can survive the acidic stomach conditions and remain stable under heat as high as 100°C. Therefore, despite the bacteria being destroyed, the enterotoxins can still cause vomiting and diarrhoea (Loir Yves Le, 2003).

Similarly, *Shigella* a rod-shaped, Gram Negative bacterium also causes gastrointestinal infection resulting in bacillary dysentery and shigellosis. Transmission can be from contaminated food and water but most commonly through the faecal-oral route. Once ingested the bacteria invades the epithelial cells and resides in the cytoplasm of cells by entering through phagosomes. As the bacterium multiplies and spreads throughout the Peyer's patch, the epithelium of M cells (immune-modulatory

cells) becomes ulcerated leading to the onset of symptoms such as stomach cramps, fever and diarrhoea (Niyogi, 2005). Shiga toxin produced by *S. dysenteriae* type 1 invades endothelial cells of the small blood vessels of the small intestine by binding to glycosphingolipid. Here, cell functions are interrupted due to the toxin binding to the large ribosomal subunit responsible for protein synthesis leading to haemorrhaging and lesions in the colon. Treatment of severe cases requires the use of antibiotics such as ciprofloxacin and azithromycin, however due to high incidence of resistance use of these antibiotics needs to be carefully considered (Niyogi, 2005).

Salmonellosis known as *Salmonella* gastroenteritis is caused by the rod-shaped, Gram Negative bacterium *Salmonella*. Although several species are associated with infection most common to cause infection in humans is *S. enterica* and more specifically serotypes (subgroups) Enteritidis and Typhi. *Salmonella* is part of poultry's microbiota, therefore handling raw eggs and poultry increases the risk and spread of the infection. *Salmonella* is also part of intestinal microflora in some individuals, so infections depends on factors such as host health, dose and type of inoculum. Infection is easily preventable by handwashing and maintaining good hygiene practice when handling food. Like *Shigella*, once ingested hypersecretion and elicitation of inflammatory processes is triggered by evasion through M cells in the epithelial mucosa. Intoxication may also occur because of some *Salmonella* strains producing enterotoxin inside the body (Velge *et al.*, 2012). Although the symptoms such as fever, nausea cramps and vomiting usually subside after a few days or with the help of oral rehydration therapy, in more severe cases antibiotics are prescribed. Some antibiotics used for treatment include: fluoroquinolones, cephalosporins and ampicillin, but reports are emerging *Salmonella* has developed resistance against these front-line antibiotics (WHO, 2014).

Typhoid fever associated with *S. typhimurium* is a more serious form of salmonellosis, causing mortality in up to 10% of cases. Infected individuals shed *S. typhi* through their faeces and precautions need to be taken to avoid infecting others, especially during the use of antibiotic treatment with fluoroquinolones**,** ceftriaxone, and azithromycin (WHO, 2014). Mortality occurs due to perforation and ulceration of the intestine, which is brought on by infected macrophages lysing and releasing the bacteria into the bloodstream and lymphatic system (Gal-Mor, Boyle, & Grassl, 2014). Pneumonia and jaundice are commonly observed during dissemination of the disease.

Gastrointestinal infections can also be caused by strains of *Escherichia coli* although it is also a commensal bacterium. Pathogenic *E. coli* strains carry virulence factors, such as type 1 fimbriae which promotes colonization of the colon and produces toxins. Strains acquire their virulence factors through horizontal gene transfer, four of six pathogenic strains are transmitted via food and water. Enterotoxigenic *E. coli* (ETEC) is known to cause travellers' diarrhoea, commonly related to travel to

less developed countries. ETEC produces enterotoxin which may be heat labile and adhesins which help the bacteria attack the intestinal wall (Nataro & Kaper, 1998). Enteroinvasive *E. coli* (EIEC) shows similar pathogenesis to shigellosis due to its intracellular invasion of intestinal epithelial tissue (Van Den Beld & Reubsaet, 2012). Enteropathogenic *E. coli* (EPEC) causes life-threatening diarrhoea leading to severe dehydration, especially in infants and in less developed countries. Mode of action is through the injection of Tir protein which attaches to the surface of the intestinal epithelial cells and triggers rearrangement of host cell actin from microvilli to pedestals (Nataro & Kaper, 1998). Enterohemorrhagic *E. coli* (EHEC) is by far the most dangerous of the *E. coli* strains as it can cause epidemics. Several outbreaks have been reported due to the epidemic strain O157:H7, where the O and H stand for the antigens that contribute to the pathogenicity (Nataro & Kaper, 1998). Like EPEC and EHEC this strain causes the formation of pedestals in the mucosal lining and produces a shigella like toxin. Severe cases display symptoms leading to haemorrhagic colitis and profuse bleeding.

A serious gastrointestinal disease associated with contaminated water and food can be elicited by *Vibrio cholera*. It is a Gram Negative, flagellated curved rod-shaped bacteria sensitive to stomach acid therefore high bacterial concentrations (~10^9 CFU/ml) are required to establish infection. Once the bacteria enter the intestine due to their motility there can travel between the mucosal layer and attach to epithelial cells to release cholera enterotoxin. Changes to the adenylate cyclase results in cAMP levels rising, which activates the chloride channels, releasing ions into the intestinal lumen, causing the influx of ions into the intestinal lumen. Water enters the lumen from the osmotic pressure, resulting in water and electrolytes being depleted from the body bringing the onset of dehydration and electrolyte imbalance (Viswanathan *et al.*, 2009). In severe, disseminated disease tetracyclines are recommended but other antibiotics may also be used. Prevention of disease is usually through good sanitation practice, since the bacteria are killed by heat, proper heating of food and water is important.

Campylobacter jejuni a Gram Negative, spiral shaped bacterium causes gastroenteritis. It is contracted from poultry which becomes contaminated during slaughter (Connerton *et al*., 2011) or through unpasteurised milk and contaminated water are other potential routes of transmission. Amongst other pathogenic bacteria similar symptomatic profile is observed and treatment of severe cases usually require administration of antibiotics.

Clostridium difficile (CD) is a gram positive bacterium first isolated in 1935 from normal intestinal flora of neonates by Hall and O'Toole (Ananthakrishnan, 2011). It has been associated with hospital acquired infections throughout Europe and America (Heinlen *et al.,* 2011). It is accountable for 15 % to 25% of *C. difficile*-associated diarrhoea (CDAD) sometimes also referred to as toxin mediated

diarrhoea, one of the leading causes of infectious diarrhoea. Onset of clinical symptoms occur after 24 hours to 72 hours include fever, abdominal pain and leucocytosis (Ramesh *et al.*, 1999).

There is a risk of *Clostridium difficile* infection (CDI) accompanying antibiotic treatment. However, it can also be transmitted via the faecal-oral route in areas with poor hygiene practices. Poor hygiene in healthcare has triggered many outbreaks of CDI epidemics. Studies show the ratio of hospitalised patients with CD colonisation is higher compared to healthy adults. However, more recently, community acquired CD infection is also becoming of concern. With rise in community acquired CDI it is likely that an increase in hospital CDI cases is imminent (Heinlen *et al*., 2011).

CD is an obligate anaerobe and in unfavourable conditions (i.e. nutrient deprivation) forms spores. CD spores are thick walled resting cells and can remain viable on inanimate surfaces for up to five months (Ananthakrishnan 2011). Precautions in hospitals such as alcohol hand rubs are ineffective at killing spores. Therefore, hospitalisation can bring the onset of CDI in patients where the ingested spores germinate into vegetative cells, causing infection (Meader *et al*., 2010).

During infection CD colonises in the colon where it can actively grow in its vegetative form. Antibiotic associated CDI results from changes in gut micro-flora due to antibiotics depleting the microflora and suppressing the immune response against CDI (Burke & Lamont, 2014). As a result, opportunistic CD can colonise the colon causing CDI and CDAD. The natural microflora of the gut forms a barrier against CD colonisation in healthy conditions. 30 % of antibiotic associated diarrhoea cases are linked to *C. difficile* (Lyerly *et al*., 1988). Highest risk of CDI is amongst patients over the age of 65 years, who have been recently exposed to antibiotics. CD is also found asymptomatically in up to 15 % of the adult population. Colonisation in infants is more common and is present at a rate of approximately 35 % falling to 15 % after the 1st year of life (Eyre *et al*., 2013). Non-healthcare related cases are also coming forward which includes individuals who are suffering from inflammatory bowel disease, children and pregnant women (Ananthakrishnan, 2011).

For the above-mentioned pathogens of the gastrointestinal tract and many more, antimicrobial resistance is increasingly being reported (WHO, 2014). Many infections are cleared by the body's immune system, in other cases antibiotics are required to prevent further spread and damage. It is due to the complexity of the infection that sometimes antibiotics are unable to fully clear the bacteria, giving bacteria the opportunity for evolving resistance mechanisms. In other cases, resistance genes are transferred through horizontal gene transfer, equipping pathogens before exposure to antimicrobials. Full reviews on mechanisms and intervention of antimicrobial resistance is discussed in detail by Roca *et al.*, (2015); Holmes *et al.*, (2016).

2.2 Bacteriophages

Antibiotic resistance is causing a major concern in healthcare. With a rise in the number of antibiotic resistant pathogens, development of new therapeutics is of utmost importance. The rate at which pathogens develop resistance is also on the rise. The mechanisms that aid this process include; interconnected travel, overuse of antibiotics, non-compliance, transduction of genes and bacterial evolution. The development of new antibiotics is challenging and currently does not look promising in terms of supply of new classes of antibiotics. Therefore, in the arms race against antibiotic resistance and development of new therapeutics, bacteriophages have once again become an area of interest (Lu & Koeris, 2011). Phages are abundant in the natural environment usually found close the source of host. They were first discovered in 1915 by Frederick Twort and Félix D'Hérelle in 1917. They were used as therapeutics shortly after, however, were soon swept away by the introduction of antibiotics after World War II (Alisky et al. 1998; Nobrega et al. 2015). Phage research has been continuing since their discovery in Eastern Europe particularly at the Eliava Institute of Bacteriophage, Microbiology and Virology, Georgia since 1923 (Merril *et al.*, 2003).

A $25 billion a year antibiotic industry by far over shadows the advancement of phage therapy which was the reason for ceasing research into phage therapy in France in 1970 (Merril et al., 2003). Lack of knowledge about phages, their efficacy and pharmacokinetics have been the reasons why phages were not considered fit for therapeutic use. Side effects from using phages in previous studies led to failures during clinical trials, mainly due to the lack of knowledge on purifying phages (Housby & Mann, 2009). Method to purify phages such as chromatography have been developed (Adriaenssens *et al*., 2012) although large pharmaceutical companies are still reluctant to invest in phage therapy research. This is largely due to the struggle of gaining intellectual property rights for phage products (Nobrega *et al*., 2015).

Developing new antibiotics against pathogenic bacteria may be ineffective as the process can take up to ten years or more and resistance may still develop (Centres for Disease Control and Prevention 2013). Nevertheless, alternative antibiotics are being investigated and the research into phage therapy has also risen.

Bacteriophages have been functional in nonclinical applications. Phage mixtures are applied to food products to reduce the number of potentially harmful bacteria that can result in food associated infections. Some of these have also passed FDA approval in the USA and are sold commerically (Abuladze et al., 2008). Phages have also been used to detect bacterial infections as diagnostics, such as Methicillin-resistant *Staphyloccocus aureus* is detected by an infection of phage in the blood culture

test (Hagens & Loessner, 2007). These approved applications show the potential use of phages as therapeutics and diagnostics.

Many animal models have effectively shown the positive attributes of phages being able to clear their target bacteria, minimal disruption of normal flora and no side-effects. For example an hamster model study showed phage therapy prevented CD induced iliocecitis (Ramesh *et al*., 1999). There are many advantages of phage therapy. Phages are highly specific and have narrow host ranges. This allows specific targeting of the pathogen producing an infection. Infections of the colon and rectum where the microflora is under the threat of elimination by antibiotics can easily be targeted whilst keeping natural flora intact. The self-replicating process of phages after infection of the suitable host is ideal when targeting a population with a specific dose. The phage replication will be amplified in relation to the amount of host present. An inflamed colon during infection can process and eliminate consumed substance at a faster rate. This results in lower bioavailability of drugs; therefore ability of the phage to replicate rapidly is a great advantage in this scenario (Rea *et al*., 2013).

Phages unlike drugs are non-toxic and are unable to attack mammalian cells or tissue. As a result, there is minimal tissue damage and inflammation is significantly low. Studies have shown the use of phage therapy in controlling *Psuedomonas aeruginosa* infection in a mouse model. *P. aeruginosa* associated with the condition cystic fibrosis causes many hurdles in treatment with antibiotics due to the development of a biofilm. However, Alemayehu and colleagues have demonstrated that administration of a phage combination significantly reduced bacterial numbers by 4-log10 and phages could penetrate through the biofilm (Debebe Alemayehu *et al*., 2012; Rea *et al*., 2013)

Nevertheless, like any therapeutic option there are challenges associated with phage therapy. Resistance is the key issue when it comes to antibiotics and similarly, bacteria are able to evolve and alter their surface receptors specific for phage binding and render them ineffective. Sulakvelidze and Alavidze (2001) showed bacteria that developed resistance to the phage initially administered were retargeted by a different phage able to infect the bacteria. They found overall 92% of the treatments showed success. This study showed that although the bacteria were able to develop resistance they could be targeted using a different phage (Sulakvelidze and Alavidze 2001). One way to move forward from this knowledge is to target bacteria with a mixture of phages and subsequently increase the host range of the phages used. Alternatively, phage screening to isolate a phage with the most extensive host range may also be beneficial (Tiwari *et al* 2014)

Alternatively, Betts *et al*., (2013) and colleagues have demonstrated the concept of phage evolution with increased effectiveness against the host. *Psuedomonas aeruginosa* strain PAO1 resistant to the

phages in study was effectively infected and killed by evolved phages. Through continuous passage (adding to exponentially growing host) of phages varying from one to six rounds (Betts *et al*., 2013) and colleagues were able to demonstrate the effect of evolution on increasing host range and impact on host population. The findings in this study show a potential alternative to counteract phage resistance in addition to isolating new phages with wider host ranges.

2.2.1 Bacteriophage life cycle

There are two types of life cycles a phage can undergo; lytic and lysogenic cycle (Figure 2.2.1). Phages approach and adsorb onto a bacterium cell wall where they attach using phage receptors. Lytic phages inject their DNA into the host and hijack the bacterial metabolism. The bacterial machinery is manipulated by the phage DNA to produce more phage progeny. As result of producing more phage, the bacterial cell metabolism comes to a halt rendering the bacteria weak. Phage progeny disrupt and break the bacterial cell wall to release mature phage into the surrounding environment which goes on to infect more bacterial cells (Campbell *et al*., 2006). Lysogenic (temperate) phages also attach and adsorb on bacterial cell walls injecting their DNA. They can initiate the lytic cycle but can also integrate their DNA into the bacterial genome (prophage) and exist as plasmids. As the bacterial cell replicates so does the incorporated prophage; causing the inheritance of phage DNA in all daughter cells (Sulakvelidze and Alavidze 2001; Merril *et al*. 2003). The prophage will remain dormant until certain conditions cause it to revert to the lytic cycle. Conditions that cause this change could be the bacterial state or the addition of antibiotics which causes the excision of prophage (J. Y. Nale *et al*., 2012).

Lysogenic phages can integrate their DNA into the bacterial genome due to the presence of the integrase gene. Integrase enables the phage to catalyse site-specific integration allowing incorporation into the bacterial genome. This gene is not present in lytic phages (Fogg *et al*., 2014). To prevent integration the gene can be excised from the phage DNA to only allow for the lytic cycle to take place (Goh *et al.*, 2007). This will enable the use of lysogenic phages in phage therapy as currently only lytic phages are researched in therapeutic use (Nobrega *et al.*, 2015).

One of the issues with using lysogenic phages for therapy is that they may carry bacterial virulence factors and antimicrobial-resistance genes which can be transferred via transduction (Nobrega *et al*., 2015). An example of this is studied by Goh *et al.* (2013) where a CD phage ϕC2 transduced the antibiotic resistance gene against erythromycin. Other risk factors that phages can transduce include toxin genes such as the Shiga toxin gene *stx*. *Echerichia coli* strains that produce Shiga toxin is encoded by prophages (Imamovic & Muniesa, 2012).

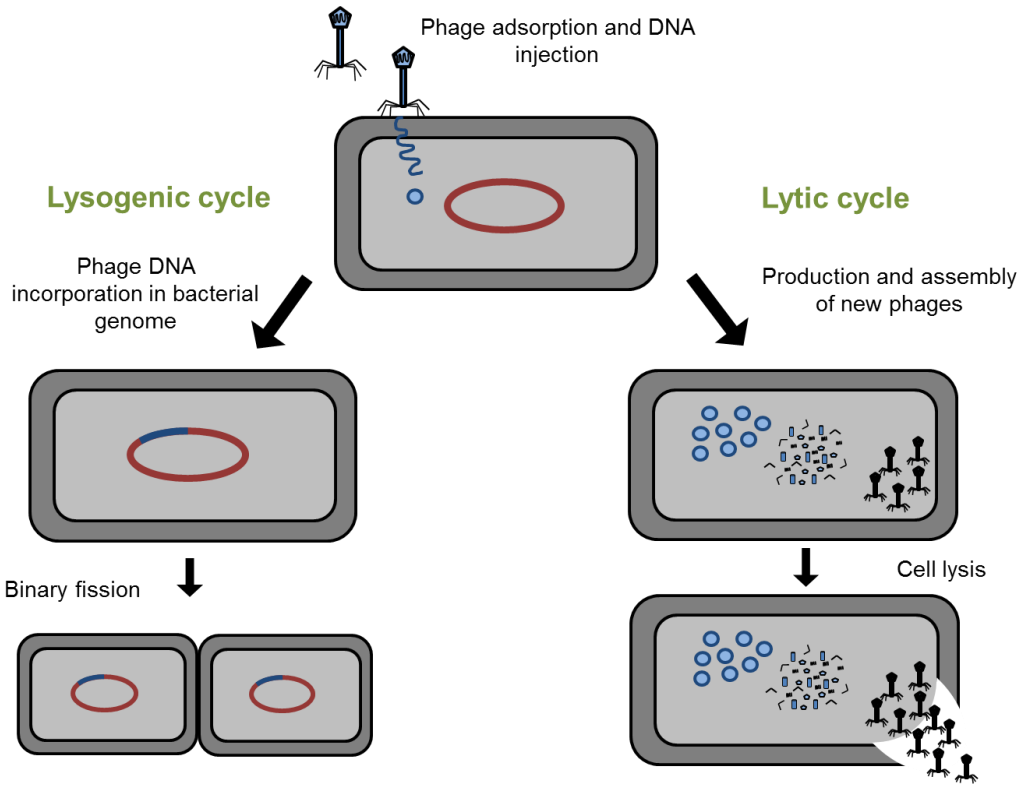

Figure 2.2.1 A schematic to show the steps in a phage infection cycle. Phages can follow the lytic cycle which leads to the lysis of bacterium or the lysogenic cycle where the phage DNA is incorporated in the bacterial genome.

2.2.2 Structure and classification of phages

The structure of phages consists of an icosahedral head also known as the capsid, this protects the genome (nucleic acid) that can be in the form of RNA or DNA (Figure 2.2.2). The genome of phages can be single stranded RNA (ssRNA), double stranded RNA (dsRNA), ssDNA or in 90% of sequenced phages dsDNA. Visualisation of phages via transmission electron microscope (TEM) and properties of the nucleic acid has enabled the classification of phages (Clokie & Kropinski 2009; Monk *et al.* 2010).

The structure of phages within one family is similar, however between families the tail length, phage size and genome length can vary between 24 nm to 400 nm and 18 kb to 400 kb respectively. *Caudavirales* comprise 96 % of the phage population and consist of tailed phages. This group is further phylogenetically divided into *Siphoviridae*, *Myoviridae* and *Podoviridae*. 61% of the tailed phages are *Siphovridae,* which are characterised by their non-contractile tails. *Myoviridae* comprise 25 % of the

population with contractile tails and *Podoviridae* characterised by their short non-contractile tails make 14 % of the population of tailed phages.

The capsid is attached to the tail via an adaptor (Figure 2.2.2), which connects the capsid to the tail. It serves to pack dsDNA in the capsid and take part in release of DNA into the host upon detecting a signal from the tail. The DNA is delivered via the tail to the host cell after the tail fibres and needles have specifically bound to the corresponding bacterial receptor. The phage genome is released as the connector opens into the host cell (Ackermann 2009).

Upon successful replication of phage inside the host cell, phage is released via bacterial cell lysis (Figure 2.2.1). Bacterial cell wall is lysed by the actions of holin which produces pores in the cytoplasmic membrane alongside endolysin, which produces hydrolytic enzymes that cleave bacterial cell wall (Schmelcher & Loessner, 2014).

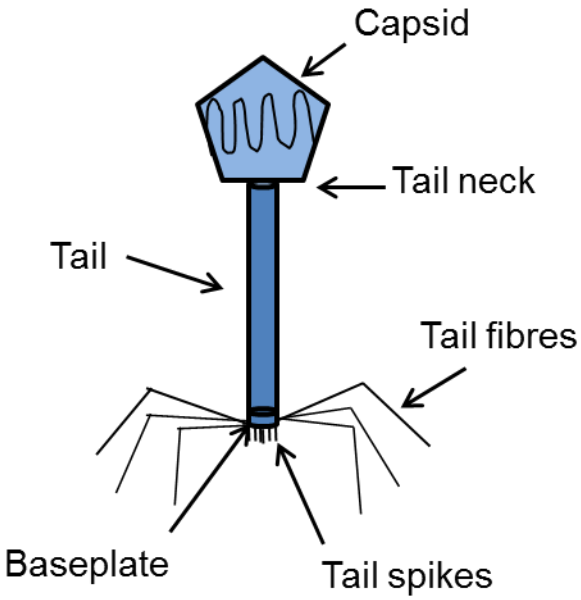

Figure 2.2.2. Schematic to show the overall structure of a single phage.

2.2.3 The need for phage encapsulation

Phages are a protein and like all biologically active ingredients, is susceptible to environmental stresses. When considering its use for therapy, formulating the delivery of phage in its optimum form and dosage are important parameters. However, considering this it is imperative to identify and understand the possible stresses the phage is prone to and may be subjected to during delivery for

therapy. In addition to that phage and bacterial population dynamics give useful insight into how phage can be utilised as a useful therapeutic tool to combat and minimise the problem of antimicrobial resistance.

Lysis of bacteria by phage is dependent on the adsorption of phage virions to the surface of a their target bacterial cells (Cairns, Timms, Jansen, Connerton, & Payne, 2009). Phage amplifies in proportion to the concentration of the bacteria present, in a first order process. Several studies have modelled phage and bacterium kinetics during different stages of growth and concentration with consideration of the immune system also playing a part in eradicating infection (Levin & Bull, 2004; Malik *et al.*, 2017; Payne & Jansen, 2001; Yasunori Tanji *et al*., 2005). These models are useful tools in helping determine the dose required, rate at which the phage is released at the site of infection, which can be pivotal factors in deciding whether infection can be eradicated before mutants emerge (Cairns *et al*., 2009). For high bacterial loads (10^9 CFU/ml), a high dose of phage shows an early arrest of bacterial population with no reappearance of bacterial growth (Malik *et al.*, 2017; Yasunori Tanji *et al*., 2005).

Efficacy of phage therapy is dependent on the phage dose and release rate. Therefore, to prevent loss of phage viability due to formulation, storage or through *in vivo* parameters (acid and digestive enzymes) is important for phage therapy. Furthermore, phage cocktails are thought to be a promising approach in combating infection and emergence of resistant mutants (Chang *et al*., 2017a; J. Nale *et al*., 2018). Tailoring formulations for each phage may be an option to maintain viability at its optimum.

2.2.3.1 Environmental stresses and phage stability

During phage formulation there are several parameters both mechanical and chemical, which can impact on the viability of a phage. Phages have previously been reported to be sensitive to organic solvents, temperature, pH and ionic concentration (Briers et al., 2008; Knezevic et al., 2011; S. W. Lee & Belcher, 2004; Puapermpoonsiri, Spencer, & van der Walle, 2009). Similarly, mechanical stress has also been reported to effect phage viability- during encapsulation the technique employed to capture the phage may use shear or agitation, which can physically render the phage inactive. A more popular technique for producing encapsulated phage; spray drying uses high temperatures, desiccation and atomisation a combination which has been reported to effect phage titre (S. S. Y. Leung et al., 2016; Tang *et al*., 2014). Electrospinning for example, uses current and solvents to produce nanofibers entrapping phages, both of which impact on the phage titre (R. Korehei & Kadla, 2013). To contest the effect of these stresses on phage viability, suitable excipient carriers or bulking agents need to be carefully considered for optimisation to minimise the loss of phage titre.

Another aspect that needs to be investigated when considering the use of phage for therapy, is the storage stability. Phages are generally propagated and stored (4°C) in growth media such as brain heart infusion (BHI) for short-term, and in 50 % glycerol at -80°C for long-term storage. Storage of dry powder containing phage is usually done by incorporating a sugar, such as trehalose and freeze drying the phage. Clark, (1962) found that freeze drying phage showed the highest loss of phage titre between 1-2-log during lyophilization but produced the most stable phage over a two-year storage period in comparison to storing phage in the fridge. All conditions investigated showed decline in phage titre after two years with storage in the fridge showing better results than storage at room temperature and in glycerol (Clark, 1962).

A study by Knezevic *et al.*, (2011) demonstrated the effect of external factors on four *P. aeruginosa* phages. The study found phages to be highly sensitive to pH 1.5 with complete loss of titre after 30 mins, however at pH 7 they remained viable. All phage lost viability upon exposure to silver nitrate, other factors such as temperature and polysaccharides and rat serum were also examined for their effect on these phages. The results reveal that there are some similarities on phage responses (such as loss in titre upon acid exposure) to external factors, but differences were also observed (the degree of titre loss) indicating each phage may react differently to external environmental factors. This directly influences the formulation ingredients that may or may not be used for encapsulation of phages and need careful evaluation if encapsulating a cocktail of phages.

2.2.4 Bacteriophages against enteric pathogens

Phages are ideal for treating enteric infections due to their specificity as mentioned previously which will prevent disruption of the surrounding microbiota in the gut as seen with the use of antibiotics (Meader *et al*., 2013). For therapy, lytic phages are ideal to prevent phage entering the lysogenic cycle and remaining dormant inside the bacteria. Experimentally lytic phages can prevent the growth and colonisation of enteric bacteria. Therefore, phages have been approved by the FDA for their use on produce such as salads and leafy vegetables, where enteric bacteria may be present. Phages against *E. coli* O157:H7, *Salmonella* spp. and *Listeria monocytogenes* are shown to be effective in reducing bacterial loads in vegetables to prevent food poisoning (Sharma, 2013).

To date, no lytic phages have been isolated for *C. difficile* however Ramesh *et al.*, (1999) showed the use of temperate CD specific phages *in vivo* to treat hamster models with CDI induced by clindamycin. The results showed the clearance of infection and survival of 14 out of 18 hamsters given phage doses

in comparison to the control where all hamsters died. Nale *et al.*, (2016) also showed reduction in *C. difficile* carriage 36 hours post administration of phage in a hamster. Further delay in symptoms was also observed in comparison to control (J. Y. Nale *et al*., 2016).

In other studies, artificial human colon and fermentation models have been employed to observe the effects of phages to treat CDI. Results show a promising decline in CD population with phage therapy (Meader *et al*., 2010, 2013). Despite these promising results research on CD specific phages in therapy is challenging due to the need for anaerobic conditions for bacterial growth (Hargreaves & Clokie, 2014).

2.3 Encapsulation techniques

In this section different encapsulation techniques currently used to encapsulate active agents are discussed. The review will focus mainly on colon targeted delivery and wound dressing applications. Examples included for each method are obtained from a literature search in the following order:

>name of encapsulation method > microencapsulation >colon drug delivery.

This review will provide an insight into the advantages and disadvantages of using each system for encapsulation of bacteriophages for colon delivery.

The review is divided into different sections as described in Table 2.3.1.

Table 2.3.1 Different encapsulation techniques

Physio-chemical processes	**Physio-mechanical processes**
Coacervation	Fluidized bed
Solvent Evaporation	Spinning disk
Gelation	Interfacial polymerisation
Sol-gel	Interfacial polycondensation
Liposomes	Spray Drying

	Microfluidics
	Membrane Emulsification
	Electrospinning

2.3.1 Physio-chemical processes

2.3.1.1 Coacervation and phase separation

Coacervation is the separation of a mixture of one or two colloid liquids into two phases; one phase containing the coacervate (colloid particles electrostatically held together) and the second phase consisting of an aqueous solution. It is sometimes referred to as phase separation. Coacervation was the first industrially adapted method for microencapsulation and was reported by Bungenberg de Jong and Kruyt in 1929 (Jong, 1929).

The process of coacervation is shown schematically in Figure 2.3.1 below. There are two types of coacervation methods, known as simple and complex coacervation. The process for microencapsulation in both methods is alike; the only difference is in the way the phase separation is carried out. Firstly, the material that will form the wall/coat is solubilized in a solution (a), (b) Figure 2.3.1. Then an active agent (to be encapsulated) is suspended in the solution containing the previously dissolved wall forming material (c) Figure 2.3.1. The wall material is induced out of the solution at stage (d) Figure 2.3.1. This induction in simple coacervation is propagated by the addition of a desolvation agent such as acetone or ethanol. Once out of solution, the wall material adsorbs onto the droplets and is cross-linked (e) Figure 2.3.1 to form a coat around the active agent as demonstrated in (f) Figure 2.3.1.

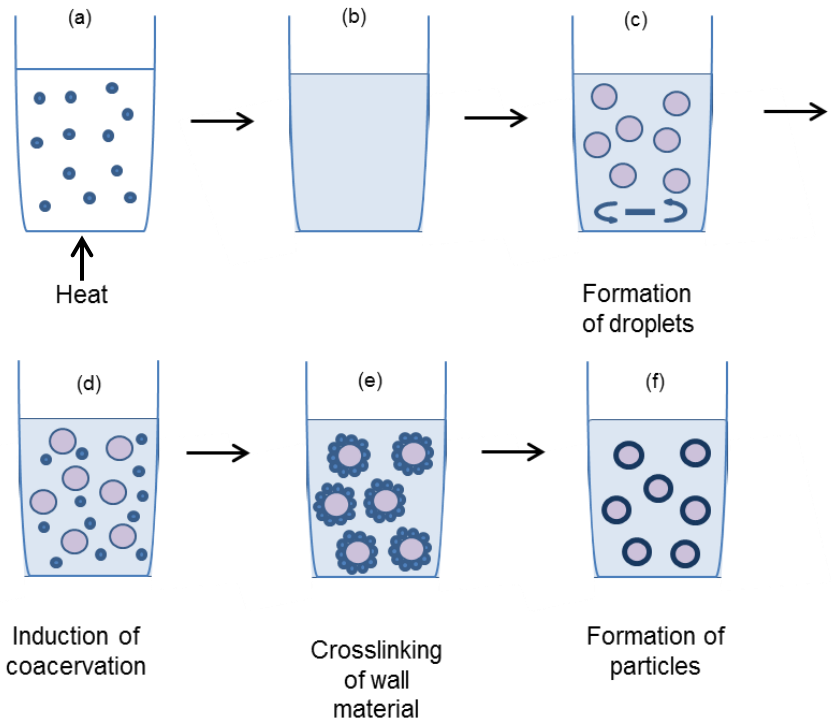

Figure 2.3.15 Schematic representation of the steps in the coacervation process. (a) The wall material is added to an aqueous solution. (b) Heat is applied to dissolve the wall material. (c) The active ingredient is suspended in the solution and stirred at a rate that produces the required droplet size. (d) The suspended wall material is induced to come out of solution by adding a desolvation agent. (e) The wall material adsorbs on the surface of droplets and (f) crosslinks to form a shell around the active ingredient.

In complex coacervation on the other hand, the polarity of two oppositely charged polymers in the Step (d) Figure 2.3.1 in complex coacervation is propagated by adding an oppositely charged polymer to that of the wall material. This difference results in charge-mediated induction of the wall material out of solution. Cross-linking of polymer in the last step is usually induced by altering properties that would render the polymer capable of forming chemical links between molecular chains. This is usually prepared by changing properties such as pH and salinity (Yin & Sto, 2003), solubility or adding cross-linking agents such as formaldehyde (Y.-I. Huang *et al.*, 2007). A classic example of this technique that has been exploited for many years is gum-arabic and gelatin. Positively charged gelatin (at pH <8) forms a complex coacervate when it is counterbalanced with negatively charged Gum Arabic. This system can be used for phage encapsulation since both gelatin and gum-arabic are derived from natural resources. Dispersing phage in gelatin which can form the wall material whilst the process of coacervation may initiated by guar gum which then further coats the microparticles leading to phage encapsulation. Another polymer combination that can employ coacervation for encapsulation is

alginate and chitosan, both are oppositely charged essential for the formation of microparticles (Y.-I. Huang *et al*., 2007).

Particle sizes using coacervation technique range from 2-1200 µm (Ghosh, 2006) although smaller size particles have been reported. Coacervation is a highly conventional method however; the importance of oppositely charged phases can limit the use of the system for applications involving non-charged substances such as an uncharged polymer. The system requires a specific formulation without which the formation of microspheres is challenging. It is also limited to the application of external stimulus (heat, pH etc.) for specific stages for the coacervation to progress. The size of droplets is also dependent on the agitation rate, which gives a large coefficient of variation (CV).

2.3.1.2 Solvent evaporation

Frequently used to encapsulate drugs (Carreras *et al*., 2012; Doan *et al*., 2011; Y. Wang *et al*., 2013) solvent evaporation is a straight forward method involving two or three phases. The core material carries the active agent surrounded by a coat material, which acts as a barrier for site specific delivery. The third phase is usually the manufacturing vehicle in the form of a liquid. The agent to be encapsulated is dissolved with the polymer in a volatile solvent and this is known as the dispersed phase. This phase is then emulsified using a stirrer in an aqueous phase in other words the continuous phase to generate droplets. Subsequent solvent extraction takes place from the dispersed phase via the continuous phase. This process results in the formation of solid particles, which is then subjected to further drying to remove residual solvent.

Solvent evaporation for single oil-in-water (O/W) emulsion is frequently used for insoluble or poor water-soluble drugs. The drug to be entrapped (e.g. Salmon calcitonin a hormone for the treatment of osteoporosis) is dispersed in the inner phase containing a volatile solvent (i.e. methanol) and polymer (i.e. PLGA which acts as the coating material), which is emulsified in an aqueous phase comprising a dissolved surfactant (i.e. sodium oleate) (Jeyanthi, Thanoo, Metha, & Deluca, 1996). The drug-polymer and solvent are emulsified in the aqueous phase using shear to generate droplets. The methanol is soluble in water and therefore leaches into it by diffusion followed by evaporation from the free surface of the aqueous phase (being more volatile than water). Solvent extraction results in the formation of solid particles that contain the encapsulated drug.

During the process of solvent removal, the solubility characteristics of the composition are considered which directly affect the rate of removal. Elevated temperature results in a higher solvent removal leading to the formation of highly porous particles. This is not ideal because in controlled systems it

leads to undesirable drug release profiles (Jeyanthi *et al.*, 1996). Double emulsion methods can be applied to situations where the drug to be encapsulated is hydrophilic, therefore it is immiscible with the organic inner phase and will likely diffuse out to the aqueous phase. In these circumstances water-in-oil-water (W/O/W) emulsions stabilise the entrapment of the drug whilst utilising removal of solvent as a method of creating microspheres. An example of double emulsion solvent evaporation was demonstrated by Doan *et al*., (2011) for the encapsulation of inhalable antibiotic rifampicin (RIF) in PLGA microspheres. The inner water phase contained the RIF along with buffer which was emulsified in an organic solution containing PLGA (PLGA is a polymer) and later added to the outer aqueous phase containing PVA (Doan *et al.*, 2011).

The variation in microsphere sizes that can be obtained via this method can vary from couple of microns to hundreds of microns. Although, solvent evaporation is an effective method, it is limited in its criteria to using volatile solvents to obtain particles which is not suitable for phage encapsulation. Phage are not compatible with an organic solvent which form an important parameter in encapsulation by solvent evaporation (Matsubara *et al.*, 2007). Additionally, like coacervation the CV of particle sizes is largely dependent on the rotary motion of a homogenizer, which gives low control of droplet size.

2.3.1.3 Gelation (Ionotropic gelation)

Gelation for encapsulation is usually used when alginate is the main component of the formulation. Alginate is linear, non-branched polysaccharide composed of varying ratios of 1, 4-linked β-D-mannuronic acid (M) and α-L-guluronic acid (G) residues. Alginate is water soluble and forms a reticulated structure which can be crosslinked to form an insoluble meshwork. It has a distinctive ability to form a gel when it encounters divalent cations i.e. Ca^{2+} (Liu, Yu, *et al*., 2002). When divalent ions (i.e. from $CaCl_2$) diffuse into an aqueous alginate solution they bind and induce guluronic acid residues to crosslink, causing internal gelation (C. M. Silva *et al*., 2006). Several studies have used gelation of alginate as a carrier for phage to protect from low pH (Colom *et al*., 2017b; Cecilia Dini *et al*., 2012; Yongsheng Ma *et al*., 2012; Stanford *et al*., 2010b; Tang *et al*., 2013; Yongsheng *et al*., 2008)

In addition to alginate there are other polymers which are utilised for encapsulation via the gelation method. Fermentation by aerobically submerging Sphingomones Eloda produces gellan gum. This is an exopolysaccharide of bacteria which is usually prepared commercially. Increasing the temperature of a concentrated aqueous solution of gellan gum induces gelation. Subsequently lowering the temperature, gellan chains form double helices forming junction zones through sol-gel transition. This feature gives a thermos-reversible hydrogel (Patil *et al*., 2012).

Chitosan is another naturally occurring poly-amino-saccharide; it is non-toxic and is easily bio-absorbable. Other properties include its ability to tolerate acid and has anti-ulcer characteristic preventing irritation that results from drug administration (C.-X. Zhao, 2013). Therefore, Chitosan is considered an attractive polymer for drug delivery and phage formulations (Tang *et al.*, 2015; Yongsheng *et al*., 2008). Carboxymethyl cellulose and pectin are also used in the gelation process. These polymers are naturally occurring with properties that allow cross-linking/ gelation by altering chemical bonds (Patil *et al*., 2012).

Polymer and crosslinking electrolyte concentration, temperature, pH of solution, drug concentration and gas forming agents influence ionotropic gelation. These factors can determine the efficiency of crosslinking between units because in order for crosslinking to commence the optimal conditions need to be present (Patil *et al*., 2012). Not being able to control these factors results in poor gelation and therefore a decline in the number of microspheres formed. The size of particles depends on the manual agitation applied by a stirrer as well as proficiency of gelation. The sizes can be varied greatly from a couple of microns to hundreds. The control over size determination of particles is limited and dependent on the factors influencing cross-linking. Encapsulation by gelation has been effectively proven and is on the rise due to the use of eco-friendly compositions and avoidance of toxic organic solvents. It is however limited by its own mechanism of action as the availability of natural polysaccharides with the ability to crosslink is limited. In addition to that the encapsulation efficiency is low and the controlled release of the loaded agent is poor due to problems with porosity (Martins *et al*., 2007).

2.3.1.4 Liposomes

Liposomes are used to encapsulate aqueous solution with a membrane of phospholipids. Phospholipids form a barrier between the aqueous phase and the oil phase, the polar head pointing towards the aqueous phase and non-polar tail towards the lipid phase. This method encapsulates a hydrophilic drug in the aqueous inner phase and can also encapsulate lipophilic drugs in the lipid bilayer. The interactions of the membrane bilayer with the hydrophilic and lipophilic properties of the drug directly affect the encapsulation efficiency (Kulkarni *et al*., 1995 Barenholz, 2003). The preparation of the liposomes can also contribute to encapsulation efficiency; some of the factors include the volume of aqueous phase, surface area and membrane robustness (Kulkarni *et al*., 1995).

The process for preparation of liposomes is referred to as microencapsulation vesicle, starting with water-in-oil emulsion. The drug to be encapsulated may be water or oil soluble. Regardless, of the solubility of the drug the primary emulsion is water-in-oil. The primary emulsion is then dispersed in

another water phase to generate drug loaded liposomes. This double emulsion is subjected to shear force which breaks up the emulsion into homogenous droplets. The process is described by Nii & Ishii (2005).

Liposomes have been successfully applied to encapsulate drugs; one such example is outlined in the U.S. Pat. No. 3,993,754, by inventors Rahman Yueh-Erh, Elizabeth (1976). Here, they described the use of encapsulating anti-tumour drugs provided for chemotherapy of malignant tumours using liposomes. The liposomes encapsulating the drug are administered intravenously, penetrating the tumour cells to induce death. Similarly, further patents including US 4515736, method for encapsulating materials into liposomes (Deamer, 1985) and patent US 4485054 A.

Several patents on the process exist and have shown the use of liposomes as an effective method for drug encapsulation. Phages have also been encapsulated in liposomes for oral delivery and release in the gastrointestinal tract (Colom *et al*., 2015; Nieth *et al.*, 2015; S. Singla *et al*., 2016; Singla *et al*., 2016). The size of the liposomes produced is usually very small ranging from nanometres to a few micrometres. Due to the small size of liposomes it is difficult to separate non-encapsulated phage from encapsulated phage.

2.3.1.5 Sol gel

The precursor is the initiator of the sol gel process; it undergoes hydrolysis by the addition of water and presence of a catalyst which can be a base, acid or a metal alkoxide. The commonly used precursors are tetraethyl orthosilicate (TEOS), alkoxymetallate and, or alkoxysilane which form hydroxyl derivatives such as silica acids and hydroxysilanes etc. The hydroxylated monomers produced, undergo polymerisation followed by phase separation generating either a semi-metal oxide or a hydrated metal hydrogel. As the aqueous phase is removed from the hydrated gel, the formation of pores occurs producing a porous xerogel (Gill & Ballesteros, 2000).

Silica alkoxides are prone to hydrolysis and form silica (SiO_2), subsequent condensation causes the bridging of two oxygen atoms causing silicon atoms to come together. Continuation of this reaction causes the silica atoms to be added and grow the polymeric chain, Figure 2.3.2. This type of reaction can occur at different location growing the silicon oxide or alkoxide particles. The term ‘sol’ refers to the stage where these particles are dispersed in a colloid system with solvent. As the particles continue to grow they start to interlink with chains from other locations forming a ‘gel’ network that encompasses pores of trapped fluid. Aerogels are formed from the aqueous phase being replaced by gas in such a way that its solid network is retained, with only slight shrinkage in the gel. Originally this

was achieved under super critical conditions. However, it is now possible to carry out the process in ambient drying conditions.

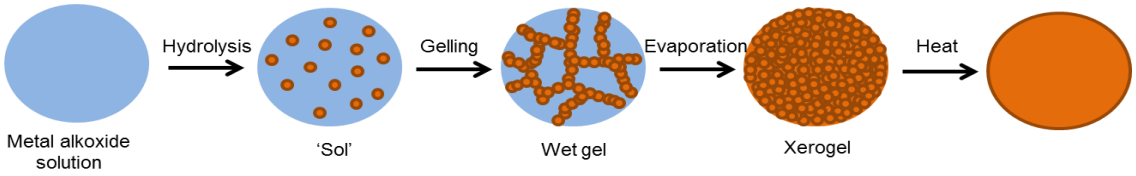

Figure 2.3.2. A schematic of the sol gel process in the formation of a dense ceramic.

The common sol-gel matrixes are comprised of silica, metallosilicates and titanium, zirconium and aluminium oxides. The matrixes formed from these materials are in a hard-transparent glass form and can be further modified to be applied for different applications one of which is for biosensors. However, they have also been successfully applied for the encapsulation of bioactive materials such as enzymes, proteins, antibodies and cells (Avnir *et al*., 1994).

The process eliminates any harsh conditions which can easily denature and destroy bioactive material. Sol-gel is carried out at room temperature which is suitable for many bioactive agents without any rigorous applications. Sol-gel compared to conventional polymers is durable, strong and highly resistant to mechanical, biological and chemical degradation. Manufacturing and engineering of products desires such properties for efficient, viable and scale-up purposes. The disadvantage of this technique is that ceramics can be frail; the presence of pores reduces the rate of chemical interaction. Further to this, following polycondensation the hydrogel ages causing it to shrink through loss of liquid phase. Although used in the food industry as an anti-caking agent, it is not ideal for oral phage therapy due to the use of metal oxides.

2.3.2 Physio-mechanical processes

2.3.2.1 Interfacial polycondensation

Interfacial polycondensation is the process of polymerisation between two immiscible phases. Two different monomers (reactive when brought together) are dispersed in each phase of the heterogeneous system. These monomers react at the interface of the two phases leading to the

formation of a polymeric membrane around the inner face. Figure 2.3.3 shows the generic steps; first water-in-oil emulsion is prepared. The inner phase carries one of the two monomers and the agent to be encapsulated in dissolved or dispersed in the inner phase. The outer phase contains the surfactant and the second monomer. Mechanical agitation results in the formation of droplets. Figure 2.3.3 (a) shows a single droplet representing the elements acting upon all droplets in the emulsion (Benita, 2006).

The monomers in the inner and external phase Figure 2.3.3 (b) are particularly reactive. The two monomers react at the interphase of water and oil to form a polymeric membrane around the droplets Figure 2.3.3 (c).The microcapsules are usually obtained from water-in-oil or oil-in-water emulsions although oil-in-oil emulsions have also been used for interfacial polycondensation (K. Bouchemal *et al*., 2003). Solubility and partition co-efficient determine the localization of the reaction Figure 2.3.3 (c), (d). The reaction can take place at the outside of the droplet or in the inner wall.

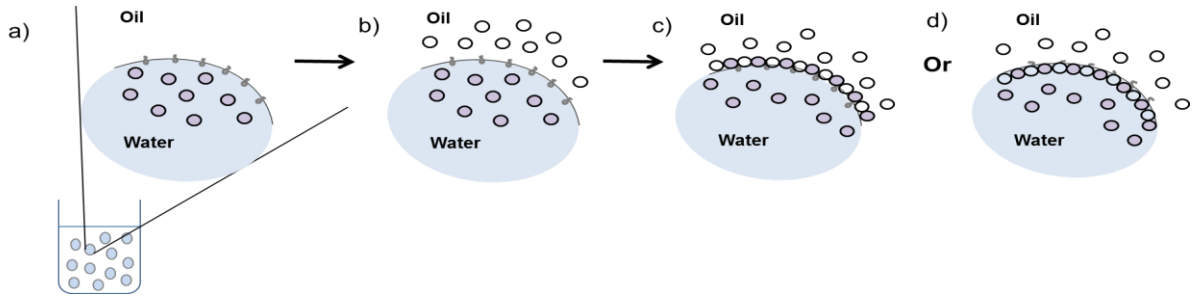

Figure 2.3.3. Schematic representation of polymeric membrane formation in the interfacial polycondensation process. (a) Enlarged single droplet from water-in-oil emulsion with monomer in the water phase and surfactant in the oil phase. (b) Second monomer added to oil phase resulting in a reaction (c) with the water phase monomer at the water-in-oil interface. Alternatively, the reaction may take place at the inner surface of the droplet (d).

The reaction only commences when there is a sufficient concentration of monomers in each phase which determines the partition coefficient. The solubility of the monomers determines where the reaction takes place which can result in either microspheres (in droplets) or microcapsules (outside droplets). The size of the droplets is hugely influenced by the initial emulsion step with the properties of both phases and the choice of surfactant. The duration and input of energy from mixing via mechanical stirring, homogenization or ultrasonication also determine the droplet size. The thickness of the wall is dependent on the concentration of monomers.

Polyurethane is a polymer already utilized in various fields of medicine due to its mechanical properties and biocompatibility. Polyurethane can undergo gradual biodegradation in the human body, making it a suitable candidate for microparticle preparation. Kim *et al*., (2006) encapsulated an anti-tuberculosis drug, isoniazid in polyurethane using interfacial polycondensation. This water-in-oil emulsion was made by adding the water phase to the oil phase whilst stirring. The water phase contained isoniazid, poly(ethylene glycol) (PEG) (monomer one) in water. This was gradually added to a solution of Toluene and surfactant Tween 20. Once the emulsion was complete Tolylene 2,4-diisocyanate (TDI) the second monomer is added. The addition of the second monomer results in a rapid reaction with PEG causing crosslinking at the water/toluene interface and subsequent encapsulation of drug (M. D. Kim *et al*., 2006). Applying this method for phage encapsulation can be challenging due to the limited use of polymers and need for organic solvents.

2.3.2.2 Interfacial polymerisation

Although sometimes difficult to distinguish from interfacial polycondensation, interfacial polymerisation performs in a slightly unique way. The presence of a monomer in this case is also essential however the mechanism of crosslinking differs somewhat from polycondensation. In the case of interfacial polycondensation when two monomers come together the reaction produces a molecule like water as a by-product hence the term polycondensation. On the contrary, for interfacial polymerisation the double bond between two carbon atoms of a monomer open during an addition reaction and form a polymer chain. This phenomenon is also referred to as addition polymerisation. During addition polymerisation the chain can be extended by addition of any number of monomers. The three steps in this process are; initiation, propagation and termination (Figure 9.1 appendix). During initiation a double bonded monomer is activated by a free radical. The activated monomer radical interacts with other monomers and attaches during propagation as the chain grows. The termination of the reaction takes place when two radicals come together to reform a double bond and stabilise. The length and other properties of polymers can be precisely controlled for synthetic polymers. Figure 9.1 (appendix) demonstrates the process using an example of the polymer, polyethylene.

The formation of polymer around an active agent seals it and therefore encapsulates the agent for site specific delivery. Interfacial polymerisation is commonly used in synthetic polymer industry however it can also be applied for drug encapsulation. Kobaslija *et al* encapsulated Coumarin-1 (model encapsulant) in polyuria microcapsulaes. Polyethylemine was the polymer used for this study. 2,4-

Tolylene Diisocyanate was added to initiate solution polymerisation and an immediate reaction resulted in formation of solid polymer. In this case mechanical stirring was applied to obtain small microcapsules (Kobašlija & McQuade, 2006). As previously stated, mechanical agitation does not give narrow size distribution of particles. Interfacial polymerisation can produce particles sizes ranging from a 1 to a couple of hundred micrometres.

2.3.2.3 Extrusion

Extrusion is a common technique used for the formation of microcapsules of a hydrocolloid solution. It is used extensively in the food industry for the encapsulation of microorganisms aimed to improve gut health by replenishing and maintaining a rich micro-biota. This method utilises the properties of a hydrocolloid solution to generate a shell around a bioactive agent. Alginate is the polysaccharide of choice for this method due to its ability to form a gel, in conjugation with calcium chloride as explained in the gelation section above.

To form droplets, a cell suspension (e.g. at concentration 10^6) is added to a mixture of sodium alginate solution. The mixture is passed through a syringe, where droplets are formed when they are pushed through needle. The diameter of the needle determines the size of the droplet as well as the distance of the fall into the setting solution. Once droplets are formed they fall into a solution of calcium chloride, as mentioned previously this causes the alginate to harden and form a shell around the bioactive material Figure 2.3.4. This method is preferred due to its low cost, ease of use and the general mild conditions necessary for retaining viable cell concentration (Krasaekoopt *et al*., 2003).

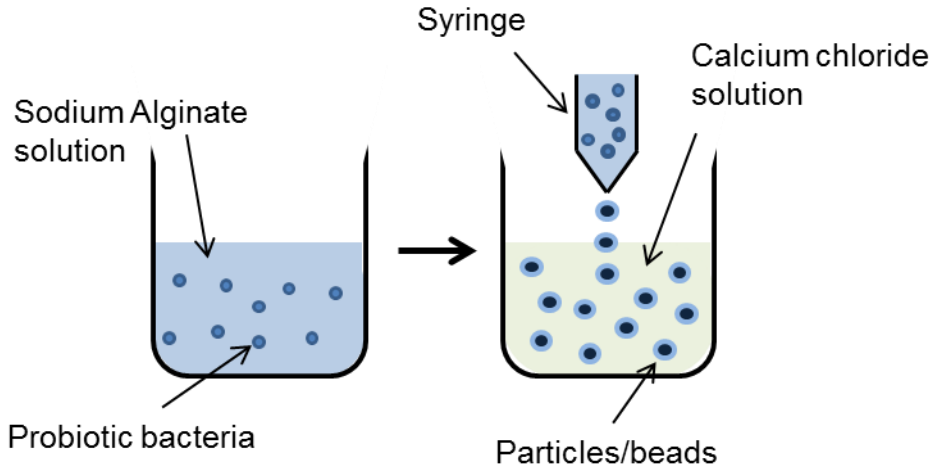

Figure 2.3.4. A schematic of the extrusion process. Bacteria are suspended in a solution of sodium alginate which is transferred into a needle with a defined size needle. The droplets formed by the syringe are collected in a solution of calcium chloride which solidifies the droplets into particle or beads.

The size of beads obtained from this method is usually bigger than what most techniques can generate. The beads are in millimetres and in some cases a couple of hundred micrometres. The large size of beads is usually desirable especially when capturing probiotics for the likes of yogurt or yogurt drinks.

The principle of extrusion has been applied with other methods to obtain droplets and subsequently particles. One such method is the double capillary method, two immiscible phases; inner (core substance) phase and outer (wall material or polymer) phase. The two phases are passed separately through the inner capillary (core substance) and outer capillary (polymer). The two phases meet at the tip to form a jet and break downstream to form droplets. Similarly, the same principle is applied to a centrifugal extrusion device. Except the break-up into droplets is mediated by rotating motion which breaks up the stream of wall material coating the inner phase (Madene *et al*., 2006).

2.3.2.4 Spinning disk

As the name suggests spinning disk produces particles with the use of a rotating disk at a certain speed. It is also referred to as spinning disk atomization and is similar to the extrusion technique. The feed comprises of a liquid which undergoes disintegration when exposed to the spinning disk at the centre of the chamber. The shear forces exerted by the speed of the disc cause the liquid to form a thin film on the disc. As the feed is continuously introduced into the chamber, the droplets are released via centrifugal forces exerted at the edge of the disk and collected (Figure 2.3.5). The droplets undergo further processing by cooling to solidify droplets into particles (Ghosh, 2006). The size of the droplets is dependent on the rotational speed of the disk. The size of microspheres produced can vary from 5-1500 micrometres, although with a multistep process nanoparticles can also be generated (Huanbutta *et al*., 2013). The simplistic approach of this technique is scalable with a production capacity of tons per day, usually using a multi-disk system.

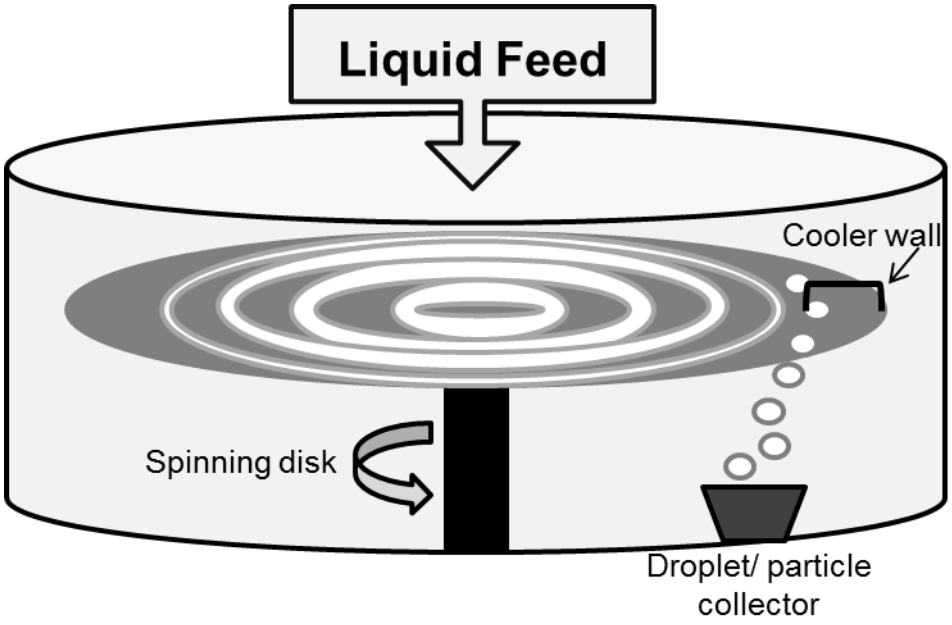

Figure 2.3.5. Schematic of a spinning disk reactor

This technique was utilised by Huanbutta *et al*., (2013) to encapsulate diclofenac sodium (an anti-inflammatory drug). The group showed successful production of nanoparticles encapsulated in poly(methyl acrylates)-coated chitosan. Eudragit S100 and L100 (co-polymers) were also utilised to increase colon targeted drug delivery efficiency. Similarly, gelation (previously mentioned) can also be applied to the spinning disk method to produce particles of a narrow size distribution. Senuma *et al* (2000) encapsulated yeast in a alginate microspheres. The principal of encapsulation in general terms remained the same (as shown in Figure 2.3.5) where the alginate and yeast were fed by a peristaltic pump into the rotating disk reactor. The resulting droplets were collected in a bath of calcium chloride to convert droplets into particles.

There are several applications of this method due to its simplicity and ease of use. It is inexpensive and produces products on a large scale. However, the encapsulation efficiency and product size distribution are marginally better than other conventional methods. The range of product particle size shows a significant range from nanometres to several hundred micrometres.

2.3.2.5 Fluidized bed

Fluidized bed technology has been commercialised and well established to produce industrial polymers amongst many other applications. The reactor can carry out multiphase chemical reactions, a porous plate (distributor) at the bottom of the chamber supports the solid substrate (usually a catalyst which coats the fluid and undergoes chemical reactions) through which the fluid is forced into the chamber under high velocity. The high pressure keeps the solid substrate suspended and it behaves like a fluid a process known as fluidization. At this stage the contents of the reactor swirl around much like a tank of water under agitation. This technique can be used to achieve a shell layer of any kind around solid particles. Double coatings or a mixture of coatings can be challenging when working with other technologies to produce double layer shells. This is because to achieve double shell layers the emulsion is aqueous requiring stabilisers. In this case however, solid particles can undergo further coating; an example of this would be chitosan particles encapsulating a drug undergoing Eudragit enteric coating in a fluidized bed (Kaur and Kim 2009).

There are several steps of this technology including; drying, agglomeration (granulation or spray drying), spray granulation, micro-encapsulation and coating. The positions of the spray nozzle (e.g. bottom or top spray) refer to Figure 2.3.6 determine the process type. Bottom spray (also known as Wurster's coater) position of the nozzle is better applied in granulation or agglomeration process where as the top spray position is better suited for coating purposes. Batch size, air velocity, inlet temperature, humidity, nozzle diameter and position, viscosity, surface tension, spray rate, atomization and air pressure are all major variables in fluidized bed process.

Particles are sprayed with a liquid coating; the process of solvent evaporation aids the formation of a coat around the particle. By controlling rate, concentration and flow of the coat material and particles in the chamber the thickness and formulation can be changed according to preference. Gravity force compensation is the basic concept of fluidization of particles. Top spray bed introduces the coat material downwards, encapsulating particles with high efficiency as they move up the chamber towards the coat spray. The originally developed bottom spray coater sprays the coat material towards the top. The particles are introduced into the chamber via a perforated plate, from the bottom of the chamber; the air flow from the bottom ensures the complete fluidization of particles. There are many modifications that can be made to enhance the process and increase the efficacy of atomization and fluidization, such as a rotating drum to enhance fluidization of particles (Gouin, 2004).

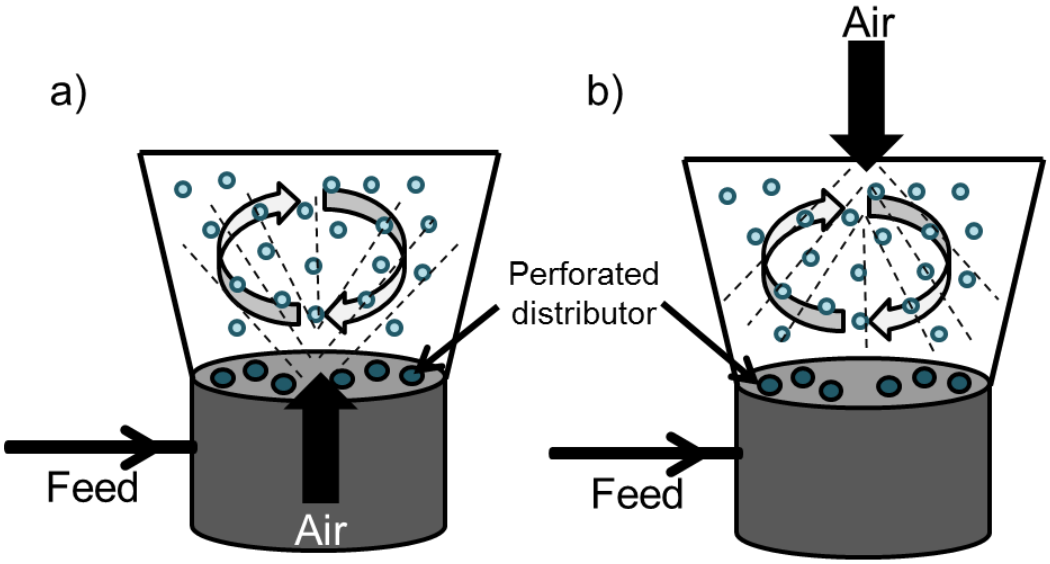

Figure 2.3.6 Schematic of a fluidized bed showing (a) a bottom nozzle spray (b) Top nozzle spray coater.

The applications of fluidized bed can range significantly; food industry and pharmaceutical industry have adapted the method. Preparation of pellets containing Glipizide (drug) for type II diabetes (Yadav *et al*., 2011), Oxytetracycline (OTC) antibiotic against various bacteria (Kleinubing *et al*., 2014), salmon calcitonin for treating osteoporosis (Yang *et al*., 2012) are all drugs which have been encapsulated using fluidized bed technology. The pH responsive methyl-methacrylate Eudragit co-polymer with alginate/chitosan was used to encapsulate the drug OTC by Kleinubing *et al*. 2014 for gastro-resistant controlled release. The size of the particles produced via fluidized bed usually ranges from micrometres to millimetres. In some cases, nano-sized particles may be produced but the process are challenging, and the impact of electrostatic forces needs to be considered.

2.3.2.6 Spray drying

This technique uses the flow of hot dry air moving through a chamber to nebulise a solution into a spray to form particles. It is widely used in the food, chemical, biochemical and pharmaceutical industry. A hot gaseous drying medium converts the feed from a fluid state to a dry form. There are three stages in spray drying, the first is the atomization which largely determines the particle size, second is solvent evaporation and finally particle collection. Atomisation is the initial stage of the entire process; here the phases are fed into a specific atomizer for conversion of the phases into droplet form. There are different atomization systems available and usually vary in their nozzle design.

The purpose of this stage is to increase the surface for heat transfer between the liquid and dry air to elevate heat and mass transfer. The nozzle design can be rotary, pressure or two-fluid atomization. There are further modifications available to these designs. Nevertheless, the feed is fed through these nozzle systems and the type of design determines how the droplets are formed (Walters *et al*., 2014).

Atomization with a rotary atomization nozzle the feed is sprayed via a spinning disk or wheel into the drying chamber creating droplets. Pressure atomization introduces the feed into the chamber under high pressure causing the fluid to break into droplets. The two-fluid nozzle carries the feed and atomization air via two separate nozzles which come to together, the air causes disruption of the fluid into droplets producing a spray. Each system has a direct impact on the particle size produced and each is useful for a different type of feed. For example, more viscous feeds benefit from the rotary nozzle system producing particles of up to 200 µm. The other two nozzle systems can produce particles less than 10µm dependent on the diameter of the nozzle. The size of the particle is affected by the viscosity as well as the surface tension of the initial feed, with high viscosity and surface tension the particle size increases (Benita, 2006).

Temperature plays a vital role in a spray drying system. The hot air contact marks the start of the drying stage; this is usually instantaneous resulting in solvent evaporation. There are two flow arrangement that can be used to introduce hot air to cause drying, the flow of hot air can be co-current or counter current. Feed is sprayed in the same direction as the hot air in a co-current set-up. Temperature between 150-200˚C of the hot air in-let causes rapid solvent evaporation. A much lower temperature is kept for dried powder to maintain the integrity of particles. However, in the counter-current flow the feed is fed at the opposite side of the hot air in-let resulting in a much higher temperature contact. The dried particles remain exposed to elevated temperature causing some constraints to its applications when requiring thermo-sensitive particles. The water in the droplets diffuses from the core to the surface due to the surface evaporation rate. This is determined by the heat and water vapour partial pressure which causes the water to diffuse away from the droplet and heat is transferred to the droplet. Because of these forces the crust of the droplet solidifies and forms a particle. This process is instantaneous especially given the higher surface area to volume ratio of droplets which increases the rate of solvent removal (Gharsallaoui *et al*., 2007).

The product is collected in a cyclone located outside the dryer chamber. This helps trap fine particles from the humid air to avoid product loss. The denser particles are usually recovered from the bottom of the drying chamber. Some spray dryers also contain bag houses which are filters capable of retaining the finest of powders (Walters *et al*., 2014). The typical process of spray drying is demonstrated by (Dobry *et al*., 2009) in Figure 2.3.7.

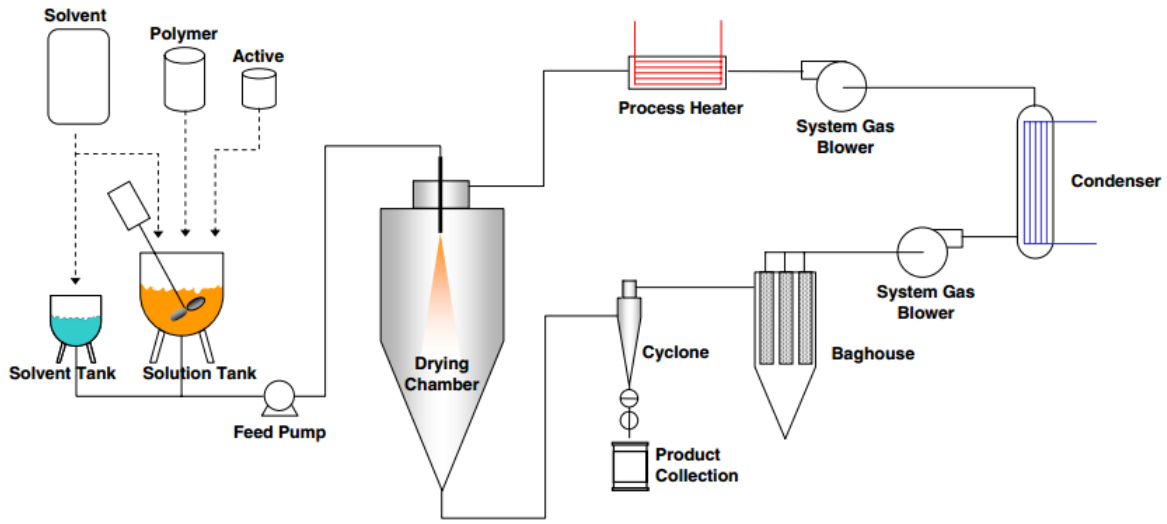

Figure 2.3.7 A typical spray drying process showing key equipment involved (Dobry *et al*., 2009). The feed is mixed and prepared before being added to the atomization chamber. Once the feed is added formation of droplets and drying takes place. The product is passed through a cyclone and a bag house to separate the particles from the humid which is then eliminated via a condenser.

Spray drying has been used in various applications including encapsulation of drugs. Inventors Thomas E. Waddell et al (2013) have described the use of spray drying to encapsulate bacteriophages in the pH sensitive polymer Eudragit S100 and L100 for site specific delivery in the patent CA 2463827 C (Thomas E. Waddell, Roger Johnson, 2013). The successful encapsulation via this method has proven the diversity of its application in various industries.

2.3.3 Membrane emulsification

Membrane emulsification was proposed in 1988 by Nakashima and Shimizu as a new emulsification system. Before this, conventional methods included shaking, injecting, stirring, and ultrasonic, aerosol, spray drying, homogenizing etc. This method is suitable for any emulsion for particle production (Nakashima *et al*., 2000). It can produce droplets sizes of 1 micrometre and above with coefficient of variance less than 10 %. Membrane emulsification allows better control over droplet size production than other conventional methods. This technique is simple and allows production of narrow size distribution droplets with low shear stress with lower energy consumption. The well-defined

production of droplets is dependent on the type of membrane used. This technique has the potential to be scaled from a laboratory to an industrial production process.

There are several types of membranes categorised as surface or sintered membranes. The most commonly used membranes are the Shirasu-porous-glass (SPG) and microsieve membranes. SPG membranes offer a uniform, flawless surface. They can have pore sizes ranging from 0.05-20µm and are commercially available. The surface of the SPG membrane can be further modified to suit the emulsion system. Microsieve membranes are essentially microfiltration membranes with a controlled pore geometry and spatial arrangement. These membranes are popular when requiring low transmembrane pressure but a high transmembrane flux.

There are several factors that can influence the size of droplets including; membrane microstructure, wetting properties, spore shape and size, spatial distribution of pores etc. In addition to these, forces that act upon the phases also contribute to droplet size. Transmembrane flux and shear stress acting at the surface of the membrane control the movement of the droplets. Viscosity of the dispersed and continuous phase, surfactant type and the concentration also contribute to droplet size. Droplets can further be processed during or after membrane emulsification to produced solidified particles. Particles sizes are directly dependent on the droplet size and the chemistry of the transition process. There are various particle morphologies that can be achieved via this process including porous and core-shell particles. The most common application of membrane emulsification is the synthesis of particles. Particles are applied in various fields including drug delivery. Advantage of using membrane emulsification for particle production is that organic, inorganic, metal, hydrogels, carbon, polymer etc. can be used.

Holdich *et al.,* (2010) describe the use of oscillating and stationary membranes for the production of droplets with a narrow size distribution. They describe the shear-based detachment of the droplets in a stirred and oscillating membrane system. The study describes the application of shear at the membrane surface that can reduce the breakup of previously formed droplets. In one case the shear is applied in the direction of injected phase, by an oscillating membrane surface (frequency 10 to 90 Hz). The frequency is kept low to allow comparison with a stationary membrane (same material) with a shear applied by a stirrer in the dispersion cell. The method allows comparison of droplets above 30µm produced in a controlled manner to allow for industrial scale-up. In conclusion, oscillating membrane system produced smaller more uniform droplets than the stirring dispersion cell. This study highlights the robustness of using membrane emulsification to produce droplets with a controlled result. In addition to that it shows promise for industrial scale up by simply increasing the membrane surface area. To allow, for a better controlled final product membrane can be exploited in many ways

such as by surface treatment or physical modifications to change rates of forces being applied during the process.

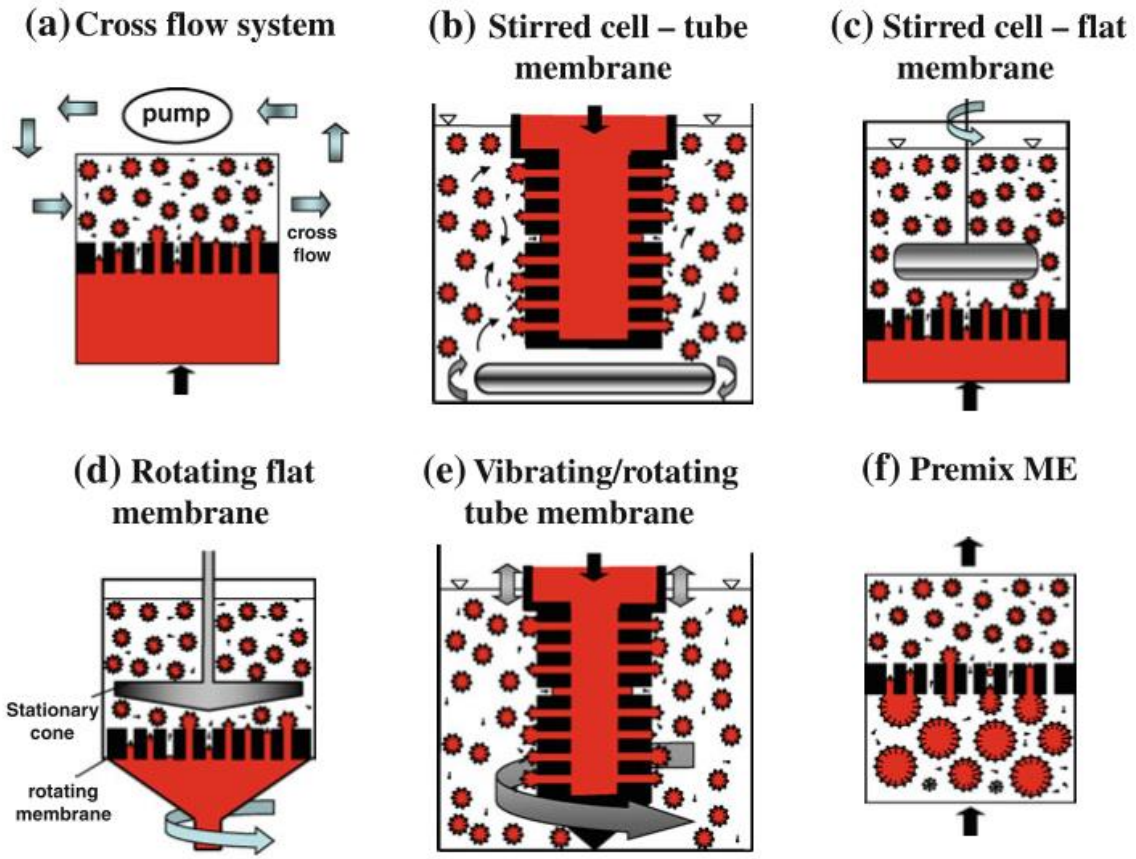

Figure 2.3. 8.16 Membrane emulsification systems (G. T. Vladisavljević *et al*., 2012)

Direct membrane emulsification systems are depicted in Figure 2.3.8 a-e. The dispersed phase (red) is injected into the immiscible continuous phase (white) forming droplets. The membrane can be hydrophilic or hydrophobic depending on whether water-in-oil or oil-in-water emulsion is required. Droplets can be formed in the absence of shear at the membrane surface relying only on the interfacial tension (Kukizaki 2009; Kosvintsev 2008). From a commercial standpoint this method is not viable as the production rate is low therefore; shear force may be applied at the membrane surface. Droplet detachment at the membrane surface can be aided by applying shear stress via cross-flow geometry of the feed fluid or stirring Figure 2.3.8 a-c.

Membrane emulsification can also be used for premixes Figure 2.3.8 f, which give the advantage of producing double emulsions such as water-in-oil-in-water or oil-in-water-in-oil. The primary water-in-oil or oil-in-water emulsion is fed through the membrane into another immiscible phase. This technique is useful to produce smaller droplets in a big drop but more importantly for encapsulation. A model water soluble drug (blue dextran) was encapsulated with 100% efficiency in poly(D,L-lactic-*co*-glycolic) (PLGA) microparticles using membrane emulsification by Gasparini *et al*., (2008). Preparation and characterization of PLGA particles for subcutaneous controlled drug release by membrane emulsification was demonstrated.

Depending on the pore size of the membrane (5 to 50 µm) droplets with controlled size are produced. Membrane emulsification is a useful platform to produce microparticles with drug encapsulation with the potential to upscale. For double emulsions, required for many encapsulation procedures membrane emulsification has also proven useful. Van der Graff *et al* discusses the use of double emulsions for encapsulation of food, medicines and other high value products. Due to the increased shear sensitivity of double emulsions surfactants (lipophillic and hydrophilic) are used. The primary emulsion (w/o or o/w) is usually subjected to high shear stress to allow formation of droplets. When the external phase (water or oil) is added the high shear, stress can cause the inner droplets to break further into smaller droplets which are not desirable. High shear also results in elongation of internal droplets increasing coalescence and areas for drug release. Therefore, it is ideal to use membrane emulsification due to its low shear stresses on the system without compromising droplet monodispersity (Van Der Graaf *et al*., 2005).

Morelli *et al*., (2017) showed the use to this technique for yeast encapsulation in gelatin and or chitosan microparticles coated with Eudragit S100. The results demonstrated the use of this technique and formulation as an effective way for encapsulating active agents for colon delivery. It is therefore a promising method even for microbial cell encapsulation and certainly for bacteriophages in phage therapy. The particles produced can vary from a couple of microns to hundreds of microns.

2.3.4 Microfluidics

Microfluidics is a technology which exploits properties of various liquids to attain an enhanced application. In other words, it is a platform to perform meticulous testing, assaying, and diagnosis on a higher scale with attention to every droplet. Microfluidics has gained much recognition in every field due to its controllability.

There are different variations of microfluidic devices which suit different purposes but essentially form monodispersed droplets Figure 2.3.9. Simplest microfluidic device is the T-junction device, where droplet formation is a result of its structure. Made in a T-shape where the main channel is perpendicular to the horizontal channel Figure 2.3.9 a and b. The dispersed phase flows through the main channel and the continuous phase from one end of the horizontal channel. The dispersed phase flows down into the continuous phase while the continuous phase flow across the horizontal channel. The formation of droplets occurs at a short distance from where the two phases meet due to shear stresses and upstream pressure (Thorsen *et al*., 2001).

Using the same principals as the T-junction device of formation of droplets, a cross junction device is also available Figure 2.3.9 f and g. The cross-junction device has 3 entry channels and one outlet channel for collecting formed droplets. All channels are perpendicular to each other in geometry. The dispersed phase is introduced into the device between two inlets of the continuous phase. This geometry configuration allows full 'engulfment' of the dispersed phase which at a short distance after encountering the continuous phase forms droplets in the outlet channel. As the jet from the dispersed phase becomes too thin when entering the continuous phase, it forms a droplet. With another cross junction connected downstream of the droplets collection channel can produce core/shell particles and with further extension to this principal more complex emulsions can be produced (triple, quadruple, quintuple) (A. R. Abate *et al*., 2011; a. R. Abate & Weitz, 2009).

Y-junction microfluidic devices are also applied to produce droplets. The geometry of the channels is in the shape of a 'Y' where the dispersed phase is fed through one of the two channels on the same side Figure 2.3.9 h and i. The continuous phase enters through the channel next to the dispersed phase and both flow into an outlet channel at the opposite end. The droplet size is independent of the flow rate or the viscosity in this geometry which we observe in the case of T-junction devices. This type of device can generate a stream of two distinct fluids when the Reynolds numbers are low. This type of process has a different purpose such as forming crystals in a continuous line or to etch the inner wall of the outlet channel (Kenis, 1999).

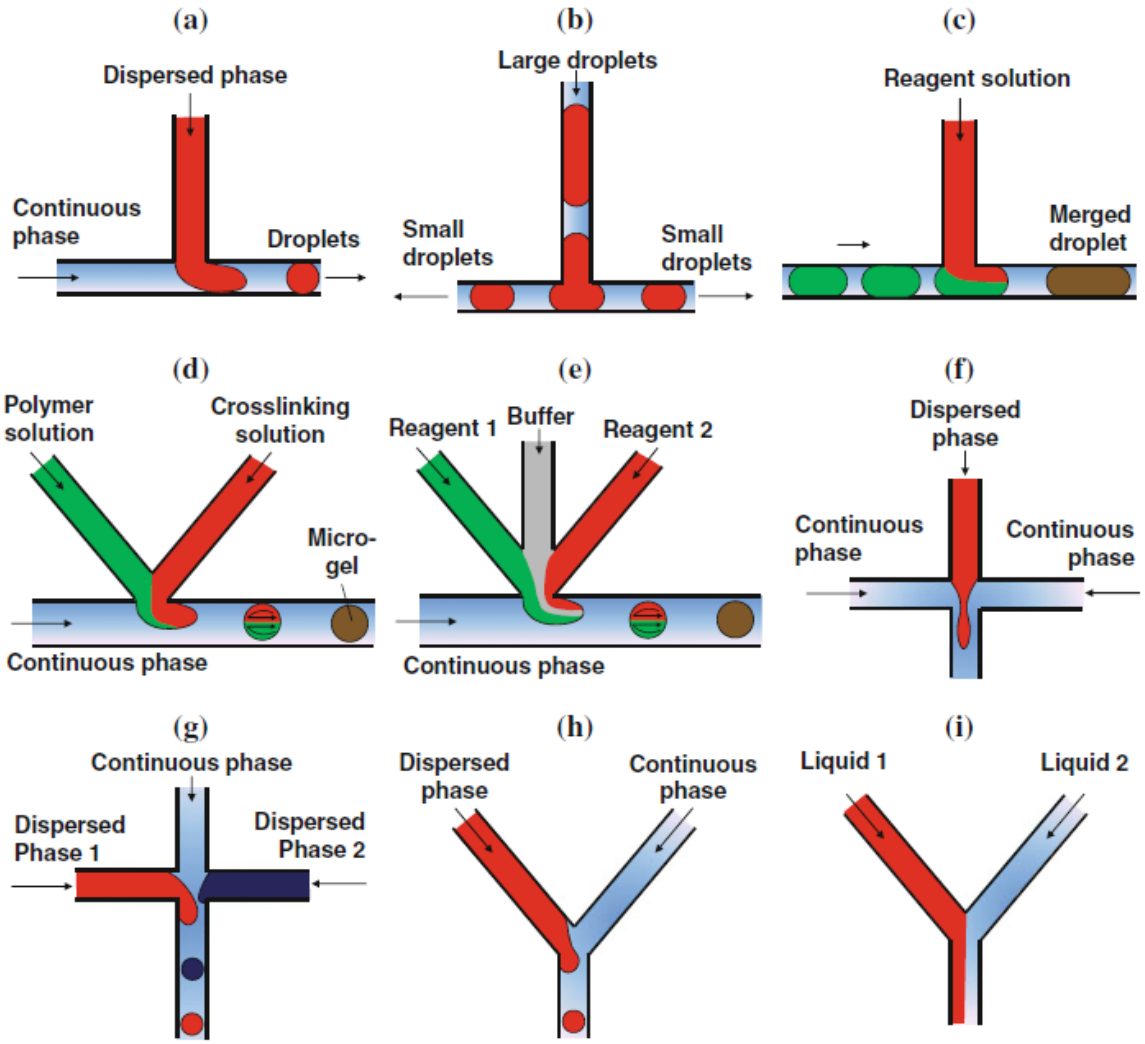

Figure 2.3.9. Schematic of different microfluidic devices (G. T. Vladisavljević *et al.*, 2012).

Microfluidic flow focusing device, combines the flow of two phases in the same direction entering into a small orifice focussing hydrodynamically to produce droplets (Q. Xu & Nakajima, 2004). The inner phase flows through an orifice surrounded by the outer phase, the device developed by Anna *et al* 2003 demonstrates this concept Figure 2.3.10 a. Core shell particles, with double emulsions can be generated with these devices, however depending on the properties of the liquids three coaxial streams (Figure 2.3.10 b) (Nie *et al.*, 2005) or a consecutive flow focusing device can be used. Consecutive flow focussing device offer the alteration of wettability at the orifice surface (Seo *et al.*, 2007). As shown by Figure 2.3.10 d, the throughput of the product can be increased by running several channels in parallel and collecting in the same outlet (M. Hashimoto *et al.*, 2008).

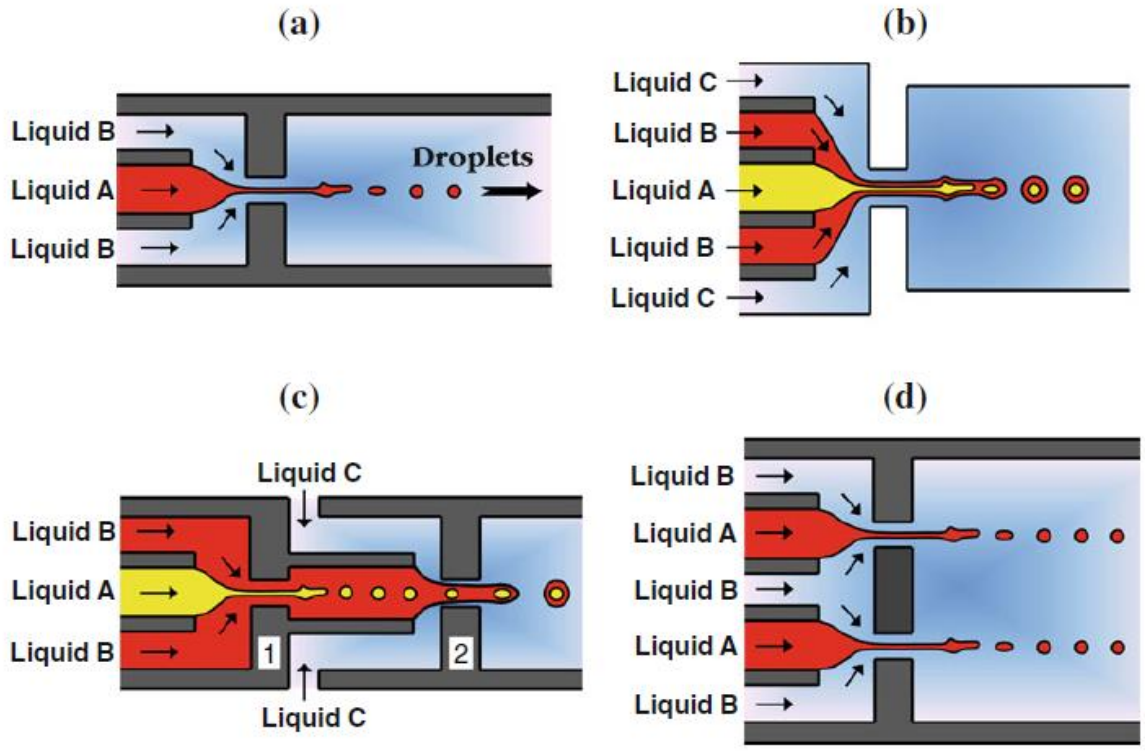

Figure 2.3.1017 Schematic of different microfluidic flow focussing devices (G. T. Vladisavljević *et al*., 2012).

Droplets are formed by the pressure and shear stress exerted on the dispersed phase to form a narrow jet which breaks near or downstream the orifice. As the inner and outer phase (liquid A and liquid B) it is seen that during focusing into the orifice the walls of the orifice are not wetted by the inner phase. Therefore, the wall is pre-treated either hydrophilic or hydrophobic to produce O/W or W/O emulsions, respectively. This step is important because if the inner phase wets the wall, then outer phase droplets will be formed and vice versa.

Microfluidic devices, whether they are junction or flow focusing, are usually devised by lithography and are commonly made of poly(dimethylsiloxane) (PDMS). Although other polymeric materials can also be used, PDMS provides good protection from contact between walls of the channels and the forming droplets. Also, the clear appearance of the PDMS device aids the visualisation during particle generation. It also helps prevent the problem of wetting by the dispersed phase and protecting droplets from shear and adhesion to the wall which can damage the droplet conformation. The shortfall of using PDMS devices however is that, the user is restricted from using organic solvents as the material is prone to swelling. In addition to that, the flexibility of the material means that the device is easily deformed with minimal pressure.

Glass capillary devices are also popular due to their tolerance to organic solvents and can be surface treated to make it hydrophilic or hydrophobic. Glass capillary devices are less prone to swelling and other changes due to chemical therefore are preferred over PDMS and other materials. The durability and surface treatment options for the use of organic solvents have made this a preferred choice.

Glass capillary devices are used in various geometric arrangements, from planar, T-junction, Y-junction, cross junction and 3 phase devices. In all arrangement the meeting of different streams of fluids form different channels at a specific region cause the formation of droplets that are collected in the converging channel (outlet). The idea behind droplet formation rests on regimes such as squeezing, dripping and jetting. In the squeezing regime, the dispersed phase occupies a large area of the capillary whilst being surrounded around the edge of the capillary by a thin continuous phase. As the continuous phase approaches the tip of the capillary the pressure exerted increases along the capillary forcing the continuous phase to squeeze and break at the neck of the capillary. As the break occurs the dispersed phase is surrounded by the continuous phase as a droplet rather than a continuous stream. In this regime the size of the droplet is dependent on the difference in flow rate of the two phases. It is not highly affected by the value of interfacial tension or viscosities of the two fluids (De Menech *et al*., 2008). The squeezing regime is commonly seen is T-junction and Y-junction.

In the dripping regime, the formation of a droplet is dependent on the interfacial tension that opposes the elongation at the neck and the drag force applied by the continuous phase on the emerging droplet Figure 2.3.11 b. The balance of these two forces determines the breakup and hence the size of the droplet. Here, the fluid flow rate is low, inertial and viscosity forces are dominated by interfacial tension.

The jetting regime on the other hand can occur in one of two ways; narrowing (Figure 2.3.11 c) or widening (Figure 2.3.11 d). In the narrowing jetting regime Figure 2.3.11 c, the high velocity of the continuous phase increases the velocity gradient at the interface and leads to high shearing. The velocity force exceeds the interfacial force. As a result of these forces a long narrow jet is produced which breaks up into droplets downstream. In the case of widening jetting the opposite occurs, the high velocity gradient at the interface is created by the high flow rate of the dispersed phase causing a long, wide jet which forms droplets downstream. The size of droplets formed in narrowing jetting are smaller than those formed by widening jetting.

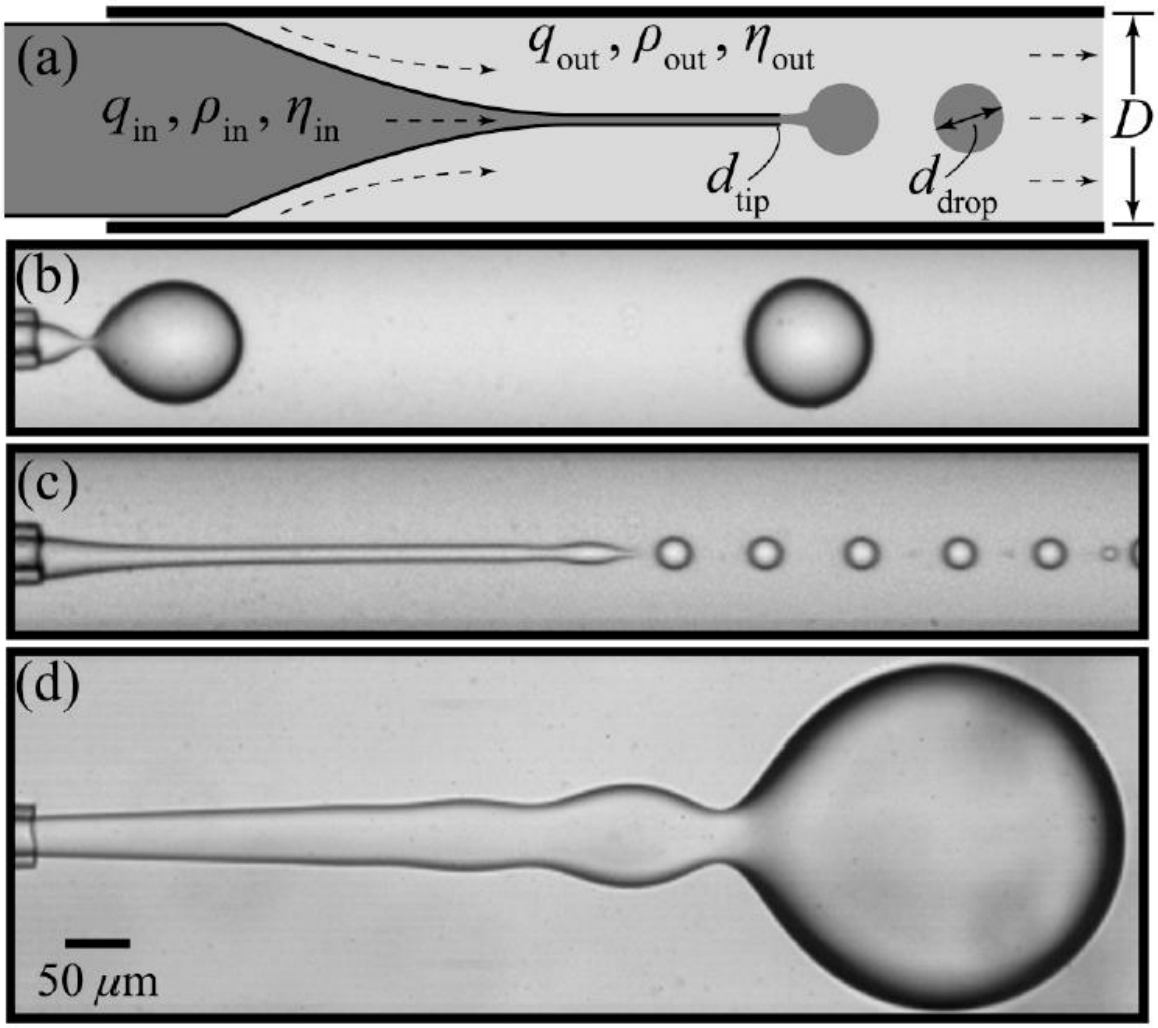

Figure 2.3.1118 Image of dripping and jetting regimes (Utada *et al*., 2007).

The capillary number (Ca) (a dimensionless quantity), can be used to predict the prevailing mechanism of droplet formation in a microfluidic device. It represents the relative effect of viscous forces against surface tension present at an interface between two immiscible liquids. For Ca_c <0.002 is within squeezing regime, 0.01 < Ca_c < 0.3 is within dripping regime (J. H. Xu *et al.*, 2008). As the capillary number further increased, the point at which the droplets breaks will move further downstream, shifting the regime from dripping to jetting. Low capillary numbers tend to result in formation of droplets closer to the junction (capillary tip) and high capillary number further downstream of the junction Figure 2.3.11. Capillary number is calculated by the equation below:

Equation 1

$$\mathrm{Ca} = \frac{\mu v}{\sigma}$$

Where, Ca is Capillary number, μ is dynamic viscosity (Pa.s), v is fluid flow rate (ms^{-1}), σ is surface or interfacial tension (Nm^{-1}).

The capillary number for a microfluidic device envisages the relative effect of different forces such as inertial, interfacial, viscosity and velocity. It enables users to predict and understand the nature of the flow and droplet formation in relation to these forces and be able to predict changes when one force is altered.

Another dimensionless number is Reynolds number (R_e), which shows the association between inertial and viscous forces in a microfluidic device. It is represented by the equation below:

Equation 2

$$\mathrm{Re} = \frac{\rho V L}{\mu} = \frac{V L}{v}$$

Where ρ (kgm^{-3}) is the density of the fluid, V (ms^2) is the characteristic flow rate, and L (m) is the characteristic length scale of flow, μ (Pas) is the dynamic viscosity of fluid and v (m^2s) is the kinematic viscosity.

At low Reynolds numbers, laminar flow occurs because viscous forces are dominant and is characterised by smooth fluid motion. High Reynolds number results in turbulent flow due to dominant inertial forces. In microfluidic devices the Reynold number must be low to achieve smooth linear flow. Reynolds number is further affected by Newtonian and non-Newtonian fluid dynamics.

Weber number is another dimensionless number which define the relationship between inertial forces and surface tension of two fluids in a microfluidic device. It is collaboration of the Capillary number and Reynolds number and is given by the equation below:

Equation 3

$$\mathrm{We} = \mathrm{ReCa} = \frac{\rho V^2 \mathrm{l}}{\sigma}$$

The Bond number identifies the importance of gravitational force in microfluidics in relation to interfacial tension and is given by the equation below:

Equation 4

$$\mathrm{Bo} = \frac{\Delta \mathrm{pgl}^2}{\sigma}$$

Where, Δp is density difference between fluids (kgm^{-3}), g is acceleration due to gravity (ms^{-2}), l is the length (m), σ is the interfacial tension between fluids (Nm^{-1}).

As demonstrated by the dimensionless number above, there are many contributors to the formation of droplets via a microfluidic device. Forces such as inertial, surface and interfacial tension, shear stress, viscosity, all play a part. However, there are other influential measures that also need to be addressed. Surfactants play a vital role in stability of an emulsion therefore should be considered when considering droplet sizes. Surfactants can also change the viscosity of fluids and consequentially influence flow rates. In addition to that, it is important to also address capillary treatment; wetting can result in increased variance in droplet size as well as the instability of the device.

Orifice size in microfluidic devices plays a key role in determining droplet size. As one would imagine with a large orifice size the volume of dispersed fluid passing through will increase hence result in larger droplets and vice versa. However, it is a combination of all these forces and geometrical arrangements that produce a given droplet size. Microfluidic devices therefore, are highly meticulous down to one drop at a time. This fine-tuning offers users the control over all aspects involved in final product generation such as particles. By changing one aspect it is possible to view the change in droplet generation in real-time.

Core shell particles can also be generated using microfluidic devices. Three dimensional axisymmetric microfluidic devices enable this and produce multiple emulsion droplets. Co-flow, counter-current flow, three phase glass capillary devices are all types of microfluidic devices which can produce droplets with multiple phases with specific properties. In Co-flow devices the two phases flow the same direction and form droplets on encountering a tapered capillary. Counter-current flow devices introduce the phases in opposite direction towards a tapered capillary forming droplets. A three-phase glass capillary device forms droplet from three phases which has a geometric combination of co-flow and counter-current device mechanism.

It is imperative to highlight the importance of microfluidics in influencing the rapid growth of lab-on-chip technology in industry. It is highly desirable in the healthcare sector as well as many others to reduce time, cost and improve sensitivity and sustainability. Keeping this in mind microfluidics offers

the ideal platform to replace or improve current methods for point of care testing. Rapid diagnostics, screening microbial libraries, viability studies are all examples of bioassay miniaturisation using microfluidics. A full review is discussed by (Ríos & Zougagh, 2015).

2.3.5 Electrospinning

2.3.5.1 Mechanism

Stemming originally from electrospraying where droplets are formed, electrospinning produces fibres. Electrospinning is a process which utilises high voltage to charge a polymer solution that is extruded through a metal needle or capillary towards an oppositely charged collector. During extrusion in the presence of charge, instead of formation of a round droplet, a cone is formed otherwise known as the Taylor cone. This is due to the attraction between the oppositely charge solution and collector but also the electrostatic repulsions between like charges of the polymer solution. Once the electric field surpasses the surface tension of the polymer solution a fibre jet in ejected from the nozzle. As the jet travels through air to the collector, solvent evaporates depositing solid polymer fibres on the collector. The onset of bending instability during acceleration of the fibre from the ejector to the collector increases the path length and time which aids fibre thinning and solvent evaporation (Yarin *et al.,* 2001).

Fibres can range from nanometres to micrometres depending on several experimental parameters. The collector can vary in geometry depending on the required state of fibres, these vary between immobile plate, rotating mandrel or aqueous solution. A schematic of electrospinning setup is shown in figure 2.3.12 with a stationary flat collector plate.

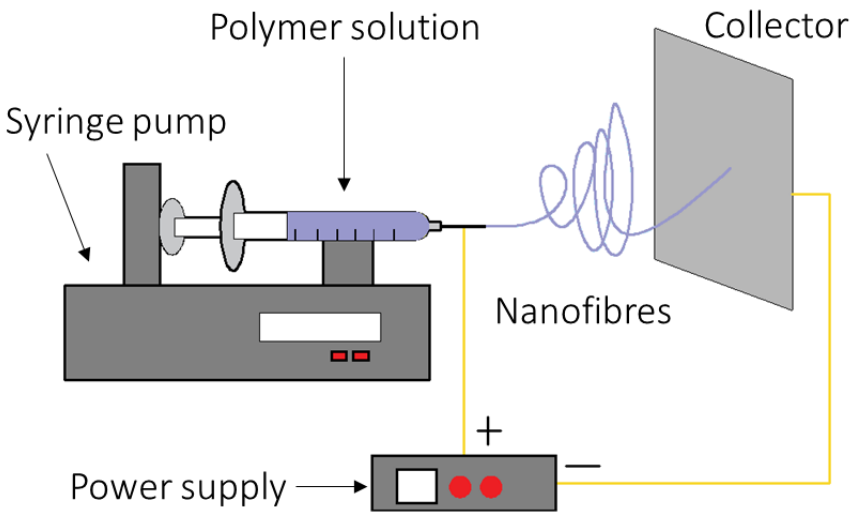

Figure 2.3.12 Schematic of electrospinning setup with a stationary collector plate.

2.3.5.2 Processing parameter

Formation of continuous defect free fibres is dependent on several factors which influence the overall size and morphology. It is therefore imperative to investigate the optimal conditions for each system to obtain the desired results. Parameters that impact the formation and structure of fibres include, voltage, flow rate of solution and the spinneret to collector distance.

The strength of the applied voltage can change the fibre diameter from nanometre to micrometres. At suboptimal levels, production of beaded fibres is usually observed or a failure to form a jet altogether. With increasing voltage Deitzel *et al.*, (2001) found that the shape from which the Taylor cone formed changed from the tip of a drop to the tip of the spinneret (Figure 2.3.13) in a polyethyene oxide (PEO) and water system. At very high voltages the taylor cone is ejected from inside capillary which often results in beaded fibres (Figure 2.3.13). A separate study by Meechaisue *et al.*, (2006) demonstrated fibres produced below the applied voltage of 20kV produced mostly beaded fibres as opposed to fibres produced above 20 kV which showed smooth fibres. Additionally, they also observed an increase in fibre diameter upon increasing the applied voltage from 2.5 µm at 10 kV to 5.4 µm at 25 kV. From these studies one can conclude that for every polymer and solvent system there lies an optimal electric field to produce defect free fibres.

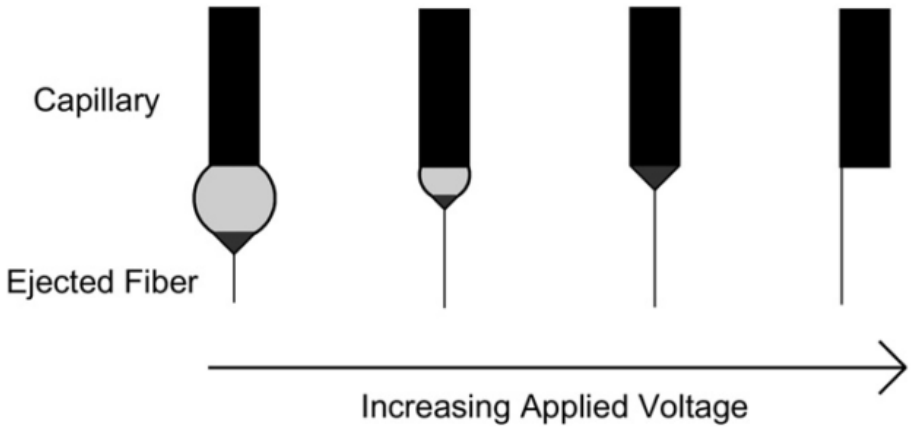

Figure 2.3.13 Influence of applied voltage on the creation of the Taylor cone. Source (Sill & von Recum, 2008)

Flow rate of the polymer solution in the syringe influences the diameter of the fibre as well as its porosity and shape. Lower flow rates fail to promptly replace the fluid at the tip of the spinneret as the polymer solution transitions into a fibre jet producing discontinuous fibres (Taylor, 1969). On the other hand, high flow rates can result in the formation bigger fibres with increased pore sizes. It can also show increased beading and flattened ribbon like structure of the fibres due to shortened time for solvent evaporation to take place (Megelski, 2002).

The distance between the spinneret tip to the collector can impact the diameter of the fibres. Increasing the distance results in thinner fibre diameter as opposed to shorter distances which produced thicker fibres. A study by Jaeger *et al.*, (1998) found that PEO fibre diameter decreased from 19 µm to 9 µm by changing spinneret to collector distance from 1 to 3.5 cm.

2.3.5.3 Solution properties

Although each polymer and solvent system will differ in their properties for producing smooth fibres, some aspects can be controlled to reach an optimised process. Solution properties that influence the production of smooth fibres include polymer concentration, solvent volatility and conductivity.

Polymer concentration determines whether fibre spinning, and therefore fibre formation, will occur or not. Both viscosity and surface tension of the solution are influenced by the polymer concentration. Within the optimal range, polymer concentration will be enough for chain entanglement. In dilute polymer solutions fibre does not form continuous threads due to effects of surface tension and instead breaks up into droplets before reaching the collector. At too high concentrations of polymer the

viscosity of the solution is increased, and the solution fails to electrospin altogether due to the lack of control on the flow rate. However, once am optimal range has been established one may observe an increase in fibre diameter upon increasing the polymer concentration (Megelski, 2002).

In electrospinning to form fibres it is important that the solvent of choice is volatile for solvent evaporation to occur, leaving polymer fibres on the collector. If the solvent is too volatile or not enough it can affect fibre morphology by increasing pore density with volatility increases and vice versa. During solvent evaporation, a phase separation occurs in the transiting jet which may be induced by vapor induced (Megelski, 2002). Conductivity of the solvent influences the fibre diameter. Highly conductive solvents have a greater capacity to carry charge as opposed to low conducting solvents. Fibre jet produced from a high conductive solvent will be exposed to a greater tensile force during fibre formation than a solvent with low conductivity. Although a study by Hayati, Bailey and Tadros, (1987) showed that solutions with high conductivity were unstable under electric field resulting in bending instability and polydisperse fibre diameter. Low conductivity solvents can be mixed with high conductive solvents given that polymer solubility is not affected. To increase conductivity (C. Zhang & Yuan, 2005) added sodium chloride ions to PVA and water solution at concentrations 0.05 to 0.2 %. Conductivity of the solution increased from 1.53 to 10.5 mS/cm and the fibre diameter reduced on average from 214 nm to 159 nm respectively.

2.3.5.4 Types of electrospinning

Since the establishment of electrospinning a 100 years ago, several modifications to the design of the electrospinning process have been done. Depending on the type and configuration of the spinneret; mono with and without emulsion, parallel or coaxial different results are obtained. Simplest configuration of the spinneret is the mono spinneret where only one solution is ejected. This produces single or sometimes composite fibres if polymer(s) dissolve in the single solvent system. On the other hand, if two different polymers or solutions are to be used an emulsion may be used and electrospun in a single spinneret system. Alternatively, a parallel configuration may be employed to spin two immiscible polymer solutions in parallel (Figure 2.3.14). However, differences in solvent conductivity in each system may result in two Taylor cones being formed and in other cases the ratio of each polymer may vary (Gupta & Wilkes, 2003).

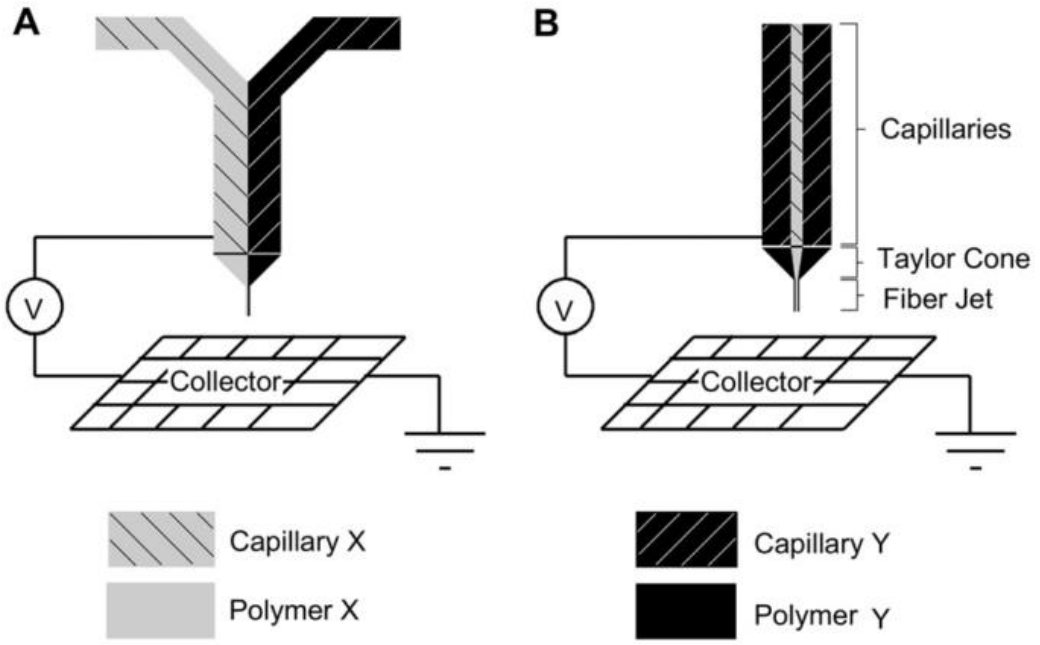

Figure 2.3.14 Schematic of spinneret configurations a) parallel b) coaxial. Source (Sill & von Recum, 2008)

Coaxial configuration is relatively new to electrospinning. Here two different polymer solutions flow simultaneously via separate capillaries with one smaller capillary inside a bigger capillary (Figure 2.3.14) . This configuration is popular for drug delivery application due to its ability to form fibre within a fibre otherwise termed core-shell. Biologicals prone to inactivation via electric charge or incompatible with solvents can now be encapsulated in fibres via this mechanism. For instance, fluorescein isothiocynate conjugated bovine serum albumin was encapsulated with poly (ethylene glycol) (PEG) in poly(Ɛ-caprolactone) (PCL) fibres using coaxial electrospinning. The resulting fibres showed prolonged release as opposed to burst release previously observed (Y. Z. Zhang *et al.*, 2006).

2.3.5.5 Applications

Tissue engineering has benefited from electrospinning application due to its ability to form scaffolds with desirable mechanical and biological properties. Several factors need to be considered carefully including material, application, orientation and porosity. Natural, synthetic or a combination of both materials can be used to achieve optimal fibre properties.

2.4 Polymers for drug delivery

Overview

Site specific delivery of drugs and other active agents is highly desirable yet challenging. A biocompatible carrier is required to overcome hurdles posed by the natural processes of the biological system. To be more specific, colon-targeted drug delivery is studied across the world to improve and find novel methods for site specific delivery. The harsh environment of the digestive system renders many drugs and active agents inactive when administered alone (Amidon *et al*., 2015; Choonara *et al*., 2014; Philip & Philip, 2010).

One of the key constraints for colon targeted drug delivery is the change in pH. Other factors are also contributors such as temperature, osmotic pressure, transition times, enzymes etc. It is important for a drug carrier system to withstand these changes and successfully deliver the drug to its site. It is also highly desirable for the drug carrier to release the drug in a time specific manner when encountering the appropriate trigger (Ibekwe *et al*., 2008).

Table 2.4.2. pH and transition times through the GI tract (McConnel *et al*., 2008).

	Stomach	**Small intestine**	Jejunum	Ileum	**Large intestine**	Proximal colon	Distal colon
pH	**1.0-3.0**	**5.5-7.4**	**6.0-7.4**	**5.7**	**6.8-7.2**	**6.8**	**7.2**
Time (hours)	**1 to 2**	**3 to 4**			**6-72 hours**		

The pH of the stomach can range from pH 1.2 to pH 3 depending on the fed or fasted state. The low acidic pH renders many biological agents inactive including bacteriophages. It is expected during fed state the transition from the stomach to the small intestine takes up to 2 hours (Vandamme, Lenourry, Charrueau, & Chaumeil, 2002). Pepsin and Lipases also contribute to cleaving biologically active compounds in the stomach. Small intestinal pH ranges from pH 5.4 to pH 7.5 with a longer transition time. Here many digestive enzymes (i.e. maltase, lactase and enterokinase) further degrade endogenous substrates (Jose *et al.*, 2009). Further along the gastrointestinal tract (GI tract) at the cecum, increase in mucus layer is observed with high absorption capability. This would prevent any active agents targeted for the colon being delivered. On approach to the large intestine (colon) the pH increases ranging between pH 5.6 to pH 7.7. As well as the change in pH, enteric bacteria, residual food and gases (Carbon dioxide and methane) are found which can all influence the delivery and

release of an active agent (Amidon *et al*., 2015). Therefore, for colon targeted delivery a robust polymer which can withstand the changes of the upper GI tract and show controlled release in the colon would be ideal.

2.4.1 Gut physiology during disease

The pathophysiology of the GI-tract is subject to further change due to the action of the infecting bacterial species. The intestinal barrier provided by the mucosal surfaces is disabled by distortions and ulcers. Mucus production is increased, and infiltration of inflammatory cells trigger an inflammatory response which initiates the onset of infection associated symptoms.

2.4.1.1 Transit time and microflora

A common change associated with GI diseases is the dysbiosis of the microbiome in the colon. During infection the reason for this is usually associated with administration of antibiotics which wipes out commensal species. The transit time during diseased state is also faster due to the onset of diarrhoea which increases the expulsion of fluid from the body. Further to this, the decreased osmotic gradient between the colon and the epithelia means increased leakage of fluid with minimal reabsorption which decreases viscosity and dilutes the action of enzymes present (Van Citters & Lin, 2006). This directly affects the transit time which can alter the way conventional dosage forms are delivered to the colon.

2.4.1.2 pH and volume

Owing to the nature of the infection (colon related), fluctuation in the stomach and small intestine pH has been little investigated. The pH of the colon however, is observed to be significantly lower than in healthy adults. Under normal conditions the pH of the colon between the proximal and distal colon is 6.8 and 7.2 respectively. However, in diseased state the pH drops below 5.5 (Hua *et al*., 2015; McConnell *et al*., 2008). The change in pH affects the microbial population in the colon which can directly affect the transit time, preventing encapsulation formulations from releasing the drug.

2.4.1.3 Mucosal integrity

The purpose of the epithelial barrier in the colon is to control movement of molecules in and out of the lumen to the underlying tissues. This regulation is aided by transmembrane protein complexes

referred to as tight junctions (TJ). The transport of cytokines, ions and glucose etc. is due to multi-protein complexes which act downstream to selectively move substances in an out depending on appropriate stimuli. The epithelial layer is surrounded by a tightly attached mucus layer, which lacks the presence of bacteria. This firmly attached mucus layer is surrounded by another mucus layer which is attached less compactly and is colonised by bacteria. The main mucin (glycoproteins) that comprises the mucus in the intestine is MUC2. MUC2 protects the epithelial barrier from bacterial interaction and is continuously shed to reduce host-bacterial interactions. If the bacteria are successful in penetrating the outer mucus layer, they will be able to interact with MUC1 which is attached to the epithelial cells via a transmembrane domain. The mucus layer not only acts as a barrier but also provides food sources for commensal bacteria to maintain their niches. There are many sugars such as oligosaccharides, galactose and fucose which are attached to the mucin glycoproteins available for bacteria. It is found that in CDI patients produced higher amounts of galactose which is known receptor for toxin A in animal models ((Voth & Ballard, 2005).

Although these properties make good pharmacological targets, they become dysfunctional during the diseased state. Bacterial toxins enter the cytosol via receptor mediated endocytosis; the endosome used for transport is acidic. Upon reaching the cytosol these toxins exhibit their enzymatic actions by glycosylating the Rho resulting in actin condensation, membrane blebbing and eventually apoptosis of cells (Voth & Ballard, 2005). Toxin receptors for some bacteria in humans have not been identified therefore better understanding of pathogenesis is required for therapeutic development.

A study by Engevik et al. (2014) showed the production of acidic mucin is largely composed of MUC1. The decreased production of MUC2 indicated a disabled barrier system for preventing bacteria crossing the epithelial barrier. The 'leaky' mucosal gel layer alters the viscosity which affects the permeability of mucoadhesive drug formulations (Keely *et al*., 2009).

2.4.2 Drug Delivery

Polymers can be natural or synthetic and have been exploited as drug carriers due to their biocompatibility. Polymers offer diversity in topology, chemistry, biodegradability, flexibility and resilience. Polymers also show controlled and sustained release at a specific site as they have proven to overcome being metabolised by pancreatic enzymes. Such polymers are used to carry drugs for the treatment of ulcerative colitis, Crohn's disease, colorectal cancer inflammatory bowel disease and many more (Dubey *et al.*, 2010; Souza *et al.*, 2013).

There are many advantages of colon drug delivery systems (CDDS). The colon has a long transit time and is the optimal absorption site for proteins and other molecules. It offers prolonged drug absorption and release which can be desirable for treatment of diseases that show symptoms during specific times. Alternatively, abrupt release can also be triggered with certain polymer formulations. Also, CDDS reduces toxicity, incidence of adverse effects and lowers the conventional dosage required (Choonara *et al*., 2014).

There are many drug carrier systems for site specific drug delivery such as poly(lactic)acid, chitosan, PEG, sodium alginate, dendrimers and Eudragit series. All these polymers respond to different stimuli at the target site. Types of stimuli from the environment can vary from temperature, ionic strength, pH, osmotic pressure and glucose levels. Therefore, it is important to consider the site delivery and purpose of the encapsulated drug when deciding which polymer to use. Release mechanisms play a vital role in delivering drugs and should be evaluated for changes in diseased states (McConnell *et al*., 2008).

Properties of the polymer including hydrophilicity, lubricity and surface energy direct the biocompatibility of the polymer with blood and tissue. These properties help decide the suitability of a polymer for a site-specific delivery. Permeability, degradability and durability also influence the physical properties. Hydrogels which undergo hydrolytic degradation and swelling are influenced greatly by their surface properties (Angelova & Hunkeler, 1999). It is now also possible to graft active agents (enzymes, proteins, antibodies) to the surface of the polymer for targeting of specific organs and cells (Pillay *et al.*, 2013).

The number of bacteria in the upper GI tract is approximately 10^3-10^4 CFU/ ml, largely composed of Gram positive facultative anaerobic bacteria. In the colon however, this increases significantly to 10^{11}-10^{12} CFU/ml (Sekirov *et al.*, 2010) and is largely composed of anaerobes such as *Bacteriodes, Bifidobacteria, Eubacteria, Clostridia, Enterococci* and *Enterobacteria*. To survive this, bacteria utilise undigested substrates from the small intestine. Carbohydrates like di- and tri-saccharides and polysaccharides are fermented by these organisms (Nicholson *et al*., 2012). Microbes produce enzymes such as β-glucoronidase, α-arabinosidase, β-xylosidase, β-galactosidase, nitroreductase and urea dehydroxylase. (Mountzouris *et al*., 2007). These enzymes metabolise polysaccharides which the body is unable to produce enzymes against.

Colon drug delivery strategies can also vary depending on the mechanism that is exploited such as pH, time dependent and biodegradability. Prodrugs use the strategy of cleavage of bonds between the drug and carrier by reduction or hydrolysis using enzymes present in the GI tract. pH dependent

systems utilise a combination of polymers to withstand the pH changes of the GI tract. However, due to certain pH overlaps between the small intestine and colon, site specificity can be affected. However, time dependent systems can survive through the transit times of each segment of the GI tract and only released upon reaching the colon. This approach can somewhat be unpredictable due to variation in transit times influenced by various inter/intra factors (McConnell *et al*., 2008). Microflora-activated systems depend on the microbial presence in the colon for the fermentation of polysaccharides present in the coat material of the encapsulated drug. Although this approach is positive, the enzymatic process can take several hours (approx. 12 hours) for complete degradation. Other strategies include osmotic systems and peristaltic pressure which is also subject to variation and instability, decreasing the site-specific response.

2.4.3 Natural polymers

Natural polysaccharides are widely used for drug encapsulation and colon targeted drug delivery. These polysaccharides are desirable due to their biodegradability, hydrophilicity, and limited swelling characteristics in acidic environment. The diverse population of microbes in the colon metabolise these polysaccharides by hydrolytic cleavage of the glycosidic bonds (Jose *et al*., 2009). They are inexpensive, low cost and available in a variety of structures and properties (Hovgaard and Brondsted *et al* 1996; Vandamme *et al.,* 2002). Examples of polysaccharides in drug delivery include; Pectin, Chitosan, Guar gum and dextrans.

Chitosan is a cationic aminopolysaccharide co-polymer of glucosamine and N-acetylglucosamine extracted by alkaline deacetylation of chitin (Garcia-Fuentes & Alonso, 2012) (Figure 9.2 appendix). Chitosan is soluble at low pH and therefore for effective use in colon targeted drug delivery it requires an enteric layer for protection against acidic environment. The enteric layer is stripped off in the intestine where the pH increases, releasing the chitosan coated core. Microbes in the colon act on the chitosan by degrading it and releasing the drug (Sinha & Kumria, 2001).

Chitosan microcores have been shown to encapsulate sodium diclofenac using the spray-drying method. These microcores were then further encapsulated within a methacrylate polymer Eudragit. Eudragit is the enteric layer which protects the chitosan from dissolving in the presence of low pH. Upon entering the intestine the enteric layer is stripped off which is also pH triggered causing the chitosan microcores to swell and subsequently release the drug upon entering the colon (Lorenzo-Lamosa *et* al., 1998).

Pectin is a non-starch, linear polysaccharide obtained from plant cell walls (Figure 9.3 appendix). It is effective in delivering both water soluble and insoluble drugs however due to its poor ability to form a film it is often used in combination with other polymers. Curcumin was encapsulated in pellets consisting of pectin and hydroxypropyl methycellulose (HPMC) showed effective protection against premature drug release and efficient release in the intestine (Kumar *et al*., 2009).

Guar gum is a polysaccharide composed of two sugars, galactose and mannose (Figure 9.4 appendix). It can be used for colon targeted drug delivery due to its release retarding property and susceptibility to microbial degradation. Fluoruracil (drug) was encapsulated in pellets consisting of guar gum and Eudragit. It was observed that the guar gum acted as a retardant and worked in a time-controlled manner. Eudragit also help protect the drug in the acidic environment. Due to microbial aided degradation of guar gum the drug was released in the proximal colon (Ji, Xu, & Wu, 2009).

Alginate is a linear polymer (Figure 9.5 appendix) which is commonly used for its ability to gel in the presence of calcium ions. This gelation results in the formation of calcium alginate beads which are capable of encapsulating drugs. Ma *et al*., (2008) and Ma *et al*., (2012) showed the encapsulation of phage Felix O1 against *Salmonella enterica* into chitosan and alginate microspheres. Upon exposure to simulated gastric fluid 2-log reduction was observed, but full release was obtained in intestinal fluid. Similarly, there are other polysaccharides namely, amylose, lectins, inulin, dendrimers and pullulan which all have been exploited for their ability to encapsulate drugs for colon targeted delivery and can be applied for phage encapsulation.

The mechanism in all polysaccharide-based polymers is the same in that they are degraded by the diverse population of microbe produces enzymes which target different chemical bonds. However, this process is constrained by the changing environment of the GI tract which can dissolve, swell or essentially inactive the polysaccharide ability to protect the drug. Therefore, as seen in many cases they are almost always used in combination with synthetic polymers such as the Eudragit series which is pH responsive.

2.4.4 Eudragit S100

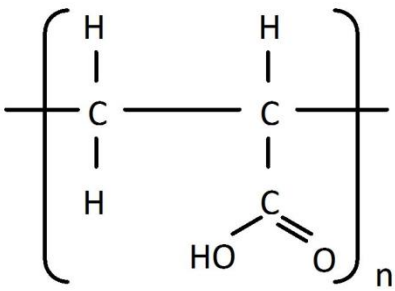

Figure 2.4.1 Monomer of Eudragit S100

Eudragits are a family of polymethacrylate polymers (Figure 2.4.1); Eudragit S100 (ES100) and L100 are the most commonly used pH-dependent methcrylic acid copolymers. Dew et al. (1984) developed the first pH-responsive colon targeted delivery system. Eudragit L100 dissolves at pH 6 and Eudragit S100 at pH 7. Therefore, it is commonly found that anionic ES100 is used in combination with other polysaccharide polymers for colon targeted drug delivery due to its ability to bypass acidic environment (low pH) of the upper GI tract. These polymers are commercially available (Evonik, Darmstadt, Rohm Pharma Germany) and are widely used in the preparation of microspheres.

The ES100 mechanism of action is largely based around the COOH group of its chemical structure. In its raw powder form, the polymer is anionic and remains that way unless a hydroxyl group is present for its neutralisation and subsequent dissolution. The common solvents used are ethanol, isopropanol, methanol, DCM etc. It does not dissolve in water; however, in the presence of hydroxyl ions in the water it has the capability to dissolve. The phenomenon is the essence of its pH triggering response. When the pH increases the hydroxyl ion concentration increases therefore, prompting the dissolution of the polymer. The mechanism of action is demonstrated in Figure 2.4.2.

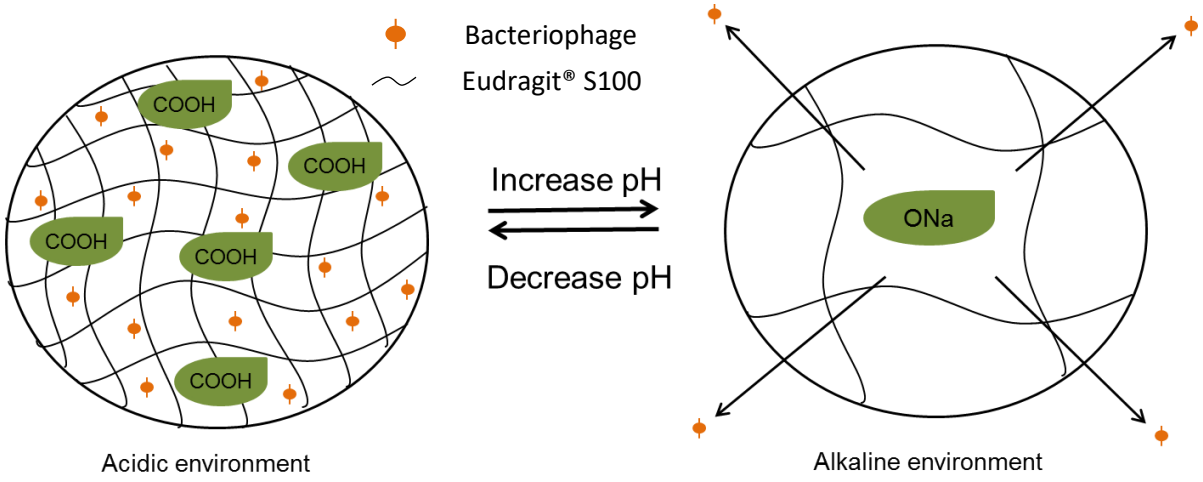

Figure 2.4.2 Schematic to show the mechanism of pH responsive polymer.

Eudragit have been successfully used for the production of microspheres encapsulating drugs for colon delivery (Chawla *et al.*, 2012; de Arce Velasquez *et al.*, 2014; Jain *et al.*, 2005; Kietzmann *et al.*, 2010; C. M. Silva *et al.*, 2006). As ES100 has a response to the highest pH (pH 7) it is ideal for colon targeted

delivery. By combining this copolymer with other biodegradable polymers (mentioned above), it makes a promising delivery system of phages to the colon. Bacterial infection of cattle can be detrimental; phages are an alternative to antibiotic treatment. (Stanford *et al*. 2010) has shown the use of ES100 for *Escherichia coli* specific phage encapsulation for cattle treatment. Here, they show the high sensitivity of the phage to the acid in the gastric environment. However, encapsulated phage showed higher viability and the aptitude to reduce bacterial population at the site of infection. The potential of ES100 in encapsulation can also be observed in the patent CA 2463827 C (Waddell *et al.* 2013).

Other, synthetic polymers are also available that have been FDA approved for food additive, pharmaceutical ingredients and as drug system carriers. Examples of this include Pluronics® and Tetronics®, they present a sol-gel transition at varying temperatures. The drug release is temperature and diffusion triggered (Escobar-Chavez, 2006). However, the application of such system is not suitable for colon targeted drug delivery. Poly(ethylene glycol) (PEG), poly(ethylene oxide) (PEO), poly(acrylic acid), poly(vinyl pyrrolidone) (PVP) and Boronate-containing polymers are all synthetic polymers. Semi-synthetic polymers which are derivates of cellulose are also used.

2.4.5 Combination of polymers for colon targeted drug delivery

2.4.5.1 Eudragit and chitosan

Polysaccharides are an effective way to encapsulate bioactive agents but on their own they are weak delivery systems. In most cases, enteric coating is required to protect the polysaccharides from the gastric environment. Chitosan for example, is a cationic, hydrophilic, crystalline polymer with the ability to undergo gelation but in the presence of acid it dissolves. Therefore, to keep chitosan intact during transition through the GI-tract until it reaches the colon where it undergoes hydrolysis of its glycosidic bonds, an enteric coating with synthetic polymer such as Eudragit is usually applied (Lorenzo-Lamosa *et al*., 1998).

Chitosan is an approved food ingredient; therefore it is an acceptable excipient for oral administration. It possesses a mucoadhesive character and is cleavable by lysozyme, produce by intestinal bacteria in the mucosa. Although efforts have been made to crosslink this polysaccharide using aldehydes, the toxicity remains a concern. Therefore, by applying an enteric coating it is possible to target drug delivery in the colon. Chitosan microspheres containing the drug are usually produced by one of the

encapsulation techniques, which is followed by the addition of the enteric coating by solvent evaporation. This ensures encapsulation efficiency and stability of the two polymers.

Delivery of mesalamine (drug) in Eudragit S100 coated chitosan microspheres for the treatment of ulcerative colitis was demonstrated by Badhana *et al.,* (2013). The mechanism behind its delivery relies on the ability of the enteric coating to protect the encapsulated drug during transition from the stomach and small intestine. Upon reaching the colon where the pH increases, the enteric layer strips off exposing the chitosan to the local mucosal environment to be natural degraded by lysozymes. At colonic pH (pH > 7.2) the chitosan sphere swells but do not dissolve. This prompts the release of the drug into the local environment where the site-specific action commences.

A similar study by Lorenzo-Lamosa *et al*., (1999) showed the encapsulation of sodium diclofenac (anti-inflammatory drug) is chitosan cores, coated with either Eudragit S100 or L100. Release profiles show faster release with enteric coating Eudragit L100 due to its response to lower pH in comparison to Eudragit S100 (pH 7). The swelling of chitosan cores was observed with water diffusion resulting in drug dissolution and release. Protection against gastric pH was seen with a total release time between 8 to 12 hours. The chemical properties of the polysaccharide and the enteric coating are compatible, in that infrared analysis showed ionic crosslinking between the amine groups of the chitosan with the carboxyl groups of Eudragit.

2.4.5.2 Eudragit and PLGA

Eudragit® has been used to coat poly(lactide-co-glycolide) (PLGA) particles (Figure 9.6 appendix). For similar reasons to chitosan microspheres, PLGA particles require protection from gastric pH due to its susceptibility to dissolution. Enteric coating provides this protection until colon pH is reached where the dissolution of the enteric coating triggers swelling of the PLGA core encapsulating the drug. PLGA chains undergo cleavage into smaller low molecular weight fragments upon hydration. These undergo further erosion and degradation releasing the drug in the colon site (Y. Wang *et al*., 2013).

In vivo models analysing the efficacy of PLGA and Eudragit nanoparticles in a trinitrobenzenesulfonic acid (TNBS) colitis rat model was investigated by Makhlof et al., (2009). The investigation highlighted the bioavailability of budesonide (anti-inflammatory drug) in the proximal region of the colon with specific adhesion of the nanoparticles to the inflamed mucosal tissue. It is found that smaller particle sizes demonstrate better attachment to the mucus layer and penetrate through the disrupted, ulcerated mucosal barrier site during inflammatory colitis (J. Stein *et al*., 1998; A. Lamprecht *et al*.,

2005). Inflammatory cells such as macrophages engulf these nanoparticles which further contribute to their accumulation at the site of inflammation (H. Nakase *et al*., 2001).

2.4.5.3 Eudragit and sodium alginate

Alginate is another polysaccharide regarded safe by the FDA and is widely used in the food industry as an emulsifier and stabiliser. It is an anionic polymer with carboxyl end groups giving it mucoadhesive properties which are reported to be higher than any other polysaccharide polymer such as chitosan. This property means the drug bioavailability due to localisation at absorptive surfaces is increased. In response to low pH alginate does not release the encapsulated drug but shows shrinkage with porous morphology. As the pH is increase sodium alginate converts into a soluble viscous layer, giving it a pH responsive property. However, it is noted that pH changes result in burst release which can easily denature the bioactive agent encapsulated. Mechanism of release is dependent on the porous network through which the bioactive agent can diffuse out or due to the polymeric degradation. The pore size of sodium alginate is between 5 nm to 200 nm.

Thus, to protect alginate microspheres during passage through the GI tract enteric coating can be applied to protect shrinkage in low gastric pH. Crosslinking sodium alginate with calcium chloride whilst encapsulating the drug is a common procedure. This can be followed by Eudragit coating for protection. Naproxen (anti-inflammatory drug) was encapsulated in sodium alginate and Eudragit S100 for colon targeted delivery (Chawla *et al*., 2012). Sodium alginate has demonstrated to be biocompatible with phages. Encapsulation of phages has been demonstrated with this polysaccharide with positive results showing site specific delivery (Cecilia Dini *et al*., 2012; Yongsheng Ma *et al*., 2008, 2012).

Dextran is another polysaccharide prone to ester cleavage by dextranase produced by microflora in the colon. It is hydrophilic with a reactive hydroxyl group which can react with other carboxyl groups on co-polymer or drugs.

2.4.6 Commercially available technologies

There are various systems that are widely used to further coat microspheres into pellets. Coat technologies for colon targeted drug delivery such as CODES^{TM} are used for this application. CODES^{TM} technology is comprised of a three-layer system; the core containing the drug is surrounded by the inner acid soluble layer (Eudragit E), the middle layer is made of HPMC which acts as barrier, and the outer enteric layer. The core is comprised of a polysaccharide which is hydrolysed by enzymes

produced by bacteria in the colon. The enteric coating protects the drug from the stomach acid but dissolves in the small intestine along with HPMC where the pH is 6 or above. Eudragit E (inner layer) dissolves at pH less than pH 5, it is only slight permeable and swellable in the small intestine. On arrival in the colon the polysaccharide core diffuses and dissolves through the inner coating to be broken down into organic acid by enzymes. Because of this the microenvironment pH is reduced causing the dissolution of Eudragit E and release of the encapsulated drug. The purpose of this technology is to reduce the variability associated with pH and time during drug delivery.

Another tableting technology called COLAL™ employs a simpler method with a two-layer coating. The inner coating is made of a polysaccharide which is prone to degradation by colonic bacteria and the outer layer is the enteric coating to protect degradation during passage through acid pH in the stomach and small intestine. The enteric coating dissolves at pH above 7 in the colon exposing the polysaccharide layer. Enzymatic action of the bacteria in the colon degrades this slowly releasing the drug. Ethylcellulose and amylose blend as the polysaccharide inner coating was researched by Wilson and Basit (2005) for mesalazine (anti-inflammatory drug for ulcerative colitis) release. It was found that the system was susceptible to colonic bacterial induced degradation. The formulation is now available as COLAL®, which is used to coat tablets containing corticosteroid prednisolone sodium metasulphobenzoate (COLALPRED®; Alizyme Therapeutics Ltd, Cambridge UK). It is currently in phase III clinical trial for the treatment of ulcerative colitis. To delay release until reaching the colon Eudragit® coating dispersion has been used (Thompson *et al*., 2001; Basit & Ibekwe 2007).

The third technology known as the multimatrix system (MMX™) utilising a combination of pH triggered and diffuse based method. This technology is designed to release the drug in the colon. The drug is dispersed in a lipophilic matrix which is surrounded by a hydrophilic matrix. The third outer layer is comprised of a pH-dependent coat which prevents release in stomach acid. As the enteric coating is removed in the colon, fluid is absorbed into the remaining layers causing swelling and eventually formation of a gel. Bacterial fermentation breaks of the gel in fragments allowing the drug to diffuse out into the colon (Sandborn *et al*., 2007).

Single coat tabletting technology, PHLORAL™ combines pH responsive polymer Eudragit S100 with polysaccharide (resistant starch). Eudragit S100 prevents drug release and swelling of starch in the stomach and small intestine. The 'resistant' starch is capable of resisting degradation by amylase produced by the pancreas but is susceptible to colonic enzymes. In the colon at the ileocaecal junction due to increase pH Eudragit S100 dissolves, exposing the starch to both enzymatic and pH triggered degradation (Ibekwe *et al*., 2008).

2.4.7 Chemical modification of polymers

2.4.7.1 Aliphatic polyesters

Synthetic polymers are widely used in industry for various applications from plastics, grafts, drug delivery and many more. Biopolymers with reactive groups offer the advantage of manipulating its chemical structure to suit the purpose it is used for. Biopolymers are used to protect drugs to enable them to reach the site of infection intact. Aliphatic biopolymers such as poly(lactic acid) (PLA), poly(glycolic acid) (PGA), poly(ε-caprolactone) (PCL) and their copolymers are synthetically produced using one naturally occurring substrate for example lactic acid produced by bacteria in PLA. These polymers are biodegradable, biocompatible and bio-absorbable making them good candidates to be studied for biomedical applications. Modification of their reactive groups alters their end use, some of the features include, hydrophilicity, rate of biodegradation, bioadhesion, targeting moiety attachment. These features are activated by adding chemical groups like carboxyl, hydroxyl, amino, ketal, bromo, chloro, carbon-carbon double to triple bonds to the polymer. To allow for the addition of these reactive groups either homopolymerization or copolymerisation process can be applied. The most common application of aliphatic polyesters is in clinical devices.

2.4.7.2 Polycarbonate and Poly (amino acids)

Polycarbonate is also a biopolymer with side chains (OH, NH_2, COOH) that can be tuned to meet the requirements of biomaterials. They have good biodegradability, low toxicity and biocompatibility. Peptides and drug molecules can be attached to free functional side chains of the polymer for specific drug delivery and tissue engineering. Drug attachment through esterification of 4-isobutylmethylphenylacetic acid (non-steriodal anti-inflammatory drug (NSAID)) to the copolymer was studied by Grinstaff *et al*., (2003). Poly (acidic amino acids) such as poly(L-glutamic acid) (PLG) is produced by linking amide bonds from naturally occurring L-glutamic acid and active carboxyl bonds. This too can be modified by changing functional side chains by esterification, polymerisation, condensation or aminolysis.

- Biopolymers with responsive activities

Biopolymers that are responsive to specific stimuli have gained increased attention. Transition to their physical-chemical properties (conformation, polarity, phase structure and chemical composition) enables them to respond to small changes in the environment. Modifying synthetic biopolymers for smart function is vital in targeting constraints faced in biomedical research. At present they are being used in biomedical applications for drug delivery, tissue engineering and biosensor design.

2.4.7.3 pH responsive

pH in the body can vary from acidic to alkaline which can be challenging when targeting a drug to a specific site. Biopolymers responsive to pH exhibit this function through the addition ionisable groups which respond to changing pH. The polypeptides usually acidic or basic depending on the amino acid attached. Poly(histidine) for example gets protonated at the imidazole groups at pH 5 to 6.5. Hydrophobic groups can be incorporated into their structure to alter their pK_a.

2.4.7.4 Prodrugs

Polymers with modifiable reactive groups, biodegradability and responsive characteristics have been studied for drug delivery. Drugs can conjugate to carboxyl groups on polymers like poly(α-malic acid) to form prodrugs (biodegradable macromolecules) to decrease the side effects encountered during free drug administration. As the polymer degrades in response to a stimulus (i.e. pH) the attached drug is also released. Prednisone acetate showed burst release at pH 7.4 in vitro as the polymeric micelle composed of poly(acrylic acid-b-DL-lactide) dissolved at this pH (Huang et al., 2009). Kim et al., (2009 and 2012) reported metronidazole prodrugs in two forms; (N-nicotinoyl-2-{2-(2-methyl-5-nitroimidazol-1-yl)ethyloxy}-D,L-glycine (NMG)) and sulfate conjugated metronidazole. In both cases the prodrug was metabolised by nitoreductase present in the cecal contents of rats. Similarly, metronidazole-pectin prodrug was researched by Vaidya *et al.*, (2012), results showed no release in acidic pH but subsequent release was observed at alkaline pH.

Other prodrug designs include incorporation of the active agent to the carrier polymer which is susceptible to colonic enzymatic action. Here, azo-link is established by conjugating the drug for example 5-aminosalicylic acid (Mesalamine) (drug for ulcerative colitis) to the carrier example, sulfapyridine to form azo-linked prodrug, sulfasalazine (Azulfidine®). In the colon sulfasalazine is metabolised by reductase into 5-ASA and sulfapyridine. In the same way, addition of β-D-galactose to the active agent (5-ASA dexamethasone) via a glycoside bond will enable release of the drug by hydrolyses by glycosidases in the colon (Lautenschlager *et al.*, 2014). Hydrogels formed by

crosslinking for example dextran to diisocyanate, show the ability to withstand conditions in the upper GI-tract with minimal swelling. In the colon however, the hydrogel swells to its maximum capacity exposing the crosslinks to enzymatic action, in this case by dextranase (Hovgaard and Brondsted 1994).

2.4.7.5 Modifying size, charge and surface ligands

Colonic drug delivery has significantly improved over the years with increased bioavailability and site specificity. However, challenges arise when infection of the colon results in physiology changes rendering conventional formulations ineffective. In diseased state they have poor specificity for the site of infection and reduced efficacy in comparison to healthy conditions (Hebden *et al*., 2000). Nanoparticle associated delivery systems are designed to target the site of infection through passive transport. The size of nanoparticles (nanometers) increases their efficacy and bioavailability at the target site with no adverse effects to the surrounding environment.

2.4.7.6 Size, charge and PEGylation dependence

Studies have found that by reducing the size of particles to nanoscale enhances their ability to reach deep routed site for targeted drug release. The residence time of nanoparticles is also higher compared to bigger particles, as bigger particles are more prone to peristaltic action and movement through the colon. Nanoparticles are able to present an epithelial enhance and retention (eEPR) effect enabling elective delivery of active molecules into the colitis tissue (Collnot *et al*., 2012; Xiao *et al*., 2012). Conventional formulations lack this ability due to their size, causing deposition in regional areas. Smaller particle sizes are able to take advantage of endocytosis for internalisation into the epithelial cells of the colon. They attach to specialised epithelial M cells which are responsible for antigen transport form the lumen to the immune system. These M cells are also responsible for uptake of nanoparticles by transcytosis (Pichai *et al*., 2012). Microparticles demonstrate adherence to inflamed mucosal wall whereas nanoparticles absorbed across the epithelial barrier (Schmidt *et al*., 2013).

The charge of the particles can also contribute to the deposition in the colon. Cationic delivery systems adhere to the negatively charged intestinal mucosa which promotes their cellular uptake and subsequent drug release (Coco *et al*., 2013). The mucins which comprise the mucosa are also known to be negatively charged. Anionic systems adhere to inflamed tissue via an electrostatic interaction, as the presence of positively charged proteins in the inflamed regions increases. Unlike cationic

particles which get immobilised on the mucus, anionic particles can interdiffuse through the mucus network due to decreased electrostatic interaction (Hua *et al*., 2015).

Incorporating poly(ethylene glycol) (PEG) on the surface of particles builds a hydrophilic surface chemistry that allows an unobstructed diffusion of nanoparticles through the epithelium. The reason for this is that the surface modification prevents strong interaction of nanoparticles to the mucus which can prevent diffusion to the colitis tissue (Cu *et al*., 2008).

2.4.7.7 pH dependence

As previously mentioned the difference in pH through the GI tract is exploited by many formulations for targeted drug delivery. The most common pH-dependent coating used in oral delivery is methacrylic acid copolymers (Eudragit). By varying the number of carboxylate side chains, the polymer can be induced to dissolve at different pH. These polymers are usually used in combination to allow drug release within a range for example Eudragit S100 and L100 for release at pH between 6 and 7. This polymer series also exhibits mucoadhesive properties (Asghar and Chandran 2006). A study found that Eudragit coated liposomes in simulated gastric and intestinal fluids was not able to withstand the presence of bile salts. The instability of the enteric coating in bile salt can greatly affect the stability of drug in vivo (Barea *et al*., 2012).

2.4.7.8 Biodegradable systems

There are some aspects which are consistent amongst patients with IBD which can be exploited to formulated biodegradable systems for drug delivery. Laroui et al produced nanoparticles (400nm) encapsulating anti-inflammatory drug, tripeptide Lys-Pro-Val using calcium and sulfate ion cross-linked chitosan and alginate. This hydrogel was prone to degradation by enzymes in the colon which subsequently released the drug. Similarly, poly(epsilon-caprolactone) (PCL) can be used to micro-coat, nanoparticles to protect degradation by acidic environment, adsorption by enzymes and proteins. The drug is released in the colon via the action of lipases which degrade PCL (Bhavsar and Amiji 2007). Hydrogels are susceptible to hydrolytic cleavage by colonic enzymes and can also be used for targeted biodegradable delivery systems (Han *et al.,* 2008).

2.4.7.9 Active targeting systems

Active targeting by surface imbedding ligands for selective drug accumulation at the site of inflammation can help reduce adverse effects and increase therapeutic efficiency. Monoclonal antibodies and peptides specific for target site are used to increase specificity and enhance mucopenetrative properties (Saltzman *et al*., 1994). It is thought that by incorporating ligands for receptors present at the site of infection will improve binding and intensify endocytosis. Possible receptors for target in the inflamed colon can include, ICAM-1 which is upregulated during inflammation, mannose receptors and macrophage galactose-type lectin (MGL) (expressed by activated macrophages). By combining the effect of small particle size, PEGylation and integration of mannose ligands an increased penetration ability of macrophage was observed (Xiao *et al*., 2012).

The combined effect of different enhancement to specific targeting may be the future for colon drug delivery. It is important to understand the changing physiology of the colon from healthy to diseased state and to consider patient to patient variations. The gut microflora can also vary greatly between healthy individuals therefore biodegradable coatings should be formulated to cover the variability between individuals.

2.4.8 Phage encapsulation for the treatment of enteric infections

2.4.8.1 Phage and probiotic (2 in 1) delivery potential

Probiotics (live microbial feed) are thought to be beneficial for host by improving and maintain the gut microbial population. Probiotics are approved by health authorities and require delivery to the colon for maximum effect. Encapsulation is seen to be the best way to avoid killing the live bacteria and deliver it to the colon (Albertini *et al*., 2010; Govender *et al*., 2015; Han *et al*., 2008). Probiotics may help in replenishing or repopulating the intestinal flora after an infection. Therefore, the most common bacterial species such as *Bifodobacterium* and *Lactobacillus* may be incorporated with the bacteriophage during treatment. The bacteriophage is self-replicating, if the host (bacteria) is present. During the process of treatment (with phages) to prevent further colonisation and improve recovery, incorporation of probiotics may be another approach to lower the number of sick days and subsequently cost associated with treatment, recovery and possible relapse.

2.4.8.2 Phage and phosphatase

In addition to that Alam *et al.,* (2014) studied the effects of brush border enzyme intestinal alkaline phosphatase (IAP) in restoring the gut flora after infection. Streptomycin and clindamycin induced

infection in mice resulted infection with *Salmonella Typhymurium* and *Clostridium difficile* respectively. Administration of calf IAP (cIAP) showed protection against infection from *S. Typhymurium* and *C. difficile*. IAP is produced by enterocytes in the proximal region of the small intestine and is secreted into the lumen. It functions to detoxify bacterial toxins, dephosphorylates ATP, regulates host microbial interaction, guts mucosal defence, maintains gut immunity and preserves intestinal microbiotal homeostasis (Alam *et al*., 2012). IAP is another possible candidate which could be incorporate alongside bacteriophages to speed up recovery and repopulate colonic microflora.

2.4.9 Mechanisms for testing encapsulation

Studying the effect of encapsulation *in vitro* has often involved using buffers with varying pH values. This is a straightforward way to demonstrate resistance of the formulation to gastric pH and intestinal pH with subsequent dissolution in slightly alkaline pH mimicking the colon. However, it can be argued that although it is a great test to test the key constraint encountered in the GI tract but it lacks the ability to examine other factors present in vivo that may influence dissolution. pH responsive polymers that resist gastric pH, can be tested via this method however it is found that the presence of bile salts (Barea *et al.*, 2010). Therefore, it is important to evaluate the influence of as many parameters seen in vivo, in vitro testing.

For a better understanding of the GI tract environmental influence on the encapsulation formula, there are USP standards that state the composition of a simulated gastric and intestinal environment. Simulated gastric and intestinal fluids consider the presence of bile salts, surfactants and enzymes in the upper GI tract in addition to the pH. Presence of pepsin in the stomach and protease in the small intestine is considered. Simulated fluids give a better understanding of the possible interactions between the delivery system and the upper GI-tract. Simulation of the colon is difficult due to its complex network of microflora. Nevertheless, studies have been undertaken to address this issue and develop better systems for understanding the physiology.

To better test the dissolution of a delivery system in the colon presence of the microflora under certain pH conditions is seen to be important especially when evaluating pH responsive and biodegradable polymers. Efforts have been made to mimic the microflora in the human gut, in an in vitro model. Hamster (animal) models have been extensively employed to study CDI. It is found that the microflora of these animals is closely related to the gut microbiota of humans. This however is controversial, as the microflora fingerprint is thought to be distinct for everyone. Ex-germ free mice have been

inoculated with human micro flora (HFA) in order to better mimic the human gut physiology (Sekirov et al., 2010).

Using human faecal emulsions from healthy and infected individuals it is possible to evaluate the effect of delivery systems in vitro without using invasive procedures (Best *et al.*, 2012). Macfarlane et al. (1998) investigated validity of a three-stage compound continuous culture system. Here, the colonic material obtained from 4 sudden death victims at autopsy was divided into three vessels (V) representing the proximal (V1) and the distal (V2 and 3) of the colon. The fermentation system mimicked the spatial, temporal, nutritional and physicochemical characteristics of the human colon. The retention time could be controlled, and pH of each vessel could be monitored. It was found that the pH of the digestive material in the cecum and the ascending bowel was acidic but increased towards neutrality in the distal gut. Carbohydrate breakdown largely occurred in V1 and aromatic amino acid fermentation was shown to be affected by retention time. Overall the correlation between in vivo chemical and bacteriological measurements to this vitro study was positive (Macfarlan *et al.,* 1997) suggesting that this three-stage fermentation system is a suitable model system to study dissolution of colon targeted delivery systems.

The next step after in vitro testing is to apply the encapsulated active agent in vivo, using animal models. Hamsters especially Syrian hamsters are commonly used to study factors associated with CDI. This is because they share recognised features isolated form human samples and contract infection after administration of antibiotics as seen in humans (Best *et al*. 2012). Better understanding of the human gut under normal and diseased conditions is necessary to improve analysis of delivery systems. In addition to that further research to understand the effect of virulence factors produced by pathogens and receptors involved in colonisation is required to formulate active delivery systems.

Chapter 3: Clostridium difficile specific bacteriophage encapsulation using microfluidic glass capillary devices for colon delivery

Abstract

The prevalence of pathogenic bacteria acquiring multidrug antibiotic resistance is a global health threat to mankind. This has motivated a renewed interest in developing alternatives to conventional antibiotics including bacteriophages (viruses) as therapeutic agents. The bacterium *Clostridium difficile* causes colon infection and is particularly difficult to treat with existing antibiotics; phage therapy may offer a viable alternative. The punitive environment within the gastrointestinal tract can inactivate orally delivered phages. *C. difficile* specific bacteriophage, *myovirus* CDKM9 was encapsulated in a pH responsive polymer (Eudragit S100 with and without alginate) using a flow focussing glass microcapillary device. Highly monodispersed core-shell microparticles containing phages trapped within the particle core were produced by *in situ* polymer curing using 4-aminobenzoic acid dissolved in the oil phase. The size of the generated microparticles could be precisely controlled in the range 80 μm to 160 μm through design of the microfluidic device geometry and by varying flow rates of the dispersed and continuous phase. In contrast to free 'naked' phages, those encapsulated within the microparticles could withstand a 3 h exposure to simulated gastric fluid at pH 2 and then underwent a subsequent pH triggered burst release at pH 7. The significance of our research is in demonstrating that *C. difficile* specific phage can be formulated and encapsulated in highly uniform pH responsive microparticles using a microfluidic system. The microparticles were shown to afford significant protection to the encapsulated phage upon prolonged exposure to an acid solution mimicking the human stomach environment. Phage encapsulation and subsequent release kinetics revealed that the microparticles prepared using Eudragit S100 formulations possess pH responsive characteristics with phage release triggered in an intestinal pH range suitable for therapeutic purposes. The results reported here provide proof-of-concept data supporting the suitability of our approach for colon-targeted delivery of phages for therapeutic purposes.

3.1 Introduction

C. difficile is the most common cause of infectious antibiotic-associated diarrhoea (Burke & Lamont, 2014) that occurs in the developed world (He *et al*., 2013). There is a significant cost associated with the treatment of *C. difficile* infection (CDI); a single CDI case in the UK costs ~£7,000 (Public Health England 2012) and the annual cost in Europe is ~€3 billion. In the USA, treatment for a single case

costs ~$12,800 with the annual additional cost to healthcare providers reaching ~$800 million (Bouza, 2012; He *et al.*, 2013).

The clinical outcomes of CDI range from asymptomatic colonisation to mild diarrhoea and in severe cases, inflammatory lesions and formation of pseudomembranes in the colon (pseudomembranous colitis), bowel perforation (toxic megacolon), sepsis, shock and even death (Rupnik *et al.*, 2009). *C. difficile* is only susceptible to three marketed antibiotics, Metronidazole, Vancomycin and Fidaxomicin and recurrence rates are high and indicate that spores surviving treatment results in re-infection (Vardakas *et al*., 2012).

3.1.1 *C. difficile* biogeography

CD is extensively distributed in the general environment and exposure to CD in healthcare facilities is high. A study by (Al Saif & Brazier, 1996) in South Wales found CD to be widespread in freshwater supply including taps, drainage channels, communal pools, rivers and lakes. In addition to freshwaters, CD was also found to exist in soil, produce and faeces of farmyard animals.

Farmyard animals and laboratory animals are found to carry CD as an enteric pathogen. Spores of CD were also isolated from meat and poultry; contamination with spores could be a result of the slaughterhouse environment and processing (E. R. Dubberke *et al*., 2011).

3.1.2 Prevalence of *C. difficile*

Globally CD has caused significant concerns in healthcare over several decades (Kuijper *et al.,* 2008; Wiegand *et al*., 2012). Statistics show that in the USA alone 250,000 cases with 14,000 deaths were reported due to CDI annually (Centres for Disease Control and Prevention 2012;Lessa *et al*., 2015). Different countries show the consistent prevalence of community acquired CDI ranging from 11 % to 28 %. According to the National Health Service (NHS) Trusts in England and Wales (effective April 2007) all CDI cases occurring in patients 2 years and above must be reported.

The epidemiological study of CD is monitored by Public Health England (PHE) in England and Wales, who collect data every three months on CDI incidences in Healthcare settings. PHE publish surveillance reports monthly, quarterly and annually on CDI cases and data are available to the general public via the PHE website (Erik R Dubberke *et al*., 2015). A decline from 44,563 cases in 2004 to 13,785 in 2014 was observed. The highest number of cases was recorded in 2006 (55,653).

Health Protection Agency (HPA) (previously known as Public Health England) in 2010 reported that decrease in CDI cases may be due to increased awareness of protocols for infection control in the healthcare environment. To further manage the reduction rate of CDI the HPA has put in several strategies such as mandatory reporting, financial penalties for CDI outbreaks in hospitals and antibiotic stewardship (Wilcox 2011; Hargreaves & Clokie 2014). Another reason may be due to variation in diagnostic tests across hospitals (Wilcox & Smyth 1998; Goldenberg & French 2011). Under reporting may also contribute to the decline in cases of CDI. K. A. Davis *et al*., (2014) reported that in a study of 428 hospitals spanning several European countries 23 % of CDI cases failed to report. Community associated CDI are not included in the report which will increase the numbers furthers.

3.1.3 Antibiotic treatment of *C. difficile*

Onset of CDI is often related to antibiotic treatment more commonly with clindamycin and fluoroquinolones. However, prescribing terminal doses of these antibiotics usually clear CDI (Burnham and Carrol 2013). If this is not successful then vancomycin or oral metronidazole is given, which has been the gold standard for over 30 years (Ivarsson *et al.*, 2015). Metronidazole is able to clear 77.6 % and vancomycin 85.8% of cases however there is a 27.1 % and 24 % chances of reoccurrence respectively (Vardakas et al., 2012). The treatment therefore, is not permanent; relapses of infection are probable. Antibiotics do not work in all patients, in 55 % of cases relapse follows antibiotic treatment. Complications occur after antibiotic treatment which disrupts the function of the microbial flora of the intestinal tract predisposing patients to infection with other pathogens (Ramesh *et al.*, 1999; Rupnik *et al*., 2009).

Fidaxomicin (Optimer Pharmaceuticals) a new antibiotic approved in 2011 by the US Food and Drug Administration (FDA) for the treatment of CDI. Comparatively, much lower levels of reoccurrence were observed with fidaxomicin but the use is limited by its high cost ($2800). Vancomycin ($680) is more expensive than metronidazole ($22) therefore the first recommended treatment is metronidazole (Ivarsson *et al.*, 2015).

The FDA has fast tracked the approval of Cadazolid (Actelion) and Surotomycin two other antibiotics currently in Phase III clinical trials (Cubist Pharmaceuticals) (Ivarsson *et al*., 2015). The development of antibiotic resistance is on the rise, the bacteria are able to infect and colonise in the presence of antibiotics (Rupnik *et al.*, 2009). Vancomycin resistance is of great concern due to the microflora of the gut being wiped out and the emergence of vancomycin- resistant CD and enterococci as a consequence of this vancomycin is only prescribed in severe cases, as a last resort drug (Ananthakrishnan, 2011; Ramesh *et al.*, 1999).

New treatment options are under investigation to counteract the problem of antibiotic associated infection and antibiotic resistance. Some of the new therapeutics include, vaccines containing monoclonal antibodies against toxin A and B, faecal microbiotic transplantation (Shields *et al*., 2015) which has demonstrated a success rate of almost 90 % and also the use of bacteriophages for the treatment of CDI (Hargreaves & Clokie, 2014).

3.1.4 Subgrouping *C. difficile* strains

In order to differentiate between prevailing strains of CD across the world, and to sub-group CD strains a common distinguishable method called PCR ribotyping is used (Goldenberg & French, 2011). The genome of CD contains an operon with many variations in copy sizes of the rRNA operon. This operon consists of intergenic spacer regions of 16S to 23S, which is used to characterise the CD strain by amplification and carrying out PCR. A pattern of bands between regions 238 to 566 base pairs is observable on an agarose gel which is used to distinguish CD into different ribotypes (Sadeghifard *et al.*, 2006). This method enables discrimination between different subgroups and classifies similar banding patterns as the same ribotype. The use of different analysis software across laboratories showed difficulties in reproducibility so Indra *et al*., (2008) updated the PCR ribotyping method to a high-resolution capillary based gel electrophoresis. So far 350 ribotypes have been reported and the number is expected to rise (Fawley et al., 2008; Public Health England 2014).

3.1.4.1 Prevalence of CD PCR ribotypes

Healthcare outbreaks associated with ribotype 027 (R027) also referred to as North American pulsed-field type 1 (NAP1) have been thought to a consequent from the excessive use of fluoroquinolones. The majority of reported CDI cases across North America, Canada and Europe have been due to R027 (Fawley *et al*., 2008; Rupnik et al., 2009; Smits, 2013). R027 is capable of sporulation, which is likely a contributing factor to its widespread dissemination and persistence (Smits, 2013; Noren, 2010). The presence of the binary toxin and deletion of toxin repressor gene, *tcdC* in R027 may further lead to increased production of toxins A and B (Ananthakrishnan, 2011; Sirard *et al*., 2011).

Another hypervirulent strain, ribotype 078 (R078) has also been associated with CDI worldwide, mainly due to excessive production of toxins A and B. In comparison to R027, R078 is known to cause more community acquired CDI cases (Cartman *et al.*, 2010). It was first isolated in pigs and calves but now is the second most prevalent ribotype in the Netherlands increasing from 3 % to 13 % from the

year 2005 to 2008 respectively. Numerous CDI outbreaks have been, such as the outbreak in Ireland. Consequently R078 is the second most prevalent ribotype after R027 (Burns *et al*., 2010).

A change in the R027 epidemiology has been observed with marked decrease in CDI associated with this ribotype. This may be explained by the control measures put in healthcare settings (Public Health England 2014) which may also be contributing to the increased prevalence of other ribotypes (Sutter *et al*., 2012). Other ribotypes seen in clinical settings are R001 in China and Korea, R002 in Japan and Hong Kong, R014/020 in European counties and the US, R017 in Northern Europe and R078 across Europe (Burke & Lamont, 2014; Goudarzi *et al.*, 2014).

In the U.K. PHE have been using the capillary-based gel electrophoresis method since 2007 to observe trends in the national prevalence of CD ribotypes. A recent report highlighting ribotype trends from 2007 to 2013 and showed there wa a decline in ribotype R027 from 65 % to 5 % respectively. Smaller reductions were noted for ribotypes R001 decreasing from 10 % to 5 %, R106 from 8 % to 2 %, from years 2007 to 2013 respectively. The changes reflect the reduced cases of CDI and motility in England and Northern Ireland (Wilcox *et al.*, 2012). Because of ribotype reduction rates, other less prevalent ribotypes have been on the rise. Some examples according to Public Health England (2014) include, R002, R005, R014/020, R015, R023 and R078. It is hoped that by identifying the ribotypes responsible for causing infection using the CDRN method would enable new control measures to be put into place to limit further spread of CDI across healthcare (Wilcox *et al.*, 2012).

3.1.5 Ribotype 076 a Model Strain

The bacteriophage T9 was chosen as a model phage which can effectively infect *C. difficile* strain T6, ribotype 076. Although strain T6 was isolated from an environmental sample, it represents strains that have the potential for transmission to a clinical setting through community acquired infection. The ribotype 076 was found in several clinical studies during a prevalence study of ribotypes (Rotimi *et al.* 2003; Huber *et al.* 2014). In healthcare settings (15-25 %) infections are predicted to occur due to transmission between patient to patient contact or transmission through the environment example surface to hand contact (Walker *et al.*, 2012). Whilst the presentation of ribotype 076 is small in the clinical setting, it highlights the transmission from environment to clinical setting. This therefore, makes it a clinically relevant strain suitable for studies.

3.1.6 *C.difficile* phages

A lack of suitable *C. difficile* phages has limited research on phage therapy for CDI. A recent study (Nale *et al.*, 2016) however, showed the potential of phages to treat CDI in a hamster model using combinations of *C. difficile* phages. A polyvalent cocktail containing between 2 to 5 phages covering a suitable host range was used; the phages delivered to the hamsters were given as simple phage suspensions and bicarbonate was administered to the animals prior to phage delivered orogastrically to reduce the stomach acidity. The phages used in this study all encoded integrases, and though they can infect lytically they can follow the temperate phage lifecycle and thus are not ideal phages for phage therapy. However no strictly virulent phages have been isolated for this pathogen and the phage cocktail demonstrated efficacy in multiple model systems suggests that they have significant potential to reduce the *C. difficile* burden in the gut environment. Data presented by Nale *et al.*, (2016) showed that phages were effective both *in vitro* and *in vivo* versions of a relevant hamster infection model, where use of phages reduced colonisation and increased time of survival in the hamster model. Further work has shown that the same phage combinations can be used to prevent and treat infection in a biofilm and an insect model (Nale *et al.*, 2016).

3.1.7 Oral delivery of phage

When free phages are delivered orally for phage therapy or for modulating microbiota (Young & Gill, 2015), there is likely to be variable but significant losses of phage titre by the time phages reach the intended infection site. Potential reduction in phage titres due to phage inactivation attributed to stomach acidity may in part have been responsible for failure of a recent clinical trial aiming to show reduction in acute bacterial diarrhoea symptoms in children using phage therapy (Sarker *et al*., 2016). This is primarily due to the acidic conditions encountered in the stomach, and the presence of bile and digestive enzymes and other proteases in the intestinal tract and stomach (Choinska-Pulit *et al.*, 2015; Yongsheng Ma *et al*., 2008; Tang *et al*., 2013). Therefore, there is a clear need to protect phages against these adverse gastrointestinal conditions by protecting them via encapsulation (S. Kim, Jo, & Ahn, 2015a; Yongsheng Ma *et al.*, 2008; Tang *et al.*, 2013), and to control their targeted release at the site of infection e.g. in the colon for CDI. The goal of encapsulation is to create a suitable micro-environment to protect phages from the harsh environmental conditions found in the stomach, and also to protect the phages during processing and storage prior to use (Merabishvili *et al*., 2013).

Encapsulation technologies are well established for many pharmaceutical drugs however, for phages such technologies may not be suitable. This is because the techniques suitable for conventional therapeutic compounds often involve the use of organic chemicals that may inactivate phages (S. W. Lee & Belcher, 2004; Puapermpoonsiri *et al.*, 2009). To overcome this, recent phage encapsulation

strategies have used basic homogeniser and extrusion techniques that appear to be less harmful and they maintain phage viability to some extent (Yongsheng Ma *et al*., 2008, 2012; Puapermpoonsiri *et al*., 2009; Shi, Zheng, Zhang, & Tang, 2016; Tang *et al.*, 2013). The lack of suitable encapsulation techniques that allow the precise control of phage encapsulation has been the motivation behind the present work discussed in this chapter where we have used microfluidic technology to encapsulate phages.

Unlike homogeniser and extrusion techniques microfluidic based microencapsulation allows exquisite control over each droplet that allows the control of desirable properties (Brouzes *et al.*, 2009) including precise loading of phage per particle and uniformity of the particle size and release kinetics. We suggest that combining microfluidic encapsulation with the possibility of being able to select a wide range of available stimuli responsive polymers will enhance the utility of phage encapsulation for a range of therapeutic applications. As such, the encapsulation strategy taken in this work was to microencapsulate *C. difficile* specific phages in a pH responsive polymer.

The main desired feature of phage microencapsulation presented here is to protect the phages from the stomach acid, and then release them in the infected colon at the typical pH of 7 (Figure 3.1a). Previously published studies that have used Eudragit S100 as an enteric coating for colon targeted drug delivery in combination with alginate have shown promise (Chen et al., 2016). Alginate is a natural biopolymer which is biocompatible, in other words nontoxic to tissue, biodegradable and relatively cheap. The gelation of alginate may be achieved by addition of high molecular weight polycations such as chitosan, or the addition of low molecular weight polyvalent Ca^{2+} cations (K. T. Lee & Mooney, 2013). Eudragit S100 is an anionic copolymer composed of methyl methacrylate and methacrylic acid with monomers arranged randomly on a polymer chain (Figure 3.2ai). The presence of weakly acidic carboxyl groups in the polymer chain results in the pH responsive behaviour; in an acidic environment, the groups are uncharged whilst at pH values greater than their pKa (pKa ~ 4), the polymer chains begin to disentangle due to the electrostatic repulsion between the negatively charged carboxyl groups (Figure 3.2aii) (Nguyen & Fogler, 2005). The suggested mechanism of phage release is illustrated in Figure 3.2 b. Prolonged exposure to acid will enable the protonation of the carboxyl groups, allowing precipitation of the polymer.

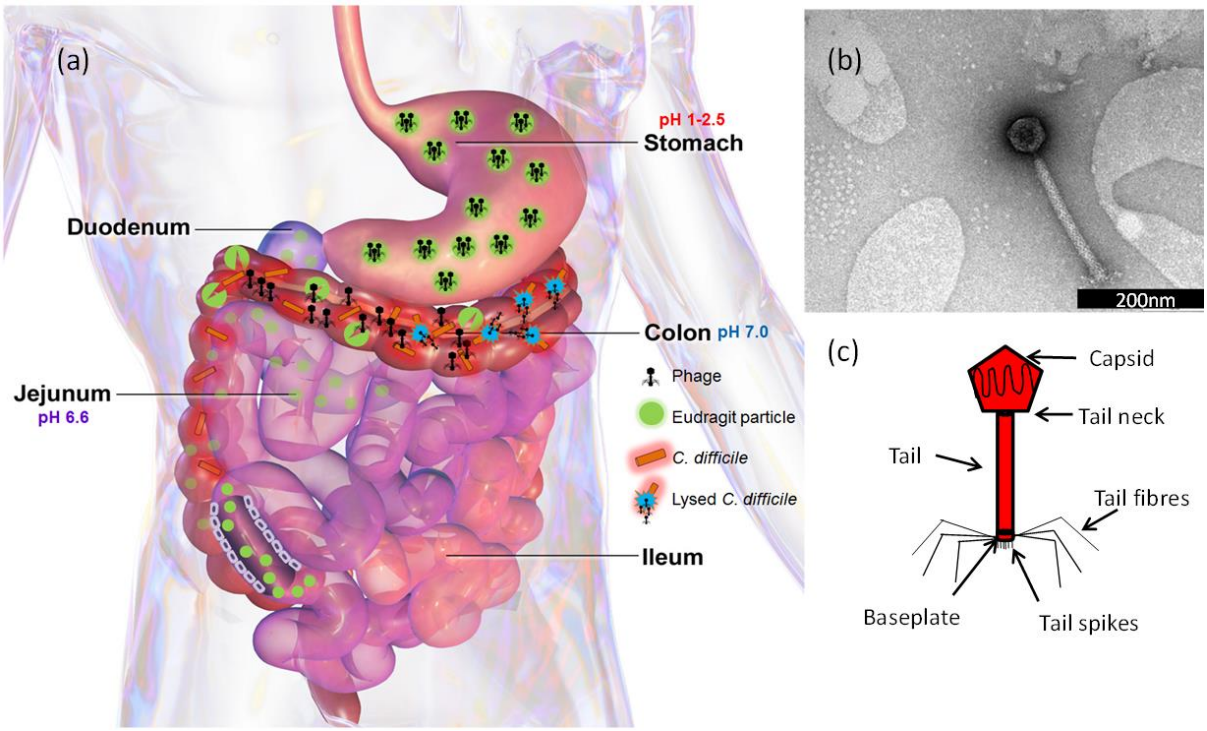

Figure 3.1. Overview of the delivery of encapsulated phage through the GI-tract to the colon. (a) Schematic of the gastrointestinal tract, depicting transit of intact encapsulated phage-loaded microparticles through the stomach and their subsequent disintegration in the colon at pH 7 leading to the controlled release of phages from the microparticles; (b) Transmission Electron Microscopy and (c) schematic of bacteriophage Phi9CD-KM, Myovirus.

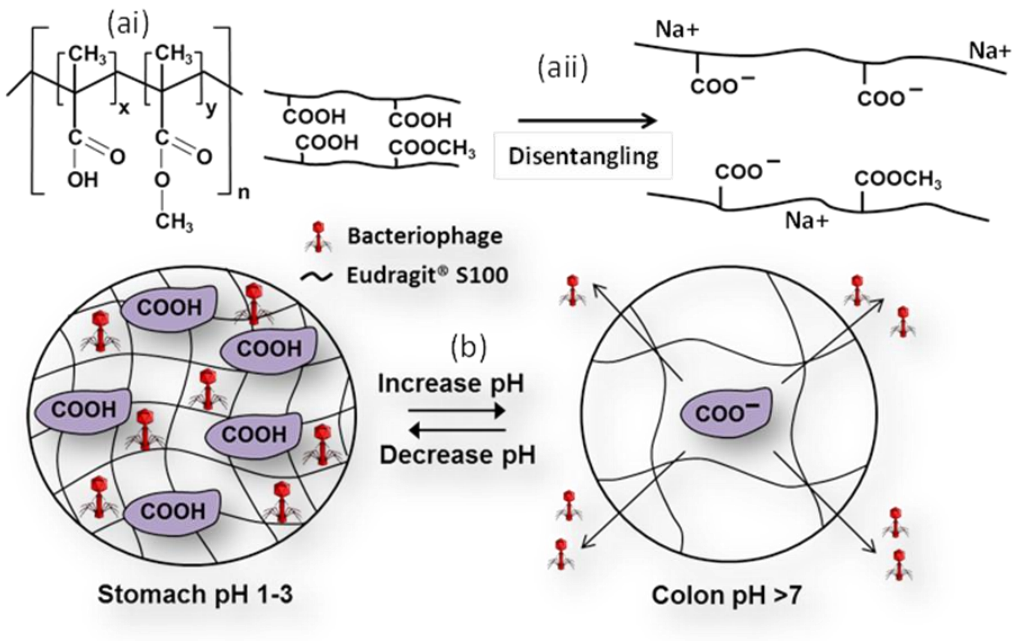

Figure 3.2. Mechanism of phage release from microparticles. Schematic of ai) the chemical structure of Eudragit S100, y:x = 2:1 aii) Eudragit S100 polymer chain separation due to dissociation of weakly acidic functional groups, electrostatic repulsion and polymer swelling; (b) Phage loading/release mechanism from pH responsive Eudragit S100 microparticles.

Composite Eudragit S100 and alginate particles have been used to deliver 5-aminosalicylic acid (5-ASA) and curcumin (both model drugs) to the colon. Duan et al. (Duan *et al.*, 2016) found that the Eudragit S100 coating enables resistance to the acidic environment of the stomach, whilst alginate provides muco-adhesive properties which prolong the residence time of the microparticles within the body. Similar investigations carried out by Sookkasem *et al.*, (2015) showed the release of curcumin in simulated intestinal fluid at pH 7.4. Pleasingly, as predicted, the curcumin released from the beads was shown to be cytotoxic to the cell line HT-29, demonstrating the efficacy of encapsulation. Vemula *et al.,* (2015) investigated the transit of Flurbiprofen to the colon in healthy volunteers through X-ray imaging. The composite tablets released the drug in the colon without disintegrating in the upper GI-tract.

A further novelty of the work reported here is the microencapsulation of phages using microfluidic technology which allows the manufacture of highly uniform micron-sized core-shell particles (G. T. Vladisavljević *et al.*, 2012) and using acidified oil for the precipitation of Eudragit S100. The technique affords exquisite control over the morphology of the microparticles including their size and size distribution, shell thickness and thereby phage release kinetics, phage loading and encapsulation efficiency.

Aim of the study

The aim of the study presented here was to demonstrate the application of microfluidics in encapsulation of bacteriophages for the first time. Microparticles with *C. difficile* phage CDKM9 in the core, surrounded by a shell of either Eudragit S100 or ES100 /alginate matrix were produced using this device. The pH sensitive microparticles were designed to survive the transition of phages delivered orally via the mouth, through the stomach and intestine with phage release in the colon. We demonstrate the ability to manufacture uniform phage entrapped particles for pH responsive site-specific delivery.

3.2 Materials and Methods

3.2.1 Materials

Eudragit S100 was purchased from Evonik, Germany. Miglyol 840, a propylene glycol diester of caprylic/capric acid, was obtained from Sasol, Germany and used as carrier oil for the continuous phase. Polyglycerol polyricinoleate (PGPR) soluble surfactant was purchased from Abitek, USA and used to stabilise the water/oil interface. 4-amino-benzoic acid, p-toluenesulfonic acid and sodium chloride (Acros Organics, UK) were purchased from Fisher Scientific, UK. The organic acids 4-amino-benzoic acid and p-toluenesulfonic acid were used to trigger *in situ* curing of the droplets in the oil phase. Ethanol and n-hexane were of analytical grade (Fisher Scientific, UK). Ethanol was used to dissolve calcium chloride as the alginate crosslinking agent and n-hexane was used to remove oil from the emulsion respectively. 5(6)-Carboxyfluorescein was purchased from Sigma Aldrich, UK and used to visualize the generated particles. Ultrapure water was obtained from Millipore 185 Milli-Q Plus water filtration system. Sorensen's buffer 0.2 M was used as a dissolution media for the microparticles and was prepared by mixing sodium phosphate (NaH_2PO_4) (for pH 7, 39 ml and for pH 6, ~88 ml) with sodium phosphate dibasic (Na_2HPO_4) (for pH 7 6, 1 ml and for pH 6, ~12 ml) (Fisher Scientific UK). Low viscosity alginate was purchased from Sigma Aldrich, UK.

3.2.2 C. difficile strain and bacteriophage CDKM9

Clostridium difficile strain CD105HE1 ribotype 076 was used to propagate the phage as per the method of Nale et al. (Nale *et al.*, 2016) Bacteriophage CDKM9 is a *myovirus* previously isolated from an environmental water sample as described by Rashid et al. (Rashid *et al.*, 2016)

C. difficile, CD105HE1, was cultured in brain heart infusion (BHI) (Oxoid, Ltd., UK) agar supplemented with 7% defibrinated horse blood (TCS Biosciences, Ltd., UK). Liquid cultures were grown in fastidious anaerobic (FA) broth and BHI broth. *C. difficile* was cultured anaerobically in an anaerobic chamber (Ruskinn Technology, UK) using an anaerobic environmental gas mixture composed of 10 vol % H_2, 10 vol % CO_2 and 80 vol % N_2.

Phage CDKM9 was propagated on CD105HE1. Phage stocks were prepared as follows: 0.5 ml of an overnight culture of *C. difficile* was grown in FA broth was transferred to 50 ml of pre-reduced BHI broth and incubated in the anaerobic chamber at 37 ˚C. The optical density (OD_{550nm}) was measured at hourly intervals until it reached 0.2, after which 100 - 300 µl (dependent on phage titre of stock) of phage stock was added. The 50 ml tube was incubated overnight in the anaerobic chamber at 37 ˚C for phage amplification to occur. The following day the tube was centrifuged at 2,000 x g for 10 min at 4˚C. The supernatant was filtered through a 0.2 µm filter (Millipore, USA), collected and stored at 4˚C until further use.

Plaque assays were carried out using the double layer agar method.(Clokie & Kropinski, 2009). Briefly, 1.5 ml of 0.4 % BHI semi-solid agar and 1.5 ml of salt mixture (0.4 M $MgCl_2$ and 0.1 M $CaCl_2$, Oxoid Ltd. UK) were added to 250 µl of overnight *C. difficile* FA broth culture and poured onto 1 % BHI agar plates and set under a laminar flow hood. 10 µl of phage solution was spotted on the plate (in triplicate), left to dry and incubated in the anaerobic chamber at 37˚C overnight. The following day the resulting number of phage plaques was enumerated.

The phage titre was determined by carrying out serial dilutions from the phage collected and each dilution (in triplicate) was spotted on host lawn (same as the propagation host). Phage titre was determined by counting plaques and expressed as plaque forming units (PFU) per ml.

3.2.3 Phage sensitivity to pH

Phage inactivation (sensitivity) to different experimental parameters used to encapsulate the phages was assessed as follows. The polymer solvents analysed were deionised water (dH_2O), 0.2M NaCl and BHI broth. The polymer was dissolved in each of these by adjusting the pH to 7.4. Effect of pH on phage was analysed by adding phage to a 0.2 M solution of NaCl with pH adjusted to 2, 3, 4, 5, 6 or 7 by adding 0.1 M HCl or 0.1 M NaOH. To analyse the survival of phage in each parameter 270 µl of each solution was added to a 96 well plate (in triplicate), with BHI broth as positive control, 30 µl of phage stock (10^8 PFU/ml) was added to each well. At time points 0 h, 6 h and 24 h serial dilutions in BHI broth (270 µl) were performed for each test and spotted (10 µl) on host lawn (prepared as described in the

plaque assay section previously). 32 repeats of each dilution were performed for each time point. The spotted plates were dried for 5 min and then incubated in the anaerobic chamber at 37 ˚C overnight. The following day, plaques were counted and PFU/ml calculated.

3.2.4 Experimental set-up of microfluidics

The controlled production of microdroplets and microparticles was achieved using in house fabricated glass capillary devices. The experimental setup for drop microfluidic experiments is shown in Figure 3.3a. Two SGE (1 ml and 5 ml) syringes were mounted on two 11 Elite syringe pumps (Harvard Apparatus, UK) to deliver the aqueous and oil phase to the inner and outer capillary respectively via separate medical tubes. The microfluidic device was positioned on the GXM XD63 optical inverted microscope (GX Microscopes, USA). Formation of droplets started when the dispersed phase reached the orifice of the collection capillary and was observed with a Phantom V9.0 high-speed camera (Vision Research, Ametek, USA) connected to the inverted microscope using x4 magnification lens. The camera was connected to the computer which allowed monitoring and recording of the droplet forming process at 2000 frames per second with a resolution of 576 by 288 pixels. The droplets and particles produced from the device were collected into a glass vial via the collection tube. Table 3.1 summarises the compositions of the dispersed and continuous phases used for the experimental work reported here.

Table 3.1. Compositions of dispersed and continuous phase.

Dispersed phase	D1	0.2M NaCl pH 7.4 5% (w/v) Eudragit S100 10^7 PFU/ml
	D2	0.2M NaCl pH 7.4 5% (w/v) Eudragit S100 5(6)-Carboxyfluorescein 50µM
	D3	0.2M NaCl pH 7.4 10% (w/v) Eudragit S100

Continuous phase	C1	2% (w/v) Alginate 10^7 PFU/ml Miglyol 840 2% (w/v) Polyglycerol polyricinoleate (PGPR) 0.25% (w/v) p-toluenesulfonic acid
	C2	Miglyol 840 2% (w/v)Polyglycerol polyricinoleate (PGPR) 1% (w/v) p-toluenesulfonic acid
	C3	Miglyol 840 2% (w/v) Polyglycerol polyricinoleate (PGPR) 1% (w/v) 4-aminobenzoic acid
	C4	Miglyol 840 2% (w/v) Polyglycerol polyricinoleate (PGPR) 0.75% (w/v) 4-aminobenzoic acid
	C5	Miglyol 840 2% (w/v) Polyglycerol polyricinoleate (PGPR) 1% (w/v) 4-aminobenzoic acid ~0.15% (w/v) $CaCl_2$ ~3% (v/v) Ethanol

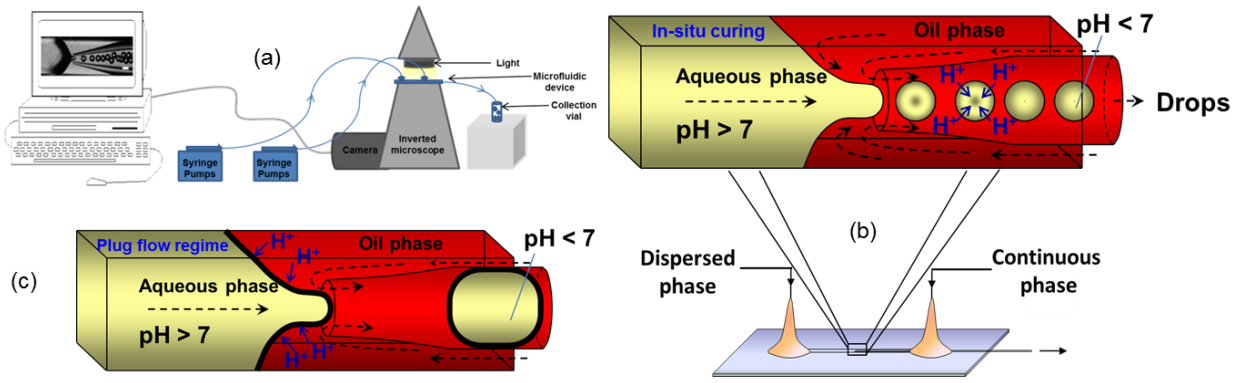

Figure 3.3. Microfluidic production of microparticles. a) Schematic of laboratory experimental set-up; b) Schematic of droplet production using a glass capillary microfluidic device followed by in situ gelation with 4-aminobenzoic acid dissolved in the oil phase; c) Schematic of the plug flow regime due to premature gelation of Eudragit S100 with p-toluenesulfonic acid resulting in a high viscosity of the aqueous phase during jet pinch-off. *p-Toluenesulfonic acid*, with a pKa of −2.8, is more than 10,000 *times stronger* acid than 4-aminobenzoic acid, with a pKa of 2.38.

3.2.5 Glass capillary device fabrication

Experiments were performed using a microfluidic device with counter-current flow focusing (Figure 3.3b). The device consists of a circular glass capillary tube (Intracel Electrophysiology and Biochemistry Equipment, St Ives, Cambs., UK) inserted into a square glass capillary tube (Atlantic International Technologies Inc., Rockaway, NJ, USA). The inner circular capillary has an internal diameter of 0.58 mm and outer diameter of 1 mm. The outer square capillary has an inner diameter of 1.15 mm and outer diameter of 1.4 mm. 5 cm length of both capillaries was used.

The inner round capillary was pulled using a P-97 Flaming/ Brown micropipette puller (Sutter Instrument Company, Novato, USA) by heating the central region of the capillary approximately 20s until it softens and separates into two parts leaving a sharp tip with a diameter of 20 µm at both ends. The orifice or the nozzle diameter was adjusted to the desired size by abrading the orifice with sandpaper (Black Ice Waterproof T402 Paper, Alpine Abrasives, UK). The orifice sizes used for the experiments were 100 µm and 200 µm. To confirm the inner diameter of the orifice of the inner capillary a Microforge MF-830 microscope (Intracel Electrophysiology and Biochemistry Equipment, St Ives, Cambs., UK) was used. After abrading, the inner capillary was cleaned by blowing compressed

air through the lumen and subsequently treated in order to create a hydrophobic inner surface using octadecyltrimethoxysilane (OTMS) (Sigma Aldrich, U.K.).

The square capillary was placed on a square microscope slide (Sigma-Aldrich, UK) and firmly attached with cyanoacrylate glue. The inner round capillary was carefully inserted inside the outer square capillary and axially centred with the help of the microscope. Two syringe needles with plastic hubs (2.5 mm outer diameter and 0.9 mm inner diameter, B-D Precisionglide®, Sigma-Aldrich, UK) were placed at edges of the square capillary and firmly held together with two component epoxy glue (Five Minute ® Epoxy, ITW DEVCON Limited, UK). The aqueous and oil phase was supplied through medical delivery tubes (0.86 mm inner diameter and 1.52 mm outer diameter, Smiths Medical International Limited, UK), attached to syringe needles. The phases entered the square capillary from two opposite ends which were enclosed inside the plastic hubs of the syringe needle. The droplets were collected through a collection tube (1.58 mm inner diameter and 2.1 mm outer diameter, Sigma-Aldrich, UK) which was attached to the inner round capillary (protruding from the plastic hub). The plug flow regime where the formed drop adopts a plug shape and occupies the entire cross section of the collection tube is demonstrated in Figure 3.3c.

3.2.6 Phage encapsulation

The dispersed (aqueous) phase was prepared by dissolving Eudragit S100 powder (final working concentration of 5 % w/v) in either 0.2 M NaCl solution or BHI. 10 M NaOH solution was added dropwise until the solution turned clear and colourless indicating complete dissolution of Eudragit S100 polymer. To prepare composite particles, 2 % (w/v) alginate was dissolved with Eudragit S100 over heat (~60 °C) stirring overnight (formulation D3 in Table 1). For phage encapsulation, the dispersed phase contained 1.6 x 10^7 PFU/ml of phages in formulation D1 and D3 (Table 3.1). For dye encapsulation, 10 mM solution of carboxyfluorescein in ethanol was added to 5 % w/v Eudragit® S100 dissolved in 0.2 M NaCl to make a final dye concentration of 50 µM (formulation D2 in Table 3.1).

The continuous (oil) phase was prepared by dissolving 2 % (v/v) of PGPR and 1 % (w/v) of 4-aminobenzoic acid (formulation C3 in Table 1) or (0.25 % or 1 %) (w/v) p-toluenesulfonic acid in Miglyol 840. The phases were introduced into the microfluidic device at different flow rates (Table 3.2), to ensure droplets formed at the entrance of the tapered inner capillary were monodispersed. The flow rates were kept constant throughout each experiment. The droplet formation was followed for periods more than 6 h as part to evaluate droplet stability over extended periods of operation. The droplet size was analysed using the Image J program (the National Institute of Health, Washington, U.S.). To evaluate droplet stability over prolonged periods of operation, the size of 20 droplets at each

time point was measured. The particles were collected in an empty glass vial. Air bubbles are a common issue in microfluidic droplet generation. Air bubbles were avoided by using high-quality gas-tight glass syringes instead of plastic syringes.

Table 3.2. Summary of samples prepared using different microfluidic experimental conditions.

Experiments	Orifice size / µm	Dispersed phase flow rate, Q_d / ml h^{-1}	Continuous phase flow rate, Q_c / ml h^{-1}
F1	200	1.2	7.0
F2	200	0.5	3.5
F3	200	0.5	3.0
F4	200	0.5	2.0
F5	100	0.09	2.0

Eudragit S100/Alginate composite microparticles were prepared as per the procedure above. The dispersed phase composition was 2 % (w/v) alginate and 10 % (w/v) Eudragit S100 (formulation D3 in Table 3.1). Formulation C5 was used for the continuous phase (Table 3.1). A 5 % w/v calcium chloride (Fisher Scientific, UK) solution in ethanol (reagent grade, Sigma Aldrich UK) was prepared and subsequently added to the Miglyol to make-up the appropriate composition of the continuous phase used for alginate crosslinking. The microparticles were left to crosslink overnight at room temperature.

After collection, the sedimented microparticles were processed by pipetting off excess Miglyol oil. Residual oil was removed by rinsing the particles three times with n-hexane and gently centrifuging at 10 g for 3 min at 4˚C. Residual hexane solvent was removed by vacuum drying the particles for 15 min at room temperature.

3.2.7 Scanning electron microscopy (SEM)

20 µl of washed microparticles prepared as outlined above, were pipetted and placed on 13 mm filter disks (0.2 µm pore size, Millipore Ltd. UK). The filter disks with the samples were placed in a -20˚C freezer for 24 h. The frozen particles were then placed in a glass freezer dryer jar and connected to a freeze dryer machine at 1 bar pressure and -50˚C. The particles were freeze dried for 24 h to allow

removal of any residual liquid. The particles were viewed using a benchtop Scanning Electron Microscope (Hitachi TM3030 Table-top Microscope).

3.2.8 Transmission electron microscopy (TEM)

To identify the purity of the phages used for encapsulation was confirmed using transmission electron microscopy (TEM) analysis was conducted. 1 ml of phage stock was centrifuged at 4,500 x g for 1 hour at 4˚C and the pellet was washed two times with 0.1 M ammonium acetate (Fisher, UK) and re-suspended in 100 µl of ammonium acetate. 4 µl of sample suspension was placed on glow discharged pioloform/ carbon coated copper grids which were allowed to stand for 5 min for bacteriophage to bind, 1% w/v uranyl acetate was added to stain the sample. 10µl of deionised water was used to rinse the sample and the prepared sample was left to dry for 24 h. The grids were examined using a JEOL 1220 electron microscope with an accelerating voltage of 80 kV. Digital images were captured using SIS Megaview III digital camera with associated analysis software.

3.2.9 Confocal microscopy

Carboxyfluorescein encapsulated microparticles were viewed using a Confocal Laser Scanning Microscope (CLSM) (BioRad Radiance 2000 MP with a Nikon Eclipse TE300 inverted microscope).

3.2.10 Encapsulated phage release

2 % (w/v) of washed particles were suspended in prewarmed 10 ml simulated intestinal fluid, 10 mg/ml pancreatin in 0.05mM KH_2PO_4 at pH 6 or 7 (Sigma Aldrich, UK) under agitation conditions at 37°C. For acid exposure 2 % (w/v) of washed particles were suspended in prewarmed 10 ml simulated gastric fluid, 3.2 mg/ml pepsin in 0.2 M NaCl at pH 2 (Sigma Aldrich, UK) for an exposure period of 3 h (reported mean gastric emptying times in human subjects is typically less than 3 hours for both pre-fed and fasted states (Ibekwe et al., 2008)), under agitation conditions at 37°C. Particles were subsequently centrifuged at 2,000 g for 15 min and re-suspended in simulated intestinal fluid (pH 7) under agitation conditions at 37°C until complete dissolution of particles. For enumeration of phage released, plaque assays were used (as described previously section 3.2.2) by removing 10 µl of sample at hourly intervals, serially diluting in BHI broth and spotting on a host bacterial lawn. The PFU/ml was determined the following day at each time point.

3.2.11 Statistical analysis

Comparison of sample means using 2 sample t-tests and evaluation of 95 % confidence intervals for data was carried out using the statistical software Minitab 18.

3.3 Results

3.3.1 Encapsulated phage (Ephage) microparticle production

Highly monodispersed core-shell Eudragit S100 droplets were produced under optimised hydrodynamic conditions using 0.75 % (w/v) 4-aminobenzoic acid to precipitate the polymer by ion exchange (a process termed polymer curing). Stable production of uniform droplets required optimisation of the hydrodynamic conditions. Microfluidic devices can be controlled *in situ* by direct microscopic observation. Hydrodynamic conditions were optimised in real-time by adjusting fluid flow rates during each experiment until uniform droplets were produced. Three different droplet generation regimes were observed depending on the relative magnitude of the shear, inertial and interfacial tension forces acting during droplet formation. These forces were modulated by changing the formulation of the phases introduced into the device and the flow rates of the continuous and the dispersed phases.

One regime which was found to be unsuitable for stable microparticle formation was 'jetting'. 'Jetting' is characterised by the long jet created inside the collection capillary away from the orifice resulting in unstable breakup of the droplets at various positions along the jet. Jet widening (Figure 3.4ai) occurred due to the high velocity of the dispersed phase compared to the continuous phase causing the velocity of the dispersed phase in the collection capillary to decrease until eventually the jet breaks into large drops due to the Rayleigh-Plateau instability. The transition from 'dripping' to 'widening jetting' occurs at the critical Weber number of the dispersed phase. The Weber number is a measure of the relative magnitude of inertial forces compared to the interfacial tension forces, $We = \rho LV^2/\gamma$, Where ρ (kgm^{-3}) is the density of the fluid, V (ms^2) is the characteristic flow rate, and L (m) is the characteristic length scale of flow and γ is the interfacial tension. In Figure 3.4aii, the inner phase is stretched into a longer and narrower jet due to the higher flow rate ratio, Q_c / Q_d compared to that in Figure 3.4ai, but the drops are still formed in 'widening jetting' regime. Alternatively, when the velocity of the outer phase in the collection capillary is much larger than the velocity of the inner phase, a narrowing jet is formed that produces relatively small droplets. The transition from 'dripping' to 'narrowing jetting' occurs at the critical Capillary number (Utada *et al.*, 2007), but this transition was not observed in this study. In either case, the droplet breakup remained unstable due to the imbalance of forces brought on by the high flow rate; either due to the inner or the outer phase. The viscosity of the phases also plays a significant role (Figure 3.4).

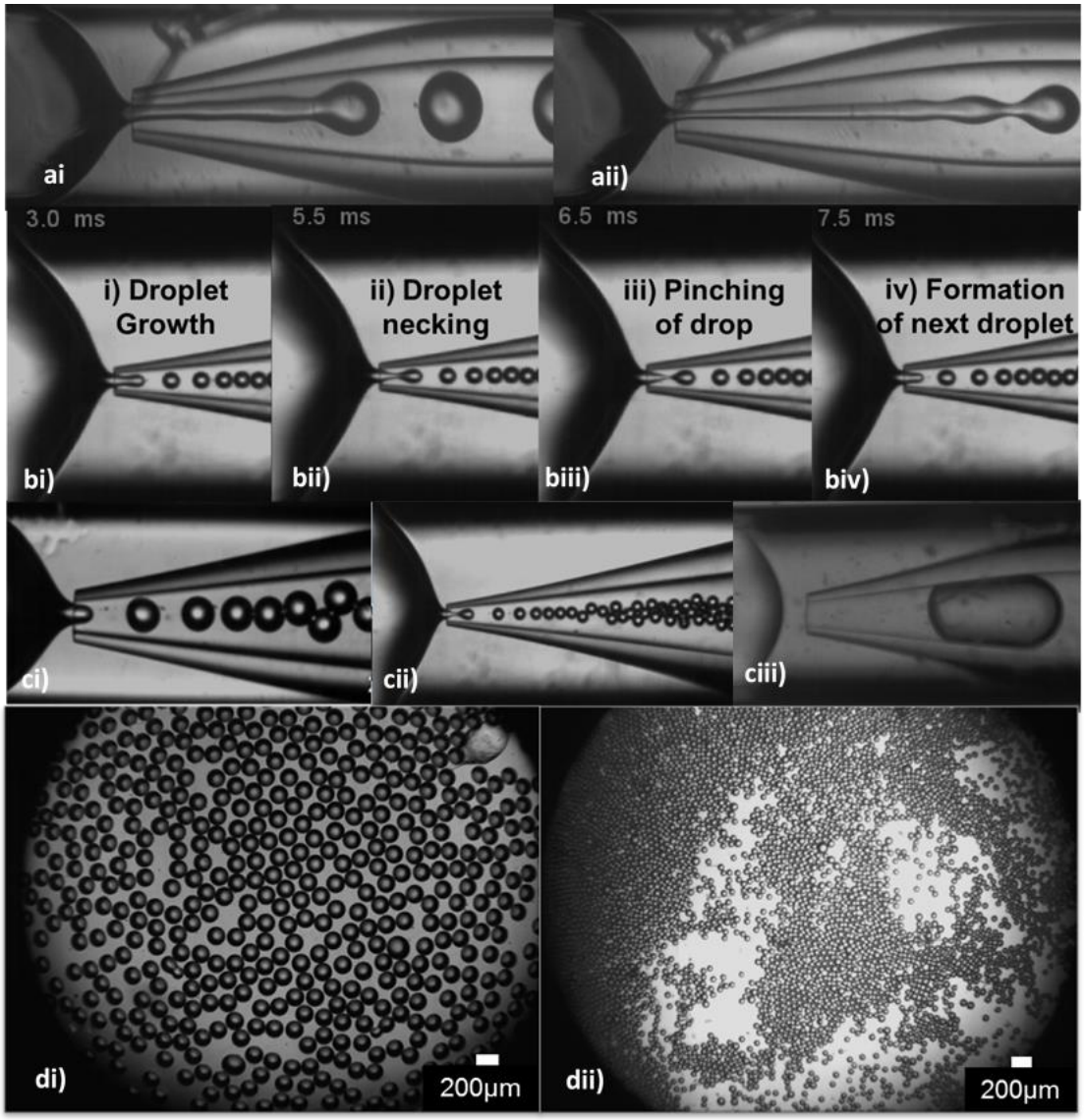

Figure 3.4. Production of W/O emulsions composed of 5 % (w/v) Eudragit S100 dispersed in Miglyol 840 with 2 % (w/v) PGPR and 0.75 % (w/v) 4-aminobenzoic acid. ai) Widening jetting at Q_c 3 $mlhr^{-1}$ and Q_d 0.9 $mlhr^{-1}$. The jet length is approximately 9 times the orifice diameter and the drop diameter was 400 µm; aii) Narrowing jetting Q_c 6 $mlhr^{-1}$ and Q_d 0.5 $mlhr^{-1}$. The jet length was approximately 11 times the orifice diameter and the drop diameter is 280µm; b (i-iv) Stages of droplet formation in the dripping regime; ci) The dripping regime during experiment F3 (Table 3.2); cii) The dripping regime during experiment F5 (Table 3.2); ciii) The plug-flow regime at the orifice diameter of 200 µm, Q_c = 0.06 $mlhr^{-1}$and Q_d = 0.3 $mlhr^{-1}$. The curing was achieved using 1 % (w/v) p-toluenesulfonic acid. The average drop diameter is ~700 µm; di) Droplets produced in (ci), average droplet size is 135 µm; dii) Droplets produced in (cii), average droplet size is 80 µm.

To enable better control of the droplet generation process and to reliably produce monodispersed droplets, the 'dripping regime' worked best. Here, the droplets were formed closer to the orifice of the collection capillary (Figure 3.4b) because the interfacial tension forces dominated over the inertia

of the dispersed phase and the viscous stress forces from the continuous phase. Droplet formation began as the dispersed phase entered the tapered collection capillary (Figure 3.4bi). The dispersed phase did not encounter the capillary wall due to repulsion from the hydrophobic surface of the treated capillary wall which resisted wetting by the aqueous phase. The continuous phase forced the dispersed phase to elongate axially (Figure 3.4bii), collapsing the dispersed phase and producing a neck behind the forming droplet. As the elongation progressed further, the neck thinned into a thread (Figure 3.4biii), eventually breaking the dispersed phase and releasing the droplet (mother plug). Following retraction, the process restarted with the dispersed phase protruding at the orifice of the collection capillary (Figure 3.4biv). In this dripping regime, the formation of one droplet took 4.5 ms^{-1}, thus 222 droplets were formed each second and subsequent droplets were produced at the same position as the previous droplets (Erb *et al.,* 2011; Fu *et al.*, 2012). The balance between the drag force and interfacial tension and negligible shear in the collection capillary after drop formation resulted in uniform droplets. The dripping regime occurs when the Weber number of the dispersed phase and the Capillary number of the continuous phase are both below their critical values. The Capillary number (*Ca*) represents the ratio between the viscous forces and interfacial tension across an interface between the two phases (Ekanem *et al.*, 2015; Erb *et al*., 2011; Utada *et al*., 2007). The Capillary number of the continuous phase is given by: $Ca = \mu v/\sigma$, Where, Ca is Capillary number, μ is dynamic viscosity (Pa.s), v is fluid flow rate (ms^{-1}), σ is surface or interfacial tension (Nm^{-1}). For experiments conducted using the dispersed phase flow rate of 0.5 ml h^{-1} and the continuous phase flow rate of 3 ml h^{-1}, Figure 3.4ci, *Ca* was below 0.1 leading to a dripping regime (Erb *et al.*, 2011). The viscosity of the dispersed phase depended on the concentration of Eudragit S100 and alginate in the different formulations investigated and varied between 5 - 50 mPas.

Changing the droplet size is an important feature of microfluidics enabling control over phage loading and particle size. Droplet generation in the dripping regime was optimised over a range of flow rates thereby enabling control of the droplet size whilst maintaining a high degree of the size uniformity. This was done in real-time whilst observing (using the microscope camera) the change in the resulting droplet size. When increasing the flow rate of the inner phase relative to the outer phase, the size of the droplets increased; this trend was well documented and observed in many experimental and numerical studies (Ekanem et al., 2015). Typically, the following relationship exists between the drop diameter, d_{drop}, the orifice diameter, $d_{orifice}$, and the flow rate ratio (Goran T. Vladisavljević *et al.*, 2012): $d_{drop}/d_{orifice} = x(Q_c/Q_d)^{-y}$ where x and y are derived from the line of best fit from a plot of drop diameter against flow rate. In accordance with this equation, when the flow rate of the outer phase was increased, the size of the droplets decreased. This was due to the increased pressure and shear stress exerted by the outer phase to break-up the inner phase into droplets.

Droplet size was also controlled by changing the orifice size of the collection capillary (Figure 3.4ci and cii). The plug flow regime occurred due to the high potency of the acid (p-toluenesulfonic acid) in the oil phase resulting in precipitation of the polymer at the water/oil interface during droplet formation. p-toluenesulfonic acid, is a significantly stronger acid (compared with 4-aminobenzoic acid) and resulted in premature polymer curing and a rapid increase in the interfacial tension and the viscosity of the dispersed phase. Because of this phenomenon droplets/particles produced were bigger than the orifice size (Figure 4ciii). The dripping regime could not be established, irrespective of the fluid flow rates, and the droplet production rate was very low.

Orifice diameters of 200 µm and 100 µm produced an average droplet size of 135 µm and 80 µm respectively (Figure 3.4d) for experiments using formulation D1 (Table 3.1) and microfluidic experimental conditions F3 and F5 (Table 3.2). In both cases, the overall droplet size was smaller than the diameter of the orifice minimising the likelihood of contact between the dispersed phase and the orifice walls and associated wetting. The flow rates were reduced when the orifice diameter was changed from 200 µm to 100 µm, to prevent the transition to the 'jetting regime' which would occur due to the high velocity of the two phases entering the collection capillary. Droplets produced by varying the experimental parameters (as described above) resulted in highly uniform droplets with a coefficient of variation of their sizes of less than 2 % (Figure 3.4d).

To test the reliability of the device, the microparticle generation experiment was run for 6 h (using experimental conditions F1, Table 3.2) whilst examining the device integrity and droplet generation behaviour. Visually, the device remained stable over the 6 h period (Figure 3.5a). There was no wetting of the collection capillary which is usually observed when the aqueous phase comes in contact with the capillary wall resulting in polydispersed drops or even the inversion of the emulsion from a water-in-oil to an oil-in water emulsion (Seo *et al*., 2007). Therefore, pre-treating the collection capillary prior to device setup allowed the aqueous phase to resist encountering the capillary wall. At all times, the dispersed phase remained at the centre of the continuous phase stream due to the 3D geometry of the device and perfect coaxial alignment of the two capillaries.

(a)

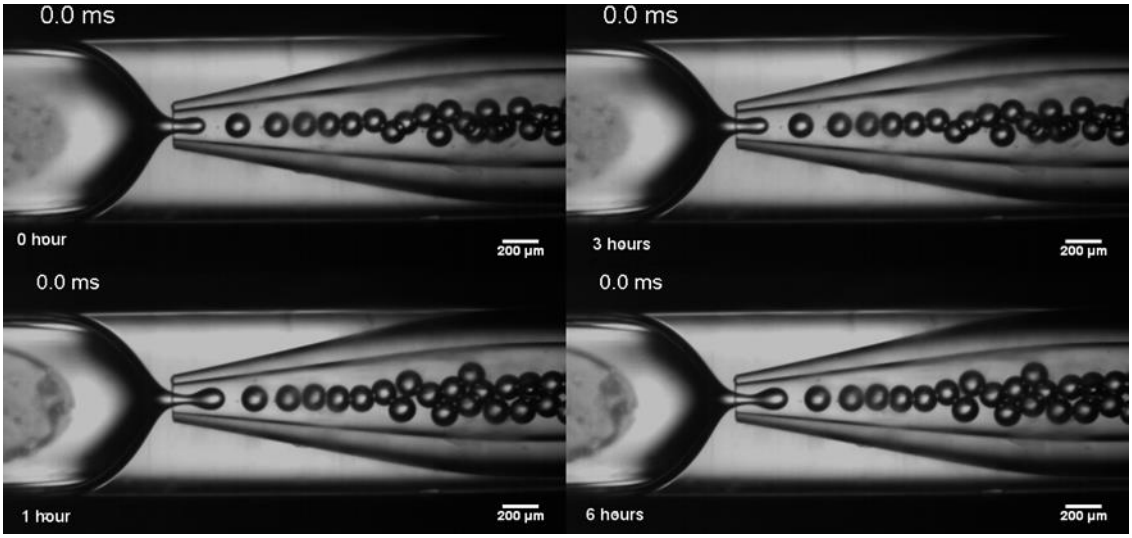

(b)

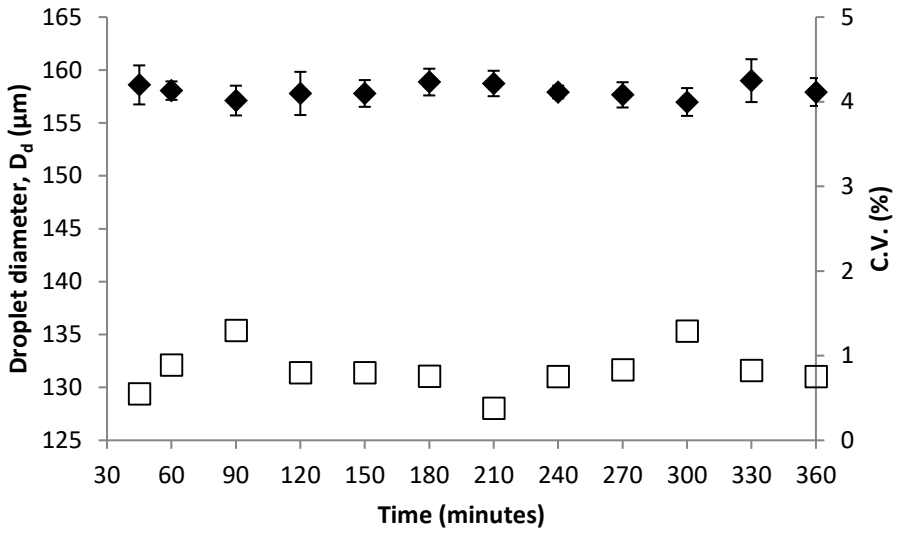

Figure 3.5. Long term stability study of a glass capillary microfluidic device in generating water-in-oil droplets. Aqueous phase: 1 % (w/v) Eudragit S100 and oil phase: 2 % (w/v) PGPR in Miglyol 840. (a) Snapshots of droplet generation over six hours (b) Device function over six hours with corresponding droplet size and coefficient of variation (CV) (D_d = ◆; CV= □). Q_d = 1.2 mlh^{-1}, Q_c = 7 mlh^{-1}, orifice size = 200 µm). Error bars represent one standard deviation (20 droplets counted per time point).

Throughout the microparticle generation process, no air bubbles were seen in the device which can affect the size of the droplets, by restricting the flow of the dispersed phase. A stable flow pattern was observed without interruption or change in phase behaviour. The device remained functional and

identical throughout the six hours of droplet generation; this demonstrated that the device was a reliable means of phage encapsulation contained in the aqueous phase. The stability of the droplet size over the six-hour period is shown in Figure 3.5b. The variation of the droplet size was less than ± 4μm. The coefficient of variation (C.V., a standardized measure of the dispersion of the particle size distribution) measuring the ratio of the standard deviation to the mean droplet size was less than 2 %; it is generally accepted that a C.V. value below 3 % for a particle size distribution is considered highly monodispersed as demonstrated here; thus the glass capillary device was able to produce highly uniform droplets. All experiments were replicated three times; in each case the flow rate and droplet diameter remained consistent. All post-processing was carried out in the same tube resulting in <1 % loss of particles due to processing. The particle sizes were reproducible after all post-processing steps.

3.3.2 Carboxyfluorescein labelled microparticles

Several formulations using carboxyfluorescein as the encapsulated agent were evaluated to find formulations suitable for encapsulation of phage in microparticles formed using the microfluidic device. Carboxyfluorescein encapsulated particles were generated using optimised flow rates of the inner and outer phase; F2, F3, F4 (Table 3.2). The average droplet diameter increased with decreasing Q_c, from 109 μm (F2), to 131 μm (F3) to 170 μm (F4); this was expected due to a decrease in shear and pressure forces acting on the dispersed phase jet with decreasing Q_c (Table 3.2). The change in particle size during curing was observable in real-time using confocal laser scanning microscopy (CLSM) (Figure 3.6). The encapsulation efficiency of the fluorescent dye was 100 %, as no emission was detected in the oil phase.

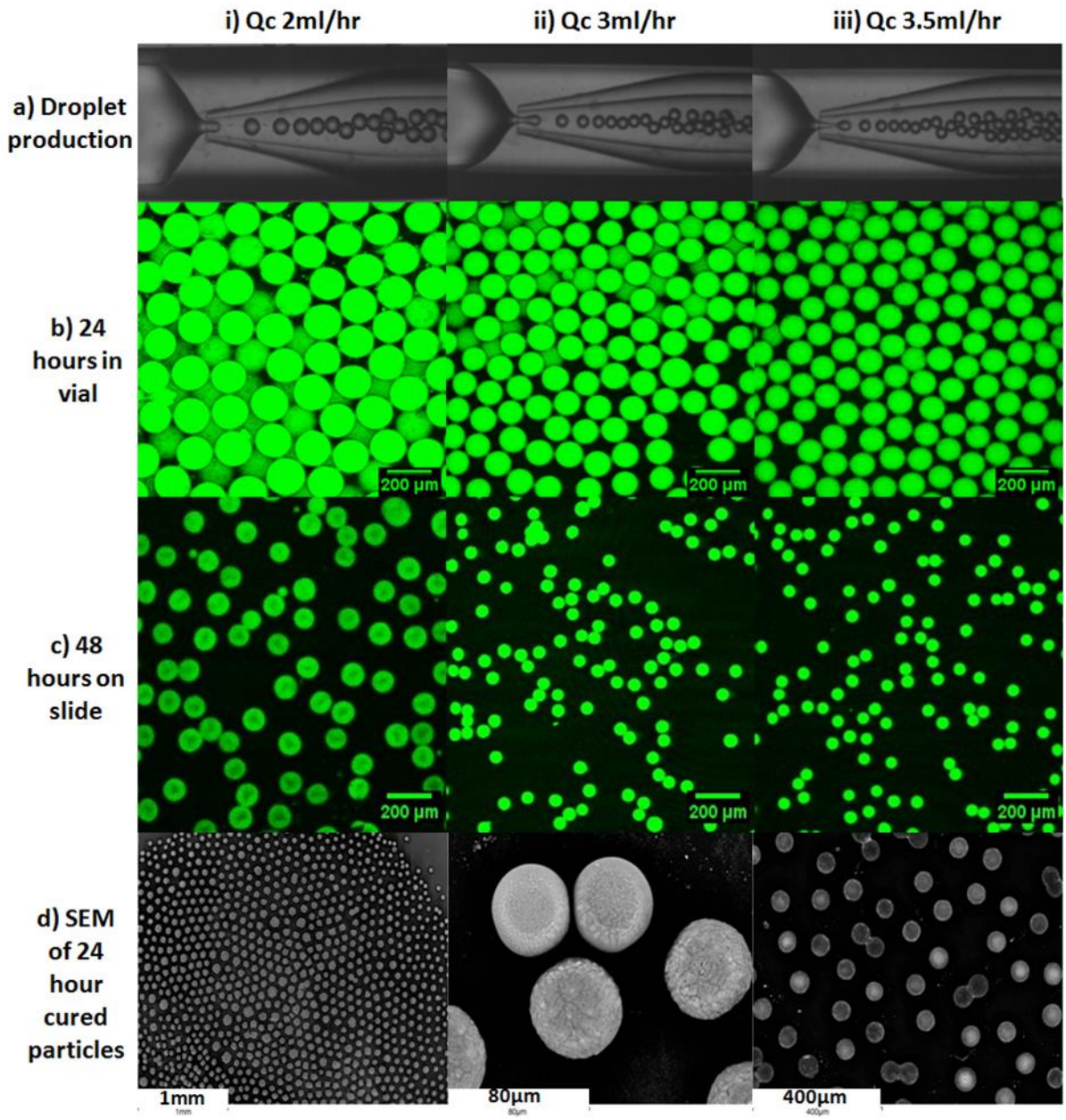

Figure 3.6. Microscopy images of carboxyfluorescein encapsulated particles cured in acidified oil, dried on a microscope slide. (ai-iii) production of droplets in microfluidic device at different Q_c flow rates; (bi-iii) corresponding confocal images of particles cured for 24 hours and 48 hours (ci-iii) produced in (ai-iii); (di-iii) scanning electron microscope images of 24 hours cured particles.

The influence of curing time on particle size was investigated for microparticles cured using 4-aminobenzoic acid. A significant difference was observed between the mean droplet size in the collection capillary just after formation (discussed above and shown in Figure 3.6a) and the mean particle size in the collection vial for samples F2 (104 µm), F3 (113 µm), F4 (155 µm). There was no significant difference between the mean particle sizes for samples F2 - F4 precipitated for 0 h, 24 h or 48 h. Shrinkage of particles was observed after being left to dry on a glass slide and a similar change

in diameter was observed with the SEM analysis, which was due to the loss of water from the particle core and associated shrinkage/collapse of the gel network (Figure 3.6).

To mimic the strong acidic environment encountered during digestion, a 0.1 M hydrochloric acid solution was added to the Eudragit S100 particles loaded with carboxyfluorescein (a surrogate hydrophilic model drug). The time lapse imaging showed no release of the dye into the surrounding environment (Figure 3.7a). This suggested that Eudragit S100 microparticles can retain the dye and maintaining the integrity of the particles in an acidic environment.

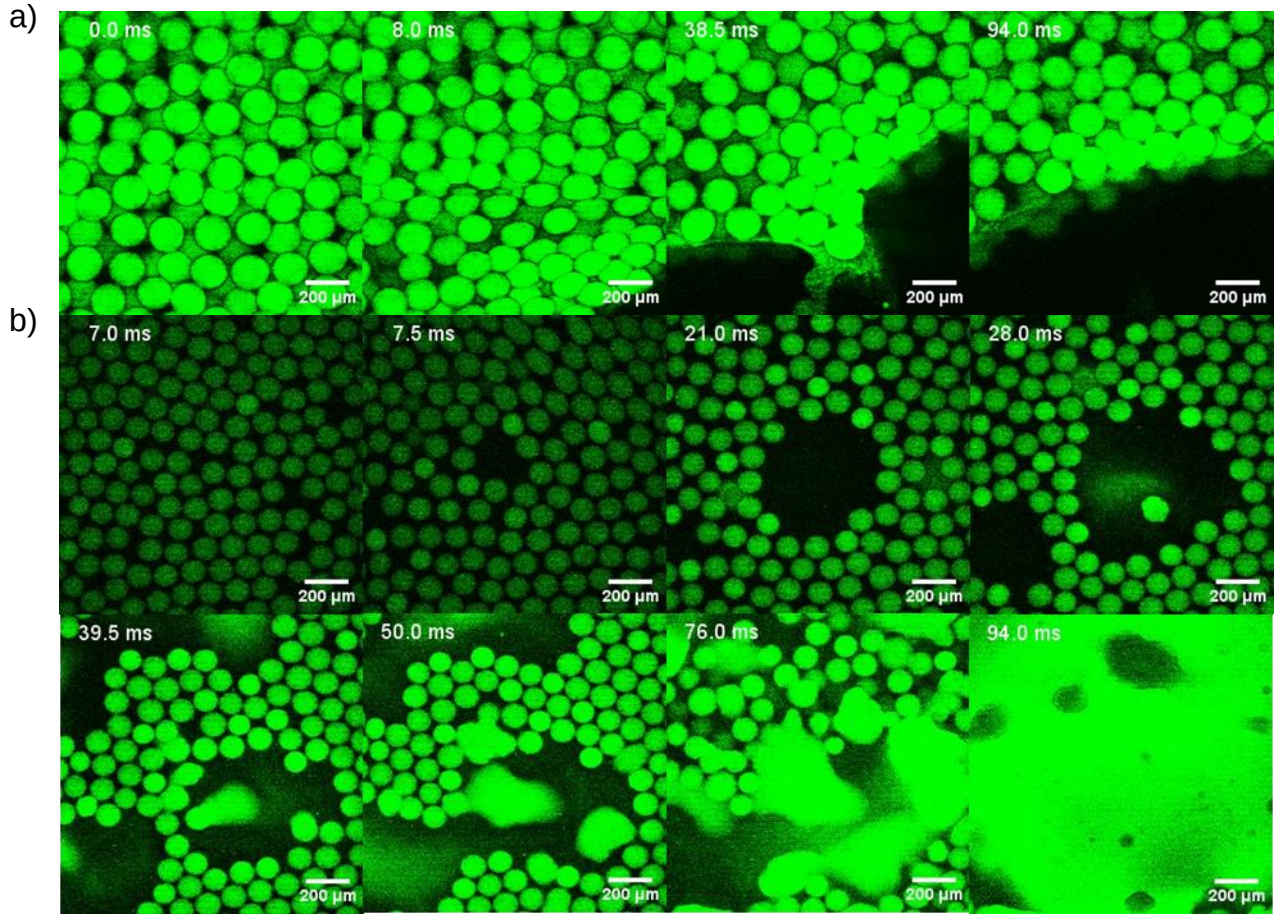

Figure 3.7. Confocal Images showing pH responsive behaviour. Time lapse snapshots (in milliseconds, ms) of carboxyfluorescein (50 µM) encapsulated particles composed of 5 % (w/v) Eudragit S100 (Formulation D2, Table 3.1). a) exposure of ~170 µm particles to 0.1M HCl; b) dissolution of ~170 µm particles in 0.1M NaOH. Snapshot time series in milliseconds (ms).

The particles were then subjected to an alkaline environment using a 0.1 M solution of sodium hydroxide, thereby increasing the pH to basic. Leaching of the dye into the surrounding environment was observed and the particles completely lost their structural integrity (Figure 3.7b). The pH response

of the Eudragit S100 was almost immediate and a burst release of the dye was observed starting from 40 ms. The ionisation of the polymer chains when exposed to sodium hydroxide was immediate with a burst release of the dye as expected due the increased concentration of hydroxyl ions. These results demonstrated the feasibility of encapsulating a water-soluble agent in pH responsive microparticles using formulations that allowed microfluidic fabrication of microparticles.

3.3.3 Transmission electron microscopy (TEM)

TEM analysis confirmed that the CDKM9 bacteriophage belonged to the *myoviridae* family. Typical features revealed a capsid head of approximately 70 nm attached to a tail and baseplate of approximately 200 nm (Figure 3.1b). *Myoviridae* phages contain dsDNA in a non-enveloped capsid; their tails are contractile enabling host cell penetration. The six tail pins and fibres are also characteristic of this type of phage (Figure 1b, c). The host range analysis for this phage has previously been reported by Rashid *et al*., (2016)

3.3.4 Phage sensitivity to formulation parameters

The effect of different formulation parameters on free phage viability and therefore their impact on phage encapsulation was evaluated. Little work has been done to date on formulation of *C. difficile* specific phages showing the effect of physical and chemical environmental factors on phage viability. Free phage in BHI alone were used as a control and compared with phage preparations subjected to different formulations. Firstly, the effect of pH on phage viability was tested for phages that were suspended in a 0.2 M sodium chloride solution at different pH. The phage lost nearly all activity after 10 min of exposure to pH 2 (Figure 3.8a). Phage viability was significantly improved when the solution pH was above pH 3. Although there was a statistically significant reduction in phage viability for phages exposed to solutions at pH 6 and pH 7 the 95% confidence intervals for the means do overlap suggesting a modest difference in means and not dissimilar to data observed for phages exposed to BHI over a 24 h period (Figure 3.8a). Phage titres reduced by about one log at pH 4 and pH 5 (Figure 3.8a).

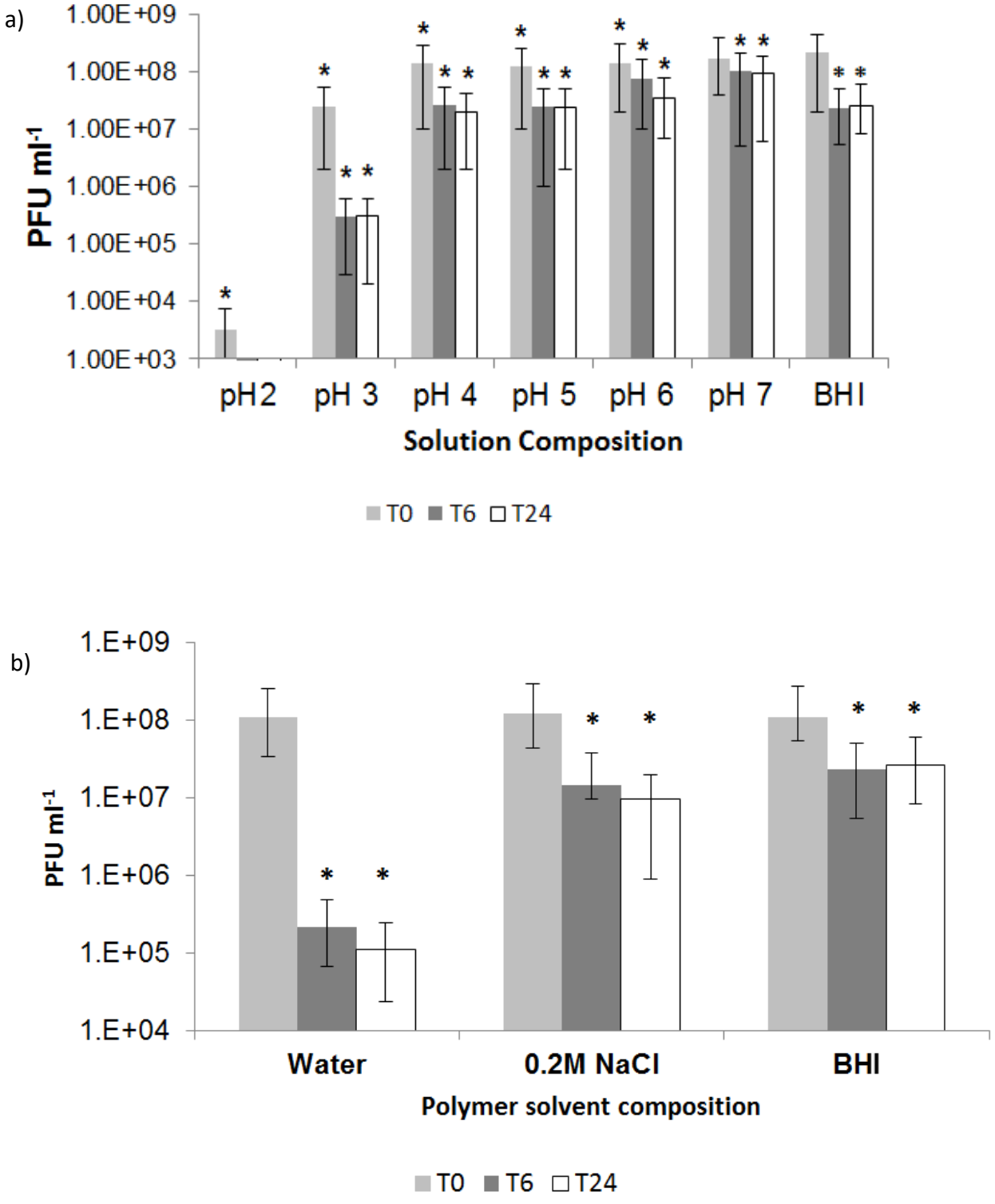

Figure 3.8. Influence of formulation parameters on free phage viability at various exposure times. a) effect of pH on free phage viability in 0.2 M NaCl solution. * indicates significantly different phage titres using a 2-sample t-test at each condition compared with phage in BHI (controls) at T0 ($p < 0.05$). Error bars indicate 95% confidence intervals for means.; b) effect of polymer solvent on free phage viability. T0 point denotes time between 0 – 10 min, T6 exposure to solution for 6h and T24 exposure

for 24h. * indicates significantly different phage titres using a 2-sample t-test at each condition compared with phage at T0 for each composition ($p < 0.05$). Error bars indicate 95% confidence intervals for means.

Phages are usually stored in broth (e.g. BHI broth used here), however, dispersing phage in a polymer solution may adversely impact phage viability. The effect of different dissolution media used to dissolve Eudragit S100 on phage activity was investigated (Figure 8b). The greatest loss of phage titre was in a polymer solution where the polymer was dissolved in water, and the pH adjusted to pH 7, a 3- log reduction in phage titre was observed. Water was therefore not used for phage formulation.

Eudragit S100 was also dissolved in 0.2 M sodium chloride solution (Figure 3.8b) as this has been previously shown to help protect phages from osmotic shock (Leibo & Mazur, 1966). Phage viability over 24 h of exposure to 0.2 M solution of sodium chloride showed that the phage titre was reduced by ~1 log (Figure 3.8b). DNA may be lost from phage capsids under high osmotic pressure and therefore the presence of salt is an important consideration for phage stability and receptor binding (S. Huang *et al.*, 2008; Leibo & Mazur, 1966). Phage viability in 5 % (w/v) Eudragit S100 dissolved in BHI broth was tested showing around ~1 log reduction in phage titre like results for 0.2 M sodium chloride.

Phage stocks stored in BHI broth at 4°C showed no greater than ~1 log reduction in phage viability stored over a period of 2 months. Storage temperature between 4˚C and 20˚C had no significant effect on the phage titre for phages stored in BHI broth (data not shown).

3.3.5 Phage release in simulated fluids

Following washing and removal of Miglyol, encapsulated phage particles were added to shaking solutions containing simulated intestinal fluid. The release of phages in simulated intestinal fluid was assayed over 24 h at two different pH values (Figure 3.9a). Eudragit S100 is a pH responsive polymer, known to dissolve at around pH 7. Near 100% (typically > 95%) encapsulation of phages was observed following the entire encapsulation and washing procedures. For pure Eudragit S100 microparticles, an initial burst release (around 10 % of the phage loading) was observed at pH 7 suggesting phages were rapidly able to permeate across the porous microparticle shell. Initially, there is a large phage concentration gradient due to the concentration of phages in the microparticle compared with the outside solution. This gradient drives phages to diffuse into the external solution. The concentration gradient gradually reduces, and the phage release slows down over time. Release of phage at pH 7 may be attributed to polymer shell swelling as polymer chains begin to disentangle upon exposure to

the buffer and ion exchange occurs between the counter ions H^+ replaced by Na^+ and dissociation of the carboxylic acid groups (Nguyen & Fogler, 2005). Phage release in pH 7 was fast (burst release) with most release taking place within an hour of exposure to buffer. Even over a 24 h exposure period to SIF at pH 6 phage only ~ 10% of encapsulated phage was released. 100% release of phage at pH 7 corresponded with a calculated phage dose of ~3.1 x 10^8 PFU ml^{-1}.

Pure Eudragit ES100 microparticles exposed to simulated gastric fluid (pH 2) for 3 hours resulted in complete inactivation of phage with no detected phage release in simulated intestinal fluid (Figure 3.9b).

a)

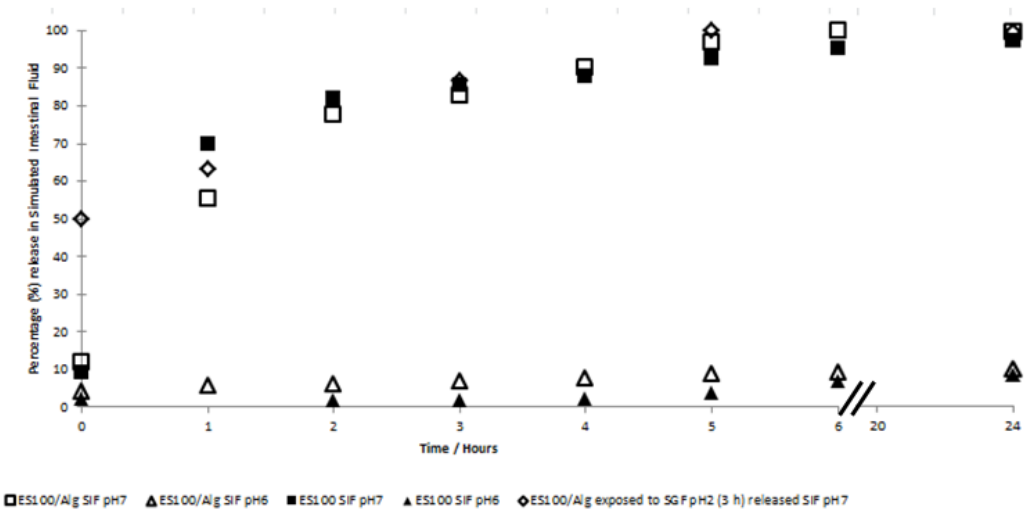

b)

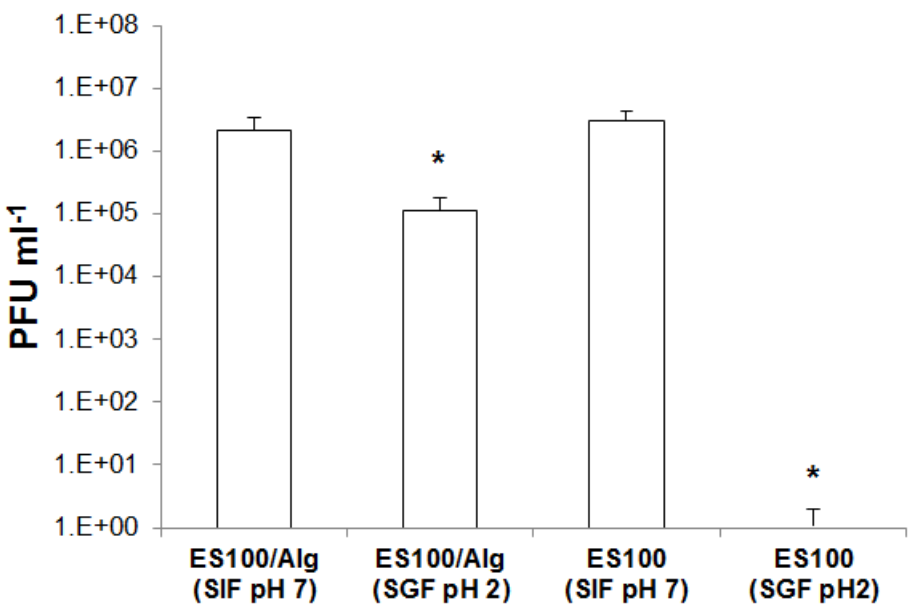

Figure 3.9. Release of encapsulated phage from microparticles. a) Phage release kinetics from Eudragit S100 (ES100) and ES100/Alginate microparticles exposed to Simulated Intestinal Fluid (SIF) at pH 6 and

pH 7 and from ES100/Alginate microparticles exposed to Simulated Gastric Fluid (SGF, pH 2, 3 h exposure) followed by release in SIF at pH 7; b) Quantitative titres of phages released at 24 h in Fig 9a above. Samples labelled pH 2 were exposed to SGF (pH 2, 3 h exposure) followed by release in SIF at pH 7. * indicates significantly different phage titres ($p < 0.05$) for a 2-sample t-test of each sample compared with phage release from ES100/Alginate (SIF pH 7). Summary statistics for data are presented in Table 3.3.

Table 3.3 Summary of microencapsulated CDKM9 release results (2-sample t-test for means).

Sample ID	**Mean / PFU ml^{-1}**	**StDev / PFU ml^{-1}**	**Lower 95% CI**	**Upper 95% CI**	**p-value**	**Sample size (n)**	**Null hypothesis**
ES100/Alg (SIF)	2.1 x10^{6}	4.5 x 10^{5}	1.4 x 10^{6}	2.8 x 10^{6}	-	4	NA
ES100/Alg (SGF)	1.1 x 10^{5}	1.8 x 10^{4}	7.6 x 10^{4}	1.3 x 10^{5}	0.000	4	Mean = 2.1 x 10^{6}
ES100 (SIF)	3.1 x 10^{6}	7.6 x 10^{5}	1.3 x 10^{6}	5.1 x 10^{6}	0.121	3	Mean = 2.1 x 10^{6}
ES100 (SGF)	0	NA	NA	NA	NA	4	NA

Notes: Reported mean values are after 24 h exposure to simulated intestinal fluid; CI = confidence interval; $p < 0.05$ indicates rejection of null hypothesis;

Phage encapsulated in pure alginate microparticles were completely inactivated following acid exposure to simulated gastric fluid (see supplementary information, S1 FIG). With the addition of alginate to Eudragit S100 particles, significant protection of phage against acidic pH in simulated gastric fluid was achieved (Figure 3.9b). There was around ~1 log reduction in phage titre in comparison with encapsulated phage not exposed to simulated gastric fluid. The calculated dose for 100% release of phage at pH 7 in SIF following SGF exposure was ~ 1.1 x 10^{7} PFU g^{-1}.

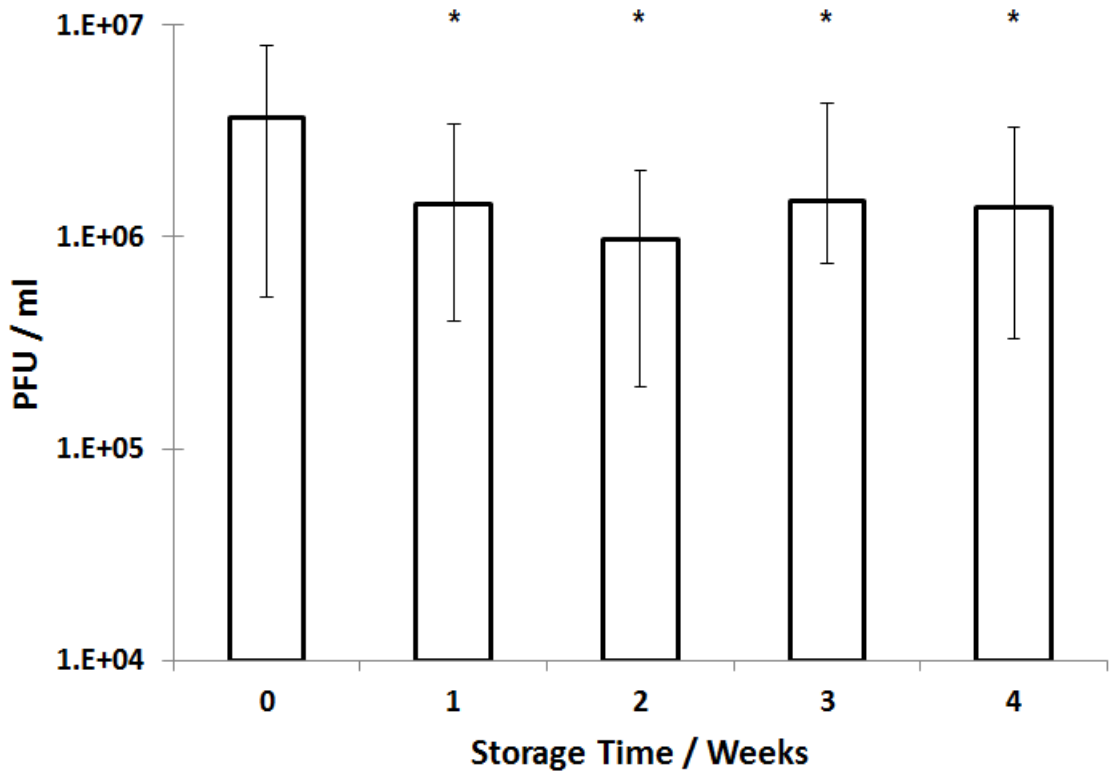

Figure 3.10. Storage stability of encapsulated CDKM9 phage in ES100/Alginate microparticles refrigerated at 4°C. Phage titre was evaluated by exposing microparticles to simulated intestinal fluid. * indicates significance as compared with sample at week 0 ($p < 0.05$) using a 2-sample t-test.

3.3.6 Storage of Ephage

ES100/Alg microparticles stored over the course of 4 weeks under refrigerated conditions (at 4°C) showed a modest drop in phage titre (Figure 3.10). Phage titre dropped from ~ 4 x 10^6 PFU ml^{-1} (4 x 10^8 PFU g^{-1} of microparticles) at week 0 to 1 x 10^6 PFU ml^{-1} (1 x 10^8 PFU g^{-1} of microparticles) after 1 week of storage. Thereafter, the titre remained stable up to week 4.

3.4 Discussion

A limited range of microencapsulation techniques have previously been employed for bacteriophage encapsulation, with extrusion based droplet formation the most frequently used method (Colom *et al.*, 2017a; C Dini *et al.*, 2012; S. Kim *et al.*, 2015a; Yongsheng Ma *et al.*, 2008, 2012; Samtlebe *et al.*, 2016; Tang *et al.*, 2014; Wall *et al.*, 2010). None have employed microfluidic fabrication techniques used here. The principle driver for encapsulation has been to protect phages from the stomach acidity. In a considerable number of previously published studies, the sizes of phage encapsulated

microparticles have tended to be considerably larger than those reported here (an order of magnitude bigger). Little consideration has previously been given to the control of the particle size distribution, the phage loading per particle and the resulting heterogeneity of the release kinetics from each particle (S. Kim *et al.*, 2015a; Yongsheng Ma *et al.*, 2008, 2012, Tang *et al*., 2013, 2014). A key advantage of the microfluidic fabrication process used here is the precision with which uniform small droplets (mean size ~100 µm) containing encapsulated phage may be prepared under low shear conditions resulting in near 100 % phage encapsulation efficiency.

The importance of establishing a stable dripping regime means that each droplet was produced at the same position; it may therefore be assumed that the disruptive forces of the same magnitude acted on each individual droplet and these forces became negligible after pinch-off. This is a rare occurrence because in conventional bulk emulsification systems, the droplets are continuously being subjected to shear which typically varies widely across the mixing container or valve (Egidi *et al*., & Kosvintsev, 2008; Stillwell *et al.*, 2007); this is true when encapsulation is carried out using conventional homogenisation or atomisation techniques (Jain *et al*., 2005; Sağlam *et al.*, 2011; Un & Lements, 2007). Continuous excessive exposure to shear results in the droplets breaking further into smaller droplets resulting in emulsions with a high polydispersity index (Kong *et al*., 2012). The microfluidic fabrication process provides a highly controlled uniform shear environment resulting in monodispersed microparticles.

It is well known that phage are sensitive to physical and chemical stresses including shear (S. S. Y. Leung *et al*., 2016; Vandenheuvel *et al*., 2013a), temperature (Vandenheuvel et al., 2013a), pH (Briers *et al.*, 2008), ionic strength (Knezevic *et al.*, 2011), exposure to organic solvents (S. W. Lee & Belcher, 2004; Puapermpoonsiri *et al.*, 2009) etc. Formulations used for phage encapsulation require careful selection of constituents and encapsulation conditions. Phage CDKM9 was shown to be highly sensitive to acidic pH. Similar results have been reported previously for a number of other therapeutic phages including a *Salmonella* phage Felix O1 (a myovirus) (Yongsheng Ma *et al*., 2008), a *Staphylococcus aureus* bacteriophage K (also a myovirus) (S. Kim *et al*., 2015a; Yongsheng Ma *et al.*, 2012) and for an *E. coli* specific phage exposed for 5 min at pH 2 (S. Kim et al., 2015a). This loss of phage activity highlights the need to protect the phage from the harsh acidic environment of the stomach if controlled doses of phage are to be reliably delivered at the infected colon. Our results show that phage CDKM9 may be acceptably formulated in a low molarity salt solution containing mixtures of dissolved polymers alginate and Eudragit. The observation that pH conditions typically found in the colon do not detrimentally affect phage activity is promising as viable phages need to be released at the site of infection in the colon (where the environmental pH may vary from neutral to

alkaline) and remain viable after release. Previously McConnell *et al.,* (2008) reported that the pH of the colon can fall during bacterial infection to around or just below pH 7; in such a case, the released phage should remain viable and capable of lysing the infecting *C. difficile* bacteria causing CDI. Osmotic damage to phage during phage processing and storage is an important consideration (Davies & Kelly, 1969). Governal and Gerba (1997) reported activity of an *E. coli* phage dropped by 2 log upon exposure to ultrapure water. Our results also suggest that phage CDKM9 titre drops upon exposure to deionised water. Phages from the *Myoviridae* family, are known to be one of the most stable types of phages however, a number of studies suggest considerable variation in phage stability exposed to identical stress conditions (Vandenheuvel *et al*., 2013a). We have shown that phage CDKM9 may be formulated with Eudragit in a 0.2 M salt solution. Merabishvili *et al.*, (2013) showed that an S. aureus phage (from the *Myoviridae* family) formulated in ~2 mM salt solution may be stored under refrigerated conditions for up to 3 months without loss of phage titre. Generally, BHI broth is the storage medium of choice for phage stocks; it is known to keep phages stable whilst stored over long periods of time (Jończyk *et al.*, 2011). Although phage CDKM9 may be formulated with Eudragit in BHI, we decided to avoid working with a complex broth medium since both saline and broth showed similar phage viability results.

A number of previous studies have used alginate as the main encapsulating agent either on its own (Colom *et al.*, 2017a; Yongsheng Ma *et al.*, 2012; Wall *et al.*, 2010) or in combination with whey protein (Samtlebe *et al*., 2016; Tang *et al*., 2013, 2014) or chitosan (S. Kim *et al.*, 2015a; Yongsheng Ma *et al*., 2008). Phages encapsulated in crosslinked pure alginate microparticles were found to be susceptible to acid damage following exposure to simulated gastric fluid (C Dini *et al*., 2012; Yongsheng Ma *et al*., 2008, 2012). Alginate hydrogel pores tend to be in the 5-200 nm range depending on the degree of crosslinking (George & Abraham, 2006). The porosity of the alginate gel microparticles affects phage susceptibility to acid damage due to diffusion of acid. A number of studies have added $CaCO_3$ within the microparticles to protect phage from acid damage (Colom *et al*., 2017a; Yongsheng Ma *et al*., 2012). Other studies have shown that by combining alginate with chitosan (S. Kim, Jo, & Ahn, 2015b; Yongsheng Ma *et al.*, 2008) or whey protein (Samtlebe *et al.*, 2016; Tang *et al*., 2013, 2014), better acid protection may be achieved. We have shown that by combining the pH responsive character of Eudragit with alginate, phage CDKM9 was significantly protected from exposure to simulated gastric fluid at pH 2 and could thereafter be readily released upon exposure to pH 7. Furthermore, the microparticles were stable upon storage under refrigerated conditions for up to 4 weeks. The combination of small particle size and pH responsive character of the encapsulating polymer resulted in rapid release of phage within the first hour upon exposure to pH 7 whereas release was negligible at pH 6. Previous studies on phage encapsulated in large microparticles (~ 1mm) have reported slower

sustained release kinetics for alginate encapsulated phage (S. Kim *et al.*, 2015a; Yongsheng Ma *et al*., 2008). Colom *et al*., (2017a) reported faster release from small alginate microparticles containing $CaCO_3$ as antacid (mean size ~ 100 µm). However, exposure to simulated gastric fluid (pH 2.8 for 60 min) resulted in between 2 log and 3 log reduction in *Salmonella* phage titre suggesting that even with the addition of $CaCO_3$, phage were highly susceptible to SGF. Particle size was found to be an important factor influencing phage protection from SGF for acid permeable beads (Tang *et al.*, 2014). Alginate-whey protein microparticles having the same composition but different mean sizes showed larger particles protected phage better compared with smaller microparticles (Tang *et al.*, 2014). The diffusion path length of acid is increased with particle size thereby affording protection to phage further away from the bead surface. We have shown that encapsulation of phage in Eudragit/alginate microparticles (mean size ~ 100 µm) may permit rapid burst release of phage cargo without significant acid damage. In future studies, it may be possible to tailor phage release kinetics through controlling the microparticle size and the shell composition (e.g. Eudragit to alginate ratio); this work is currently underway in our laboratory.

A number of *in vivo* animal studies have shown dose dependent phage therapy outcomes, with high doses of phage resulting in better clinical results (Biswas *et al.*, 2002; Cerveny *et al.*, 2002; Smith *et al.*, 1987; Wills *et al.*, 2005). Accurate control over the phage dose delivered at the site of infection and the timing of the delivery are important considerations (Sarker *et al*., 2016). Careful formulation and microfluidic loading of phage (resulting in uniform particle size) would facilitate control over the phage release dynamics and accurate delivery of the phage dosage. This has so far received little attention in the published literature. We have demonstrated that even after exposure of phage encapsulated microparticles to simulated gastric fluid at pH 2 for 3 hours, the released phage dose corresponds to ~ 1×10^7 PFU g^{-1} of phage microparticles. The encapsulated dose was ~ 2×10^8 PFU g^{-1} of phage microparticles. One gram of microparticles would therefore deliver a ~10^7 PFU dose which is similar to therapeutic doses given in a number of animal studies (Smith *et al.*, 1987; Barrow and Lovell, 1998; Chibani-chennoufi *et al.*, 2004; Abdulamir, Sabah and BakarFatimah;, 2014; Nale *et al.*, 2016; Yen *et al.*, 2017). Nale *et al*., (2016) in their hamster *C. difficile* infection model delivered an unformulated phage suspension at a dose of ~ 10^8 PFU/hamster. The actual dose delivered to the site of infection would have been considerably lower. Failure of the recently concluded phage trial for the treatment of *E coli* diarrhoea in children was attributed to the lack of clinical host range coverage of the employed *E.coli* phages to the disease-causing bacteria (faecal phage titres were not higher in patients harbouring a phage sensitive E. coli colony in the stool; around 50% of all patients). A drop in phage titre due to phage exposure to stomach acidity may also have been a factor in the consequent lack of *in situ* phage amplification (Sarker *et al.*, 2016). Stanford *et al*., (2010) previously used Eudragit S100,

for phage encapsulation and enteric delivery targeting *E. coli* infection in cattle. A spray dryer was used to encapsulate phages into a dry powder, which was administered either as a bolus or added to the feed directly. The method was not optimised to protect the phage from the stomach acidity. Some protection of phages from stomach acidic pH was seen with phage replicating *in vivo* and a lower *E. coli* faecal shedding rate was observed in phage treated cattle. We have demonstrated much improved acid protection of phage encapsulated in highly uniform Eudragit/alginate microparticles; a significant step forward compared with previously published work.

Delivery systems and their formulation require consideration of the bioavailabity of the active agent at the site of infection. The size of microparticles may play an important role by ensuring it is minimally affected by the conditions of the diseased state. The small intestine and the colon are connected via a junction known as the ileum; while *C. difficile* infection has been reported to occur and cause disease in the small intestine (Navaneethan & Giannella, 2009), in most patients the bacterium mainly affects the colon. Nevertheless, release of phage in the small intestine as microparticles transit towards the colon may prove beneficial in eradicating CDI for a wide range of patients. Other considerations for colon targeted delivery of active agents include the changes in transit times during infection. Increased loss of fluid from the colon due to symptoms such as diarrhoea result in observed shortened mean transit times. Dilution of phage due to the high fluid environment may be a particular challenge. Larger particles (~ mm size range) may be more prone to the influence of short transit times. Smaller particles may be predisposed to non-specific mucoadhesion (Alhnan *et al.*, 2010; Kietzmann *et al*., 2010) which may aid in phage retention and sustained release over a signficant time period. Colom *et al*., (2017a) showed better phage retention (for animals treated with encapsulated phage versus those treated with free phage) in the caecum of chickens and a significant reduction in *Salmonella* colonisation, attributing these results to the mucoadhesiveness of the small alginate microparticles (~ 100 µm) used for encapsulating phage. Wittaya-areekul *et al*., (2006) showed differences in mucoadhesion properties of chitosan coated alginate microparticles using an *in vitro* assay using porcine gut tissue samples.

Gastrointestinal infections can affect different parts of the gut. In future different phage fomulations may need to be developed targeting phage release in the appropriate intestinal region perhaps using more specific infection related triggers e.g. enzymes or toxins released by the bacterium causing the infection (Bean *et al*., 2014).

A limitation of phages for therapeutic use (*C. difficile* phages such as CDKM9 are no exception) is their narrow host range. Most phages only infect a small number of prevalent strains, thereby necessitating

the use of phage cocktails to provide adequate therapeutic coverage. Phages incorporated in the cocktail may require tailored formulations to ensure adequate stability (Malik *et al.*, 2017).

Microfluidic systems such as the one described in the present work have the potential to enable precise control of the particle size and loading of the phages within the microparticles. Here, we have demonstrated for the first time, proof-of-concept data in support of this platform technology for the production of encapsulated phage in a pH responsive polymer suitable for targeted intestinal phage delivery. An eight week study on the use of Eudragit coated mesalazine tablets in patients with mild to moderately active ulcerative colitis (Gibson *et al.*, 2006) showed that the tablets were well tolerated suggesting Eudragit® based microencapsulation of phages may be safe for use in humans.

3.5 Conclusions

Highly uniform small microparticles (mean size ~ 100 µm) of Eudragit S100 or Eudragit S100/alginate were generated using a flow-focussing glass capillary device. A novel mechanism of microparticle formation was demonstrated using acidified medium-chain triglycerides in a water-in-oil emulsion system. Solid core-shell microparticles were produced with a low polydispersity index enabling control over phage loading and their subsequent pH triggered release. Encapsulation of carboxyfluorescein in Eudragit S100 particles was visualised using confocal laser scanning microscopy and examined under different conditions elucidating the effect of different formulation and microfluidic experimental parameters on particle size. Phage encapsulation and subsequent release kinetics revealed that microparticles prepared using Eudragit S100 formulations possess pH responsive characteristics with phage release triggered in an intestinal pH range suitable for therapeutic purposes. The encapsulated phages were shown to be significantly protected upon prolonged exposure to an acidic environment without the addition of an antacid in the formulation. We have also demonstrated the storage stability of the encapsulated phage under refrigerated conditions over a 4-week storage period. Future work will investigate the efficacy of the encapsulated phages by controlling phage loading and release rates on bacterial inactivation in suitable *in vitro* chemostat type systems as well as in tissue culture models and long term in relevant animal infection models.

Chapter 4: Microfluidic encapsulation of bacteriophages in a commercial chip with high precision control

Abstract

A *Salmonella* specific bacteriophage Felix O1 (Myoviridae) was microencapsulated in a pH responsive polymer formulation. The formulation incorporated a commercially available pH responsive polymer Eudragit S100 (10 % w/v), with the addition of the biopolymer sodium alginate whose composition was varied (0.5 % w/v - 2 % w/v). The microencapsulation process employed a commercially available microfluidic droplet generation device. A key feature of the microfluidic process was the exquisite control over the uniformity of the droplet size, phage dose and high encapsulation efficiency (~100%). Monodispersed droplets were subsequently crosslinked into highly uniform spherical gelled microparticles containing viable encapsulated phages. A novelty of the work reported here is that the size of the generated monodispersed droplets could be precisely controlled in the range 50 µm to 200 µm by varying the flow rates of the dispersed and continuous phases. Consequently, alginate concentration and microparticle size were shown to influence the phage release profile and most importantly the degree of acid protection afforded to phages upon exposure to simulated gastric fluid (SGF). Bigger microparticles (~100 µm) showed better acid protection compared with smaller beads (~50 µm) made from the same formulation. Increasing the alginate composition resulted in improved acid protection of phages, however, high viscosity formulations containing 2 % (w/v) alginate negatively affected ease of droplet generation in the microfluidic device thereby posing a limitation in terms of process scale-up. Optimisation of microcapsule size and alginate composition was carried out. Felix O1 encapsulated in 10 % (w/v) ES100 and 1 % (w/v) alginate showed excellent protection upon exposure of the gelled microparticles to SGF at pH 1 for 2 h without the use of any antacids in the encapsulation matrix. Encapsulated phages previously exposed to SGF at pH 1 for 2 h were released at elevated pH in simulated intestinal fluid (SIF) and arrested bacterial growth in the log growth phase. The significance of our research is in demonstrating the use of microfluidic microencapsulation of phages to produce solid dosage microcapsule forms providing a high level of acid protection with a rapid pH triggered release profile suitable for targeted delivery and controlled release in the gastrointestinal tract.

4.1 Introduction

It is estimated that *Salmonella* alone accounts for 1.2 million foodborne illnesses in the United States, with 23,000 hospitalisations and 450 deaths costing an estimated 365 million dollars in medical costs each year (Scallan *et al*., 2011). Increasing centralisation and industrialisation of food supply enhances the probability of distribution of these hardy organisms. Antimicrobial resistance to 'first-line' drugs is increasingly common among *Salmonella* worldwide (Hohmann, 2001). In animals, decolonisation of the gastrointestinal tract from *Salmonella* may be beneficial for biocontrol to reduce dissemination of harmful bacteria through the food chain e.g. lairage associated *Salmonella* transmission in pigs (Wall *et al.*, 2010). Ensuring delivery and subsequent release of a precise high dose of phages to the site of infection in the gastrointestinal tract remains an important challenge to ensure that phage therapy develops its full potential as a therapeutic or prophylactic antimicrobial agent (Malik *et al*., 2017). Encapsulation may help protect phages from loss of activity during manufacturing and storage and during transit through the stomach *en route* further downstream in the gastrointestinal tract. Encapsulation in solid dosage forms e.g. microcapsules may also permit easy oral dose application allowing phage administration through feed instead of administration via oral gavage.

When free phages are delivered orally for phage therapy or for modulating microbiota, there is likely to be variable but significant losses of phage titre by the time phages reach the intended infection site (Young & Gill, 2015). Oral application of phages exposes them to stomach acidity, digestive tract contents (e.g. enzymes such as pepsin and pancreatin) which can inactivate phages (Denou *et al.*, 2009). A recent *in vivo* study in chickens (phage were added to animal feed) using alginate microencapsulated *Salmonella* Felix O1 phages showed a significant reduction in levels of phage titre (3 log reduction compared to the dose given) found in the gastrointestinal tract (Yin-hing Ma *et al*., 2014). Potential reduction in phage titres due to inactivation attributed to stomach acidity may in part have been responsible for failure of a recent clinical trial treating acute bacterial diarrhoea symptoms in children using phage therapy (Sarker *et al*., 2016). Acidic conditions encountered in the stomach and the presence of bile and digestive enzymes and other proteases in the intestinal tract and stomach may inactivate unformulated phages (Choinska-Pulit *et al*., 2015; Yongsheng Ma *et al.*, 2008; Tang *et al.*, 2013). Use of antacids may increase the risk of gastroenteritis and its use was not permitted in a recent clinical trial (Sarker *et al*., 2016). In a separate study, mice were given an oral dose (T4 coliphages in drinking water) of 10^9 PFU/g gut contents which resulted in a 1000-fold lower titer, indicating a sizable loss in phage activity (Denou *et al*., 2009). Therefore, there are clear drivers to protect phages against adverse gastrointestinal conditions by encapsulating them and to control their targeted release at the site of infection e.g. in the lower gastrointestinal tract (GIT) i.e. ileum, cecum

and colon for *Salmonella* and other enteric infections (S. Kim *et al*., 2015a; Yongsheng Ma *et al.*, 2008; Tang *et al.*, 2013).

Previous phage encapsulation strategies have used basic homogeniser and extrusion techniques and have employed formulations that are gentle in terms of avoiding use of organic solvents that would inactivate phages (Yongsheng Ma *et al.*, 2008, 2012; Puapermpoonsiri *et al*., 2009; Shi et al., 2016; Tang *et al*., 2013). These studies have shown modest protection of phages when the capsules were exposed to simulated gastric fluid at pH values in the range 2 – 2.5, for up to 2 h exposure duration. (Vinner *et al.*, 2017) recently showed for the first time the potential of microfluidic encapsulation for a *C. difficile* specific phage using an in-house developed microfluidic device (Vinner *et al*., 2017). In-house built microfluidic droplet generation devices are highly versatile however they require a high level of fabrication expertise including access to specialist micro-forging equipment, the devices are fragile, difficult to handle, prone at times to leakages and ingress of air bubbles causing contamination and production issues especially for processing of biological materials.

Aims and objectives

The aim of this study was to use commercially available low-cost glass microfluidic droplet generation systems to microencapsulate phage. Additionally, in the previous chapter the phage titre for the encapsulated *C. difficile* specific phage was rather low (10^7 PFU ml^{-1}), the formulation was not optimised, and acid protection was limited to pH 2. The objectives here were to precisely control microparticle size and hence investigate the effect of particle size and formulation parameters (alginate concentration) to prepare pH responsive microparticles that were able to withstand significantly low gastric acidity (as low as pH 1 for 2 h) without appreciable loss in phage activity at high encapsulated phage titres.

4.2 Materials and Methods

4.2.1 Chemical reagents

A methyl methacrylate co-methacrylic acid copolymer Eudragit S100 was purchased from Evonik, Germany. Miglyol 840, a propylene glycol diester of caprylic/capric acid, was purchased from Sasol, Germany and used as carrier oil for the continuous phase. Polyglycerol polyricinoleate (PGPR), an oil soluble surfactant, was purchased from Abitek USA. Para-toluenesulfonic acid and sodium chloride were purchased from Fisher Scientific, UK. Sorensen's buffer 0.2 M was used as a dissolution media for the microparticles and was prepared by mixing sodium phosphate (NaH_2PO_4) with sodium

phosphate dibasic (Na_2HPO_4) (for pH 7) (Fisher Scientific UK). Alginate was purchased from Sigma Aldrich, UK.

4.2.2 *Salmonella* strain and bacteriophage Felix O1

Salmonella enterica ATCC19585 was purchased from LGC standards, EU (Figure 9.9 appendix). Phage Felix O1 was kindly donated by Dr Cath Rees, University of Nottingham, UK (Siqueira, Dodd, & Rees, 2006). *S. enterica* strain was used to propagate and enumerate Felix O1 (Figure 9.10 and 9.11 appendix). Brain heart infusion broth and agar (Oxoid UK.) were used for all bacterial work. A single colony from a streaked overnight culture on a BHI agar plate was used to inoculate fresh BHI broth and left shaking overnight at 37˚C. The culture was diluted and regrown to log phase at 0.2 O.D. (550nm) for all phage work.

Table 4.1. Compositions of formulations and operating parameters for microfluidic device used to prepare emulsion droplets.

Formulation ID	**D1**	**D2(s)**	**D2(b)**	**D3**
Composition	10 % (w/v) ES100 2 % (w/v) Alginate ~10^9 PFU/ml	10 % (w/v) ES100 1 % (w/v) Alginate ~10^9 PFU/ml	10 % (w/v) ES100 1 % (w/v) Alginate ~10^9 PFU/ml	10 % (w/v) ES100 0.5 % (w/v) Alginate ~10^9 PFU/ml
Dispersed phase flow rate, Q_d / µl h^{-1}	50	25	100	50
Continuous phase flow rate, Q_c / µl h^{-1}	1000	1000	1000	500

Felix O1 was propagated by infecting a log phase culture of *S. enterica* at MOI 0.01. Once the culture had cleared the lysate was centrifuged at 2000 g for 15 mins at 4˚C and filtered using a 0.2 µm pore size filter (Millipore, USA). All phage stocks were stored at 4˚C until further use.

To titre the phage stocks, 10 µl of phage stock was serially diluted (10-fold) to 10^{-8} in 90 µl of BHI broth. This was spotted in triplicate on a double layer agar plate containing 10 µl of overnight culture of host, *S. enterica*. The plate was dried near a flame and then incubated overnight at 37˚C. The following day plaques were counted to determine the phage titre and expressed as plaque forming units (PFU) per ml.

4.2.3 Free phage sensitivity at different pH values

Phage sensitivity to different pH values was tested in 0.2 M NaCl with pepsin at 3.2 mg/ml for solutions of pH 2, 2.5 and 3. For pH solutions 4 to 7, 0.2 M Sorensen's buffer was used with the addition of 10 mg/ml pancreatin. Time points were taken at 0 min, 30 min, 1 hour, 3 hours, 6 hours and 24 hours. For pH 2 and 2.5 exposure time points were also taken every minute for the first 10 mins. 10 µl was removed at each time point and serially diluted 10-fold to 10^{-8} as described above. The samples were spotted in triplicate on a lawn of the host bacteria introduced via the double layer agar method. The plates were incubated at 37˚C overnight and checked for PFU the following day.

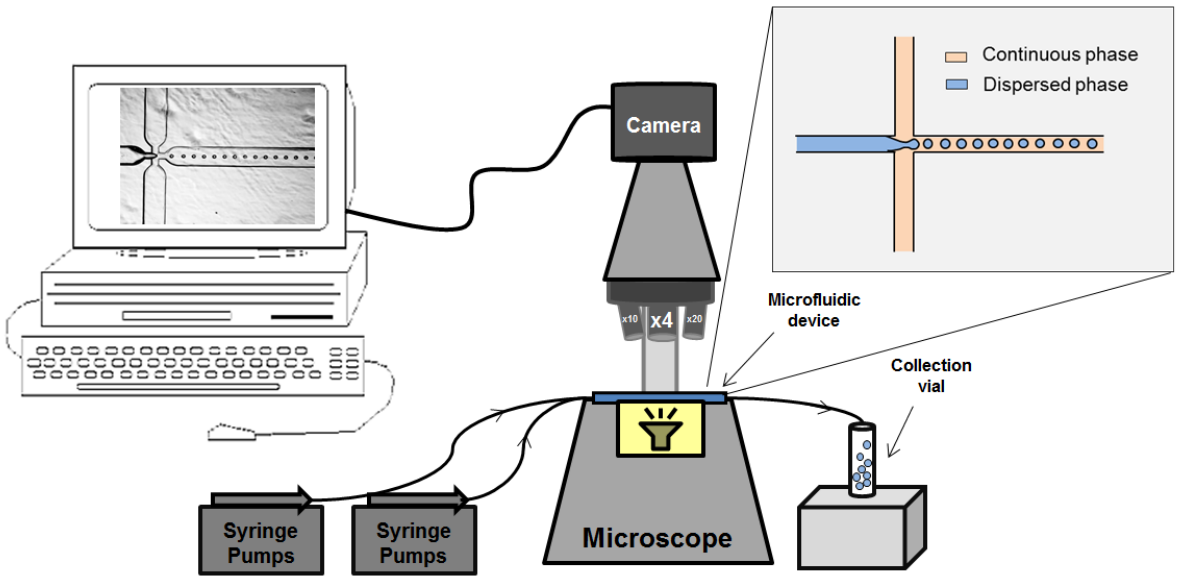

Figure 4.1 Schematic of experimental setup to produce water-in-oil emulsion for phage microencapsulation. Microscope stage with mounted microfluidic chip connected to two syringe pumps suppling aqueous (containing phage and polymer formulation) and oil phase. High speed camera connected via computer to microscope for visualisation of drop formation.

4.2.4 Felix O1 encapsulation using microfluidic droplet generation system

Eudragit S100 (ES100) was dissolved in deionised water (dH_2O) by dripping 4 M NaOH until the solution was clear. The solution pH was adjusted to pH 7 using 0.1M HCl. To this solution different concentrations (0.5 %, 1 %, 2 % (w/v)) of alginate was added and dissolved by stirring at 60°C overnight in 50 ml Duran bottles with a top equipped with a magnetic stirrer to aid mixing. The solution was left to cool before phage stock was added. Felix O1 stock was concentrated by centrifuging in Amicon tubes (Millipore, UK) with a 0.2 µm filter for 15 min and 2,000 g. This concentrated phage was added to the dispersed aqueous phase solution to make the final concentration of phage of ~10^8-10^9 PFU ml^{-1}. The continuous oil phase was made of a 50:50 mixture of Miglyol 840 and Castor oil (Elf Foods, Loughborough, UK), with 5 % (w/v) PGPR. The emulsion was collected in acidified oil, consisting of 0.05 M p-toluenesulfonic acid in Miglyol with 5 % (w/v) PGPR.

Eudragit-alginate droplets were prepared by using a hydrophobic quartz droplet junction chip with an etch depth of 190 µm purchased from Dolomite, UK (Figure 4.1). The dispersed aqueous phase was introduced through the inner/middle channel and the continuous phase from the two outer channels. The phases were pumped via 10 ml syringes (BD Plastipak, UK) mounted on syringe pumps (Harvard Apparatus, UK). The two phases were delivered and collected through medical delivery tubes (0.86 mm inner diameter and 1.52 mm outer diameter, Smiths Medical International Limited, UK). As the two phases met at the interface, the oil phase causes the aqueous phase to pinch and form droplets. The flow rates for all formulations were kept constant and maintained to keep the dripping regime. The droplet formation was observed via a high-speed camera (Micro C110 Phantom Ametek, UK), connected to an inverted microscope (Nikon Eclipse E200) using x 4 magnification objective lens. The camera was connected via computer allowing recording of the droplet formation at around 3000 frames per second. The forming droplets were collected in acidified oil and allowed to crosslink for a minimum of 2 hours.

The acidified oil was removed by pipetting off the oil layer after gentle centrifugation at 300 g for 5 mins to settle the acidified microparticles. An excess of 0.1 M $CaCl_2$ was added to the microparticles to crosslink the alginate for 1 hour. Microparticles were collected by centrifuging at 2000 g for 5 mins and removing the $CaCl_2$ solution using a pipette. The gelled particles were stored hydrated at 4°C.

The drop and particle size were analysed using the Image J program (National Institute of Health, Washington, U.S.) by counting 10 drops or particles per sample. The particle sizes for gelled microcapsules were measured using Coulter LS series 130 (Beckman Coulter Inc.), employing a Fraunhofer optical model for data regression (Figure 9.7 appendix).

4.2.5 Scanning electron microscope (SEM)

Gelled particles were frozen on filter paper (0.2 µm pore size, Millipore Ltd. UK) at -20˚C overnight. The particles were freeze dried (VirTis Wizard 2.0) for 24 hours at 50 Pa pressures and -20˚C. The particles were put on viewing stubs using double sided carbon tape, sputter coated with gold and viewed using a table top SEM (Hitachi TM3030 Microscope).

4.2.6 Encapsulated phage release in SGF and SIF

100 mg of Felix O1 encapsulated particles (approximate) were suspended in 10 ml prewarmed simulated intestinal fluid (SIF) containing 10 mg/ml pancreatin in 0.2 M Sorensen's buffer at pH 7 (Sigma Aldrich, UK). All dissolution experiments were carried out at 37^{o}C, shaking. For acid exposure to pH 1, 2, 2.5 and 3, 0.1 g particles were suspended in 10 ml prewarmed simulated gastric fluid (SGF) containing 3.2 mg/ml pepsin in 0.2 M NaCl at pH 2 (Sigma Aldrich, UK). After 2 hours exposure to SGF at each pH, the particles were centrifuged at 2000 g for 10 min, SGF removed and microparticles re-suspended in SIF (10 ml) for dissolution and phage release. Phage release was monitored over 4 hours, by taking samples to enumerate phage release kinetics at hourly time points. To do this, plaque assays were performed as described previously by taking 10 µl samples, serially diluting and spotting on a bacterial lawn using double overlay agar method. The plates were counted the following day for plaques.

4.2.7 Encapsulated phage *Salmonella* killing

Salmonella was cultured from a single colony with a starting O.D. (550nm) of <0.001, shaking at 37^{o}C overnight. 60 ul of overnight culture was added to 60 ml of BHI. 2 ml of this starter culture was added to 24 well tissue culture plates. Approximately 0.2 g of microparticles were added to multiple wells (for hourly time points) to evaluate *in vitro* phage release, amplification and arresting of bacterial growth (samples were shaken to allow mixing). Microparticles used were either virgin or previously exposed to pH 1 for an exposure period of 2 hours. At hourly intervals 1 ml aliquots were withdrawn and the O.D. measured of the controls (bacteria only), pH 1 exposed particles and non-pH 1 exposed

particles. An additional 1 ml aliquot per well was transferred to an Eppendorf tube for each sample and centrifuged at 2000 g for 3 mins for plaque assays. 10 µl was removed from the supernatant to enumerate for phage using the double-layer agar method as described previously. The pellet was separated and re-suspended in fresh BHI broth, this was serially diluted and plated on BHI agar plate to enumerate residual bacteria concentration. The control was also serially diluted and plated to determine the bacteria concentration. The plates were incubated overnight at 37^{o}C and checked for plaques and colonies the following day. The results were presented as the mean of three repeats.

4.2.8 Statistical analysis

Statistical analysis was carried out using the statistical software Minitab 18.

4.3 Results

4.3.1 Production of phage encapsulated ES100-alginate microparticles

Highly monodispersed droplets were produced for 0.5 % (w/v) (viscosity, 25 cP) and 1 % (w/v) alginate (64 cP) compositions (all solutions had 10 % (w/v) ES100). Droplet generation was stable for 0.5 % (w/v) and 1 % (w/v) alginate formulation over extended periods with drops collected for several days without interruption. Formulations with alginate compositions higher than 1 % (w/v) were highly viscous, (2 % (w/v) alginate solution having a measured viscosity of 574 cP) and this resulted in difficulties in maintaining uniformity of droplet generation for prolonged periods due to flow instabilities causing disruption in droplet generation and observation of jetting phenomena discussed elsewhere (Vinner *et al*., 2017). Stable production of uniform droplets required at-line optimisation of the hydrodynamic conditions. Microfluidic droplet generation devices can be controlled *in situ* by direct microscopic observation. Hydrodynamic conditions were optimised for each formulation in real-time by adjusting fluid flow rates during each experiment until uniform droplets were produced. Thereafter only slight changes to these values were needed to achieve droplets of similar sizes ensuring batch-to-batch uniformity of droplets.

To enable better control of the droplet generation process and to reliably produce droplets with low polydispersity, the 'dripping regime' worked best. Here, the droplets were formed closer to the orifice of the collection capillary because the interfacial tension forces dominated over the inertia of the dispersed phase and the viscous stress forces from the continuous phase. Droplet formation began as the dispersed phase entered microfluidic flow focusing zone. The dispersed phase did not meet the capillary wall due to repulsion from the hydrophobic surface of the collection capillary wall which is

designed to resist wetting by the aqueous phase (Figure 4.2a and b). The continuous phase forced the dispersed phase to elongate axially, collapsing the dispersed phase and producing a neck behind the forming droplet. As the elongation progressed further, the neck thinned into a thread, eventually breaking the dispersed phase and releasing the droplet. Following retraction, the process restarted with the dispersed phase protruding at the orifice of the collection capillary. In this dripping regime, the formation of one droplet took ~95 ms, thus ~10 droplets were formed each second and subsequent droplets were produced at the same position as the previous droplets. The balance between the drag force and interfacial tension and negligible shear in the collection capillary after drop formation resulted in uniform droplets.

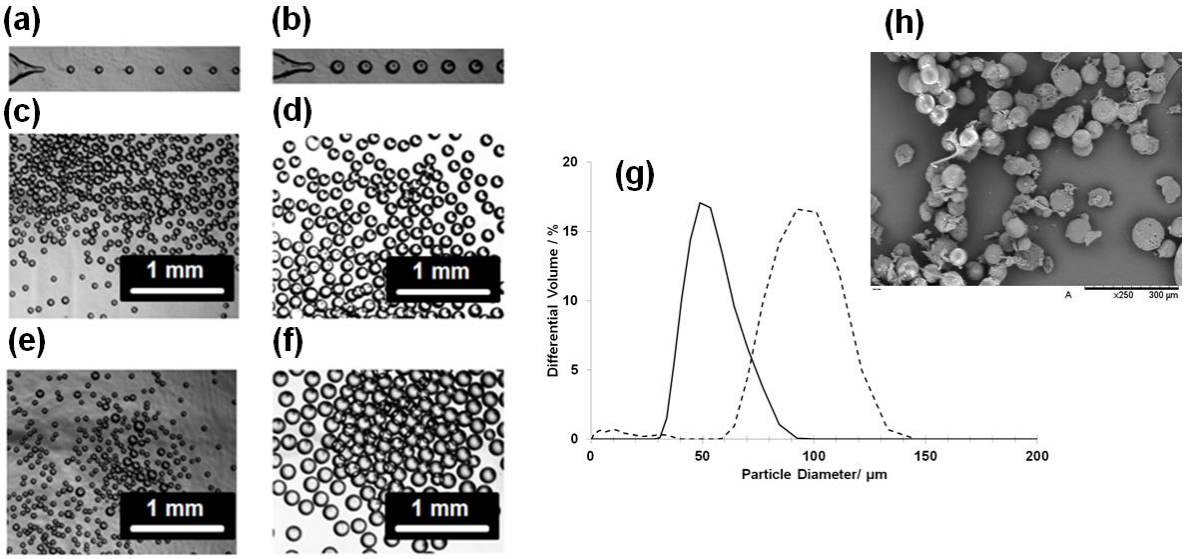

Figure 4.2 Production of pH responsive microparticles using a microfluidic droplet generation system. (a) *in situ* imaging showing generation of small droplets in the microfluidic chip using formulation D2(s) and (b) large droplets using formulation D2(b); (c) collected small droplets with formulation D2(s) (mean drop size 73 µm ± 11 µm); (d) collected large droplets with formulation D2(b) (mean drop size 190 µm ± 5 µm); (e) collected small droplets with formulation D1 (mean drop size 64 µm ± 12 µm); (f) collected big droplets with formulation D3 (mean drop size 164 µm ± 19 µm); (g) particle size distributions for gelled microparticles using with formulation D2(s) and D2(b); (h) scanning electron micrograph of freeze dried big microparticles prepared using formulation D2(b).

Changing the droplet size is an important feature of microfluidics enabling control over phage loading and particle size. Droplet generation in the dripping regime was optimised over a range of flow rates

for alginate formulations of differing viscosities thereby enabling control of the droplet size whilst maintaining a reasonably high degree of the size uniformity (Figure 4.2 c and d). This was done in real-time whilst observing (using the microscope camera) the change in the resulting droplet size. Increasing the flow rate of the inner phase relative to the outer phase resulted in increased size of the droplets e.g. for 1 % alginate formulation.

Droplet formation in the microfluidic droplet generation chip was followed by curing in acidified oil, removal of acidified miglyol and gelling of alginate in 0.1M $CaCl_2$. This resulted in distinct gelled microspheres (Figure 4.2 e and f). The gelling process resulted in significant shrinkage in the size of the final microparticles as shown by the Coulter measurements (Figure 4.2) and the freeze-dried SEM image (Fig 4.2h).

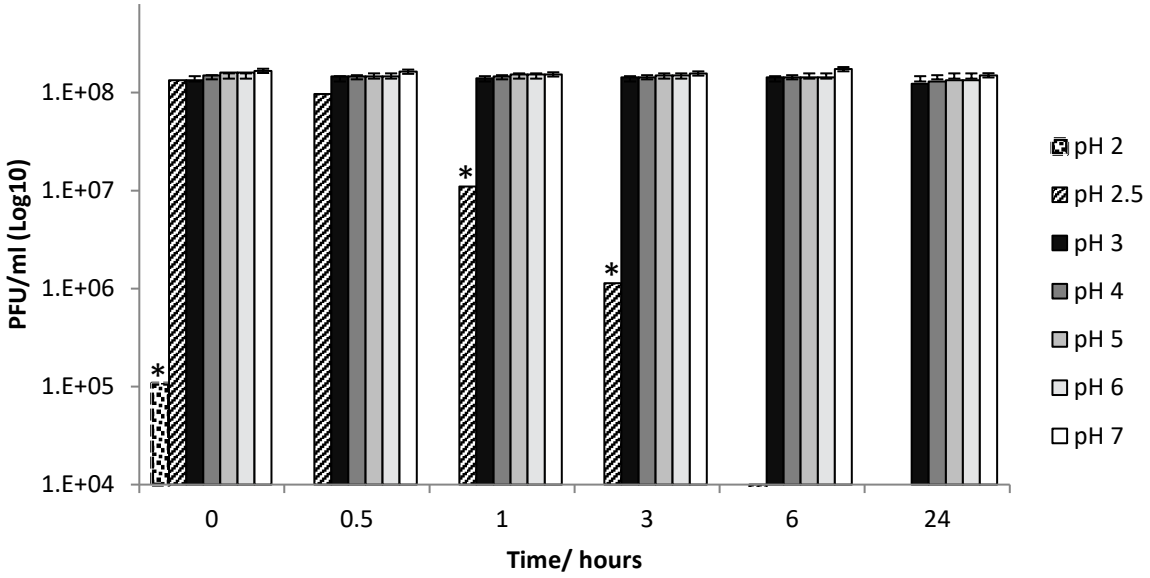

Figure 4.3. Effect of pH on free phage Felix O1 viability in 0.2 M NaCl solution. * indicates significantly different phage titres using a 2-sample t-test at each condition compared with phage exposed to pH 7 at the corresponding time point. Time point 0 hours denotes time between 0-10 minutes for phage exposed to all pH values except pH 2.5 where phage titre reduced rapidly, and data is plotted 10 seconds post exposure.

4.3.2 Effect of acid exposure on Felix O1 viability

The effect of acidic pH on Felix O1 phage viability was tested. Phages were suspended in 0.2 M sodium chloride solutions with varying pH. The phage lost nearly all activity after 10 min of exposure to pH 2

and lost activity progressively upon exposure to pH 2.5 over a period of 6 hours (Figure 4.3). Phage viability was significantly improved when the solution pH was above pH 3.

Phage Felix O1 was found to be stable and retain titre upon formulation in 10 % (w/v) ES100 containing between 0.5 % (w/v) to 2 % (w/v) alginate upon storage under refrigerated conditions at 4 ^{o}C (for up to 1 week) and for several days in syringes mounted in microfluidic pumps used during droplet generation at room temperature.

4.3.3 Microencapsulated phage exposure to simulated gastric fluid (SGF) and phage release in simulated intestinal fluid (SIF)

Near 100 % (typically > 95%) encapsulation of phages was observed following the entire encapsulation process. Gelled microparticles were added to shaking solutions containing SGF with pH adjusted to pH 1, pH 2, pH 2.5 and pH 3 and microparticles were exposed for 2 hours followed by phage release in SIF. Small 1 % (w/v) alginate microbeads (mean size 50 µm) were able to protect Felix O1 phage up to acidic pH 2.5 (Figure 4.4a). However, further lowering pH resulted in titre drop from $1x10^{9}$ PFU ml^{-1} to 4×10^{7} PFU ml^{-1} (at pH 2) and complete loss of phage titre upon exposure to pH 1. Using the same 1 % (w/v) alginate formulation and increasing the size of microparticles (mean size ~100 µm) resulted in significant improvement in phage viability with no measured loss in phage titre for microparticles exposed to pH 1 (Figure 4.4b). The release profile also changed from burst release for small microbeads to slow release for the larger microbeads with around 20 % of encapsulated phage dose released after 1 hour and near complete release after 2 hours of exposure to SIF. Increasing the alginate composition from 1 % (w/v) to 2 % (w/v) for small microbeads significantly improved phage acid protection with phage surviving exposure albeit with titre reduction upon exposure to SGF at pH 1 (Fig 4.4c). For larger microbeads lowering the alginate composition reduced acid protection with 0.5 % (w/v) alginate samples showing acid protection down to pH 3 with significant drop in phage titres at pH 2.5 (Fig 4.4d).

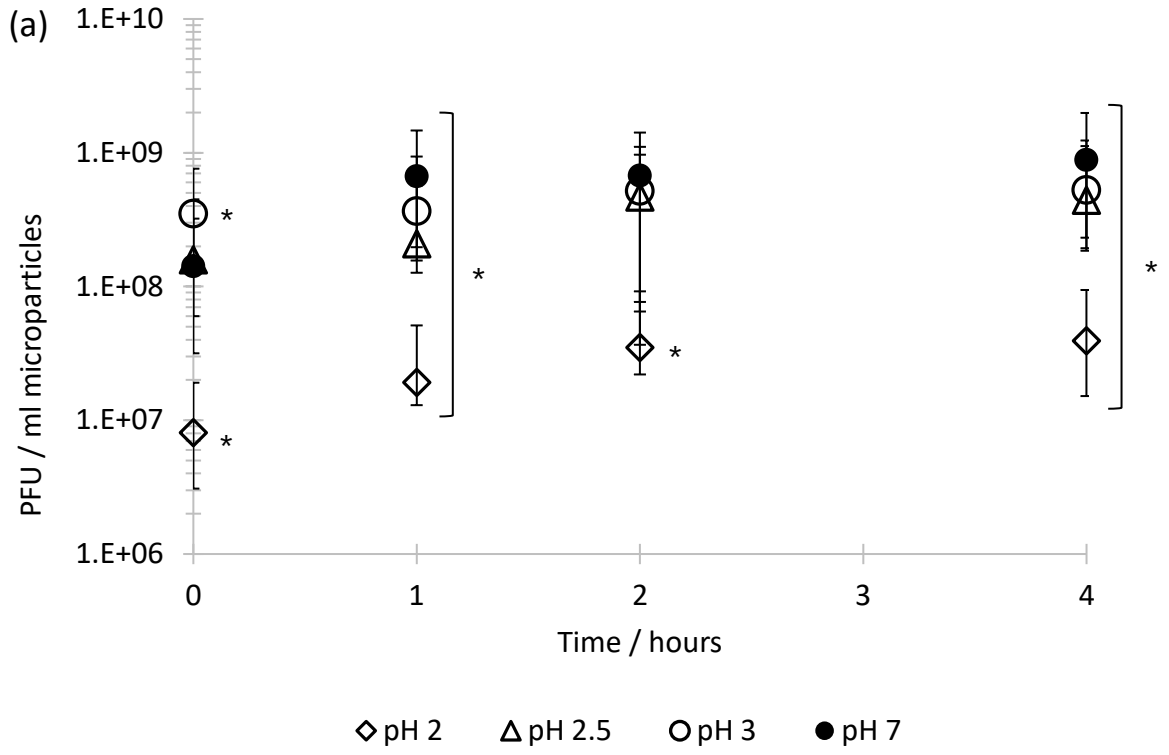
(a)
1.E+10
1.E+09
1.E+08
1.E+07
1.E+06
PFU / ml microparticles
0
1
2
3
4
Time / hours
pH 2
pH 2.5
pH 3
pH 7

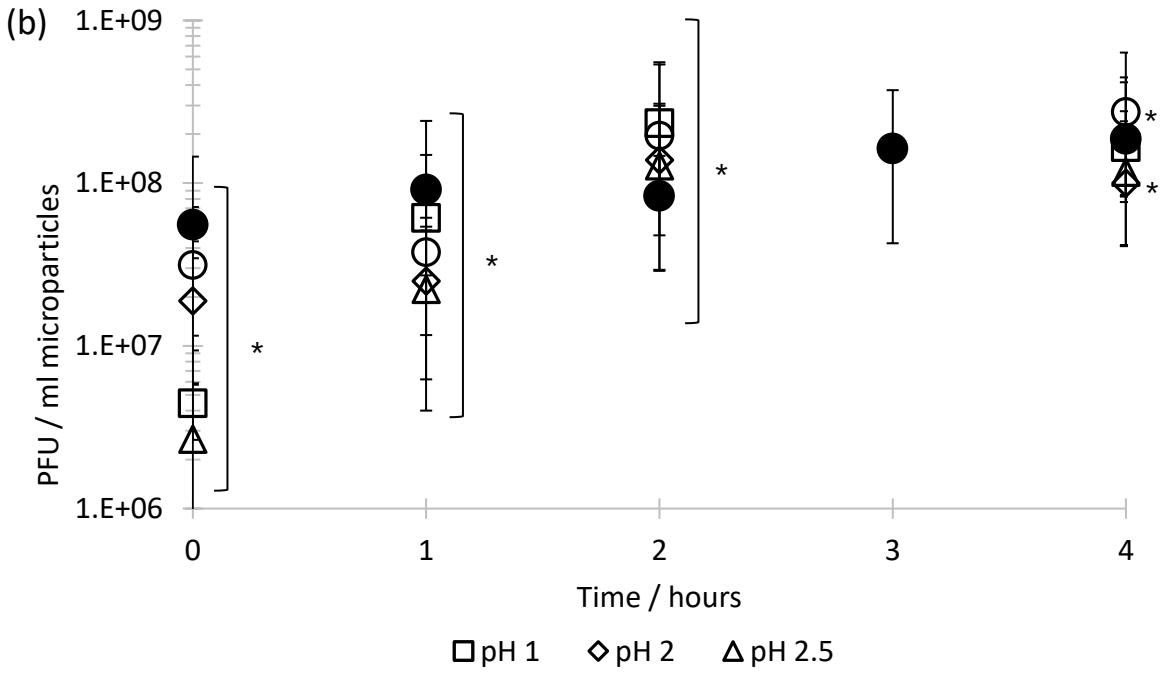
(b)
1.E+09
1.E+08
1.E+07
1.E+06
PFU / ml microparticles
0
1
2
3
4
Time / hours
pH 1
pH 2
pH 2.5

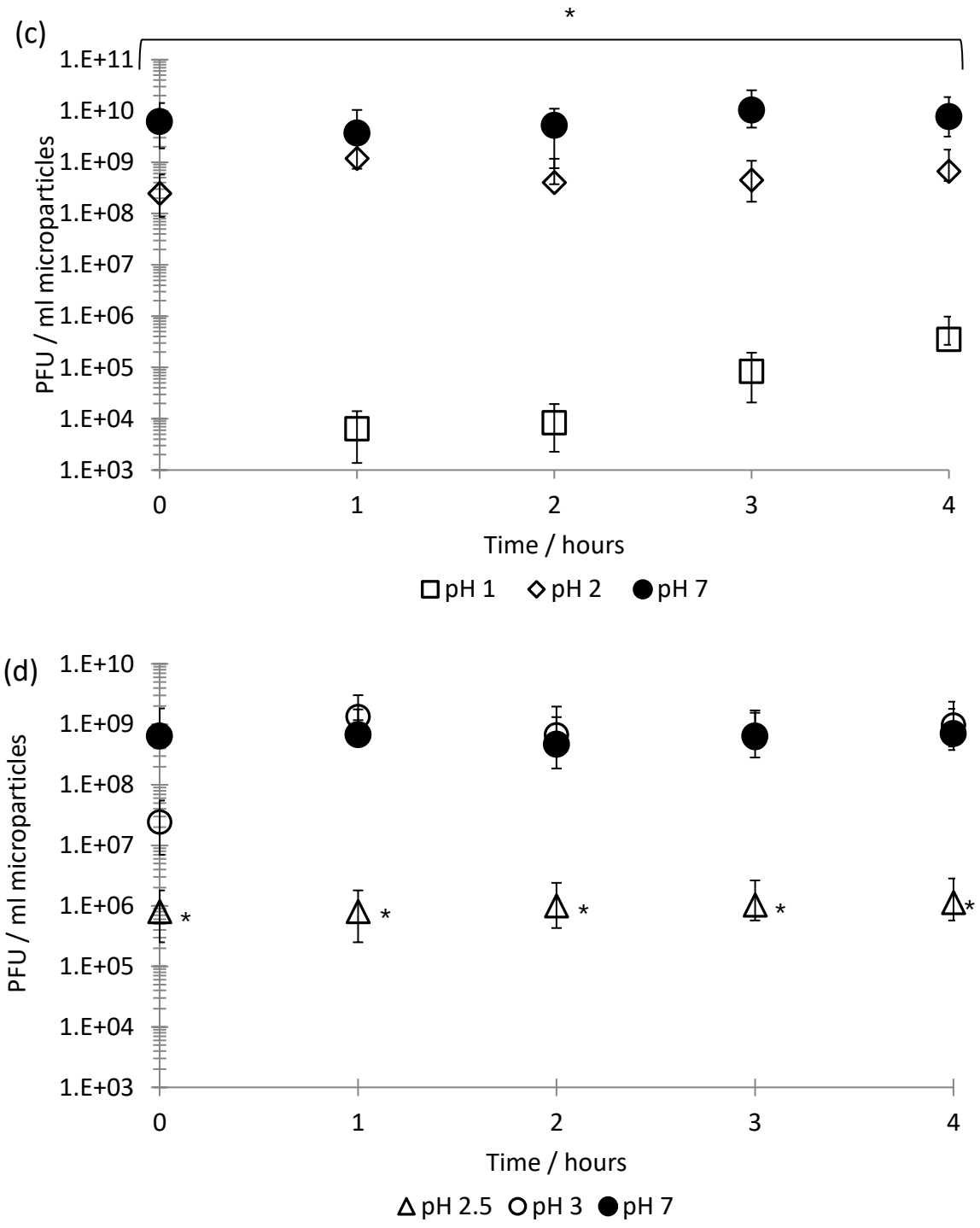

Figure 4.4. Protection of encapsulated Felix O1 bacteriophage from SGF and release of phages upon exposure to SIF. (a) acid protection and phage release kinetics for small microparticles, formulation D2(s)*;* (b) acid protection and phage release kinetics for big microparticles, formulation D2(b); (c) acid protection and phage release kinetics for small microparticles, formulation D1; (d) acid protection and phage release kinetics for big microparticles, formulation D3. * indicates significance in comparison to pH 7 for each time point ($p < 0.05$) in a two sample t-test.

4.3.4 Microencapsulated phage release and *Salmonella* killing

Large 1% (w/v) alginate microbeads pre-exposed to SGF (pH 1) rapidly released phage with the phage titre rising to 1 x 10^6 PFU ml^{-1} shortly after addition (Fig 4.5 c). Optical density measurements showed a clear deviation in *Salmonella* growth in cultures at time point 3 hours post microparticle addition for small and large microparticles that had previously been exposed to SGF at pH 1 for 2 hours (Fig 4.5 a). For big particles the CFU counts dropped sharply after 3 hours with concomitant amplification of phage titres (Fig 4.5 b, c). Exposure to SGF at pH 1 resulted in considerably lower phage titres in the small 1% (w/v) alginate microparticles, therefore phage release from the small microbeads resulted in much lower phage titre (1 x 10^3 PFU ml^{-1}). This resulted in a significant delay in both *Salmonella* CFU reduction (~ 4 hours) and subsequent phage amplification (Fig 5.5 b, c). 4 hours post microparticle addition both sets of cultures had arrested *Salmonella* growth and considerable phage amplification was noted with phage titre rising to ~ 1 x 10^{10} PFU ml^{-1} however, the time taken to arrive at this level differed significantly for the two 1% (w/v) alginate samples indicative of the effect of phage dose on phage-bacterium population dynamics.

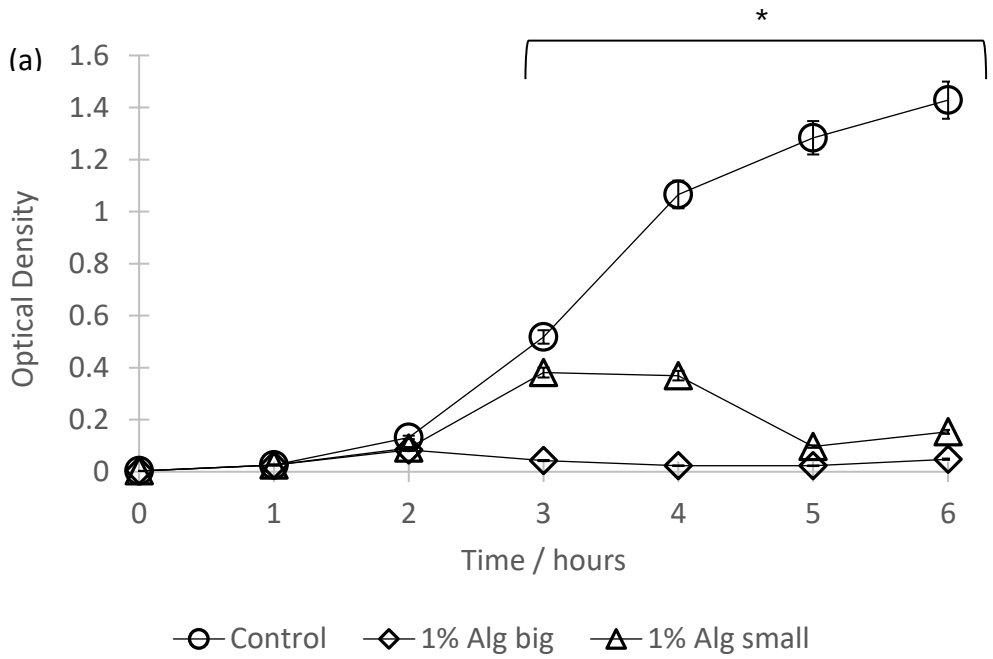

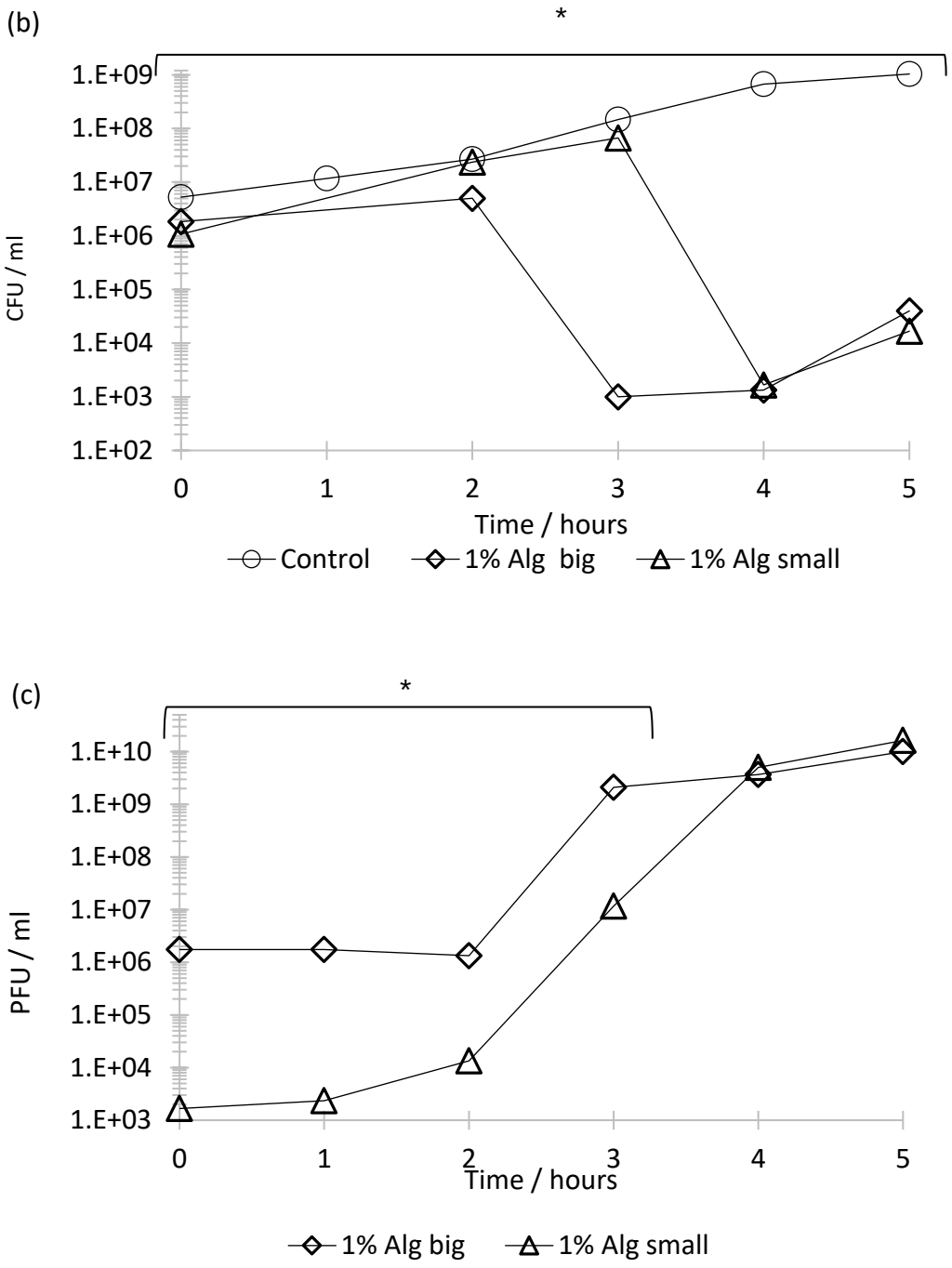

Figure 4.5 Dynamics of phage killing of *S. enterica (serovar Typhimurium)* bacteria with microencapsulated Felix O1 bacteriophage. (a) Optical density curves; (b) CFU data showing bacteria killing in the presence of added microencapsulated phage (big and small beads prepared using formulation D2) pre-exposed to simulated gastric fluid (exposure period of 2 hrs at pH 1) prior to addition to bacterial cultures; * indicates significance in comparison to the control ($p< 0.05$) (c) Phage amplification in the presence of *Salmonella*. * indicates significance in a 2-sample t-test ($p < 0.05$) n=3.

4.3.5 Storage stability of encapsulated phage

10 % (w/v) ES100 containing 1% (w/v) Alginate microparticles stored over the course of 4 weeks under refrigerated conditions (at 4°C) showed a modest drop in phage titre (Figure 4.6). Phage titre dropped from ~ 4 x 10^8 PFU ml^{-1} microparticle at week 0 to 1 x 10^8 PFU ml^{-1} microparticles after 1 week of storage. Thereafter, the titre remained stable up to week 4.

a)

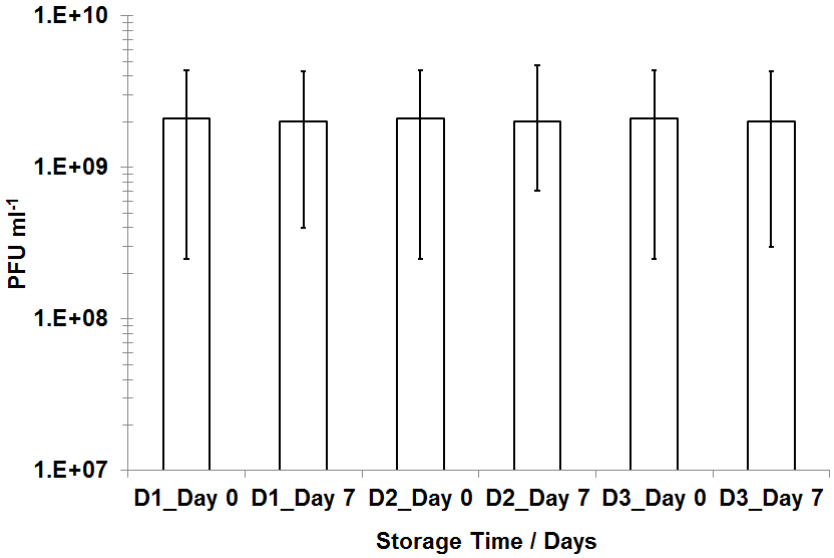

b)

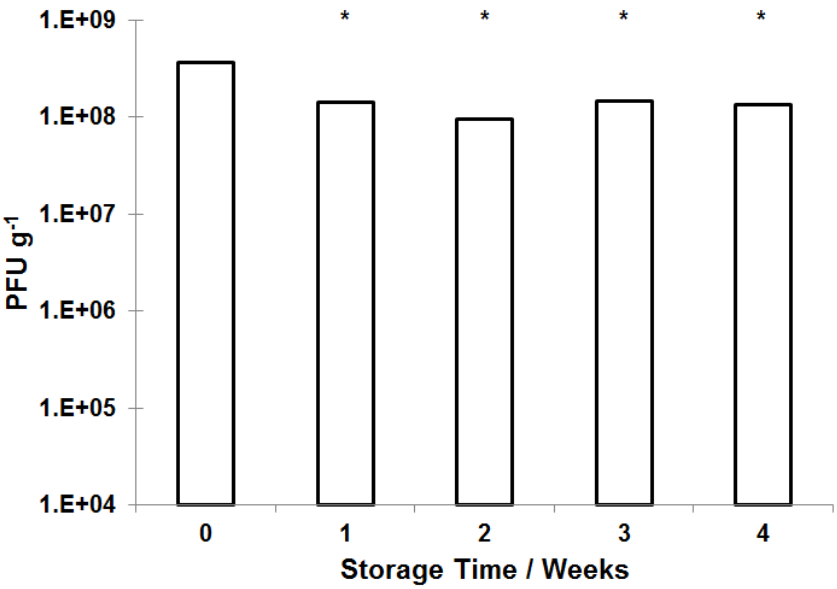

Figure 4.6. Storage stability of Felix O1 phage in (a) formulations D1-D3 and (b) microencapsulated in microparticles prepared using formulation D2 (~100 µm beads) refrigerated at 4° C. Phage titre was evaluated by exposing microparticles to simulated intestinal fluid (pH 7). * indicates significance as

compared with sample at week 0 ($p < 0.05$) using a 2-sample t-test. All measurements were done in triplicate with three biological repeats and three technical repeats.

4.4 Discussion

Fabrication of bacteriophage encapsulated microparticles using microfluidic technology allows precise control over the particle size, phage dose per particle and tailoring of the release profile for targeted delivery and controlled release of phages. The low controlled shear in the microfluidic droplet generation unit allows 100% phage encapsulation and production of highly uniform droplets. Previous published works on phage microencapsulation have employed a limited range of microencapsulation techniques with extrusion based droplet formation the most frequently used method (Colom *et al*., 2017a; C Dini *et al*., 2012; S. Kim *et al*., 2015a; Yongsheng Ma *et al*., 2008, 2012; Samtlebe *et al*., 2016; Tang *et al*., 2014; Wall et al., 2010). The significant potential of microfluidic microencapsulation for phages is relatively unexplored with only two previous published papers to date including one from our group (Boggione *et al*., 2017; Vinner *et al*., 2017). Motivation for research into solid dosage forms for oral application of phages is driven by the need to protect phages from the harsh gastrointestinal tract environment. Phage mediated reduction of bacterial levels *in vivo* requires high tires of viable phages delivered precisely at the site of infection that are able to target the host and arrest bacterial growth (Malik *et al*., 2017). *In vitro* phage stability experiments exposing phages to solutions of different acidic pH may be useful predictors of *in vivo* phage survival and a prerequisite during formulation development prior to testing in animal models (Watanabe *et al.*, 2007). In a considerable number of previously published studies, the sizes of phage encapsulated microparticles have tended to be considerably larger than those reported here (an order of magnitude bigger) due to the use of extrusion methods. Little consideration has previously been given to the control of the particle size distribution, the phage loading per particle and the resulting heterogeneity of the release kinetics from each particle (S. Kim *et al*., 2015a; Yongsheng Ma *et al*., 2008, 2012, Tang *et al*., 2013, 2014). A key advantage of the microfluidic microcapsule fabrication process used here is the precision with which uniform small microparticles (mean size 10 ~ 100 μm) containing encapsulated phage may be prepared under low shear conditions.

Droplet generation in the microfluidic device established using a stable dripping regime resulted in each droplet being produced at the same position; disruptive forces of the same magnitude acted on each individual droplet and these forces became negligible after pinch-off. In conventional bulk emulsification systems, the droplets are continuously being subjected to shear which typically varies widely across the emulsification or homogenisation unit (Jain *et al*., 2005; Sağlam *et al.*, 2011; Un &

Lements, 2007). Continuous excessive exposure to shear results in the droplets breaking further into smaller droplets resulting in emulsions with a high degree of polydispersity (Kong *et al*., 2012). The microfluidic fabrication process provides a highly controlled uniform shear environment resulting in microparticles with low polydispersity demonstrated here.

Phages are sensitive to physical and chemical stresses including shear (S. S. Y. Leung *et al.*, 2016; Vandenheuvel *et al.*, 2013a), temperature (Vandenheuvel *et al.*, 2013), pH (Briers *et al*., 2008), ionic strength (Knezevic *et al.*, 2011), exposure to organic solvents (Lee and Belcher, 2004; Puapermpoonsiri *et al*., 2009). Overcoming phage instability to gastric acid is a major concern in oral phage delivery; it has been addressed in some studies through administration of antacids e.g. sodium bicarbonate prior to oral phage treatment or co-encapsulation of calcium carbonate (Jamalludeen *et al.*, 2009). Formulations used for phage encapsulation require careful selection of constituents and encapsulation conditions to ensure phages remain viable and to prevent titre loss during processing and storage. Previous efforts targeting *Salmonella* in the food chain have attributed poor phage stability in the gastrointestinal tract for insufficient *in vivo* efficacy (Wall *et al.*, 2010). *Salmonella* Felix O1 phage (belonging to the *Myoviridae* family) was shown here to be highly sensitive to acidic pH. Similar results have been reported previously for phage Felix O1, other *Salmonella* phages as well as *staphylococcus aureus* bacteriophage K (also a myovirus) and for *E. coli* specific phages (Albino *et al.*, 2014; S. Kim *et al*., 2015a; Yongsheng Ma *et al*., 2008, 2012; Saez *et al.*, 2011). This loss of phage activity highlights the need to protect the phage from the harsh acidic environment of the stomach if controlled doses of phage are to be reliably delivered to treat *salmonellosis* in the infected gut. Our results show that phage Felix O1 titre is stable in a formulation of dissolved ES100 10 % (w/v) containing variable alginate amounts over the range 0.5 % - 2 % (w/v). Microencapsulated Felix O1 formulated using 1 % (w/v) alginate in large 100 µm microparticles was shown to survive 2h exposure to SGF at pH values as low as pH 1 without loss of phage titre. Felix O1 microencapsulated in alginate beads has previously been shown to survive and amplify in the gastrointestinal tract of pigs (Wall *et al*., 2010). *In vitro* results reported here suggest that high *Salmonella* phage titres could be delivered to the gastrointestinal tract, subsequently released there using a pH trigger and should remain viable thereafter. The pH of the colon can fall during bacterial infection to around or just below pH 7; in such a case, the released phage should remain viable and capable of lysing the infecting *Salmonella* bacteria present in the gut (McConnell *et al.,* 2008).

Alginate hydrogel pores tend to be in the 5-200 nm range depending on the degree of crosslinking (George & Abraham, 2006). The porosity of the alginate gel microparticles affects phage viability upon exposure to the acidic stomach environment. A number of previous studies have used alginate as the

main encapsulating agent either on its own or in combination with whey protein or chitosan to improve acid stability (Colom *et al*., 2017a; S. Kim *et al*., 2015a; Yongsheng Ma *et al*., 2008, 2012; Samtlebe *et al*., 2016; Tang *et al*., 2013, 2014; Wall *et al.*, 2010) Phages encapsulated in crosslinked pure alginate microparticles were found to be susceptible to acid damage following exposure to simulated gastric fluid (C Dini *et al*., 2012; Yongsheng Ma *et al*., 2008, 2012; Soto *et al.*, 2018). Previously researchers have co-encapsulated $CaCO_3$ within the microparticles to protect phage from acid damage (Colom *et al*., 2017a; Yongsheng Ma *et al*., 2012). We have shown that microparticle size and alginate composition are important in ensuring acid protection for encapsulated phage. The pH responsive character of Eudragit S100 results in phage readily released upon exposure to pH 7. The microparticles were stable upon storage under refrigerated conditions for up to 4 weeks. The combination of small microparticle size and pH responsive character of the microparticles resulted in rapid release of phage within the first two hours upon exposure to SIF at pH 7. Previous studies on encapsulated phage in large microparticles (~ 1mm) have reported slower sustained release kinetics for alginate encapsulated phage however acid protection was poor (S. Kim *et al.*, 2015a; Yongsheng Ma *et al*., 2008). Faster release from small alginate microparticles (mean size ~ 100 µm) containing $CaCO_3$ as antacid was recently reported (Colom *et al*., 2017a). However, exposure to simulated gastric fluid (pH 2.8 for 60 min) resulted in between 2 log and 3 log reduction in *Salmonella* phage titre suggesting that even with the addition of $CaCO_3$, phage were highly susceptible to SGF. Particle size was previously shown to be an important factor influencing phage protection from SGF for acid permeable beads (Tang *et al*., 2014). Alginate-whey protein microparticles having the same composition but different mean sizes showed larger particles protected phage better compared with smaller microparticles (Tang *et al.*, 2014). The acid diffusion path length increases with particle size thereby affording protection to phage further away from the bead surface. We have shown that encapsulation of phage in Eudragit/alginate microparticles with different mean sizes (50 ~ 100 µm) may permit control over the release rate with small particles showing rapid burst release of phage cargo whilst larger beads showed an initial burst and then slower sustained release over 2 hours.

A number of *in vivo* animal studies have shown dose dependent phage therapy outcomes, with high doses of phage resulting in better clinical results (Smith *et al*., 1987; Biswas *et al.*, 2002; Cerveny *et al.*, 2002; Wills *et al*., 2005). Accurate control over the phage dose delivered at the site of infection and the timing of the delivery are important considerations (R. J. Atterbury *et al*., 2007; Malik *et al.*, 2017; Sarker *et al.*, 2016). Using *in vitro* experiments, we have shown that loss in phage titre upon acid exposure to SGF may result in a significant delay in phage amplification and this would potentially allow bacteria to attain much higher bacterial cell numbers in an *in vivo* setting with adverse treatment outcomes. Failure of a recently concluded phage therapy trial for the treatment of *E coli* diarrhoea in

children was attributed to the lack of *in situ* phage amplification due low host cell numbers which were nevertheless susceptible to the phage cocktail administered (Sarker *et al*., 2016). Lack of phage formulation, no antacid administration and subsequent drop in phage titre due to phage exposure to stomach acidity may have been a factor in the consequent lack of *in situ* phage amplification (Sarker *et al*., 2016). These issues may be addressed through proper formulation development and microfluidic encapsulation of high phage titres for targeted delivery and controlled release of phages at the site of infection coupled with a better understanding of phage-bacterium population dynamics *in vivo* (C. Y. (Joey); Leung & Weitz, 2016; Levin & Bull, 2004). These aspects have thus far received little attention in the published literature. We have demonstrated here that even after exposure of phage encapsulated microparticles to simulated gastric fluid at pH 1 for 2 hours, the released phage dose was unaffected and corresponded to ~ 1 x 10^8 PFU g^{-1}. The dose was sufficient to prevent rapid bacterial growth *in vitro* and resulted in rapid phage amplification from an initial titre of 1 x 10^6 PFU ml^{-1} to ~ 1 x 10^9 PFU ml^{-1} within 3 hours of addition of microencapsulated phage. In small animal studies (e.g. mice) typical dose via oral gavage is around 100 µl which would allow dosing of around 0.1 g of microparticles containing around ~ 10^8 PFU or higher through phage stock concentration. Such a dose is indeed typical of many animal studies in literature (Abdulamir *et al*., 2014; Barrow & Lovell, 1998; Chibani-chennoufi *et al*., 2004; Malik *et al*., 2017; J. Y. Nale, Spencer, *et al*., 2016; Smith *et al.*, 1987; Yen *et al*., 2017). Bacterial killing by phage is dependent on phage particles adsorbing to the target bacteria (Cairns *et al*., 2009). Phage-bacterium binding kinetics may be modelled as a simple first order process with respect to the concentrations of bacteria and phage populations respectively (Levin & Bull, 2004; Payne & Jansen, 2001). High phage densities are needed in order to arrest the growth of phage susceptible bacteria (Malik et al., 2017). Adsorption of phage to bacteria results in an initial drop in phage concentration (Cairns et al., 2009). The timing of rapid *in situ* phage amplification is highly dependent on the concentration of the bacteria (Cairns et al., 2009). Successful amplification of phage is dependent on high bacterial concentration hence efficient killing is not achieved until both phage and bacteria concentrations are high. Resistant bacteria quickly become the dominant population unless a phage mixture (cocktail) is used containing high doses of the different phage strains capable of killing the resistant mutant population. It is known that phage clearance mechanisms rapidly reduce the phage concentration in the absence of host bacteria (Yen *et al*., 2017). We have shown here that a high phage dose is quickly able to arrest the rise of bacterial growth. Tanji *et al.*, (2005) showed similar results for *E. coli* using an *in vitro* chemostat experimental system. However, if low starting concentrations of bacteria are present, phage concentrations *in vivo* may decay significantly due to host clearance mechanisms and phage may be unable to amplify and achieve a sufficiently high concentration to eradicate the infecting bacteria until the bacteria have had time to

grow bacterial numbers substantially (Malik *et al*., 2017). In such circumstances it takes time for the bacterial population to grow before phage are able to adequately multiply *in situ* and then arrest bacterial growth (Cairns *et al*., 2009). During this delay in bacterial concentration growth, phage concentrations may decay significantly thereby resulting in poor phage therapy outcomes. If phages are administered prophylactically too early prior to infection or at the early onset of infection (when the bacteria concentration is low), clearance of phage by the host immune system or by other mechanisms (e.g. dilution or shortening of intestinal transit times during diarrhoea) may result in lowering of the *in situ* phage concentration resulting in poor phage therapy outcomes (Malik *et al*., 2017). Under such conditions mucoadhesion of phage trapped in microparticles and slow sustained phage release may be a good strategy. Encapsulation of phage and their slow controlled release may help in ensuring that the *in situ* phage concentration remains at a therapeutically effective level (over a realistic time period) allowing phage to amplify once the bacteria concentration increases to levels sufficient for *in situ* phage amplification (Malik *et al*., 2017).

Previous phage therapy studies in animals and recent human trials have paid scant attention to phage delivery systems and their formulation with little consideration to the bioavailabity of the active agent at the site of infection. The size of microparticles may play an important role by ensuring they are minimally affected by the conditions of the diseased state. *Salmonella* is typically found infecting the ileum and caecum e.g. in chickens and pigs. Solid dosage forms need to be designed to deliver their phage cargo at the site of infection. Gastrointestinal infections can affect different parts of the gut. In future different phage fomulations may need to be developed targeting phage release in the appropriate intestinal region perhaps using more specific infection related triggers e.g. enzymes or toxins released by the bacterium causing the infection (Bean *et al.*, 2014). Other considerations for targeted delivery of phage include the changes in transit times during infection. Increased loss of fluid from the colon due to symptoms such as diarrhoea result in observed shortened mean transit times. Dilution of phage due to the high fluid environment may be a particular challenge. Larger particles (~ mm size range) may be more prone to the influence of short transit times. Smaller particles may be predisposed to non-specific mucoadhesion (Alhnan *et al.*, 2010; Kietzmann *et al.,* 2010) which may aid in phage retention and sustained release over a signficant time period. Colom *et al.*, (2017a) showed better phage retention (for animals treated with encapsulated phage versus those treated with free phage) in the caecum of chickens and a significant reduction in *Salmonella* colonisation, attributing these results to the mucoadhesiveness of the small alginate microparticles (~ 100 µm) used for encapsulating phage. Wittaya-areekul *et al .,* (2006) showed differences in mucoadhesion properties of chitosan coated alginate microparticles using an *in vitro* assay using porcine gut tissue samples.

A limitation of phages for therapeutic use is their narrow host range. Most phages only infect a small number of prevalent strains necessitating the use of phage cocktails to provide adequate therapeutic coverage. Phages incorporated in the cocktail may require tailored formulations to ensure adequate stability (Malik *et al.*, 2017).

Microfluidic encapsulation technologies have the potential to enable precise control over phage loading and production of highly uniform microparticles produced using many different polymer formulations enabling high level of innovation using a multitude of different triggers including light, temperature, pH, enzymes etc (Malik *et al.*, 2017). Furthermore, the fabrication of structured mutliple emulsions e.g. composed of concentric onion-like shells around the core drop may allow production of complex microcapsules for co-encapsulation and simultaneous or sequential release of several different phages encapsulated in individually optimised formulations (Malik *et al.*, 2017). Multiple shells would allow tailored formulations within a single microcapsule e.g. an outer acid stable shell may protect phage cargo from the stomach acid, an inner burst release shell containing a phage cocktail providing broad host range coverage for typical infection causing serovars and an innermost core for perhaps a later burst release or slower sustained release of a different cocktail to target any mutants that may give a delayed surge of infection causing bacteria.

Here, we have demonstrated proof-of-concept *in vitro* data in support of microfluidic production of encapsulated *Salmonella* Felix O1 phage in a pH responsive polymer suitable for targeted intestinal phage delivery.

4.5 Conclusions

We have demonstrated the controlled production of highly uniform small composite microcapsules (using commercially available microfluidic droplet generation chips) with mean size 50 ~ 100 µm composed of Eudragit S100 and with varying alginate amounts. Highly uniform microparticles were produced with low polydispersity enabling control over phage loading, acid stability upon exposure to SGF and their subsequent pH triggered release in SIF. Phage encapsulation and subsequent release kinetics revealed that microparticle size and alginate composition are factors affecting the pH stability and release profile of encapsulated phages. 100 µm beads prepared from 10 % (w/v) ES100 and with 1 % (w/v) alginate afforded phage excellent pH protection upon exposure to SGF (for 2 hours at pH 1) with no loss in phage titre. The microparticles released all their phage cargo within 2 hours upon subsequent exposure to SIF making them suitable solid dosage forms for gastrointestinal delivery of phages. We have also demonstrated the storage stability of the encapsulated phage under refrigerated conditions over a 4-week storage period. Furthermore, we demonstrated the effect of

acid stability and high phage dose delivery on the attenuation of bacterial growth upon release of encapsulated phage after exposure of microbeads to SGF at pH 1. Future work will investigate the spatial and temporal delivery of encapsulated phage in a relevant small animal model and the suitability of these solid dosage forms to target *Salmonella* infections *in vivo*.

Chapter 5: Microencapsulation of enteric bacteriophages in pH responsive microparticles using microfluidic membrane microarray-based emulsification for oral delivery

Abstract

Phage encapsulation for site-specific release was previously studied by Vinner *et al*., (2017). The use of commercially available polymer Eudragit S100 and alginate was used for protection against acid at pH 2. Here, we report the scale-up of this system using membrane emulsification technology to produce large volumes of encapsulated phage in composite microparticles. Investigation of process parameters to determine the effect on droplet diameter was studied and reported. Impact of dose was probed in this study by performing a phage -bacterial killing assay. A three-way interaction between phage, bacteria and epithelial cells was also investigated. Changes in epithelial cells showed bacterial infection however after introducing phage, bacterial growth was arrested, and epithelial cell damage rescued. Both free and encapsulated phage showed comparable results indicating that microparticles were able to dissolve and unload phage to effectively reduce bacterial growth. For the first time, this study has shown process scale-up for phage encapsulation which can successfully target enteric pathogen *in vitro*.

5.1 Introduction to membrane emulsification

Chapters 3 and 4 have investigated the use of microfluidic platforms for phage encapsulation. Optimisation and fine-tuning the production of uniform droplet size and therefore the release kinetics of phage *in vitro* was demonstrated. When considering the use of encapsulated phage for phage therapy, large scale production is required. Microfluidic platforms lack the ability to produce large volumes of material but are an excellent tool for formulation development and optimisation. Up-scaling this process can be challenging since conventional methods lack the ability to produce uniform droplets, introduce high mechanical stress and insufficient batch-to-batch reproducibility (Spyropoulosa *et al.*, 2011).

Membrane emulsification (ME) overcomes some of the afore mentioned disadvantages. Emulsions are produced by injecting the dispersed phase through defined pores of a membrane into the continuous phase. The resulting emulsions have uniform droplets with CV below 20 % whilst permitting large volume production (Vladisavljević *et al.*, 2012). ME is suitable for large-scale

production due to the simplicity of adding more membrane area to increase the throughput of emulsion formation. Furthermore, versatility of the system is demonstrated in its ability to produce both batch and continuous production as shown by Peng and Williams, (1998) on a pilot scale. Membrane emulsification consumes low energy between 10^4- 10^6 J m^{-3} in comparison to 10^6- 10^8 J m^{-3} consumed by conventional methods (Joscelyne & Trägårdh, 2000).

Injection of one non-miscible fluid into another is termed direct membrane emulsification whereas a premade emulsion injected into another immiscible fluid is termed premix membrane emulsification (C. Charcosset *et al.*, 2004). The type of emulsion produced is dependent on the membrane type, a hydrophobic membrane produces water-in-oil emulsion whereas a hydrophilic membrane produces an oil-in-water emulsion. In both cases, the dispersed phase must not wet the surface of the membrane where droplet detachment takes place (Nakashima *et al*., 2000). Droplet detachment is aided by shear applied above the membrane e.g. via a paddle stirrer connected to a pump (Williams & Vladisavljevic, 2005).

Droplet size is affected by several parameters such as shear, membrane type, membrane pore size, dispersed phase flux, emulsifier, viscosity of both phases (Catherine Charcosset, 2009; Joscelyne & Trägårdh, 2000; Nazir *et al.*, 2010; Spyropoulos *et al.*, 2014; Williams & Vladisavljevic, 2005).

5.1.1 Membrane type

There are several types of membranes available for ME which contribute to the production of stable emulsions. The type of membrane used depends on whether a water-in-oil or oil-in-water emulsion is required. Shirasu porous glass (SPG) membranes were initially used for membrane emulsification. Available in different pore sizes varying between 0.05 to 20 µm, these membranes have a high porosity (50-60 %) (Catherine Charcosset, 2009). Naturally used as a hydrophilic membrane through chemical modification the surface can be made hydrophobic to cater for water-in-oil emulsions (Kukizaki, 2009). Microsieve membranes made from ultra-thin foils are an alternative to SPG (R. G. Holdich *et al.*, 2013). An advantage of these membranes is that they have the capacity to reach high transmembrane flux at a low transmembrane pressure (Wagdare *et al.*, 2010) and are less likely to foul. Examples of microsieve membranes include silicon nitride Aquamaijn™, nickel produced by Micropore Technology Ltd (Egidi *et al.*, 2008) as well as aluminium and stainless steel foil (Williams & Vladisavljevic, 2005). Microsieve membranes offer the flexibility to produce pores with varying geometry such as slotted pores (R. Holdich *et al.*, 2006). Pore size is an important parameter as a direct linear correlation is observed between the pore diameter and the size of the droplet produced (Williams & Vladisavljevic, 2005).

5.1.2 Role of emulsifier in drop production

The role of the emulsifier to prevent coalescence is well known, however in membrane emulsification it plays a significant role in droplet detachment from the membrane surface. The emulsifier stabilises the water- oil interface by reducing the interfacial tension between the two immiscible phases and therefore facilitates droplet detachment (Goran T. Vladisavljević *et al.*, 2012). A critical amount of emulsifier needs to be used so as to prevent lowering of the interfacial tension to the point where the dispersed phase jets into the continuous phase without forming droplets (Goran T. Vladisavljević *et al.,* 2012). Membrane fouling by surfactant can occur if these molecules adhere to the membrane surface and allow the dispersed phase to spread across the membrane (Vladisavljevic, 2015).

Katoh *et al.*, (1996) investigated the effect of different emulsifiers on the effect of stable droplet generation in an oil in water emulsion between water phase and a mixture of corn oil and kerosene. They observed that each emulsifier produced monodispersed droplet once the interfacial tension was reduced to a constant minimum value which differed for each emulsifier (Katoh *et al.,* 1996).

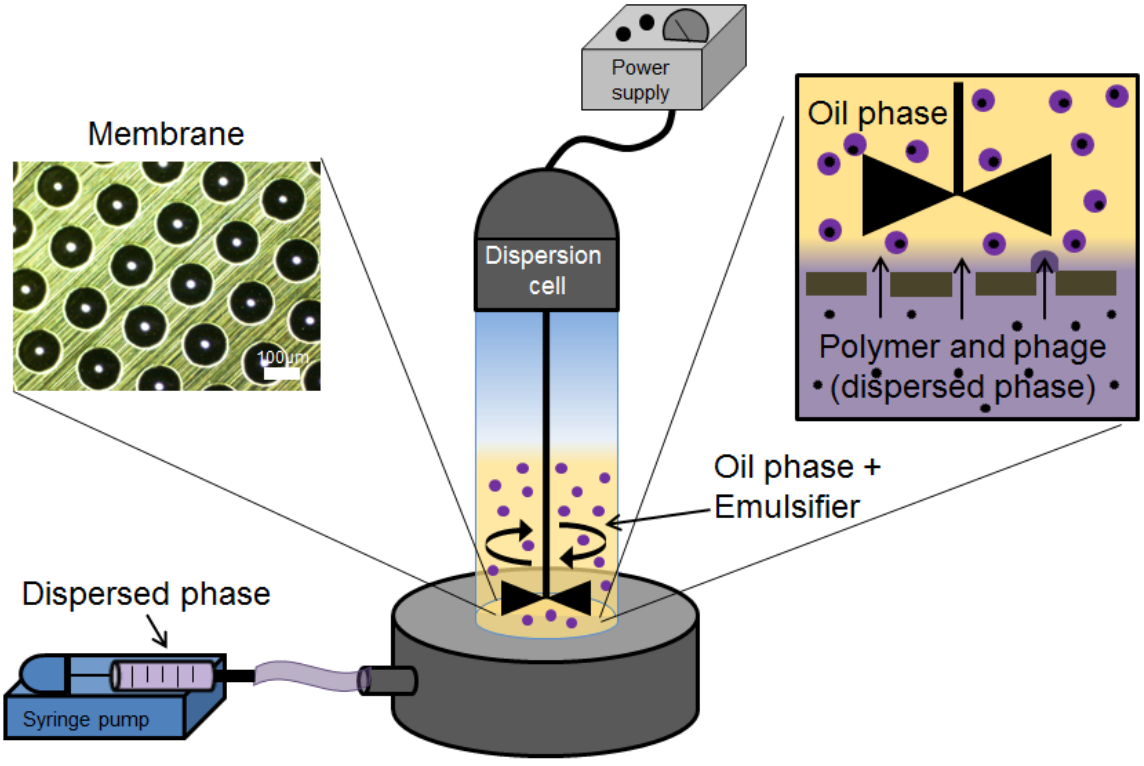

Figure 5.1 Schematic representation of the membrane emulsification system used for microencapsulation of bacteriophages.

5.1.3 Effect of shear on drop production

In a stirred membrane emulsification system (Figure 5.1), the shear produced by the moving continuous phase of the membrane surface aids droplet detachment (Joscelyne & Trägårdh, 2000; Nakashima *et al.*, 2000). Alternate arrangements have been used to provide surface shear including pulsing membrane emulsification systems and utilising crossflow in combination with the pulsing membrane for droplet detachment (R. G. Holdich *et al*., 2013). Similarly, vibrating or rotating membrane systems produce shear by vibrating and rotating the membrane respectively allowing for droplet detachment (R. G. Holdich *et al.*, 2010; Williams & Vladisavljevic, 2005). Also, a cylindrical membrane which oscillates back and forth to produce shear for droplet detachment is termed Azimuthallly oscillating membrane system (P. S. Silva *et al.*, 2015). These different membrane systems demonstrate that the shear influences the droplet size and monodispersity.

5.1.4 Flux and viscosity of the dispersed phase on droplet production

The dispersed phase is pumped through the membrane pores to form droplets. Higher transmembrane fluxes allow more filling before the droplet is detached however other parameters influence the transmembrane flux. Egidi *et al*., (2008) investigated the effect of membrane flux on droplet production with two pore sized membranes (80 and 200 µm). The study found that droplet size increased as the dispersed phase injection rate increased for a 200 µm pore sized membrane and decreased with increasing shear. However, only at low flux the most monodispersed droplets were achieved with a CV of 18 %. The opposite was true for the 80 µm pore size, where CV of less than 10 % was achieved for high transmembrane fluxes. Generally, at low shear stresses with a high flux rate, decrease in droplet size was observed (Egidi *et al.*, 2008).

The effect of increasing continuous phase viscosity on droplet size has been reported to decrease the average droplet size. However, depending on other process parameters the uniformity of the droplets may be better at low continuous phase viscosity (Goran T. Vladisavljević *et al.*, 2006). Another study by Liu *et al.*, (2002) found that viscosity of alginate affected the uniformity of droplet size with concentrations of 2 % (w/v) alginate producing droplets with average diameter of 97µm and CV of 82 %. Production of monodispersed droplets is dependent on several factors and optimisation of the various process parameters are necessary to achieve control over drop size and uniformity of the emulsion.

5.1.5 Phage bacterium kinetics

Phage therapy effectiveness in reducing bacterial load requires high phage dose to lyse bacteria. Hence, delivering of a high dose of phage at the site of infection can prove to be an effective strategy in arresting bacterial growth and clearing infection (Tangi *et al*., 2013). At present, limited work has been published to address the problem of acid inactivation of phages in the stomach when phages are delivered orally. Several studies have shown that phage are rendered unviable if the pH is acidic (typically below pH 3) and demonstrated possible routes to protect them (Colom *et al*., 2015, 2017b; Cecilia Dini *et al*., 2012; Yongsheng Ma *et al*., 2012; Stanford *et al.*, 2010a; Tang *et al*., 2013, 2014; Yongsheng *et al*., 2008).

However, so far protection against pH 2 for 2 hours has been demonstrated *in vitro* (Yongsheng Ma *et al*., 2012; Tang *et al*., 2013, 2014; Yongsheng *et al*., 2008). Targeting phage encapsulation for biocontrol applications e.g. in poultry and swine may justify the reason for studying phage protection at pH 2. Human phage therapy however needs protection at pH values lower than pH 2 due to the variation in stomach pH depending on fed or non-fed state (McConnell *et al.,* 2008). Chapter 2 addresses this, showing that the combination of Eudragit and alginate can be used to protect phage from pH as low as pH 1. This is key in delivering the correct dose of phages to the site of infection. The rate of mutation in actively growing bacteria was reported to be 10^{-5} h^{-1} (Cairns *et al*., 2009), which is fast and necessitates rapid phage killing to prevent increase in bacterial concentration. In addition, scale-up issues around encapsulated phage need to be addressed.

Ex vivo experiments showing a three-way interaction of phage, bacteria and epithelial cells may prove beneficial in understanding infection dynamics. Stressed mammalian cells in the presence of bacteria may offer insights into an *in vivo* scenario. Addition of phages in a cell culture model useful insights into understanding of phage-bacterial inhibitions and the impact of this on mammalian cells (Shan *et al*., 2018). Further analysis will prove beneficial, when encapsulated phage are introduced and results can be compared and evaluated to show the equally beneficial effect of encapsulated phage.

Aims and objectives

The aim of this work was to demonstrate scale-up of phage encapsulation using membrane emulsification technology. Formulation development and optimisation performed in chapters 3 and 4

were transferred to produce larger quantities of encapsulated phage. Optimisation using membrane emulsification was performed to achieve encapsulated phage microparticles capable of acid protection. Control over droplet size was investigated by controlling various experimental parameters. Arresting growth of actively growing bacteria with both free phage and encapsulated phage was investigated, evaluating the effect of dose on bacterial lysis *in vitro.* The potential of encapsulated phage in arresting bacterial growth and infection of mammalian cells was studied in an *ex vivo* model. Overall, the potential of using ME to up-scale the process of phage encapsulation and application was investigated.

5.2 Materials and Methods

5.2.1 Chemical reagents

Eudragit S100 was purchased from Evonik Germany. Medium viscosity alginate was purchased from Sigma Aldrich, UK. Miglyol 840, a propylene glycol diester of caprylic/capric acid, was obtained from Sasol Germany. Food grade Castor oil was purchased from Elf Foods, Loughborough U.K. both of which made the continuous oil phase. Polyglycerol polyricinoleate (PGPR) soluble surfactant was purchased from Abitek USA. Tween 20, p-toluenesulfonic acid, sodium chloride and calcium chloride (Acros Organics, UK) were purchased from Fisher Scientific, UK. Ultrapure water was obtained from Millipore 185 Milli-Q Plus water filtration system. Sorensen's buffer 0.2 M was used as a dissolution media for the microparticles and was prepared by mixing sodium phosphate monobasic (NaH_2PO_4) (for pH 7, 39 ml) with sodium phosphate dibasic (Na_2HPO_4) (for pH 7 61 ml) (Fisher Scientific UK). Pancreatin and pepsin added to simulated intestinal fluid and simulated gastric fluid respectively were purchased from Sigma Aldrich, U.K. McCoys medium, Leibovitz supplemented with CO_2, Isopropyl β-D-1-thiogalactopyranoside (IPTG) and Fetal bovine serum (FBS) were purchased from Sigma Aldrich UK.

5.2.2 Culturing *EV36 and* phage propagation

E. coli strain *EV36* and phage K1F were obtained from collaborator Dr Antonia Sagona, University of Warwick, U.K. EV36 is a K-12 and K1 hybrid which is susceptible to K1 specific phages including K1F and K1-5 (Scholl *et al.,* 2005). Phage K1F is a T7-like phage first isolated from sewage in 1984 (Scholl & Merril, 2005).

EV36 was genetically modified to express red fluorescent protein (RFP) by Dr Antonia Sagona (University of Warwick, UK). The procedure for this cannot be disclosed here due to copyright protection. RFP-*EV36* was cultured in Luria-Bertani (LB) medium (Oxoid, Ltd., UK) with the addition of 0.5 mM IPTG and 10mg/ml Ampicillin sodium salt, (Sigma Aldrich U.K) (Figure 9.11 appendix).

Phage K1F was propagated on RFP-EV36. Phage stocks were prepared by growing a fresh culture of *RFP-EV36*, shaking at 37˚C until the $O.D._{550}$ reached 0.2. Then phage K1F was added at a MOI of 0.01. Once complete lysis of bacteria was observed (as seen by a clear solution of LB broth) the culture was centrifuged for 15 mins at 2,000 x g, and filtered through a 0.2 µm filter (Millipore, USA). The stock was stored at 4˚C until further use.

Plaque assays were carried out using the double layer agar method as described by Mahony *et al.,* (1985) and Goh *et al.,* (2005). Briefly, 10 µl of overnight culture of *RFP-EV36* was added to a 50:50 mixture of LB semi-solid agar and salt mixture (0.4 M $MgCl_2$ and 0.1 M $CaCl_2$, Oxoid Ltd. UK). This was poured onto LB agar plates and set under a laminar flow hood. 10 µl of phage solution was spotted on the plate (in triplicate), left to dry and incubated at 37˚C overnight. The following day the resulting number of phage plaques was enumerated.

The phage titre was determined by carrying out serial dilutions from the phage collected and each dilution (in triplicate) was spotted on host lawn. Phage titre was determined by counting plaques and expressed as plaque forming units (PFU) per ml. Similarly, for bacterial growth serial dilutions of bacterial culture were spotted on LB agar in triplicate and incubated overnight at 37˚C. Bacteria concentration was determined by counting colonies and expressed as colony forming unit (CFU).

5.2.3 Phage sensitivity assay

Phage inactivation (sensitivity) to different pH was assessed as follows. 0.2 M NaCl was pH adjusted with HCl to achieve pH 2, 2.5 and 3. 0.05 M of KH_2PO_4 was pH adjusted with NaOH to achieve pH 4, 5, 6 and 7. To analyse the survival of phage in each parameter 270 µl of each solution was added to a 96 well plate (in triplicate), with LB broth as positive control, 30 µl of phage stock (~10^8 PFU/ml) was added to each well. At time points 0 h, 0.5h, 1h, 3h, 6 h and 24 h serial dilutions in LB broth (270 µl) were performed for each test and spotted (10 µl x 3) on host lawn (prepared as described in the plaque assay section previously). The spotted plates were dried for 5 min and then incubated at 37 ˚C overnight. The following day, plaques were counted, and PFU/ml calculated.

5.2.4 Preparation of W/O emulsions

The dispersed (aqueous) phase was prepared by dissolving Eudragit S100 powder (final working concentration of 10 % w/v) in ultrapure water. 10 M NaOH solution was added dropwise until the solution turned clear and colourless indicating complete dissolution of Eudragit S100 polymer. Next, 2 % (w/v) alginate was dissolved with Eudragit S100 over heat (~60 °C) stirring overnight. 50ml of phage was concentrated in 50K Amicon Ultra centrifuge tubes, Millipore U.K. 10 % (v/v) of concentrated phage was added to a cooled Eudragit and alginate solution with a final working solution of 10^9 PFU/ml. The continuous (oil) phase was prepared by dissolving 2 % (w/v) of PGPR in a mixture of miglyol 840 and castor oil (9:1).

A dispersion cell from Micropore Technologies Ltd. (Teesside, U.K.) was used for the emulsification process. Figure 5.1 shows the setup of the equipment, the base holding the glass cylinder cell is made of poly(tetrafluoroethylene) (PTFE). The dispersed phase was introduced via a syringe mounted on the syringe pump into this base through a nickel membrane of a specified pore size (20 µm) (Figure 9.13 appendix). The glass cell carried the continuous phase which was screwed into the base of the above the membrane. The shear stress was provided by a paddle-blade stirrer operated by a 24 V DC motor, rpm was converted to $rads^{-1}$ (Figure 9.8 appendix) necessary for droplet detachment. The dispersed phase enters the glass cell through uniformly spaced pores of the membrane and the shear allows detachment of the droplets forming an emulsion. The nickel membranes also purchased from Micropore Technologies Ltd. (Teesside, U.K.) were pre-treated with 1H, 1H, 2H, 2H-Perfluorodecyletriethoxysilane (Sigma Aldrich U.K.) as per the manufacturer's instructions (Method 9.1 appendix). They were stored in the continuous phase when not in use. The use of membrane emulsification to produce uniform droplets by changing various parameters was well studied by (Kosvintsev *et al.*, 2008; Stillwell *et al*., 2007).

For this work, phage encapsulation was studied by producing polymer droplets which were cross-linked post droplet production for 1 h. The stirrer speed setting used for all experiments was 62 rad s^{-1}. The nickel membrane with pore size 20 µm had an effective surface area of 8.54 cm^2 (Hanga *et al* 2014), with pore spacing distance of 200 µm. The dispersed phase was pumped by a Harvard syringe pump (Harvard Apparatus U.K.) with an injection rate of 4.68 $Lm^{-2}h^{-1}$. The continuous phase volume was 50 ml for every 15 ml of dispersed phase that was introduced into the glass cell.

5.2.5 Preparation and characterisation of Eudragit and alginate particles

Once the emulsion was formed, it was transferred into a sterile tube. The droplets were settled by centrifuging at 500 x g for 3 mins. The droplets were re-suspended in acidified oil phase consisting of a 9:1 mixture of miglyol to castor oil with 2 % (v/v) PGPR) and 0.05 M toluenesulfonic acid. The droplets were left to crosslink for 1h, then they were centrifuged at 500 x g for 3 mins to pellet the semi-crosslinked droplets. After discarding the supernatant, the pellet was re-suspended in 0.1 M calcium chloride ($CaCl_2$) with 1 % (v/v) Tween 20 and left to further crosslink for 2h. The crosslinked particles were centrifuged at 2, 000 x g for 5 minutes to remove $CaCl_2$ solution. Particles were stored at 4˚C in sealed tubes.

Photographs of the droplets and particles were taken with an optical microscope (Nikon Eclipse E200, U.K.). For SEM images the gelled particles were firstly freeze dried (VirTis Wizard 2.0) for 24 hours at 1 bar pressure at -20°C. The dried particles were mounted on stubs and sputter coated with gold and viewed using a benchtop Scanning Electron Microscope (Hitachi TM3030 Table-top Microscope).

5.2.6 Cell culture and imaging

For cell culture T24 (ATCC® HTB-4™) urinary bladder epithelial cells were used. To obtain a confluent culture of epithelial cells, McCoys medium was added to tissue culture flasks with 1 % streptomycin (Sigma Aldrich, UK) and seed with frozen stocks of cells. Epithelial cells were grown in Leibovitz medium supplemented with 10 % FBS when grown in parallel with bacteria. NucBlue (Thermofisher U.K.) 1 drop/ml was added to epithelial cells and left to incubate for 15 mins before imaging changes in the nucleus.

Epithelial cells were inoculated with 10 µl of bacteria and incubated for 2 hours for infection to begin. After which in control flasks bacteria were left to grow with addition of LB (20 µl) without phage. Free phage at different titres (10^2, 10^4, 10^6, 10^8 PFU/ml) (volume 20 µl) was added to the positive control flasks. Microparticles with phage K1F were exposed to pH 2 for 2 hours before they (20 µl) were added to infected epithelial cells. Imaging was taken at hourly intervals (each flask was staggered accordingly). During imaging the temperature was maintained at 37°C.

For imaging Zeiss LSM 880 confocal microscope was used at University of Warwick (U.K.) with multi-channel spectral imaging and ultra-sensitive GASP detector. Images were analysed on Zen2.3 Lite software.

5.2.7 Dissolution of microparticles

1 g of particles were suspended in prewarmed 10 ml simulated intestinal fluid, 10 mg/ml pancreatin in 0.05mM KH_2PO_4 at pH 7 (Sigma Aldrich, UK) under agitation conditions at 37°C. For acid exposure 1 g of washed particles were suspended in prewarmed 10 ml simulated gastric fluid, 3.2 mg/ml pepsin in 0.2 M NaCl at pH 2 (Sigma Aldrich, UK) for an exposure period of 2 h, under shaking at 37°C. Particles were subsequently centrifuged at 2,000 g for 15 min and re-suspended in simulated intestinal fluid (pH 7, 6, or 5) under agitation conditions at 37°C until complete dissolution of particles. For enumeration of phage released, plaque assays were used (as described previously) by removing 10 µl of sample at hourly intervals, serially diluting in LB broth and spotting on a host bacterial lawn. The PFU/ml was determined the following day. For the co-encapsulation assay each phage was spotted on its respective host for titre.

For storage tests,1 g of particles was weighed and exposed to SGF (pH 2) for 2 hours, then centrifuged at 2,000 g for 15 mins and resuspended in SIF (pH 7) at 37°C until complete dissolution of particles. Phage release was enumerate as described above.

5.2.8 Coulter particle size analysis

A Coulter LS 130 (Beckman Coulter Inc.) (Figure 9.7 appendix) was used to determine the droplet and particle size distribution. The device is laser modulated and uses the optical model Fraunhofer, to detect laser diffraction caused by droplets and particles (appendix). The equipment feeds the information to a computer where data is collated via the LS software program. Droplets or particles were loaded into the sample cell containing the continuous phase and directly placed inside the coulter equipment to carry out the measurements.

5.2.9 *In vitro* phage bacteria dynamics

The effect of free phage and encapsulated phage in arresting bacterial growth was investigated. Firstly, bacteria were grown until log phase was reached, at 0.2 (O.D. 550) (approximately 10^8 CFU/ml). The assay was performed in LB and cell culture media, (Leibovitz). Each well contained 2 ml of bacteria to which 20 µl of free phage was added at different concentrations (10^2, 10^4, 10^6, 10^8 PFU/ml), 20 µl of encapsulated phage (Ephage) was also added to 2 ml of bacterial culture with and without pH 2 exposure for 2 hours. Separately, a negative control contained 20 µl of Ephage in LB media or cell culture media without bacteria and the positive control contained bacteria only. After phage addition, the infection was allowed for one hour before samples were taken at hourly intervals up to 5 hours.

Upon sample collection, 1 ml was removed to record the $O.D._{550}$ and 1 ml was centrifuged, and plaque assay carried out (as per the procedure above). For the positive control, bacterial counts were determined by spotting 10 µl of sample on LB agar plates. The following day the plates were counted and CFU determined.

5.2.10 Statistical analysis of results

Comparison of sample means using 2 sample t-tests and evaluation of 95 % confidence intervals for data was carried out using the statistical software Minitab 18.

5.3 Results

5.3.1 Acid sensitivity of free phage

Model phages against enteric pathogens such as *Salmonella* and *E. coli* were analysed for their sensitivity to different pH. The results for each phage, demonstrates susceptibility to low acidic pH and highlights the need for encapsulation. In the case of phage K1F, all phages were inactivated after merely 10 secs of pH 2 exposure whereas Felix O1 showed more resilience as viable phage were detectable after 10 mins of exposure. Nevertheless, in both cases no detectable phages were measured after the initial 10 minutes of exposure time. The results underpin the motivation behind this study which is to encapsulate and protect the phages from acid damage.

The pH sensitivity of K1F to low pH was evident even at pH 2.5, the phage was completely inactivated after 10 minutes of exposure. On the other hand, Felix O1 showed more tolerance at this pH, with viable phage measured up to 3 hours (Figure 4.3). However, the titre of the phage significantly dropped indicating a clear need for encapsulation. The stomach pH of some animals may be as high as pH 3, therefore it is important to consider the phage viability at this pH. Phage K1F showed more tolerance at this pH but there was over a log reduction in titre whereas Felix 01 showed greater stability over time (Figure 5.2). In either case, phages were stable over 24 hours as the pH increased, this is important when using pH responsive polymers such as Eudragit S100, because to dissolve this polymer the pH needs to be neutral or alkaline.

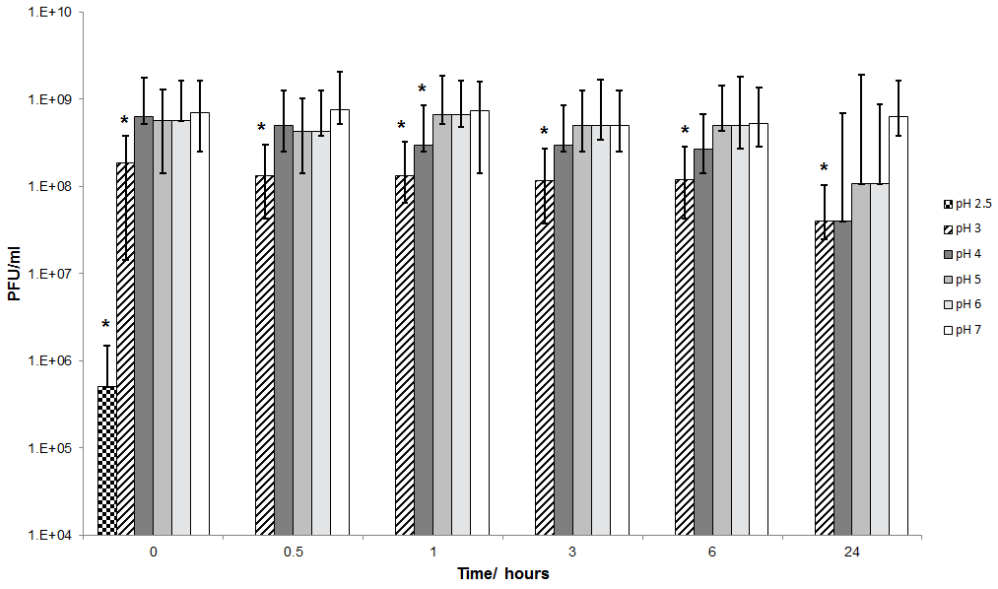

Figure 5.2 Effect of pH on free phage K1F viability in 0.2 M NaCl solution pH 2 not shown since no detectable phage was recovered at time point 0. * indicates significantly different phage titres using a 2-sample t-test at each condition compared with phage exposed to pH 7 at the corresponding time point. Time point 0 hours denotes time between 0-10 minutes for phages exposed to all pH values except pH 2.5 where phage titre reduced rapidly, and data are plotted 10 seconds post exposure. P-values can be found in Table 9.1 (appendix).

5.3.2 Effect of stirrer speed on droplet diameter

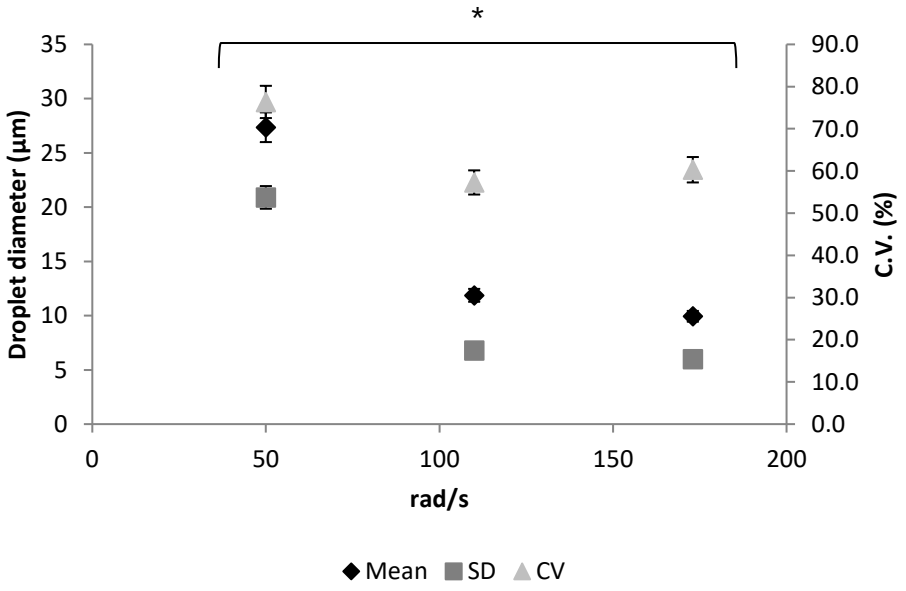

Figure 5.3 Effect of stirrer speed on the mean droplet size (300 droplets analysed) composed of 5 % (w/v) ES100 with infusion rate of 100 mlh^{-1}, membrane pore size 20 µm. * indicates significantly

different droplet sizes when comparing the mean sizes of each parameter for each time point ($p < 0.05$).

Shear is an important parameter when determining the size of droplets in membrane emulsification. Hence, the influence of shear rate on droplet size was investigated using 5 % (w/v) Eudragit S100 in the dispersed phase. A total of 300 droplets were measured for each parameter investigated. Uniform droplets were measured ranging between 10 to 30 µm (Figure 5.3). With increasing shear the average droplet diameter reduced. However, this was not necessarily linear. It was found that further increasing the shear did not result in smaller droplets but rather the C.V. was compromised. The influence of droplet size on phage loading was also analysed (Figure 5.4). There was a slight decrease in phage loading observed when the droplet size was reduced from 27 µm to 10 µm. This may be attributable to the shear stress; by increasing the frequency of droplet breakup at the membrane interface the resulting droplets were smaller in size. This translated to smaller particles, the larger surface area to volume ratio increased the likelihood of phages encountering acid during crosslinking in acidified oil. This may be attributable to the decrease in phage loading in smaller particles. These findings formed the basis for further work, which included increasing polymer concentration and introducing alginate as a co-polymer. Changing the dispersed phase composition also meant changing the viscosity which influenced the droplet size.

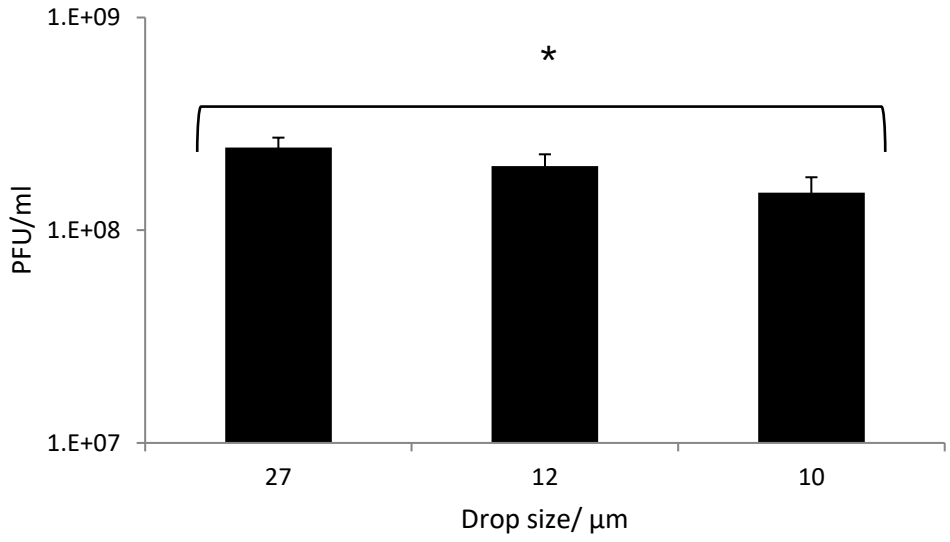

Figure 5.4 Effect of droplet size on phage encapsulation. Phage released in pH 7 (without acid exposure) and titre measured after 5 hours. * indicates the significance mean was compared ($p < 0.05$) using a 2-sampel t-test. All measurements were done in triplicate (n=3)

5.3.3 Effect of alginate concentration on drop diameter

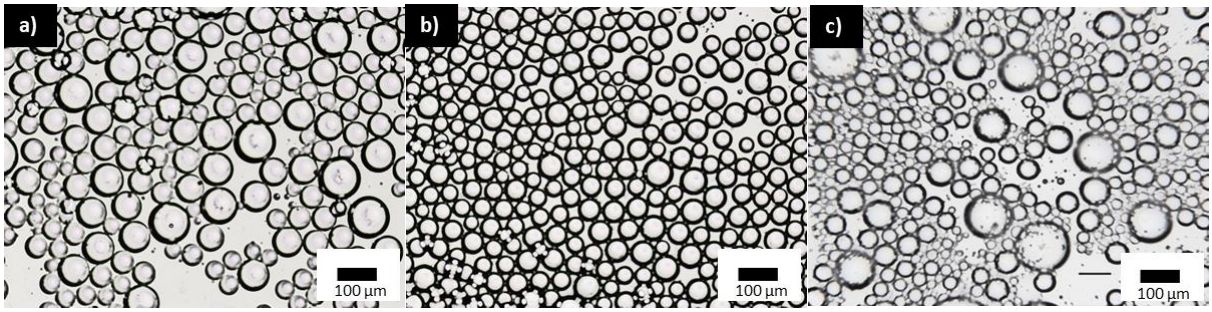

Figure 5.5 Effect of alginate concentration on droplet size, all other parameters were kept constant at, 10 % ES100, 40 mlh^{-1}, 62 $rads^{-1}$, 20 µm pore nickel hydrophobic membrane a) 0.5 % (w/v) alginate, b) 1 % (w/v) alginate c) 2 % (w/v) alginate.

Changes in droplet size were investigated through changing alginate concentration whilst keeping Eudragit S100 concentration constant at 10 % (w/v). In comparison to Eudragit droplets alone the average droplet size increased (Figure 5.5). The viscous nature of the alginate meant the infusion rate was increased to allow for enough dispersed phase to enter the pore to form a droplet. Droplets were bigger for 0.5 % (w/v) alginate formulation (Figure 5.5a) in comparison to other formulations. As the concentration of alginate increased so did the viscosity. Therefore, at the same infusion rate the lowest concentration of alginate (0.5 % (w/v)) caused an increase in the dispersed phase flux. As viscosity increases with higher alginate concentration, the dispersed phase flux decreased resulting in smaller droplets.

The most uniform droplets were observed with the 1 % (w/v) alginate formulation, due to better balance between viscosity and interfacial tension. With increasing viscosity, the interfacial tension also increases which theoretically should result in larger droplets due to instability of droplets, and their tendency to coalesce. The amount of surfactant required to overcome interfacial tension was higher therefore the variation in droplet size was observed at higher concentration of alginate (Figure 5.5c). The formulation prepared with 2 % (w/v) alginate gave the best results during acid exposure of phage therefore, this was taken forward for further analysis.

5.3.4 Effect of membrane pore size and flow rate on droplet diameter

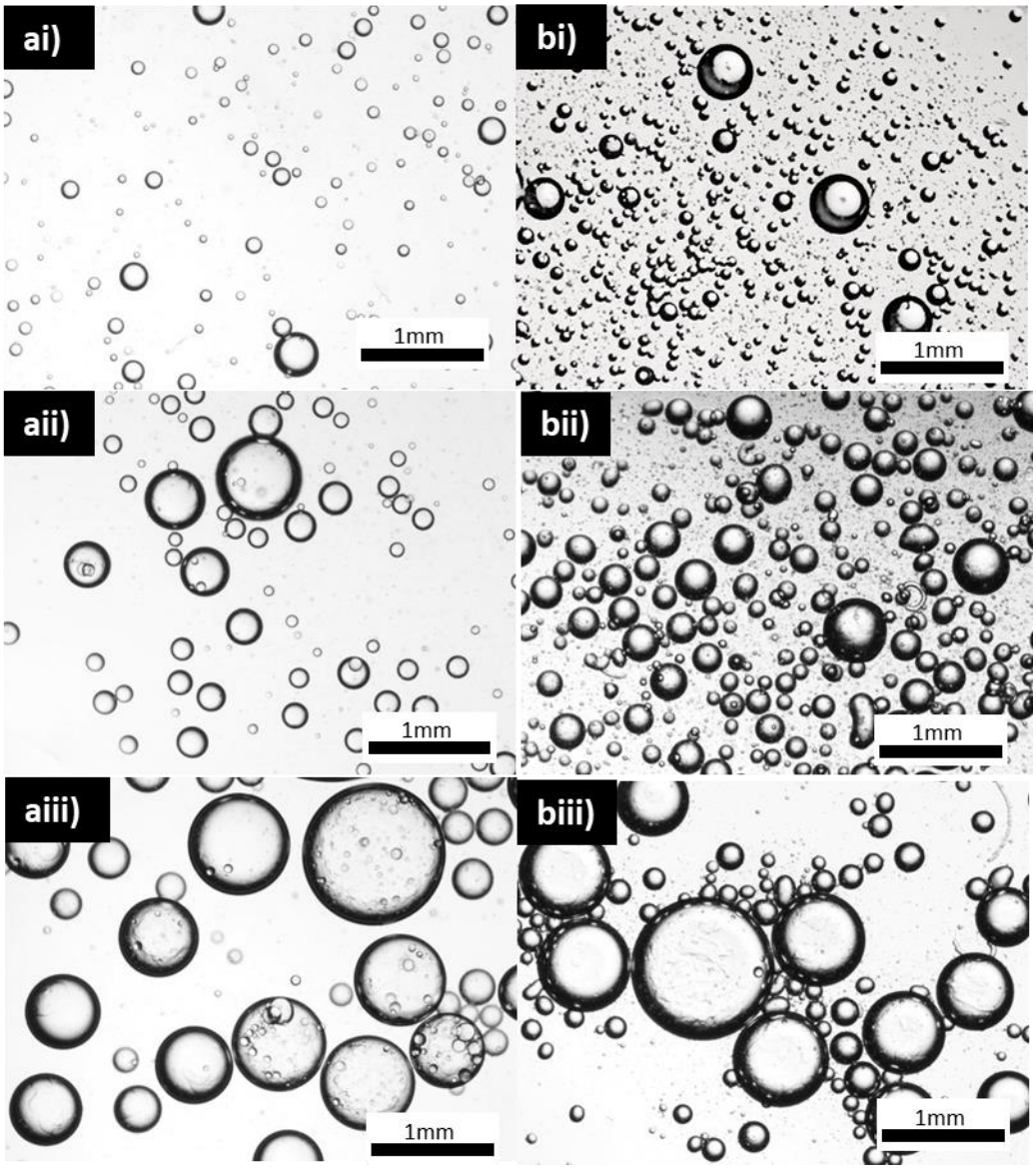

Figure 5.6 Effect of membrane pore size and dispersed phase flow rate on drop size. ai) 40 µm pore membrane with 10 mlh^{-1} aii) 40 µm pore membrane with 40 mlh^{-1} aiii) 40 µm pore membrane with 50 mlh^{-1} bi) 20 µm pore membrane with 10 mlh^{-1} bii) 20 µm pore membrane with 40 mlh^{-1} biii) 20 µm pore membrane with 50 mlh^{-1}.

Another set of parameters that can affect the size of the droplets is the membrane pore size. The influence of a 20 µm and 40 µm pore size nickel membrane was investigated with formulations containing 2 % (w/v) alginate and 10 % (w/v) ES100 as the dispersed phase (Figure 5.6). The shear was kept constant, but the dispersed phase the flow rates were changed to observe changes in drop size. Droplets produced using the 40 µm membrane produced larger droplets for the respective flow rates in comparison to the 20 µm membrane. For both membranes the uniformity of the droplets was compromised due to the viscous nature of the dispersed phase. As the flow rate was increased the droplet size was also seen to increase. Droplets as large as 1 mm were produced at the highest

flowrate (Figure 5.6 aiii and biii). Desired droplet size could be achieved by either membrane by changing the dispersed phase flux.

5.3.5 Effect of continuous phase on droplet diameter

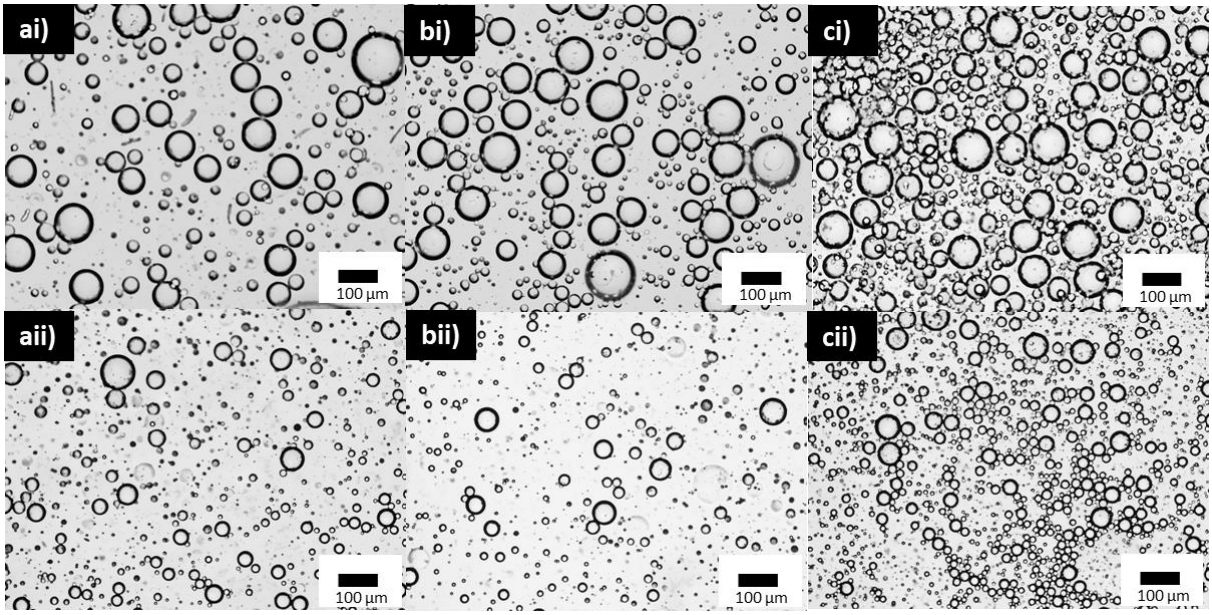

Figure 5.7 Effect of continuous phase viscosity on droplet size and particle size. Miglyol and castor oil (M:C) were mixed in varying ratios to alter viscosity ai) M:C 9:1 droplets aii) M:C 9:1 particles bi) M:C 4:1 droplets bii) M:C 4:1 particles ci) M:C 2:3 droplets cii) M:C 2:3 particles.

Typically, in literature on emulsions the dispersed phase viscosity tends to be less than that of the continuous phase, however the present case, dispersed phase viscosity was higher. Therefore, to gain further control over droplet size in the membrane emulsification process, the continuous phase viscosity was changed. Viscosity of the continuous phase was increased by adding castor oil at different ratios to miglyol whilst keeping PGPR concentration the same at 2 % (w/v). Figure 5.7 shows the droplets produced with the corresponding particles. With increasing viscosity, the droplet size decreased (Figure 5.7). The coulter analyses put into perspective the average droplet size for each parameter showing as the viscosity of the continuous phase was increased, the mean droplet size increased (Table 5.1). Droplets were also crosslinked with TSA and $CaCl_2$ and the size was analysed for any changes. Shrinkage of the particles was observed in all cases, with approximately 50 % reduction in the mean droplet to particle size.

Table 5.1 Cumulative size distribution by volume of (10 %, 50 %, 90 %) droplets and particle with changing miglyol to castor oil ratios with 10 % (w/v) Eudragit and 2 % (w/v) alginate as aqueous phase.

Droplet/ particle size in µm						
M:C	**D10**		**D50**		**D90**	
	Droplets	Particles	Droplets	Particles	Droplets	Particles
9:1	8	6	54	24	64	59
4:1	8	3	49	24	111	70
2:3	5	1	16	10	54	31

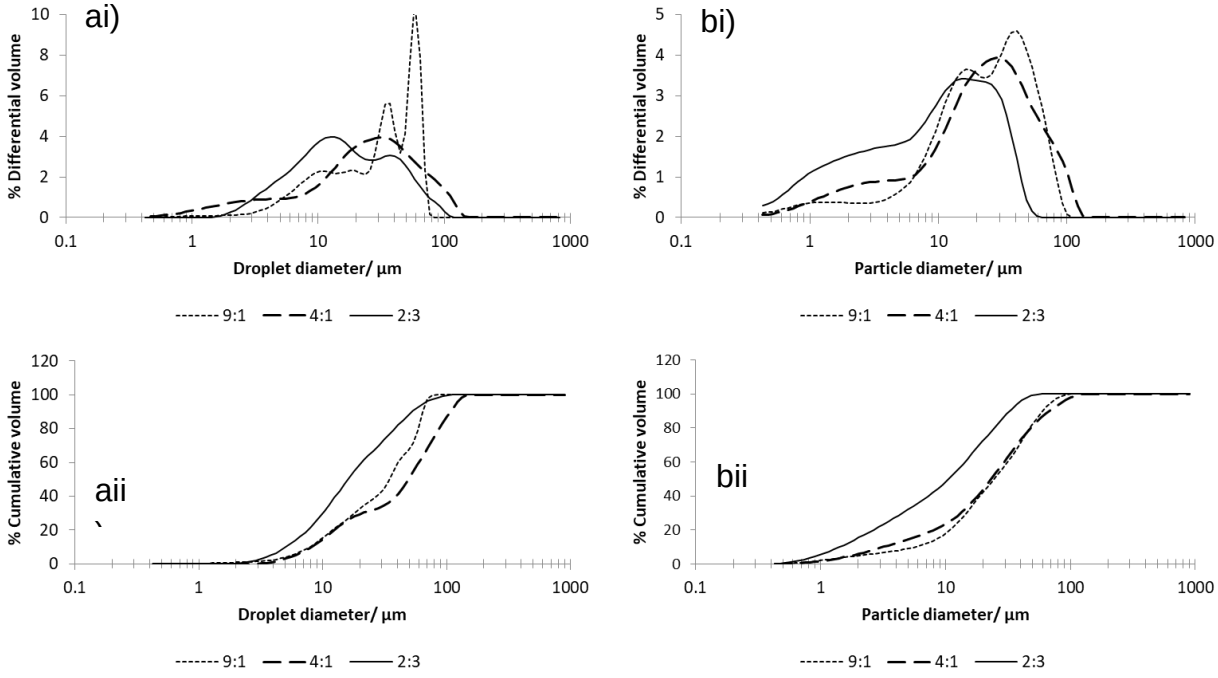

Figure 5.8 Coulter analysis of a) drops and b) particles produced by varying miglyol to castor oil ratios (M:C 9:1, 4:1, 2:3). ai) volume percentage of droplets aii) cumulative volume percentage of drops bi) volume percentage of particles bii) cumulative volume percentage of particles.

Coulter volume distribution analysis showed the bulk of the volume consisted of bigger drops/particles as opposed to the smaller drops/particles. The graph shifted to the left as the continuous phase viscosity was increased, showing that the average drop or particle size by volume decreased (Figure 5.8a). Bulk of the volume was carried by the bigger drops for each parameter even though the smaller drops/particles may be higher in number. The phages are carried in the bulk volume therefore the release profile will be largely influenced by the larger droplets. Figure 5.8b shows the cumulative volume for each parameter with drop/ particle size varying between 10 to 100 µm. A shift is noticeable

as the continuous phase viscosity rises and can be a useful tool to manipulate the production of a certain range of drop/particle sizes.

5.3.6 Effect of dispersed phase flow rate on droplet diameter

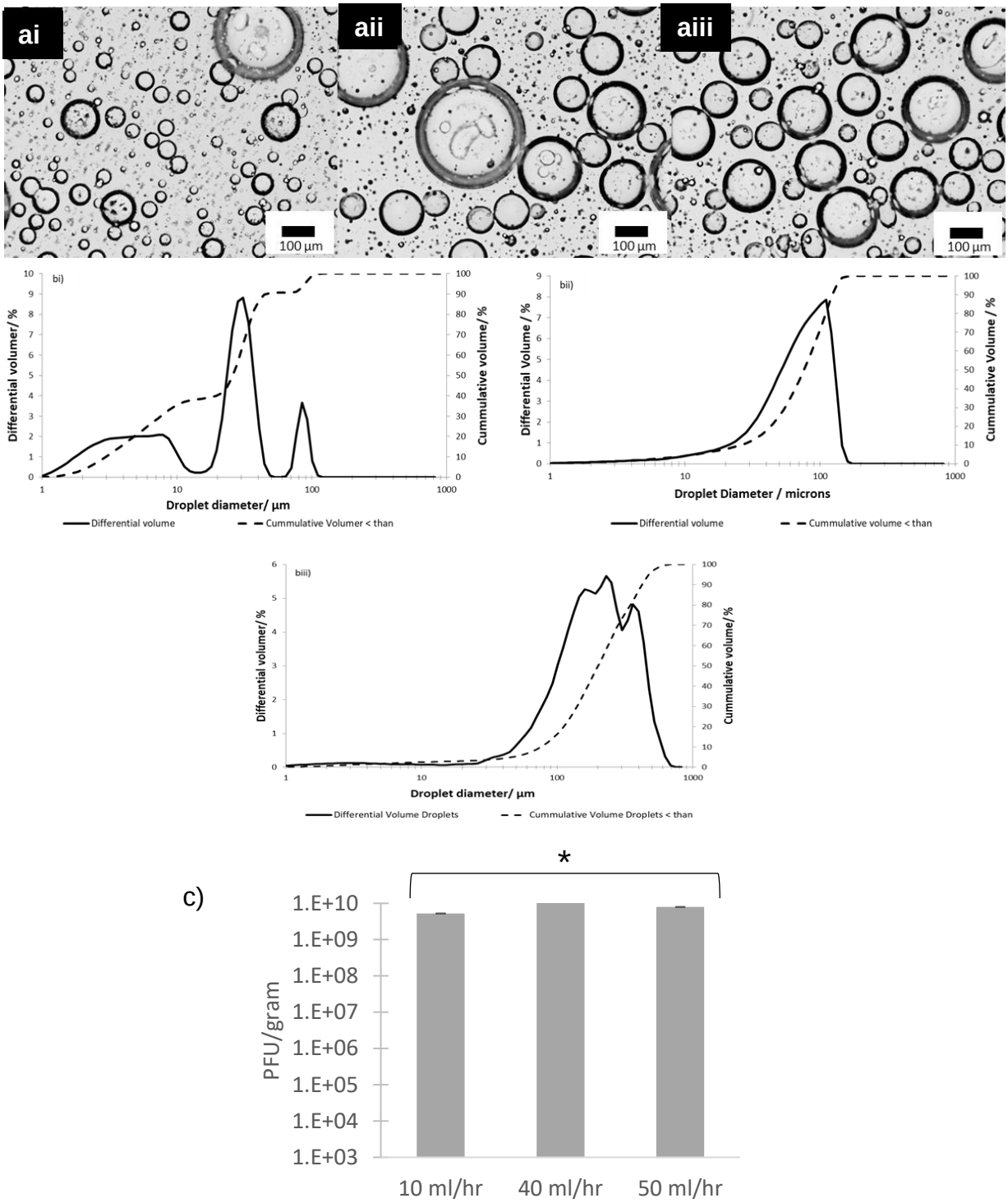

Figure 5.9 Effect of flow rate on droplet diameter a) optical images ai) 10 mlh^{-1} aii) 40 mlh^{-1} aiii) 50 mlh^{-1} b) coulter analysis bi) 10 mlh^{-1} bii) 40 mlh^{-1} biii) 50 mlh^{-1} c) phage encapsulation with release in pH 7 Sorensen's buffer with no acid exposure.

Flow rate plays an important part when manipulating droplet size. The dispersed phase flux controls the amount of liquid flowing through the pores before shear breaks them away from the membrane surface. Low dispersed phase flux results in smaller droplets in comparison to high fluxes (Figure 5.9 ia-c). Although the size is also influenced by continuous phase viscosity, in this case this parameter was kept constant to observe the impact of dispersed phase flux.

The change in droplet size was further confirmed by coulter analysis (Figure 5.9ii). There was a clear shift in the average droplet diameter towards the right (bigger drops) as the dispersed phase flux increased. This is a key factor when using membrane emulsification to control drop size. The smallest droplets were produced at the lowest flux with a high proportion of drops in the 10 μm region. This increased for 40 mlh^{-1} and 50 mlh^{-1} to below and above 100 μm.

For all three parameters, the effect on phage encapsulation was analysed (Figure 5.9c). Phages were present in all samples and were protected at pH 2 (exposure for 2 hours). For further experiments, 40 mlh^{-1} was used due to the narrow distribution of drop size in coulter and phage loading. 10 mlh^{-1} was not chosen due to increased length of time required to run the experiments and 50mlh^{-1} was not chosen due to a broader distribution of drop size in coulter. The experiment was then repeated with the following parameters, dispersed phase flux 40 mlh^{-1}, shear rate 62 $rads^{-1}$ and 9:1 ratio of Miglyol to castor oil with 2 (w/v) alginate. Figure 5.10 shows the results for phage encapsulation in these particles. The optical images are presented at different magnification for droplets Figure 5.10a and particles Figure 5.10b). The coulter sheds light into the droplet and particle size distribution where there is a slight shift of particle size to the left (smaller size) in comparison to droplets. The particles were then freeze dried and viewed under SEM (Figure 5.11). Here the morphology of the particles shows that they are non-porous, smooth and spherical.

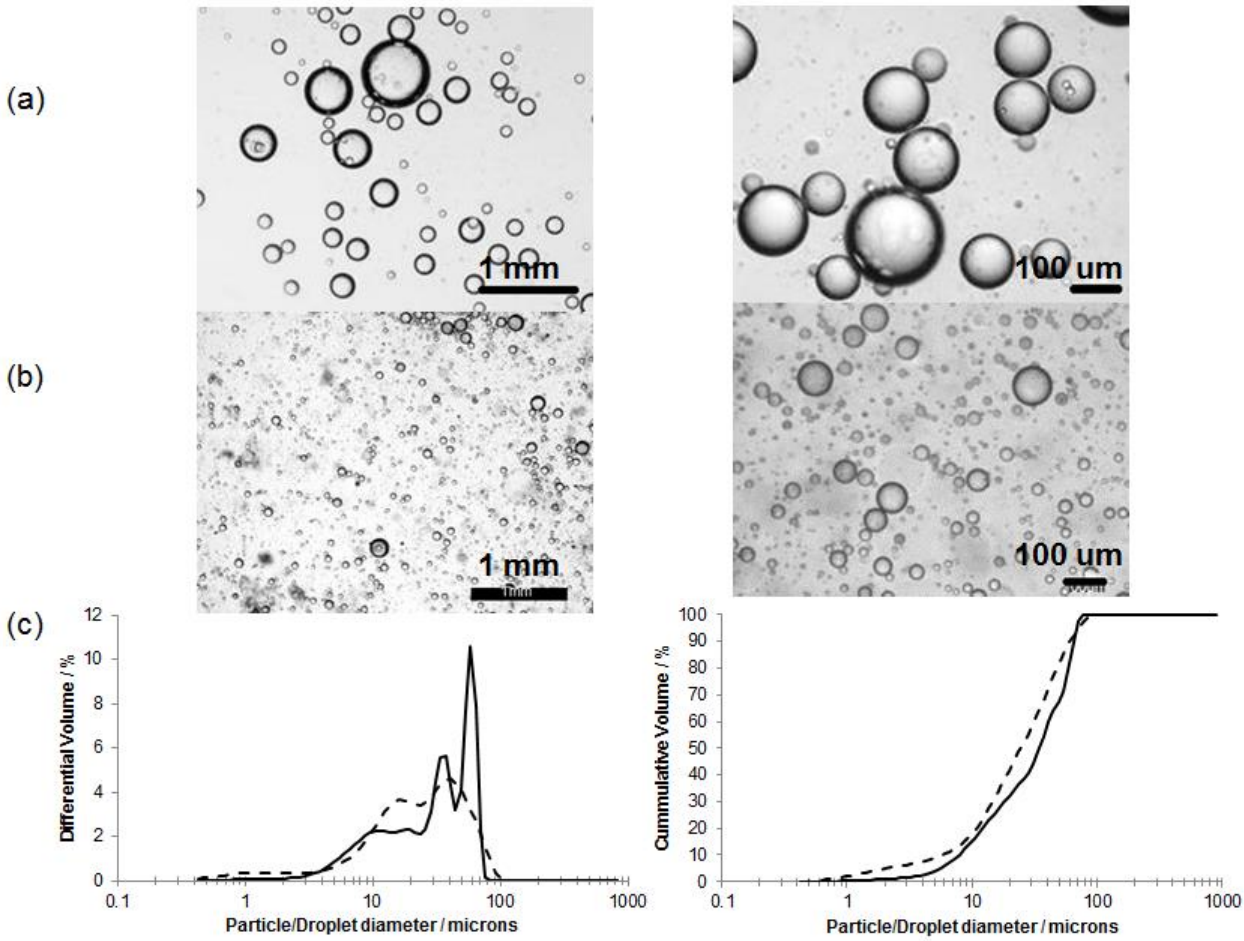

Figure 5.10 Optical microphotographs of w/o emulsion droplets, crosslinked particles, and size distribution of phage containing emulsion droplets and particles. (a) emulsion produced using dispersed phase flow rate of 40 $mlhr^{-1}$ and paddle rotation speed of 62 $rads^{-1}$at different magnifications. Dispersed phase composition: Eudragit S100 10 % (w/v), Alginate 2 % (w/v). Continuous phase composition: M:C ratio 9:1, with 2 % (w/v) PGPR. (b) Microparticles produced from emulsions following TSA and $CaCl_2$ crosslinking at different magnifications. (c) Droplet and particle size distribution, solid lines – droplets; dashed lines – particles.

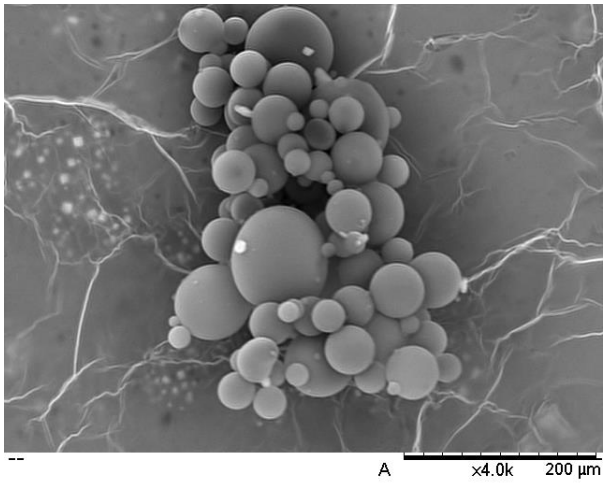

Figure 5.11 SEM image of particles produced by membrane emulsification (phage K1F) from 10 % (w/v) ES100, 2 % (w/v) alginate.

5.3.7 Effect of crosslinking parameters on phage encapsulation.

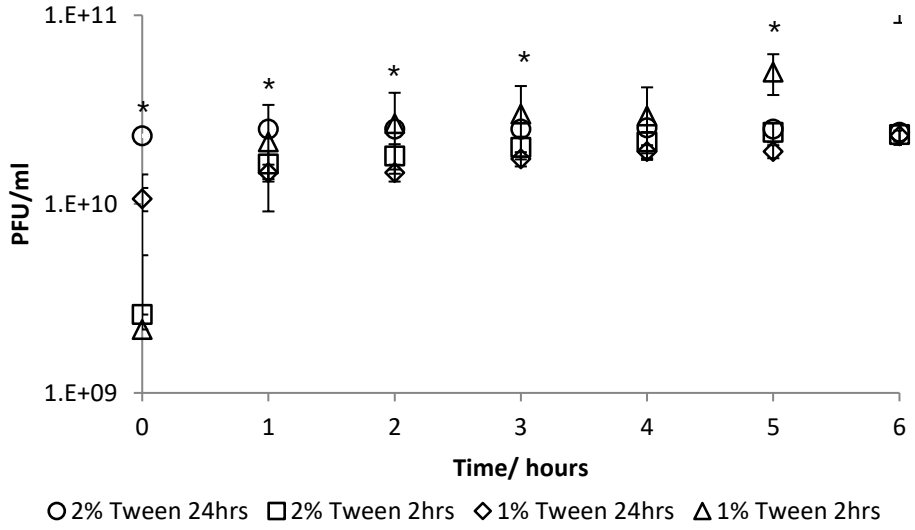

Figure 5.12 Effect of Tween concentration and crosslinking time on phage viability (10 % (w/v) ES100, 2 % (w/v) alginate at 62 $rads^{-1}$, 20 µm mem, M:C 9:1 Felix 01). 1 % and 2 % (v/v) of Tween 20 was added to $CaCl_2$ for crosslinking composite particles. After crosslinking the particles were release in SIF for 6 hours. The plotted results are mean of 3 repeats. *indicates a significance difference between the mean PFU/ml for each parameter comparedto the mean of every other parameter within each time point ($p<0.05$).

The effect of crosslinking times and surfactant concentration in the crosslinking solution was investigated. The influence of Tween concentration was studied because the pH of the solution changes with the addition of surfactant. With higher Tween concentrations the pH of $CaCl_2$ falls, so at

2 % tween the pH was 3 and at 1 % tween the pH was 4. The effect was further examined by allowing different crosslinking times (2 hours and 24 hours). Figure 5.12 shows that there was no significant difference in each of the parameters investigated. Phage titre was unaffected by tween concentration and crosslinking time.

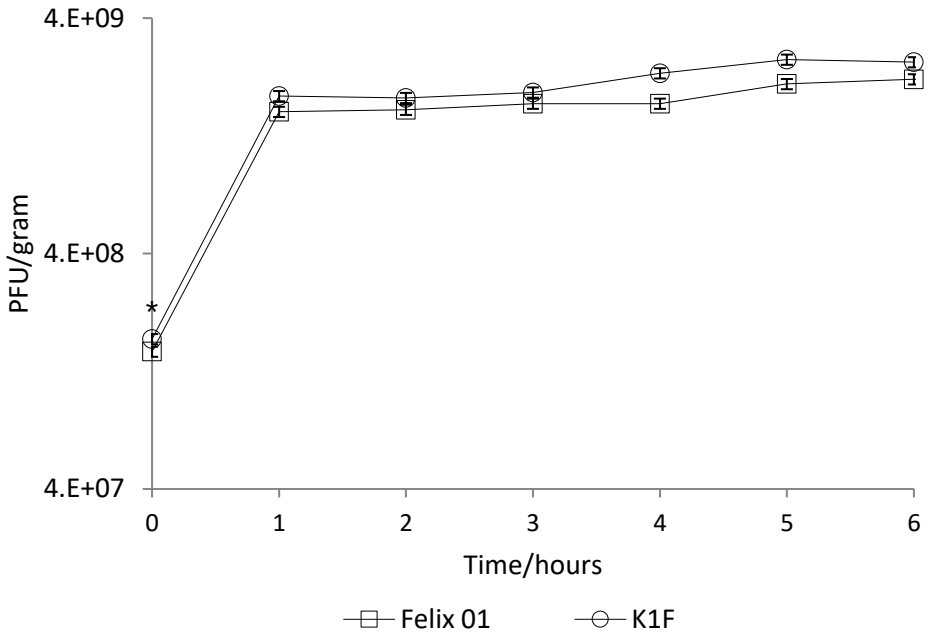

Figure 5.13 Phage Felix 01 and K1F encapsulated together in 10 % (w/v) ES100, 2 % (w/v) alginate at 62 rads^{-1}, 20 µm membrane, M:C 9:1. The plotted results are mean of 3 repeats. *indicated a statistical difference for the PFU/gram at each time point in comparison to the final value at 6 h ($p<0.05$)

Since the formulation was used for more than one phage against enteric pathogens, both Felix O1 and K1F were encapsulated together. This was to observe any interactions between the phages that may affect the encapsulation process. Figure 5.13 shows the results for the two phages encapsulated together and their release profile at pH 7 (plaque assay carried on the appropriate host). The encapsulation showed 100 % efficiency with the titre remaining ~ 10^9 PFU/ml for both phages. The release profiles also showed similarities with a burst release within the first hour and slow increase thereafter. The two phages did not have a negative effect on the encapsulation of the other, the formulation was suitable for co-encapsulation of more than one phage. Both phages belong to the *myoviridae* family and are in similar in size, therefore they occupy a similar spatial area.

5.3.8 Encapsulation of phage K1F

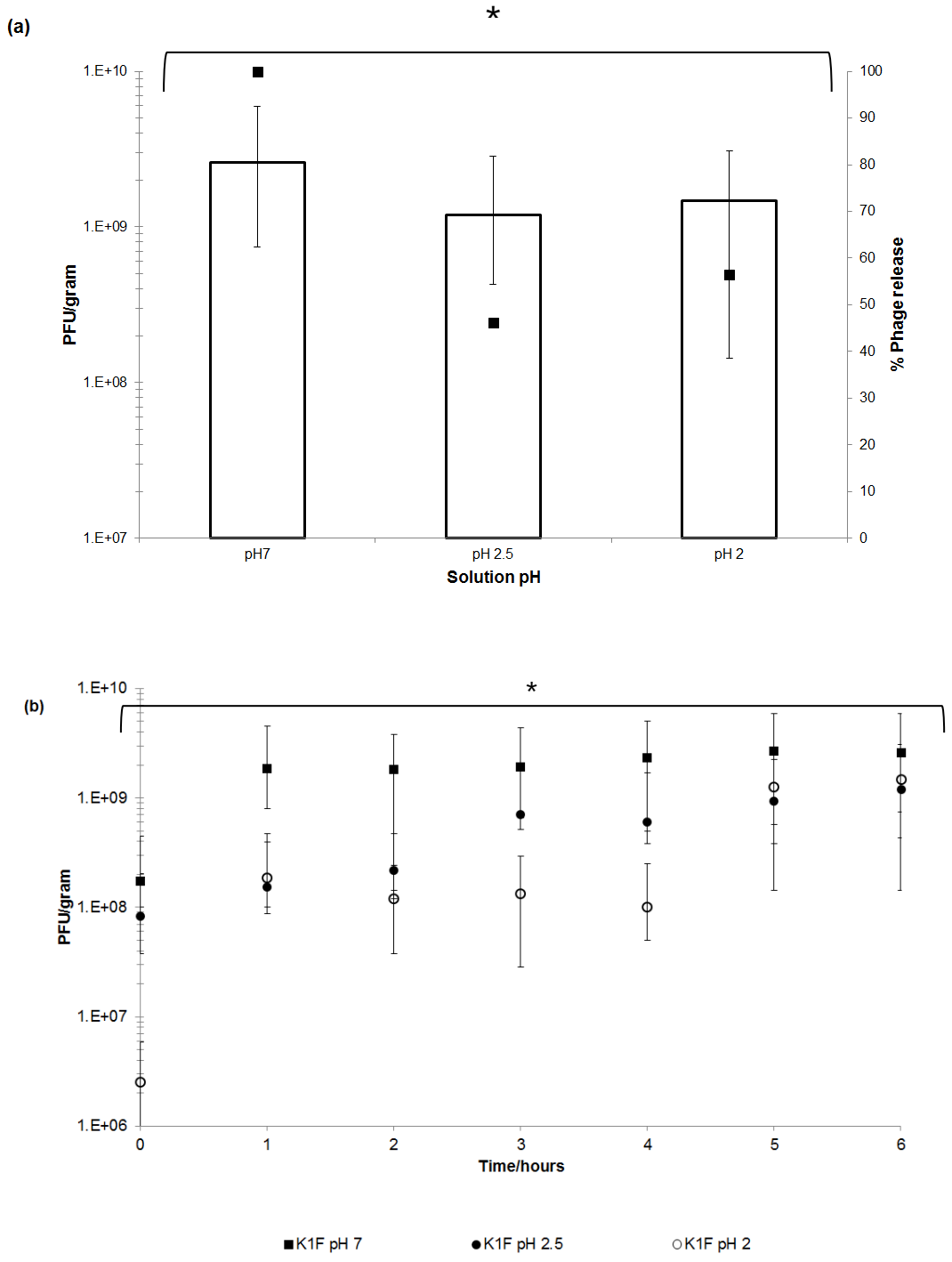

Figure 5.14 Release of encapsulated phage from 10 % (w/v) ES100, 2 % (w/v) alginate at 62 rads^{-1}, 20 µm mem, M:C 9:1 microparticles. (a) Total phage release from ES100/Alg microparticles after 6 h exposure to SIF at pH 7 with and without exposure to SGF at pH 2 and pH 2.5 (exposure to SGF for 3h).

(b) Phage release kinetics from ES100/Alg microparticles over a 6 h exposure period to SIF at pH 7 without (K1F pH 7) and with exposure to SGF at pH 2 (K1F pH 2) and pH 2.5 (K1F pH 2.5). *indicates a statistical difference between the average mean of each parameter in comparison to pH 7 within each time point in a two-sample t-test ($p<0.05$).

Phage K1F was encapsulated and exposed to SGF pH 2 and 2.5 for 2 hours, after which phage was released at pH 7 SIF Figure 5.14a. Over 70 % of the encapsulated phages were released after 2 hours exposure to pH 2, this was comparable to pH 7 as there was less than 1-log reduction in phage titre. The release profile showed a burst release of the phages with most of the phages being released within the first hour and then slowly rising over five hours to complete full release (Figure 5.14b). For pH 2 and 2.5 the phage titre after complete release was of the same order and statistically indifferent to pH 7 as shown by the error bars.

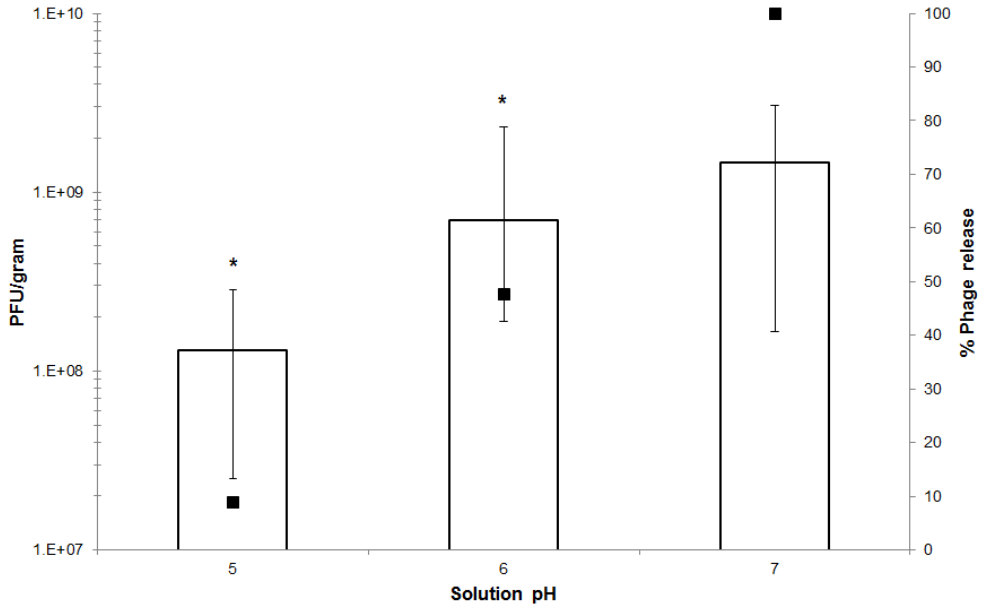

Figure 5.15 Release of encapsulated phage from 10 % (w/v) ES100, 2 % (w/v) alginate at 62 $rads^{-1}$, 20 µm mem, M:C 9:1 microparticles. Phage release (PFU g^{-1}) after 5h from ES100/Alg microparticles in SIF at different pH values following prior exposure of microparticles to SGF at pH 2 (3 h exposure to SGF). Black squares represent the % phage release. * indicates significantly different phage titres ($p < 0.05$) for a 2-sample t-test with each sample compared with phage release from ES100/Alg exposed to pH 7.

The phage was further investigated for its release kinetics at pH 5 and 6 (Figure 5.15). The pH in the lower gastrointestinal tract rises slowly therefore release of phage at these pH was a crucial factor to consider. Post pH 2 exposure encapsulated phage K1F microparticles were added to pH 5, 6 and 7 (Figure 5.15). Less than 40 %/ 10^6 PFU/ml of phages were released at pH 5 and approximately 60 %/ 1

x 10^9 PFU/ml were released at pH 6. This phenomenon was observed due to the hydrolysis of the carboxylate groups on the Eudragit polymer which are present at pH 5 and these begin to increase as the pH rises to pH 6 and 7 hence increase in phage release. Similarly, with increasing pH alginate also begins to swell and dissolve. Upon a 5-hour exposure to pH 5 and 6 the particles were then suspended in pH 7 solution to complete the dissolution and release of the remaining encapsulated phage which corresponded the phage titre at pH 7 only.

5.3.8 Kinetics of bacterial lysis by encapsulated phage

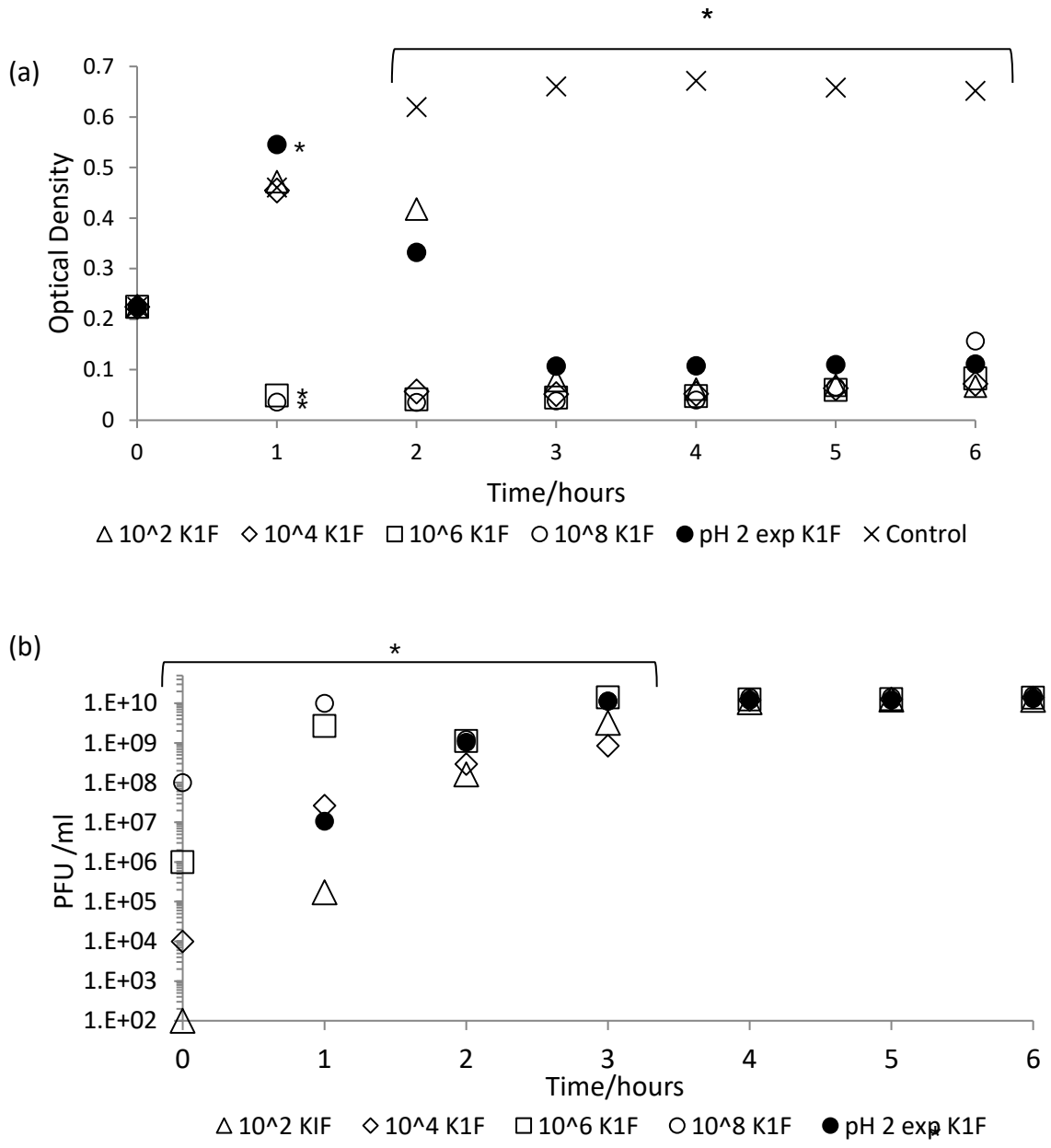

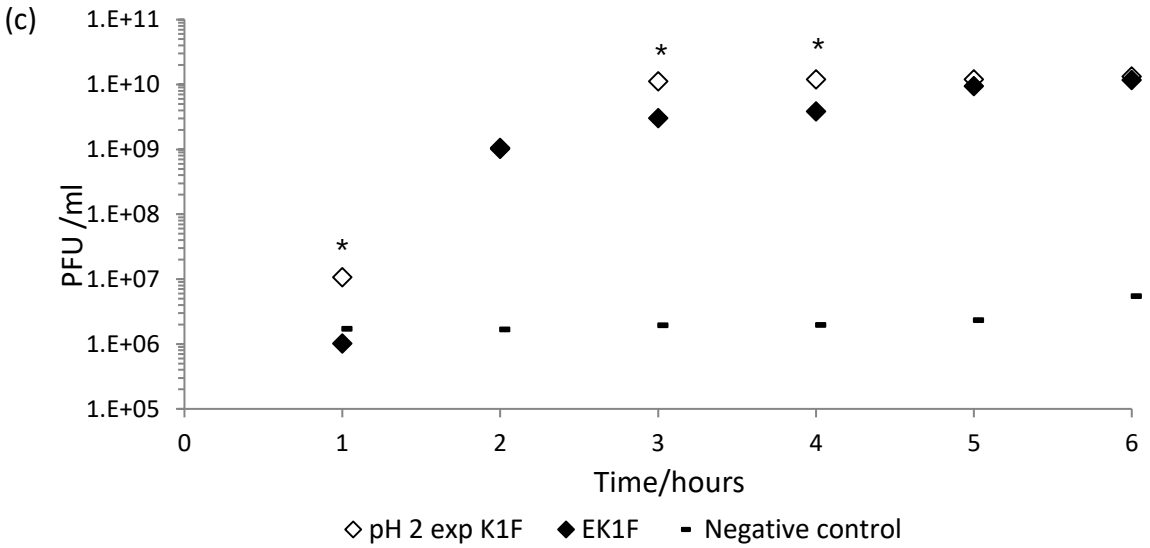

Figure 5.16 Dynamics of phage killing of *E. coli* EV36 bacteria with K1F bacteriophages. (a) Optical density curves showing bacteria killing in the presence of different concentrations of added phage. *indicates significance difference in comparison to the control ($p< 0.05$) n=3 (b) Phage amplification in the presence of *E. coli* EV36. *indicates significance difference between all parameters within each time point ($p<0.05$) n=3 (c) Comparison of phage amplification of EK1F phages encapsulated in microparticles with and without exposure to SGF (3 hours). *indicates the significance difference in the mean PFU/ml between pH 2 exposed K1F and EK1F within each time point in a two-sample t-test ($p < 0.05$) n=3.

Encapsulated phage killing of bacteria in comparison to free phage was examined in a series of experiments. The control which monitored the growth of bacteria over the course of the experiment showed exponential growth Figure 5.16a as shown by the optical density. Different concentrations of free phage were added to an exponentially growing culture of bacteria. High concentration of free phage (10^6 PFU/ml and 10^8 PFU/ml) were able to arrest bacterial growth early on approximately within the first hour the O.D. of the bacteria dropped significantly. Low free phage concentrations such as 10^2 PFU/ml and 10^4 PFU/ml were also able to arrest bacterial growth however this took longer around 3 hours post phage infection.

Ephage pre-exposed to pH 2 showed similar killing profile to the low pH phage concentrations. Ephage was also able to arrest bacterial growth but 3 hours post infection. Low phage concentration lags due to the time required for phage amplification. Phage amplification catches up to the growing bacterial population however there was a time delay in comparison to a high titre phage Figure 5.16b. Ephage

and 10^4 PFU/ml showed similar phage amplification Figure 5.16b meaning the phage released from the ephage was of the same order (10^4 PFU/ml). All phage was amplified by hour 3 Figure 5.16b meaning low titre phage can catch up due to amplification.

Figure 5.16c demonstrates the comparison between ephage with and without exposure to SGF and release of ephage in the absence of bacteria. Ephage with and without SGF exposure showed similar amplification profiles, meaning the exposure to SGF did not affect the phage titre. Encapsulation enabled the phage to stay viable even after pH 2 exposure which was an important finding since free phages alone were not able to survive pH 2 exposure.

5.3.9 Three-way interaction of phage, bacteria and epithelial cells

(a,i)

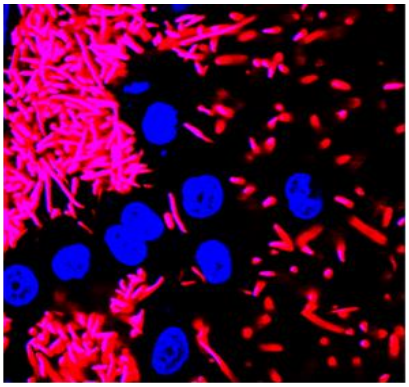

(b,i)

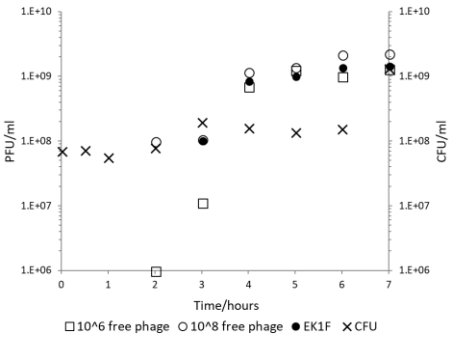

(a, ii)

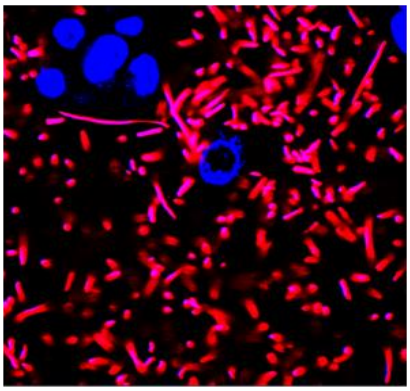

(b, ii)

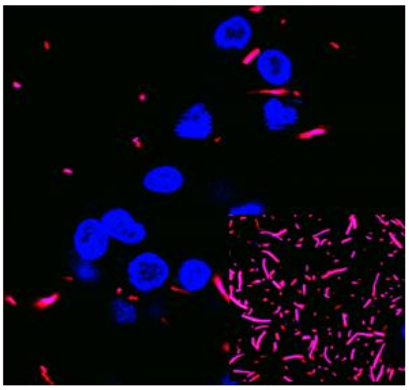

(a, iii)

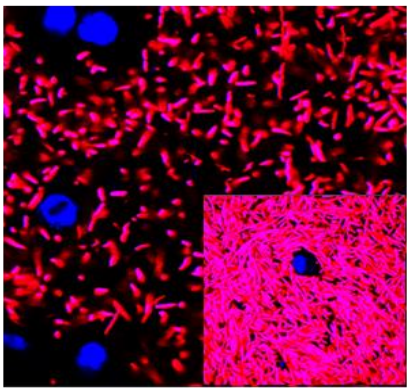

(b, iii)

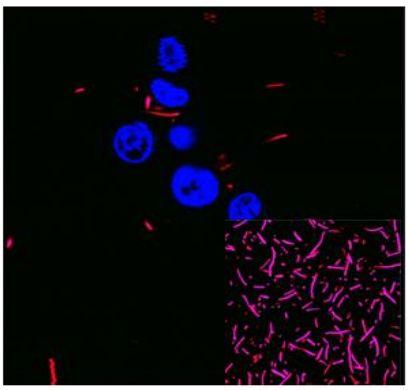

(a, iv)

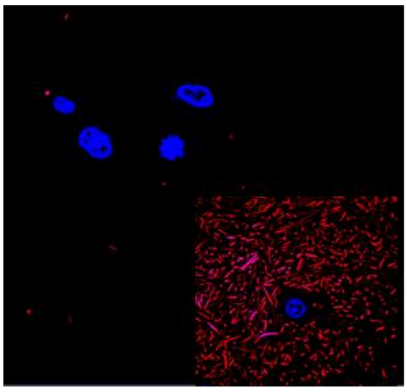

(b, iv)

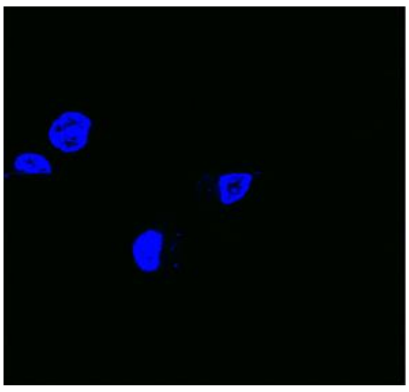

(a,v)

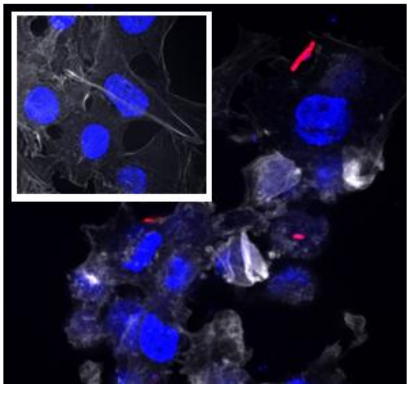

(b,v)

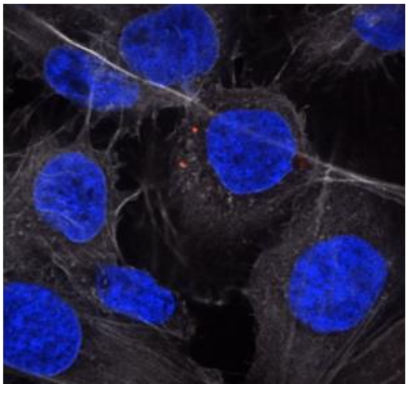

Figure 5.17 Confocal microscopy images of RFP *E. coli* EV36 cells (red) treated with microencapsulated EK1F in the presence of epithelial cells (blue). (a) controls without phage: (i) 2 h, (ii) 3 h, (iii) 3.5 h and (iv) 5 hours following incubation of epithelial cells with EV36; (v) image showing damage to actin (using phalloidin staining) – inset showing control epithelial cells not exposed to EV36. (b) (i) Phage amplification of free phage and microencapsulated phage in the presence of EV36; Confocal images of EK1F treated sample: (ii) 3 h, (iii) 3.5 h and (iv) 5 hours following incubation of epithelial cells with EV36; (v) image showing condition of actin of epithelial cells exposed to EV36 and treated with phage K1F.

A cell culture assay was carried out to investigate the arresting potential of ephage of the bacteria *in situ*. Mammalian cells were grown until confluent, to which bacteria EV36 (host for phage K1F) was added and allowed to grow and infect for 2 hours. After which ephage was added to one culture, whilst one was used as a control. Figure 5.17ai-iv shows the epithelial cells and the growth of bacteria. It was evident the bacteria had actively grown in the presence of epithelial cells as shown in Figure 5.17ai-iv highlighted by the pink/red fluorescence rods. Confocal imaging showed stressed epithelial cells in the presence of growing number of bacteria as shown by the blue fluorescent dye. This was evident due to the shrinking cell morphology Figure 5.17aiv and damaged actin cytoskeleton found around the cell structures Figure 5.17av actin provides support for cell shape, cell division and other cellular processes). The cell morphology deteriorated over time due to the presence of growing number of bacteria.

On the other hand, cells treated with phage after SGF exposure showed a different profile Figure 5.17b. Upon release phage amplification took place in the presence or bacteria, lysing them and preventing further cell damage. In comparison to the control the number of bacterial cells at each time point were seen to be reduced Figure 5.17biii the morphology of the mammalian cells was showed some recovery and further damage was prevented Figure 5.17biv-v. The actin cytoskeleton also showed better morphology with taut microtubules rather than collapsed ones seen with the control.

5.3.10 Storage stability of Ephage

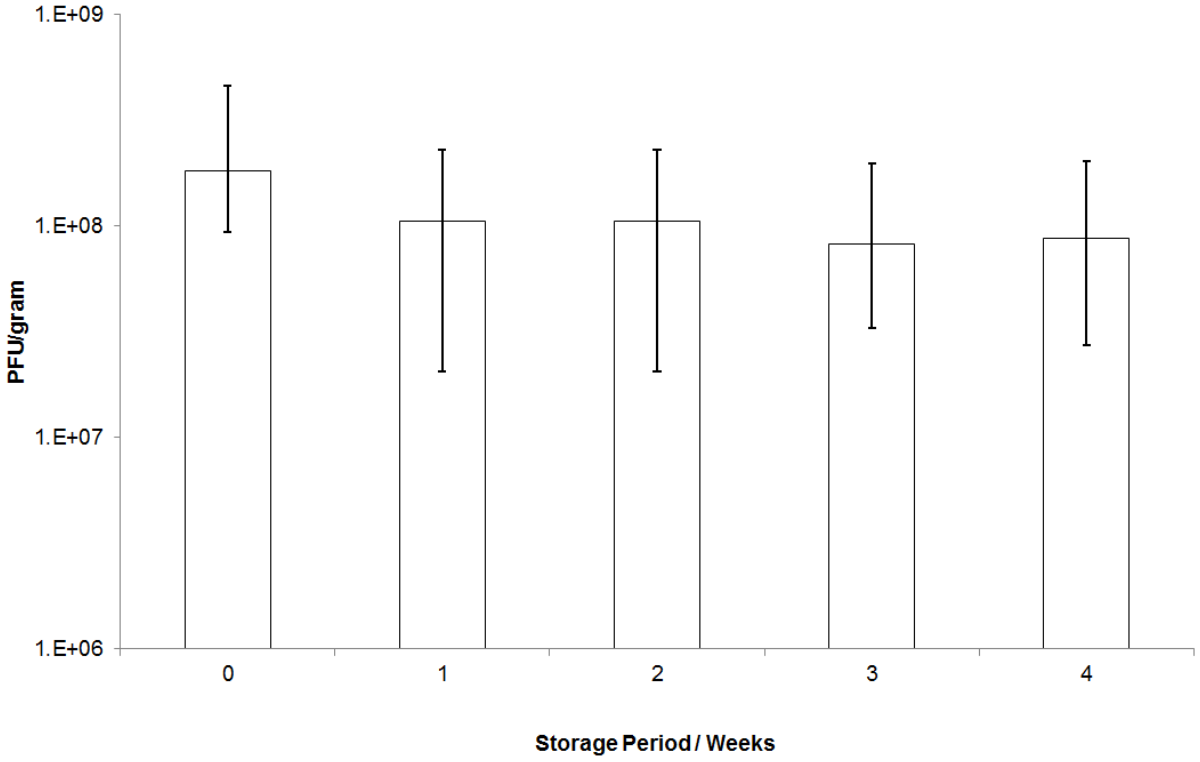

Figure 5.18 Storage stability of encapsulated K1F phage in 10 % (w/v) ES100, 2 % (w/v) alginate at 62 rads^{-1}, 20 µm mem, M:C 9:1 microparticles refrigerated at 4°C**.** Phage titre was evaluated by exposing microparticles to simulated intestinal fluid. Absence of * indicates sample means were not significantly different as compared with sample at week 0 ($p < 0.05$) using a 2-sample t-test.

Table 5.2 Summary of microencapsulated EKF1 storage results from Figure 5.18.

Storage period / weeks	**Mean / PFU g^{-1}**	**Lower 95% CI**	**Upper 95% CI**
0	[a] 1.8 x10^8	8.9 x10^7	2.8 x10^8
1	[a] 1.1 x 10^8	8.4 x 10^7	1.3 x 10^8
2	[a] 1.1 x 10^8	8.4 x 10^7	1.3 x 10^8
3	[a] 8.3 x 10^7	5.0 x 10^7	1.2 x 10^8
4	[a] 8.8 x 10^7	6.0 x 10^7	1.1 x 10^8

Notes: CI = confidence interval; different superscripts in the same column indicate significantly different mean values at $p < 0.05$ (2-sample t-test) comparison with storage period 0 weeks.

Ephage was stored at 4˚C for 6 months (Figure 5.18) The results indicate that there was no significant drop in titre of the phage over this period. There was an initial significant drop in titre after 1 week however this seemed to have stabilised for the remaining storage period. This could be due to the phage adjusting to the unfamiliar environment otherwise kept at room temperature of 37˚C for all experimental work. The confidence intervals shown in Table 5.2 are evidence to the results in Figure that the titre of the phage remained unchanged over the storage period. This concluded that the phage was not affected by the formulation or process parameters of encapsulation.

5.4 Discussion

Phage encapsulation is an integral part of phage therapy. Limited studies on phage encapsulation demonstrate that much is yet to be done to develop formulations and techniques to enhance the efficacy of phage therapy. A key motivation for this piece of work was to demonstrate the route to scale-up phage encapsulation using a pH trigger responsive polymer system. Also, to show the transferability of the system to phages of different enteric pathogens. Previously, focus has been on developing the formulation with precise control of droplets and protection against acidic pH. Phage are sensitive to acidic pH to a different degree as demonstrated in this study, nevertheless this raises an important question regarding the development of cocktails against enteric pathogens. With the intention of delivering an equal titre of phage in a cocktail or alone, acid inactivation may disable the desired effect of phage. Hence, it is imperative to study the resilience of each phage to pH and ensure that sufficient protection is provided to deliver an expected dose to the site of infection.

Membrane emulsification was found to be a suitable method for scale-up since large scale production can be achieved through adding more membrane area. The narrow droplet size distribution achieved via microfluidics can be difficult to replicate during scale-up. However, with membrane emulsification droplet size distribution is homogenous in comparison to conventional shear dependent methods. Hanga & Holdich, (2014) found that despite the high viscosity of alginate, droplets size ranged from 0.2 to 1.5 µm where span less than 1 is considered as monodispersed. In this study this was difficult to achieve since coefficient of variance was observed to be at 60 %. Usually, CV values below 20 % are considered monodispersed. Droplet size is said to be influenced largely by the choice of membrane and not by the shear in the dispersion cell (Charcosset *et al.,* 2004). Many studies have however, shown the influence of shear in the dispersion cell on droplet size. Here, we demonstrated that shear influenced droplets size to a small degree and therefore the phage loading.

Size analysis revealed that particles at D50 ranged from 10 to 24 µm for different continuous phase viscosities. Previously, we have reported particle size ranging around 100 µm (Vinner *et al.*, 2017) with others reporting particle size as big as 900 µm (Yongsheng Ma *et al.*, 2012). Bigger microparticles have shown to have better acid protection and slower release kinetics (Yongsheng Ma *et al*., 2012; Yongsheng *et al*., 2008) whereas release in this study displayed a burst release with up to 90 % of phage being release within the first hour. Although a burst release was observed during dissolution in SIF, phages were protected after a two-hour pH 2 SGF exposure. This observation indicated that the formulation was a crucial factor in determining acid protection in addition to the physical parameters of the microparticles produced. Incorporating properties from a combination of polymers ensures that the microparticles produced as a result can protect phage from hostile environment.

A combination of parameters was investigated to better understand and optimise the production of monodispersed droplets and hence particles using membrane emulsification. This did however prove challenging in that up-scaling from microfluidic platforms where fine-tuned uniform droplets were produced (chapters 3 and 4), the same could not be replicated with membrane emulsification. There are several factors which contributed to this, the change in geometry of the emulsification played a crucial role. In comparison to microfluidics, where a single capillary was used to produce droplets, and every single drop was subjected to the same fluid dynamic forces, in membrane emulsification this drastically changed. Here, formation of a droplet was dependent on the flow rate, membrane pore diameter, membrane type and coating, the shear applied by the paddle stirrer, viscosities of both phases and the presence of surfactant. The majority of these parameters played a role in determining the droplet size in microfluidics; however, the major difference with membrane emulsification was the emphasis on the membrane and the shear applied. As the droplet grew whilst entering through the membrane pore it was continuously subjected to shear which was heterogenous throughout the dispersion cell. Hence, depending on the formulation droplets were further broken into smaller droplets producing polydisperse droplets.

In the presence of these parameters, monodispersed droplets were successfully been produced with a low coefficient of variance even in the case of high viscosity alginate (Hanga & Holdich, 2014; Liu, Bao, *et al*., 2002). Despite the change in droplet diameters for each parameter the phage loading was not significantly affected. Microparticle produced showed smooth non-porous solid surface confirming the microparticles were sufficiently crosslinked. Crosslinking of microparticles was further investigated by looking at the influence of Tween (emulsifier) on phage titre due to pH of the solution being acidic (pH 3). Results showed there was no impact of the acidic solution on phage viability which

also confirmed acid protection at pH 3 after a 24-hour exposure where otherwise phage sensitivity to pH 3 has previously been reported (Yongsheng Ma *et al*., 2012; Yongsheng *et al*., 2008).

Precision control of droplet size can help predict the release profile of the microparticles hence the production of monodispersed microparticles is highly desirable. Microparticles produced via membrane emulsification showed an average droplet diameter of 50 µm going up to of 100 µm and lows of 5 µm. Phage release kinetics demonstrated that despite there being an initial burst release as previously seen, a slower sustained release was observed after 1- hour which may be attributed to the presence of poly-size microparticles. The initial burst from smaller microparticles in the first hour changes the solution properties, slowing the rate of diffusion of hydroxyl ions which then prolonged the release of the larger microparticles.

Encapsulation of phage was a crucial step in ensuring a known dosage was delivered to the site of infection to eradicate the pathogen. Studies have shown phage cocktails with broad host ranges were better at targeting bacteria (Connerton *et al.*, 2011; Nale *et al.*, 2016; Nale *et al.*, 2018). Therefore, every formulation must be tailored for each phage to be encapsulated and address possible interactions between different phage. Phage K1F and Felix O1 were co-encapsulated and subsequently released in SIF, the results revealed no effect on phage viability in either case. This was a crucial first step in devising formulations and platforms for phage encapsulation engineered for phage therapy.

A high phage dose was required to arrest bacterial growth (Malik *et al*., 2017; Y. Tanji *et al*., 2004) hence when designing formulations, release profiles need to be carefully considered. In this study, the release of composite Eudragit and alginate microparticles was studied at different pH which may be encountered during transit through the digestive system. This has not previously been reported and therefore not taken into consideration when calculating phage dosages. Up to 10 % and 50 % phage was released at pH 5 and 6 respectively, demonstrating that although polymers maybe pH responsive at neutral to alkaline pH their release starts prematurely. Presence of hydroxyl ions start to increase as the pH values increase which initiate the dissolution or swelling of polymer resulting in release of phage. In certain circumstances, this can be a useful occurrence where the infection has spread over a large area such as colon or the pH has changed due to infection (McConnell *et al.,* 2008; Lalezari, 2012). The premature release may help prevent the spread of bacteria to other sites. It is however important to account for the premature release of phage during transit to better understand dosing during phage therapy.

Further investigation led us to conclude that even very low amount of phage has the capacity to arrest bacterial growth with a short delay given that bacteria are actively growing. These findings confirm

phage-bacterial infection mathematical models (Malik *et al.*, 2017; Payne & Jansen, 2001; Y. Tanji *et al.*, 2004). *In situ* analysis of phage killing of bacteria showed a positive arrest of mammalian cell deterioration and rescue of the actin cytoskeleton. Bacterial lysis was observed with both free and encapsulated phage. These findings provide a useful insight into how not only free phage work *in vivo* but also how encapsulated phage may behave. Phage in the presence of human cell lines predicts the response of the bacteria and cells to phage which potentially could have adverse effects on mammalian cells (Mirzaei *et al.*, 2016). Phage have reported to respond well in lysing bacterial cells in the presence of epithelial cells as found to be the case against *P. aeruginosa* (Debebe Alemayehu *et al*., 2012).

For encapsulated phage, polymer safety and toxicity need to be evaluated. Eudragit is FDA approved and considered safe for use in biological applications, its use in commercially available medicine is evidence of its low toxicity. A study by Coco *et al.*, (2013) also showed very low toxicity of Eudragit nanoparticles on Caco-2 intestinal epithelium cells mimicking the inflamed epithelium. A study by Shan *et al.,* (2018) showed a three-way interaction between phage, bacteria and epithelial cells. HT-29 cell line was used to mimic the colon environment to investigate the *C. difficile* infection and the effect of introducing phage. Bacterial killing by phage was shown to be more effective in comparison to *in vitro* assays thought to be due to phage adherence to epithelial cells which increased phage-bacteria interactions (Shan *et al*., 2018). pH 2-exposed microparticles carrying phage which were successfully able to lyse bacteria in the presence of epithelial cells demonstrate that the interaction of phage with cells and bacteria is not hindered by encapsulation.

Phage stability is important to ensure the titre does not drop during storage which can alter the phage dosage. Polymer properties impact phage viability during long-term storage and this study demonstrated that phage was well protected in composite particles over a 4-week period with no significant drop in titre. Composite microparticles produced via membrane emulsification showed phage encapsulation can be scaled-up to produce larger quantities without compromising on optimised properties of the formulation.

5.5 Conclusions

Membrane emulsification technique was used to scale up the process of phage encapsulation in composite, Eudragit and alginate microparticles. Experimental parameters affected the droplet diameter which ranged on average from 10 to 50 µm at D50 with the lowest CV achieved at 57 %. Phage was encapsulated at a high yield and showed protection from SGF (pH2 for 2 hours) with less than 0.5 log reduction in phage titre. Premature release of phage was also observed at pH 5 and 6

with up to 10 % and 50 % phage unloaded respectively. Further investigation of different phage titres in reducing bacterial concentration showed higher phage titres to arrest bacterial growth faster than low phage titres. Addition of epithelial cells demonstrated that encapsulated phage was released from microparticles and lyse bacteria. Overtime, bacterial concentration decreased and an improvement in epithelial cell morphology was observed. Phage was stable for up to 4 weeks in microparticles at 4°C. The study demonstrated that membrane emulsification is a viable technique for scale-up which can successfully produce microparticles for phage encapsulation. Further work is required to better control droplet size and test this formulation for a more diverse set of phages to ensure its efficacy.

Chapter 6: Microencapsulation of Felix O1 in pH responsive polymers using spray drying for tableting and improved storage.

Abstract

Treatment of enteric infections can be challenging since the harsh stomach environment (acidic pH) can render phages inactive during transit. Therefore, site-specific delivery and stability of phage over prolonged periods is essential for phage therapy. Spray drying is a conventional technique used industrially to produce encapsulated drugs, respiratory powders and even vaccines. Phage Felix O1 was used as a model phage to be spray dried in pH responsive polymer Eudragit and/or alginate. Phages are also prone to damage from desiccation and elevated temperatures usually encountered during spray drying. To further protect phage from environmental stresses trehalose was used in addition to polymers to protect phage and prolong storage stability. Spray dried powder entrapping phage was compressed into tablets with a 1 mm diameter, these were tested for dissolution, disintegration, friability and storage under different conditions. Results showed a high encapsulation yield of phage Felix O1 with stable storage at 4°C.

6.1 Introduction

Spray drying is a popular technique to produce dry powder forms carrying bioactive agents such as proteins, peptides, attenuated antibodies and phages (Ameri & Maa, 2006). Previously, spray drying has been used for the encapsulation of phages to produce powders for respirable use (S. S. Y. Leung *et al*., 2016; Matinkhoo *et al.*, 2011; Vandenheuvel *et al.*, 2013b). Dry powder forms are favoured due to their ease of handling and long-term storage stability e.g. at ambient temperatures avoiding the need for a cold supply chain for storage. Encapsulating phages in a dry powder form opens possibilities for their use in dry powder inhalers and oral solid dosage forms e.g. tablets for enteric delivery. This chapter investigates the use of spray drying for phage microencapsulation in multicomponent formulations using the following combination of excipients: the pH responsive polymer Eudragit S100, the disaccharide trehalose and the biopolymer alginate. This chapter presents results investigating the use of these excipients to produce pH responsive microparticles using a one-step method for phage microencapsulation such that the particles have high phage loading and good storage stability. The best formulations were processed further into compressed tablets suitable for blister packaging. The work reported here allows evaluation of the suitability of these methods for phage encapsulation

using highly scalable manufacturing processes that would facilitate translation of phages from bench to bedside for phage therapy in both humans and animals.

6.1.1 Excipients for spray drying phage

Phage Felix O1 belongs to the *Myoviridae* family, first isolated by Felix and Callow in 1943. Since then, it has been studied for various applications including incorporation in phage cocktail for phage therapy to treat *Salmonella* contamination in pig skin (Hooton *et al.*, 2011). The effect of temperature on phage is better understood in the dairy industry where phages can cause problems with cheese making by killing bacteria that initiate the fermentation process. These phages however are found to be prone to thermal stresses showing all or partial loss of activity at temperatures above 60°C (Capra *et al.*, 2004; Jończyk *et al*., 2011; Müller-Merbach *et al.*, 2005). It is common practice to store phages in at 4°C, in liquid nitrogen or -80°C with 50 % glycerol, these conditions keep phage relatively stable over several years (Ackermann *et al.*, 2004). Phages are essentially vehicles which carry genetic material in the form of DNA or RNA hence elevated temperatures can cause protein denaturing rendering phage incapable of binding/ adsorbing onto the host.

6.1.1.1. Trehalose

In contrast to lyophilization which often uses low temperatures, spray drying can expose active agents to temperatures as high as 100°C, which can be detrimental for temperature labile active agents such as phage. To overcome this, phages are often spray dried with excipients or bulking agents to provide protection from elevated temperatures. Good excipients prevent or minimise the effect of thermal stress on the active agent, some examples include sugars i.e. trehalose and sucrose etc. These sugars act as water-replacing agents, in other words active agents such as phage and proteins which undergo irreversible damage due to the removal of water (essential for the maintenance of the hydrogen bonds necessary to stabilise the secondary structure of the proteins) are protected by these sugars (Arakawa & Timasheff, 1982). Sugar acts to replace the hydrogen bonds which otherwise would be lost due to evaporation under higher temperatures.

Trehalose structure is made of two α-glucose units and naturally occurs as a disaccharide, it is the glycosidic linkage that makes it resistant to hydrolysis. In its amorphous form, trehalose exhibits a high glass transition temperature- around 117°C which gives it exceptional lyoprotectant properties (Miller & de Pablo, 2000). High glass transition temperature means the ability to form a glassy matrix in the amorphous form which averts the structural transformation of the active agent under higher temperatures. Therefore, under humid conditions trehalose picks up the moisture, changes in part to

its crystallisation form preventing hydrolysis- this in turn reduces the glass transition temperature. As the moisture is removed by drying, the sugar can return to its amorphous state. The instability of amorphous trehalose can be measured by Gibbs free energies of the amorphous and crystallization states at constant heat and pressure. The decrease in Gibbs free energy of changing from amorphous to crystalline equals the enthalpy minus the entropy of the system and surroundings. A bigger thermodynamic driving force for crystallisation is observed when the Gibbs free energy is high. As investigated by Miller & de Pablo, (2000) the Gibbs free energy for trehalose was found to be -17 kJ/mol which is the highest amongst sugars compared with maltose (-7.4 kJ/mol) and sucrose (-9.6 kJ/mol). This indicated that trehalose makes a good excipient for protecting active agents which are prone to environmental changes during long-term storage.

Trehalose has been used to spray dry phages to produce stable powder for applications such as dry powder inhalers. A *Podoviridae* phage LUZ19, was spray dried with trehalose, lactose and dextran 35 by Vandenheuvel *et al*., (2013) for use against respiratory infections caused by *Pseudomonas aeruginosa*. Trehalose was found to be the best excipient in protecting phage from temperature and shear stress caused during the spray drying process, less than 1-log reduction in phage titre was observed. Similarly, Leung *et al*., (2016) also spray dried an anti-Pseudomonal *Podoviridae* phage with mannitol, trehalose and leucine however, failed to achieve less than 1-log reduction in titre but showed overall better phage viability when compared to spray freeze drying. In contrast, a collection of *Myoviridae* phages was spray dried with trehalose, leucine and a surfactant by Matinkhoo *et al.,* (2011) showed less than 1-log reduction in phage titre. In addition to that enhanced performance of the spray dried powder was observed in comparison to commercial dry powder inhalers.

6.1.1.2 Eudragit S100

Application of spray dried phage has largely been for combating pulmonary infection or to increase the long-term storage stability of phages for better preservation. To date, limited work has been done to exploit the use of spray dried phage for oral dosage form to address enteric infections. Stanford *et al.*, (2010) encapsulated four anti-E. coli phages in a pH responsive polymer using spray drying, 1-log reduction in phage titre was observed. Due to the intended enteric delivery, the encapsulated phage was exposed to pH 3 for 20 mins to mimic the stomach acidic environment in cattle. Protection against pH 3 was observed for all four phages with the highest survivability at 13 %. This study demonstrated the use of spray dried powder containing phage for use in oral dosage forms to treat enteric infections. pH responsive Eudragit S100 a methyl-methacrylate copolymer ensures the stability of the phage upon

exposure to low pH. This opens the possibilities of spray drying phage with excipients other than sugar or lyoprotectants to produce tailored release powder properties of Ephage.

Eudragit S100 and its analogue copolymers such as Eudragit L100 and RS have been used for encapsulation and coating active agents in various pharmaceutical applications. Examples of commercially available products containing these polymers include Dulcolux and coated Naproxen tablets. Several patents have also been setup which have included the use of Eudragit in application for colon drug delivery (Basit & Ibekwe, 2007) and also for encapsulating phage in Eudragit copolymers (Waddell *et al*., 2013). Further studies have focussed on using the pH responsive behaviour of this polymer to encapsulate probiotics for delivery to the colon (Govender *et al.*, 2015), where the commensal flora can be repopulated after infection. Eudragit is a popular enteric coating for delivery to the lower gastrointestinal tract, however it can also be used for micro and nano encapsulation with other polymers (Collnot *et al.*, 2012).

6.1.1.3 Alginate

Alginate is naturally occurring anionic polymers extracted from brown seaweed and has been extensively used in biomedical applications due to its bioavailability and desirable physical and chemical properties. It is a non-toxic copolymer, generally regarded as safe under the FDA classification (George & Abraham, 2006) and readily dissolves in water making it highly useful when working with active agents sensitive to solvents such as ethanol. To crosslink alginate addition of multivalent cations such as calcium can be added to form a hydrogel matric which dissolves in neutral to high pH. Under acidic conditions alginate tends to contract which is desirable since the porosity of the alginate matrix is reduced, entrapping and protecting the active agents inside the hydrogel.

Alginate has already proven to be a popular choice for the encapsulation of bacteriophages (Colom *et al*., 2017a; Yongsheng Ma *et al.*, 2008, 2012; Stanford *et al.*, 2010b; Tang *et al*., 2013, 2014) mainly due to its biocompatibility and ease of use. Using alginate for phage encapsulation has shown some promise, however in light of its porous structure when exposed to SGF at pH 2 or 2.5 the acid was able to penetrate the gel matrix and reduce phage viability (C Dini *et al*., 2012; Yongsheng Ma *et al*., 2008, 2012). Therefore, some studies have proposed the use of alginate in combination with other copolymers such as chitosan (C Dini *et al*., 2012; S. Kim *et al.*, 2015a; Yongsheng Ma *et al*., 2008, 2012), guar gum, pectin (C Dini *et al.*, 2012), whey protein (Samtlebe *et al.*, 2016; Tang *et al.*, 2013, 2014) and Eudragit (Jain *et al*., 2005; Stanford *et al.*, 2010b). This highlighted that when used in combination with another polymer better phage protection maybe achieved against SGF

6.1.2 Tableting spray dried powder

6.1.2.1 Benefits of tabletting

Tableting bioactive agents has several advantages, it is the preferred dosage form in the pharmaceutical industry due to its accurate dosing, ease of manufacture at low cost and stable long-term storage stability. The ease of use and dosage is pre-empted by the uniformity and reproducibility of each tablet in the blister pack, which ensures patient compliance to the prescribed medicine. Several phage products are available on the market around the globe targeting the spread of bacteria through food, veterinary applications and environmental sanitation- many of these products offered by Intralytics Inc. (USA). However, tableted phage is manufactured by Biochimpharm, under Septaphage®. This product contains several phages against bacteria such as Shigella, Salmonella, E. coli, Proteus, Staphylococcus, Pseudomonas and Enterococcus. The commercial availability of this tablet highlights the possibility of using other formulations to produce encapsulated phage in a tablet form, with enhanced properties in terms of targeted release.

6.1.2.2 Examples of tableting by direct compression

Typically, tableting is carried out using wet or dry granulation however, an increased interest in direct compression is observed due to the simplicity of the method and by-passing many steps involved in granulation (Jivraj *et al.*, 2000). There are several ideal requirements of the powder for direct compression technique to be employed for tableting. Ensuring homogenous and quick flow of the powder for filling the punch chamber in high speed tableting machines is an important consideration. Similarly, the compressibility of the powder is also important, as the mass compressed into a tablet must remain compact once the compression force is removed. The tapped bulk density of the powder can be a good indicator of whether powder has the potential to be directly compressed, external factors can also influence the bulk density of a powder such as segregation of particles and moisture (Jallo *et al.*, 2012).

Spray dried powders followed by direct compression that are commercially available include Lactose-316 Fast Flo®, Avicel PH, Karion Instant, TRI-CFOS S and Advantose 100. Powder produced via spray drying has good flowability and retains the uniform spherical shape of particles which is advantageous for direct compression (Marwaha *et al.*, 2010). Excipients such as sugar i.e. trehalose may be used for direct compression to form tablets carrying phage- since phage has proven to be stable when spray dried with trehalose. However, without triggered release properties trehalose tablets alone do not

serve purpose for enteric delivery- adding a copolymer such as Eudragit and/or alginate can help enhance tableting potential for site specific delivery.

Enteric coating of tablets with the Eudragit series have shown their potential in site specific targeting of the active agent. Govender *et al.*, (2015) showed encapsulation of a model probiotic bacteria, *Lactobacillus acidophilus* in ovalbumin to create mini-tablets after 24-hour lyophilization (~1.87 mm). These were then separately coated with either lactose or Eudragit S100 to create a tablet in tablet system with the aim of targeting release in the upper and lower GI tract. Results revealed successful protection of the bacteria from acidic stomach environment and pH dependent release in the colon. A separate study Souza *et al.*, (2013) investigated the release of minitablets composed of Polyox®WSR 1105 carrying model drug mesalamine using dry granulation which were further coated using a fluidized bed with Eudragit L30D55. The results showed a prolonged drug release at pH 6 and 7.2 showing zero-order release kinetics.

Risedronate, an antiresorptive drug for GI tract injuries was encapsulated in pullulan (polysaccharide) and Eudragit S100 using spray drying to produce dry powder, which was directly compressed into tablets. Upon exposure to pH 1.2 the formulation containing the highest amount of Eudragit concentration showed the highest gastro-resistance with only 10 % drug release. Further release in SIF revealed a prolonged release of the drug over 4 hours (De Arce Velasquez *et al.,* 2014). The potential of using spray dried powder for tableting though direct compression has shown potential when using Eudragit and sugars as excipients. Similarly, when considering the use of Eudragit encapsulated phage in dry powder form, tableting can improve the dosage and ease of use for therapy applications.

Aims and Objectives

Previous chapters have shown and optimised the use of Eudragit and alginate in phage encapsulation using different encapsulation techniques. This study investigated the versatility of the formulation when applied to well established industrial spray drying technique. A bench-top spray dryer was used to produce phage encapsulated powder. An additional excipient, trehalose was incorporated into the process due to its protective properties of phage demonstrated in literature. Effect of each excipient on phage viability during spray drying was investigated as well in combination to produce an optimised recipe suitable for phage encapsulation. Parameters such as temperature, yield, moisture content and encapsulation efficiency were evaluated. The optimised formulation was further explored by tableting. Tablets were examined for their disintegration, dissolution and friability capabilities. For both powder and tablets the effect of long-term storage under various conditions was studied for its

effect of phage viability. Shift in glass transition temperatures for each sample was analysed and will be discussed. Conclusions, regarding the potential use of powder and tableted form for animal and human therapy will be discussed.

6.2 Materials and Methods

6.2.1 Model bacterium and phage

All work carried out for both bacteria and phage was carried out according to the method in chapter 4 section 4.2.2, salmonella strain and bacteriophage Felix O1.

To test the effect of temperature on phage viability phage in BHI broth was incubated at temperatures 40°C, 50°C, 60°C for 60 minutes. 10 µl was removed at 10-minute intervals for the first 30 mins and then at 60 minutes, which was then diluted 10-fold to 10^{-8} and spotted in triplicate on a double layer agar plate containing *Salmonella*. The plate was dried an incubated overnight at 37°C and plaques counted the following day to determine phage viability.

6.2.2 Spray drying phage Felix O1

Eudragit S100 was purchased from Evonik Germany. D- (+)-Trehalose, Dihydrate was purchased from Fisher Scientific (U.K.). Alginate was purchased from Sigma Aldrich (U.K.). Solutions containing different excipient concentrations (table 6.1) were dissolved in 500 ml of dH_2O. For Eudragit pH of the water was changed to alkaline to allow polymer dissolution. To dissolve alginate, the temperature was raised to 60°C and left stirring until full dissolution was observed. For each formulation 1 % (v/v) high titre phage Felix O1 was added. The phage solution was spray dried using a two-fluid nozzle Labplant spray dryer SD-06 (Labplant UK limited) (Figure 9.14 appendix). The diameter of the nozzle used throughout the work was 0.5 mm with liquid flow rate at 280 mlh^{-1} and air speed at 4.3 ms^{-1}. Temperature was controlled by changing the inlet temperature (table 6.2) with corresponding outlet temperature Table (6.2) which varied by 2°C between runs.

Once the dry powder was collected, it was stored at 4°C in sealed tubes unless storage conditions were changed. For storage analysis, powder was stored at 4°C and at 23°C for a period of up to 3 months. At timely intervals 0.1 g of powder was removed and dissolved in simulated intestinal fluid

(SIF) (composition 10 mg/ml of pancreatin in 0.5mM KH_2PO_4 pH 7) and phage titre enumerated using a plaque assay (described above). To ascertain the phage encapsulated in each excipient, 0.1 g of powder was removed and dissolved in SIF, 10 µl of sample was removed and plaque assay performed to enumerate phage. Similarly, simulated gastric fluid (SGF) (composition 3.2 mg/ml of pepsin in 0.2 M NaCl pH 2) exposure was carried out for 2 hours for each formulation after which release kinetics were analysed in SIF. At timely intervals (30 mins) up to 3 hours, 10 µl of sample was removed and plaque assay performed to observe phage release.

Table 6.1 Formulations used for spray drying phage Felix O1

Excipient	Concentration (w/v)						
	F1	F2	F3	F4	F5	F6	F7
Eudragit S100			3 %	3 %	2 %	2 %	2 %
Trehalose		4 %		2 %	1 %	1 %	4 %
Alginate	1 %					0.5 %	

Table 6.2 Spray drying inlet temperature with corresponding outlet temperatures.

Inlet temperature	Outlet temperature
180°C	96°C ± 2°C
150°C	82°C ± 2°C
120°C	66°C ± 2°C
100°C	56°C ± 2°C

6.2.3 Powder characterisation

6.2.3.1. Scanning electron microscope (SEM)

To analyse the morphology of spray dried powder, a representative sample from formulation containing 2 % (w/v) Eudragit and 1 % (w/v) trehalose spray dried at inlet temperature 150 °C was

taken and mounted on double sided carbon stickers. The sample was gold-sputter coated ready to be viewed using a benchtop SEM (Hitachi TM3030 Tabletop Microscope Europe).

6.2.3.2 Coulter size analysis

Coulter LS 130 (Beckman Coulter Inc.) (Figure 9.7 appendix) was used to determine the particle size distribution of the spray dried powder. The device is laser modulated and uses the optical model Fraunhofer, to detect laser diffraction caused by particles. A representative sample from formulation 2 % (w/v) ES100 and 1 % (w/v) trehalose was taken for each temperature tested and loaded into the glass sample cell containing n-hexane (Sigma Aldrich U.K.). The volume size and cumulative distribution were measured and reported.

6.2.3.3 Different scanning calorimetry (DSC)

Eudragit and trehalose powders were taken before and after spray drying at 150°C inlet temperature for differential scanning calorimetry (DSC). 10 mg of powder was weighed into aluminium pans for analysis with an empty pan for reference. The analysis was performed for temperatures 25°C to 120°C with a ramp rate of 5°C a minute. The thermographs were recorded and analysed for glass transition temperature.

6.2.4 Tableting

Spray dried powders from formulation 7 and 5 spray dried at inlet temperature of 150°C were used for tableting using Riva Minipress MII (U.K.) machine (Figure 9.15 appendix). Each powder sample was mixed with varying amount of magnesium stearate (Sigma Aldrich U.K.) (0.5 %, 1 %, 1.5 % w/v). Approximately 0.3 g of powder was loaded into the punch hole and compressed at a force of 13.5 kN. The produced tablets were weighed and stored in sealed tubes for further analysis.

6.2.4.1 Friability

Six tablets were used to test for friability using Erweka friability tester (U.K.) (Figure 9.17 appendix), and the weight of each tablet was recorded prior to the start of the analysis. Every 20-drum rotations the weight of each tablet was recorded and reported at percentage (%) loss.

6.2.4.2 Disintegration

Tablet disintegration was evaluated using Erweka ZT31 (U.K.) disintegration machine (Figure 9.16 appendix). Six tablets from each formulation were used to test for tablet disintegration in SGF pH 2

for a period of 2 hours. The weight of the tablets was recorded and subsequent release in SIF performed. At timely intervals of 30 mins 10 µl of sample was removed and plaque assay performed to ascertain the amount of phage present, for a total period of 3 hours.

6.2.4.3 Tablet storage

Tablets were stored in glass universals at 4°C tightly sealed and at 30°C with 65 % relative humidity (RH) with lids removed in a humidity chamber. Tablets were stored for 6 weeks, a tablet for each parameter was removed at 1 week, 2 weeks, 4 weeks and 6 weeks to test for phage viability. The tablets were exposed to SGF pH 2 for two hours in the disintegrator before being dissolved in SIF. The phage titre was evaluated use plaque described above.

6.3 Results

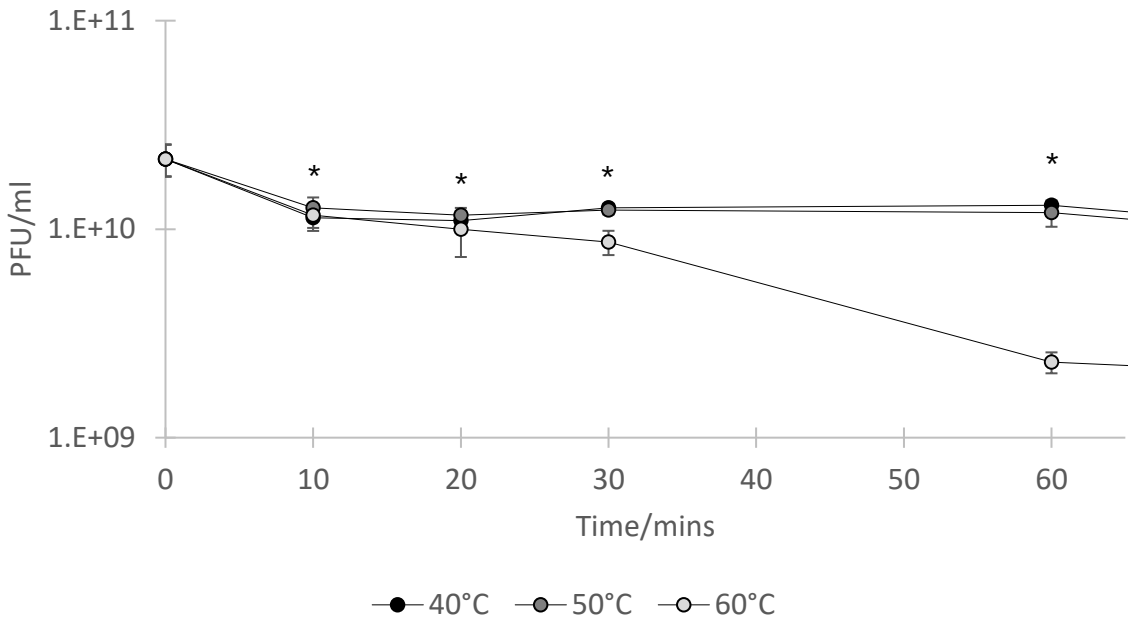

Figure 6.1. Temperature stability of free phage Felix O1 in BHI broth over a period of 1 hour.
*indicates the significance difference between the PFU/ml of each parameter in comparison to 0 h in a two-sample t-test ($p < 0.05$).

Effect of temperature on phage Felix O1 was investigated by exposing the phages in BHI broth to temperatures typically encountered during the spray drying process. The phage was unaffected by temperatures below 50°C but 1-log reduction after 60 mins exposure was observed at 60°C Figure 6.1. Phage was also exposed to 90°C (data not shown) however no phage was recovered after 10 mins of

exposure. Continued exposure to all temperatures for 24 hours showed no further loss at temperatures 40°C and 50°C but a further 1-log loss was observed for exposure to 60°C.

6.3.1 Phage encapsulation using different excipients and experimental parameters

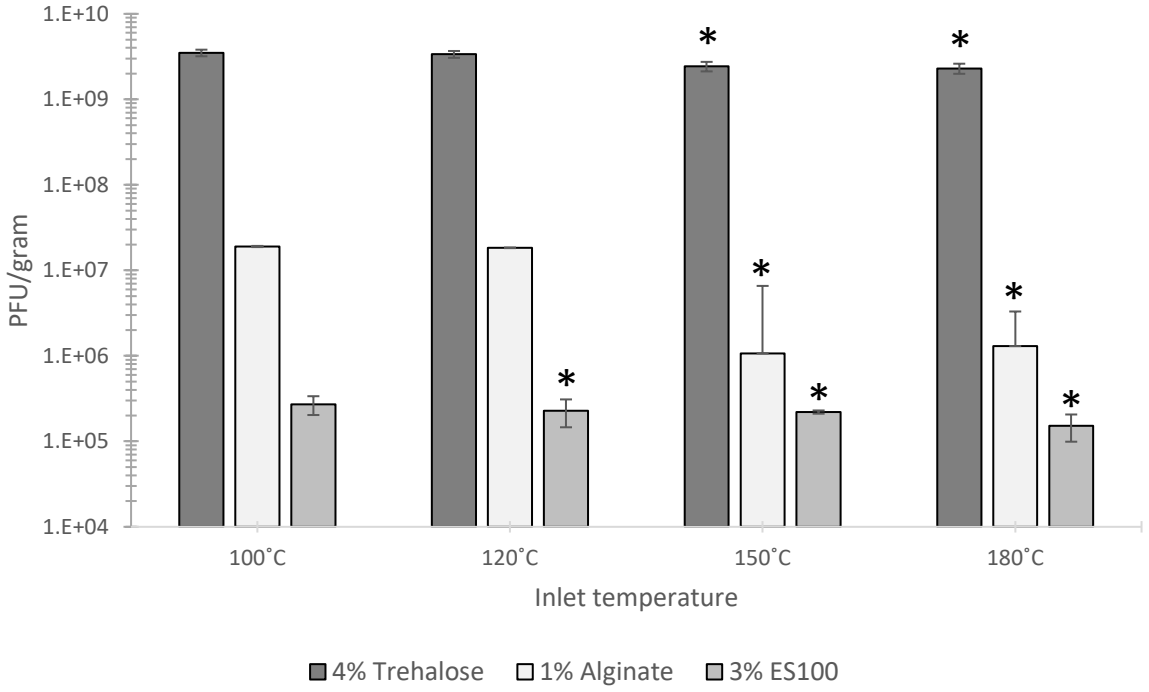

Figure 6.2. Felix O1 encapsulated at 4 temperatures and its release from each excipient in PFU/gram. * indicates significance means were compared across all temperatures to 100°C inlet temperature ($p < 0.05$) using a 2-sample t-test. All measurements were done in triplicate ($n = 3$).

Phage Felix O1 was spray dried with each excipient used in this study separately to observe effects on encapsulation. For each excipient different inlet temperatures were studied to observe the effect of temperature. Trehalose was found to be a good excipient, with phage encapsulated at high titres at all temperatures Figure 6.2. Whilst alginate and Eudragit alone showed less promise in retaining phage viability after spray drying Figure 6.2. The phage titre dropped by an average of 3-log for alginate and 4-log for Eudragit. This may be attributed to the lack of protection from desiccation and heat provided by the two excipients in comparison to trehalose which is known be an excellent excipient for the protection of bioactive agents due to its high glass transition temperature.

Effect of temperature on phage viability however was less obvious as the phage titre did not change with decreasing temperature with trehalose and Eudragit. In the case of alginate however, better

phage viability was observed with lower temperatures (120°C and 100°C) Figure 6.2. The influence of temperature on phage viability therefore may be dependent on the excipient used.

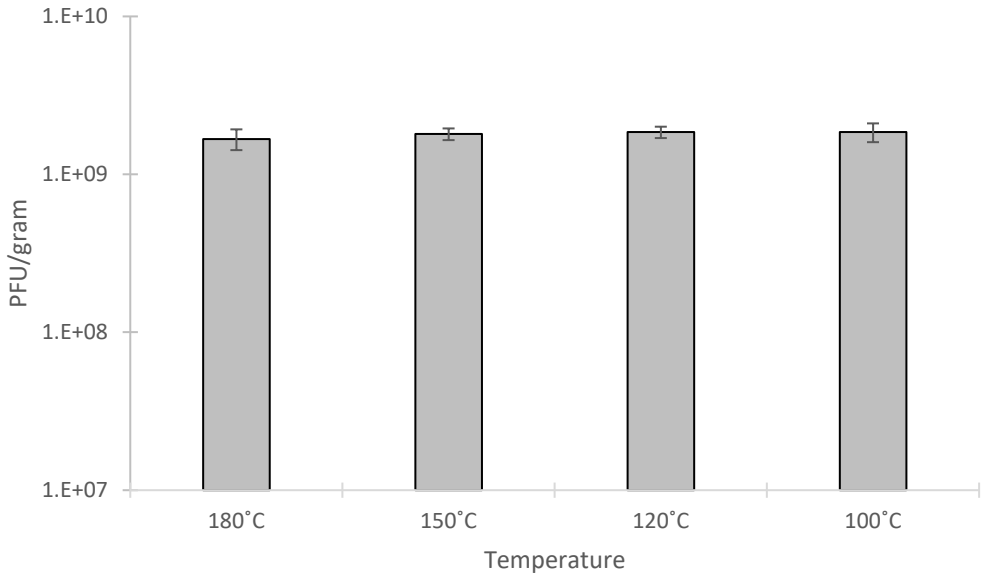

Figure 6.3. Felix O1 encapsulated in 3 % (w/v) Eudragit and 2 % (w/v) trehalose at different temperatures, with subsequent release in SIF for 5 hours. No statistical difference was found between the mean of each temperature. No statistical difference was found between the means.

Felix O1 was encapsulated with Eudragit S100 and trehalose to combine the benefits of both excipients, one being the pH responsive behaviour of the polymer and second the potential to protect phage from thermal stress and desiccation provided by trehalose. Taking forward the formulation from previous chapters, the viscosity of solutions containing between 5 % to 10 % (w/v) Eudragit was found to be too high for the peristaltic pump supplying the atomiser in the spray dryer. Therefore, the concentration of Eudragit was lowered to 3 % (w/v) (with a viscosity of 20 mPa) which was then mixed with 2 % (w/v) trehalose. The reason for using 2 % (w/v) trehalose as opposed to 4 % (w/v) as previously investigated Figure 6.2 was to prevent premature dissolution of particles in aqueous solutions. The concentration of trehalose had to be lower than Eudragit otherwise the higher solids fraction of the sugar excipient was found to dominate dissolution characteristics over the pH responsive effect of Eudragit, nullifying the encapsulation properties of the formulation.

The phage viability after spray drying remained high with virtually no loss in phage titre (Figure 6.3). The amount of phage being encapsulated (added to polymer and sugar solution before spray drying) was 5 x 10^9 PFU/ml. Encapsulated phage was released in SIF for 3 hours, until complete dissolution of powder. Despite the change in temperature during spray drying, the phage was unaffected, showing a similar profile to when encapsulated with trehalose alone Figure 6.2. By incorporating lesser (1 %

w/v) amounts of trehalose it was possible to retain a high phage titre which otherwise was not possible if encapsulating phage in Eudragit alone (Figure 6.4). Encapsulated phage was also exposed to SGF, pH 2 for 2 hours before releasing in SIF. However, only 2 x 10^7 PFU/gram viable phage was recovered after acid exposure. This may be explained by the concentration of trehalose which may have caused a premature loss of phage during SGF exposure. Trehalose was added to yield a high titre of phage during encapsulation, perhaps adding lesser amounts where up to 95 % of the microparticles are composed of Eudragit, trehalose can still exhibit its benefits. However, reducing trehalose concentration too much may result in a low glass transition temperature meaning that phage is not able to resist the effects of desiccation and high temperatures which can also affect storage stability.

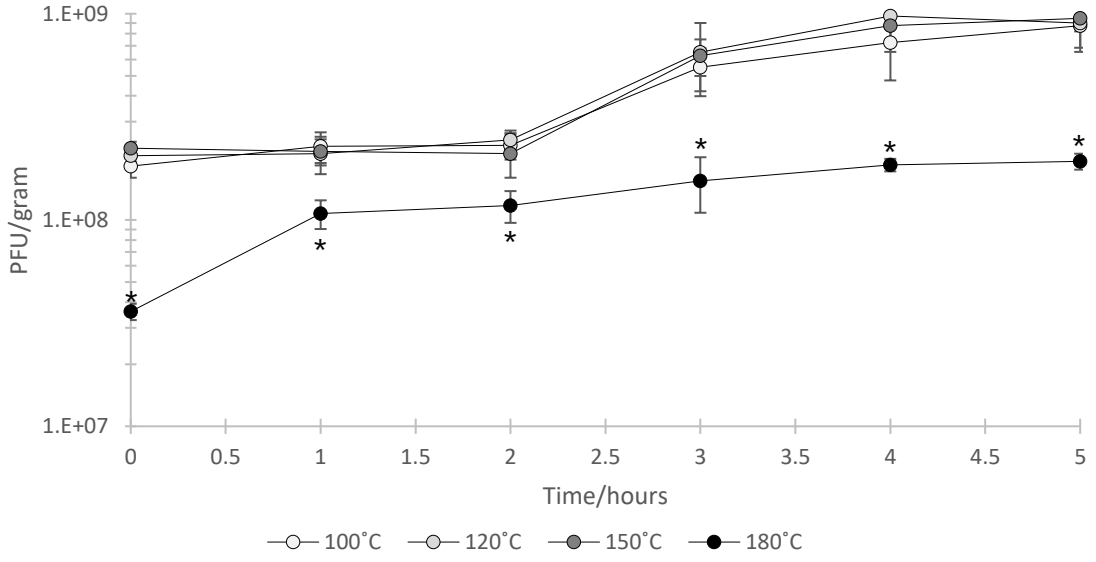

Figure 6.4. Release kinetics of encapsulated Felix O1 in 2 % (w/v) Eudragit S100 and 1 % (w/v) trehalose prepared using different spray drying temperatures. Time zero corresponds to 5 mins of microparticles release. *indicates the significance difference between the mean values for each parameter when compared within each time point ($p < 0.05$) (n = 3).

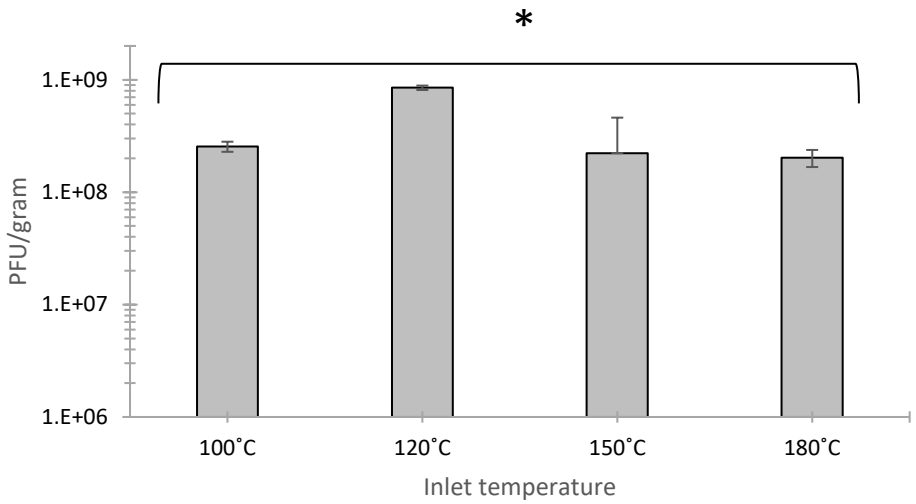

Figure 6.5. Release of Felix O1 from spray dried microparticles (2 % (w/v) Eudragit and 1 % (w/v) trehalose) after exposure to SGF (pH2) for 2 hours and subsequent release in SIF for 5 hours. * indicates significance means were compared across all temperatures ($p < 0.05$) using a 2-sample t-test. All measurements were done in triplicate (n = 3).

The concentration of trehalose was lowered to 1 % (w/v) due to the lack of phage protection from SGF. Unlike other solutions such as trehalose and alginate alone, 3 % (w/v) Eudragit was the limit in terms of how well the pump was able to function and how effective the nozzle deblocker was able to keep the spray nozzle unclogged. Therefore, the concentration of Eudragit was lowered to 2 % (w/v), still maintaining the trehalose concentration low at 50 % from 67 % previously. Once again phage was encapsulated at varying temperatures to investigate any effect of temperature on phage encapsulation.

The initial titre of phage in the solution was 1 x10^9 PFU/gram. Figure 6.4 shows the phage release kinetics in SIF over a period of 3 hours for samples spray dried at each temperature. In all cases there was burst release of phage, unloading on average 50 % of encapsulated phage in the first hour and releasing the remainder of the phage thereafter. For all spray dried temperatures, the release profile was similar with slight differences in the measured phage titre. 10-20 % less phage was encapsulated and therefore released for phage encapsulated at an elevated inlet temperature 180°C (Figure 6.4). A significant difference was found after performing a 2-sample t-test ($p < 0.05$) comparing values for 180°C to all the other inlet temperatures. Here, it may be possible to relate the effect of increased temperature on the concentration of viable phage encapsulated. Encapsulated phage particles were further investigated by exposing them to SGF for 2 hours and subsequently releasing in SIF for 3 hours (Figure 6.5). Viable phages were recovered in all cases, with the best results noted for the inlet temperature 120°C with a phage titre of 8.5 x 10^8 PFU/gram indicating a 15 % overall phage reduction.

The remaining inlet temperatures presented phage titres around 2 x10^8 PFU/gram, showing just under a log reduction after SGF (pH 2) exposure.

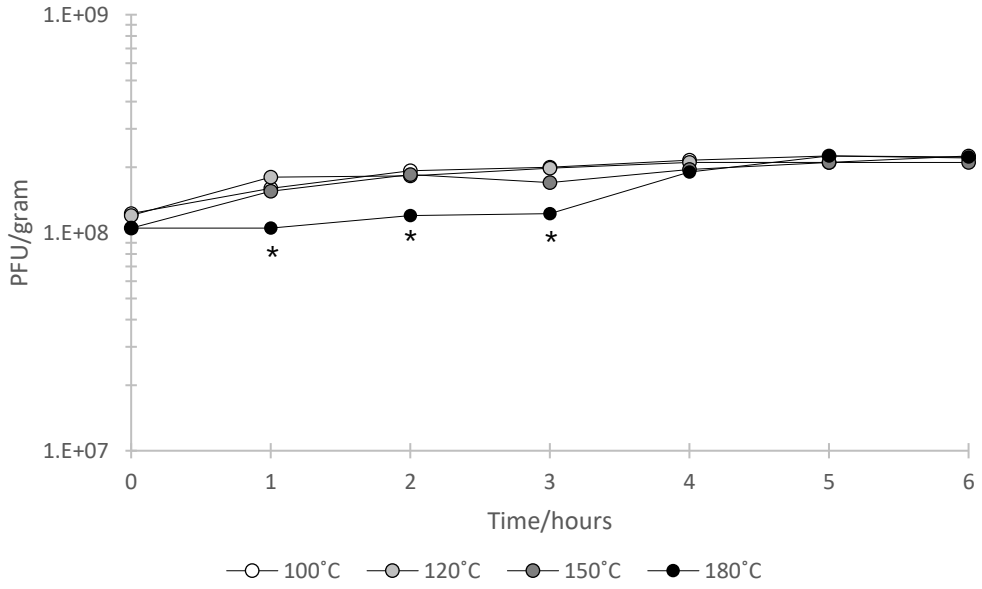

Figure 6.6 Release profile in SIF of 2 % (w/v) Eudragit, 1 % (w/v) trehalose, 0.5 % (w/v) alginate encapsulated phage Felix O1 under different spray drying temperatures in SIF for 6 hours. *indicates the significance difference between the mean values within each time point ($p < 0.05$) n=3.

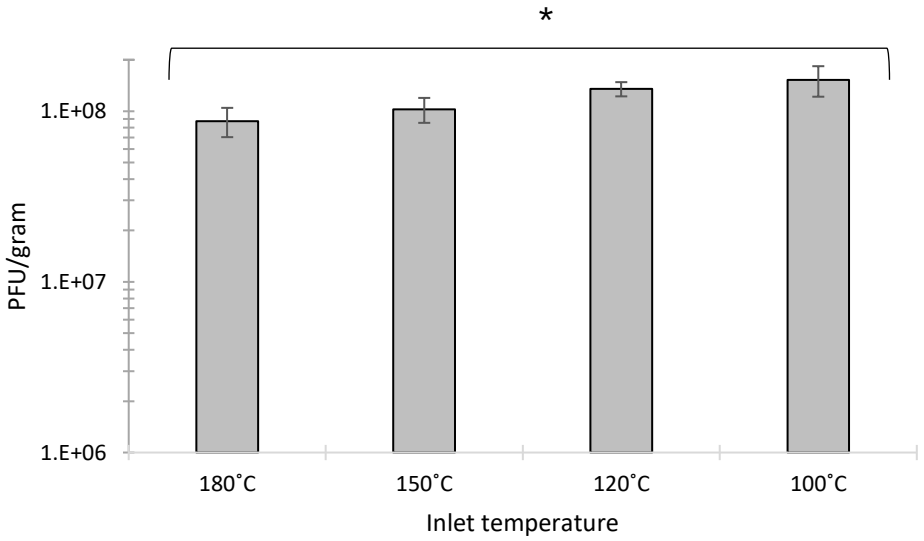

Figure 6.7. Release of Felix O1 from spray dried microparticles using formulation with 2 % (w/v) Eudragit, 1 % (w/v) trehalose, 0.5 % (w/) alginate prepared using different spray drying temperatures (release after a 2-hour SGF exposure with subsequent release in SIF for 6 hours). * indicates

significance means were compared across all temperatures ($p < 0.05$) using a 2-sample t-test. All measurements were done in triplicate ($n = 3$).

Alginate was incorporated in previous chapters to improve acid protection in hydrogel dosage forms. In the case of spray drying, the effect of alginate in phage encapsulation was also investigated by incorporating 0.5 % (w/v) in the formulation. Due to the high viscosity of alginate solutions, only a small amount was added thereby allowing the spray dryer to pump the solution through the nozzle without blocking. Unlike the phage yield for spray dried alginate alone, higher phage titres were observed for phages encapsulated in formulations containing alginate in combination with trehalose and Eudragit (Figure 6.6). Encapsulated phage was released completely in SIF for 3 hours with full dissolution of particles. Titres of 2×10^8 PFU/ml were observed after complete release, somewhat lower than the formulation containing no alginate (Figure 6.5). No statistical difference in phage viability was observed across the varying inlet temperatures. All samples showed phage protection against pH 2 (Figure 6.7) after 2 h exposure to SGF followed by release in SIF. Less than 1-log reduction was observed for all samples in comparison to phage release at SIF alone Figure 6.7. Although the loss of phage during the spray drying process was higher in comparison to formulation without alginate, the overall acid protection was better. The loss of phage viability during the spray drying process can be explained by the low titres observed during phage encapsulation in each excipient alone where alginate and Eudragit show higher loss of phage Figure 6.2.

6.3.2 Characterisation of spray dried powder

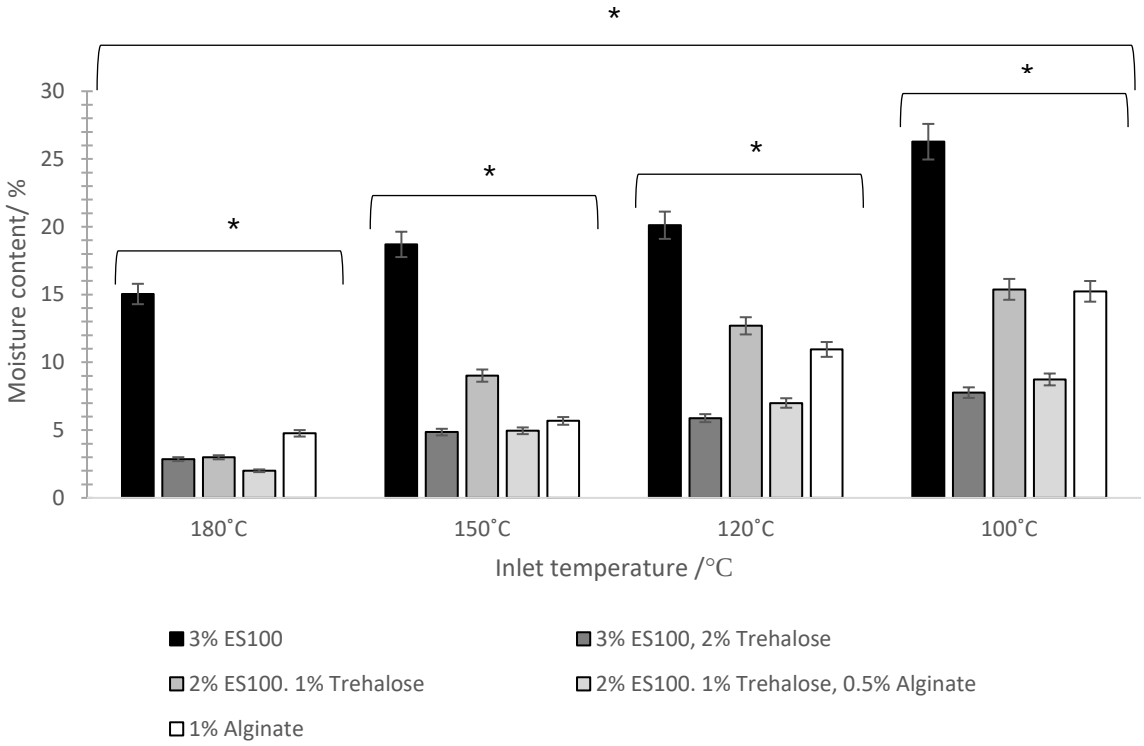

Figure 6.8 Percentage (%) moisture content of spray dried powders produced using four inlet temperatures with different excipients. * indicates significance difference between means which were compared across and within all temperatures ($p < 0.05$) using a 2-sample t-test. All measurements were done in triplicate ($n = 3$).

For each excipient examined the moisture content was analysed at each temperature Figure 6.8. The amount of moisture in the sample impacts the properties of the powder as well storage stability. So, for each sample a representative amount of powder was weighed and left in an oven overnight to remove any residual water. Highest level of moisture was found with Eudragit alone reaching 26 % moisture content at inlet temp of 100°C. For all other excipients the moisture content of the spray dried samples was 15 % or below. The second excipient with the highest moisture content was for formulations containing alginate alone. Formulation with 2 % (w/v) trehalose with 3 % (w/v) Eudragit in comparison to 1 % (w/v) trehalose with 2 % (w/v) Eudragit displayed low moisture content, indicating the influence of trehalose in sequestering moisture with increasing concentration. The general trend across all formulations was that as the temperature decreases the level moisture increases Figure 6.8. Moisture content related to storage stability, higher moisture content equally lowering of the glass transition temperature. Low glass transition temperature powder recrystalizes at low storage temperatures which can destroy the encapsulated phage.

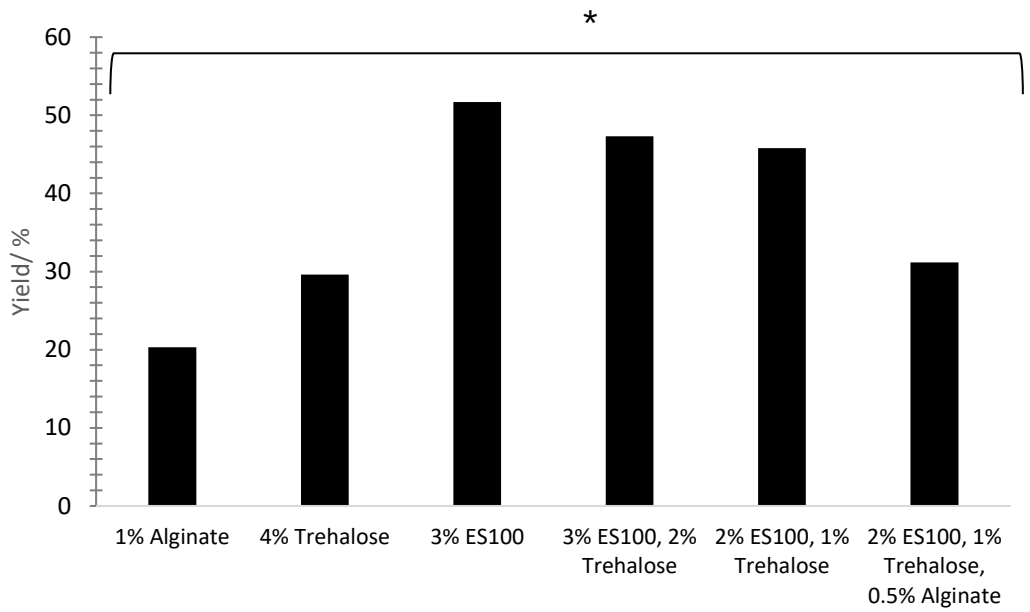

Figure 6.9. Percentage (%) yield (weight of solids collected in comparison to solid weight spray dried) of excipients used to produce spray dried powder. * indicates significant difference between the means which were compared across all formulations ($p < 0.05$) using a 2-sample t-test. All measurements were done in triplicate ($n = 3$).

The yield of powders following spray drying was evaluated for every formulation. The amount of powder produced was compared to the amount of solids dissolved in solution before spray drying. There were several challenges when the yield of excipients such as alginate and trehalose was low at 20 to 30 % (Figure 6.9) which meant several runs were required to obtain enough material for analysis. This was due to the powder being carried away through the cyclone which was unable to remain in the collection bottle. Usually, the finer microparticles are not effectively trapped in the cyclone which causes a high loss of powder during production. The yield was highest for formulations containing Eudragit (Figure 6.9) with 3 % (w/v) Eudragit showing the highest yield at 50 %. Combining Eudragit, trehalose and alginate the yield decreased in comparison to Eudragit and trehalose. On average the yield remained higher for comibined excipients when compared to spray drying these excipients alone, indicating the influence of Eudragit overall remains high.

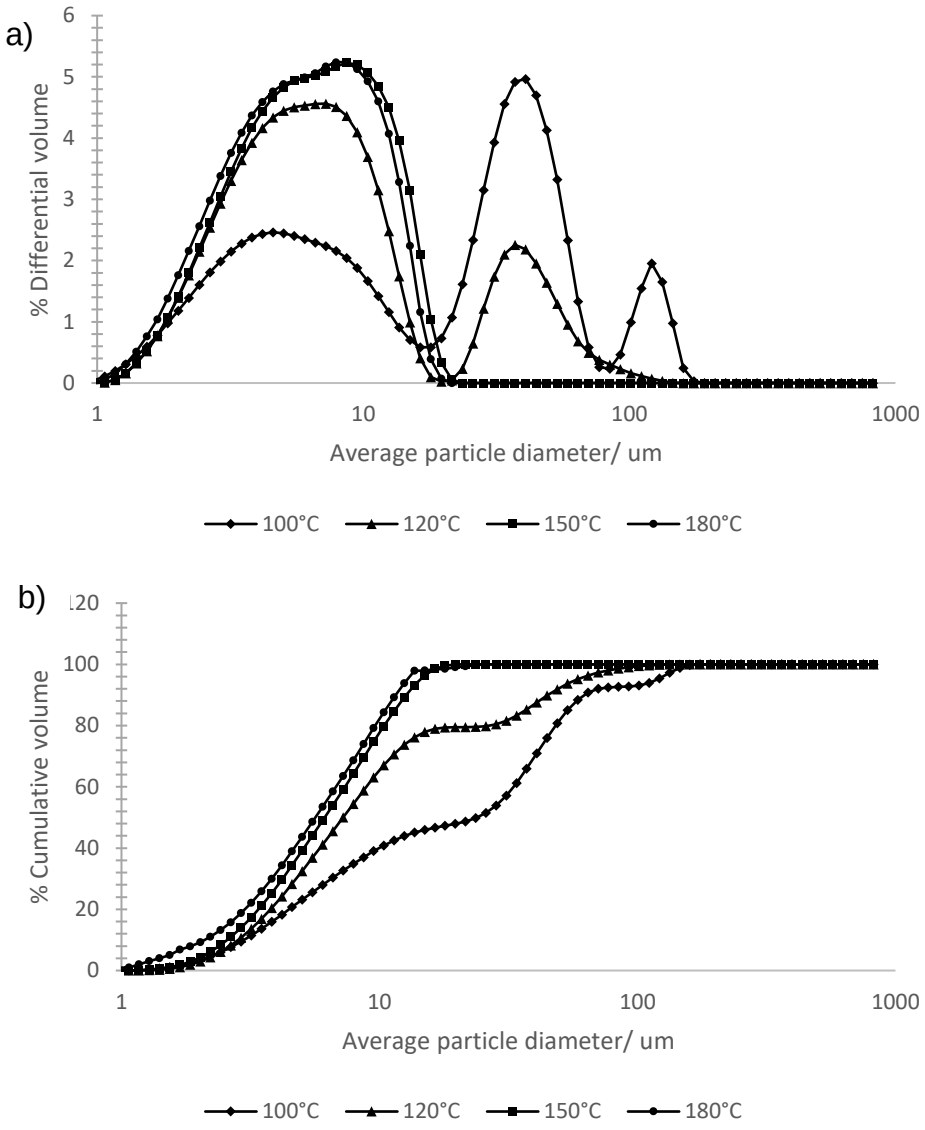

Figure 6.10. Coulter analysis on particles from spray dried 2 % (w/v) ES100 and 1 % (w/v) trehalose powder using different inlet temperatures a) differential volume distribution of particles b) cumulative volume distribution.

The two-fluid nozzle diameter used for spray drying powders was 0.5 mm, the microparticles produced from this nozzle are affected by the formulation viscosity and the spray drying conditions (temperature). Therefore, the size of microparticles was analysed using the coulter size analyser for 2 % ES100 and 1 % trehalose. Figure 6.10a shows the % differential volume distribution of all the inlet temperature according particle diameter. Multiple peaks demonstrate polydispersity of the microparticles which range from 1 to 100 µm. Marginal difference can be seen for each temperature with 180°C showing smaller particle size and 100°C showing the biggest particle diameter. This trend was further demonstrated in the % cumulative volume as shown in Figure 6.10b, where 50 % of the particle at inlet temperature 180°C were below 5 µm whereas for 100°C inlet temperature, 50 % of

particles are below 25 µm. For inlet temperatures 150°C and 120°C, 50 % of the particle are below 6 µm and 7 µm respectively.

The particles were also examined under the scanning electron microscope for morphological characterisation Figure 6.11. The particles were spherical in shape with a smooth outer surface, size range between a few microns to tens of microns. Panel one of Figure 6.11 shows the makeup of the powder from these small microparticles which were smooth in texture and the powder was flowable without course aggregated particles.

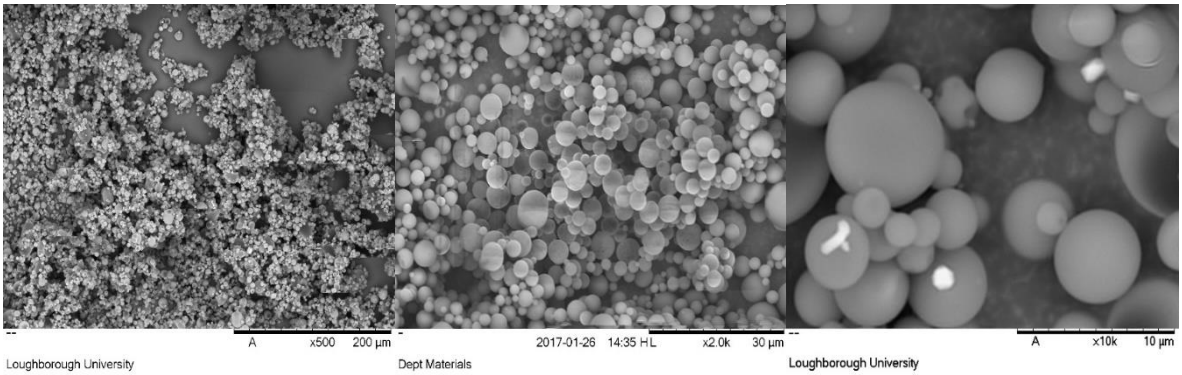

Figure 6.11. SEM of spray dried 2 % (w/v) ES100 and 1 % (w/v) trehalose powder at inlet temperature 150°C.

6.3.3. Storage of phage encapsulated spray dried powder

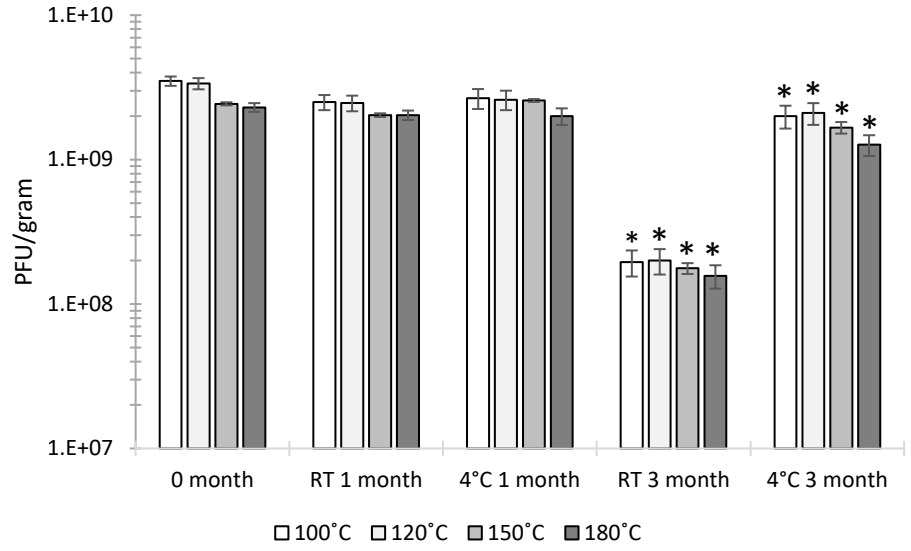

Figure 6.12. Storage results of 4 % (w/v) trehalose spray dried powder encapsulated Felix O1 under 4°C and 23°C (RT). * indicates significance mean was compared to 0 month for all parameters tested ($p < 0.05$) using a 2-sample t-test. All measurements were done in triplicate (n = 3).

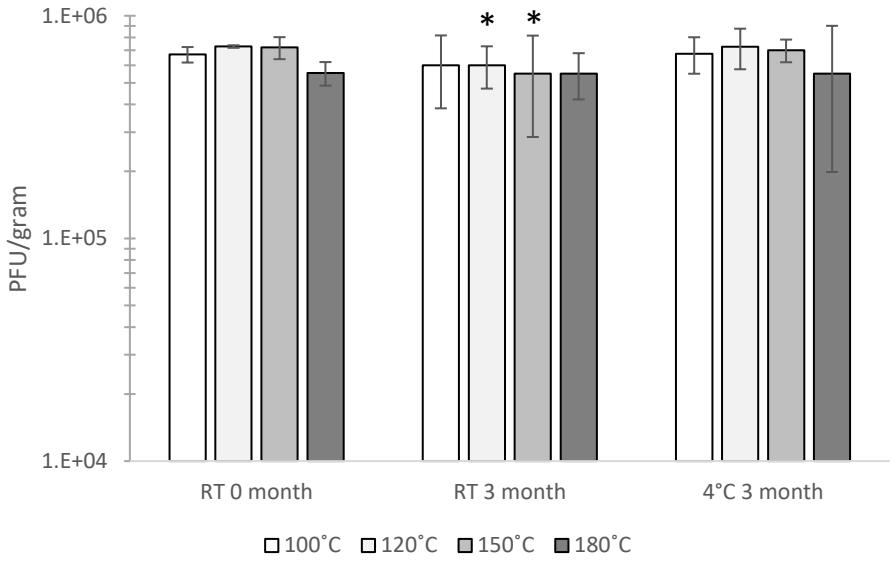

Figure 6.13. Storage results of 3 % (w/v) Eudragit spray dried powder encapsulated Felix O1 under 4°C and 23°C. * indicates significance mean was compared to 0 month for all parameters tested ($p < 0.05$) using a 2-sample t-test. All measurements were done in triplicate (n = 3).

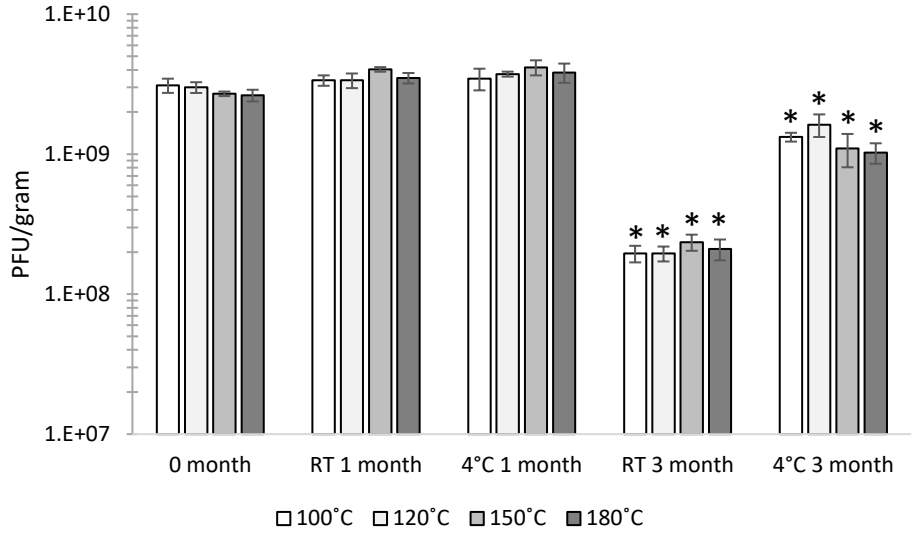

Figure 6.14. Storage results of 2 % (w/v) Eudragit, 1 % (w/v) trehalose spray dried powder encapsulated Felix O1 under 4°C and 23°C. * indicates significance mean was compared to 0 month for all parameters tested ($p < 0.05$) using a 2-sample t-test. All measurements were done in triplicate ($n = 3$).

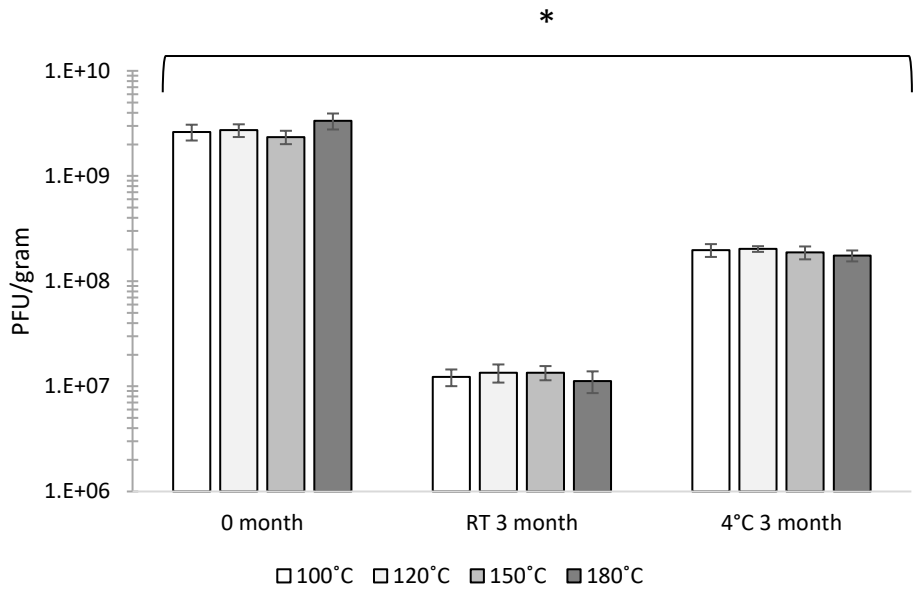

Figure 6.15. Storage results of 2 % (w/v) Eudragit, 1 % (w/v) trehalose 0.5 % (w/v) alginate spray dried powder encapsulated Felix O1 under 4°C and 23°C. * indicates significance mean was compared to 0 month for all parameters tested ($p < 0.05$) using a 2-sample t-test. All measurements were done in triplicate ($n = 3$).

Spray dried phage in all excipients were stored at room temperature (23°C) in sealed tubes and in the fridge at 4°C for a period of 3 months. A sample was removed from each tube and tested for phage up to a period of 3 months (Figure 6.12-15). Trehalose encapsulated phage showed good stability over the storage period, with minimal drop in titre at 4°C for all samples (Figure 6.12). Samples stored at room temperature showed just under a log decrease in the phage titre. Similarly, phage encapsulated in 3 % (w/v) Eudragit showed good stability after 3 months storage with little to no phage reduction in all storage conditions Figure 6.13. The formulation containing trehalose and Eudragit, Figure 6.14 displayed good stability over 3 months. No change in phage titre was detected for the first month and this remained the same for 4°C at 3 months however the titre of phage dropped by a log for all samples at RT. For the formulation containing all three excipients together (trehalose, Eudragit and alginate) Figure 6.15 phage titre was affected the most in terms of viability. The phage titre dropped by a log at 4°C after 3 months and up to 2-logs at 23°C after 3 months. The T_g may be the reason for this, crystallization of trehalose under humid condition can affect phage viability.

6.3.4 Tableting spray dried phage

Figure 6.16. Image of tablets produced using Minipress tableting machine.

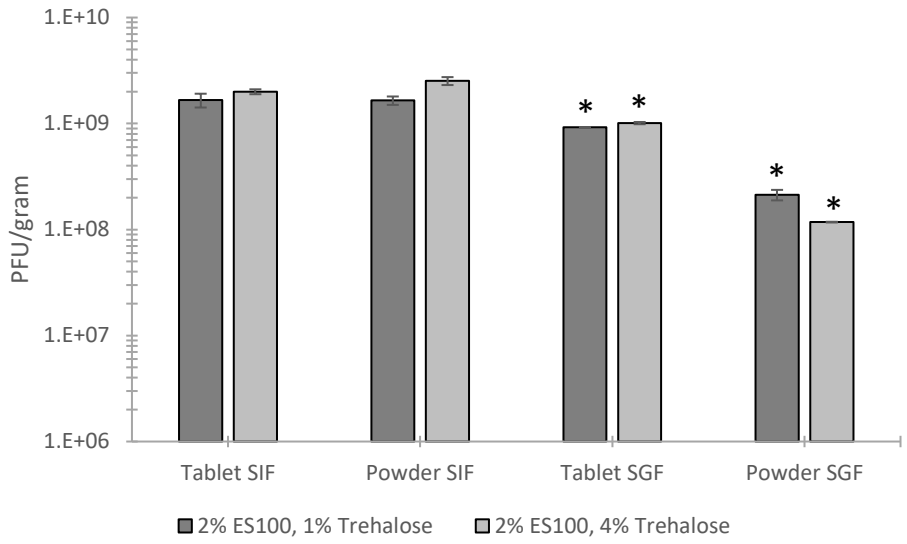

Figure 6.17. Encapsulated Felix O1 release in SIF for 5 hours from powder and tablet form using two different concentrations of excipients. * indicates significance mean was compared to tablet and powder in SIF for all parameters tested ($p < 0.05$) using a 2-sample t-test. All measurements were done in triplicate ($n = 3$).

Spray dried phage containing powders were compressed into solid round tablets which can be blister packed for ease of use and transfer Figure 6.16. The formulation used throughout this piece of work was the combination of 1 % (w/v) trehalose and 2 % (w/v) Eudragit. This formulation gave the best overall results in terms of encapsulation, yield of powder and acid protection and storage. In addition to this, 4 % (w/v) trehalose and 2 % (w/v) Eudragit was also tableted and tested- with the intention that tableting compression may halt premature dissolution of the tablet and offer protection against SGF. Increasing trehalose concentration also meant long-term storage maybe improved.

The inlet temperature used for further experiments was 150°C which was due to minor differences in encapsulation efficiency at all temperatures. 180°C showed modest adverse effect of temperature on phage viability therefore the next lower temperature (150°C) was carried forward. Industrial scale spray dryers operate at much higher temperatures, therefore the higher the temperature the easier feasibility of future to scale up of the operating at 150°C proven, hence temperatures 100°C and 120°C were not used as they were statistically no different.

As mentioned in section 6.2 (material and methods) tablets were produced using a small scale Minipress® machine and subsequent analysis was carried out using pharmaceutical grade equipment for disintegration, friability and dissolution (appendix). The spray dried powder was loaded into the tableting machine and tablets weighing at 0.3 g ± 0.5 were produced. The variation in tablet weight was due to a low bulk density of the spray dried powder largely attributed to Eudragit. A total of 6

tablets were exposed to SGF in the disintegration apparatus for 3 hours, following which each tablet was collected and dried, the weight of the tablet was measured before and after to account for any erosion during disintegration. 6 representative tablets were not exposed to SGF and were directly dissolved in SIF (Figure 6.17).

Along with the tablets the powder used to produce the tablets was tested in the same way (2-hour acid exposure under agitation conditions at 37°C and directly in SIF). The results for both powder and tableted phage are shown in Figure 6.17. Where there was release of phage in SIF without SGF exposure the phage from powder and tablets show no statistical difference and the titre was high at 10^9 PFU/gram. SGF exposure (pH 2) for 2 hours with subsequent SIF exposure showed protection in both formulations for both powder and tablet form. In the case of powder, the formulation containing 4 % (w/v) trehalose showed significant lost in phage viability. For both formulations, phage exposure to SGF and release thereafter from tablets showed similar protection with just over a log loss in titre- higher than in the powder form. A significant difference was observed in phage loss after SGF exposure in powder form for in comparison to tablet form.

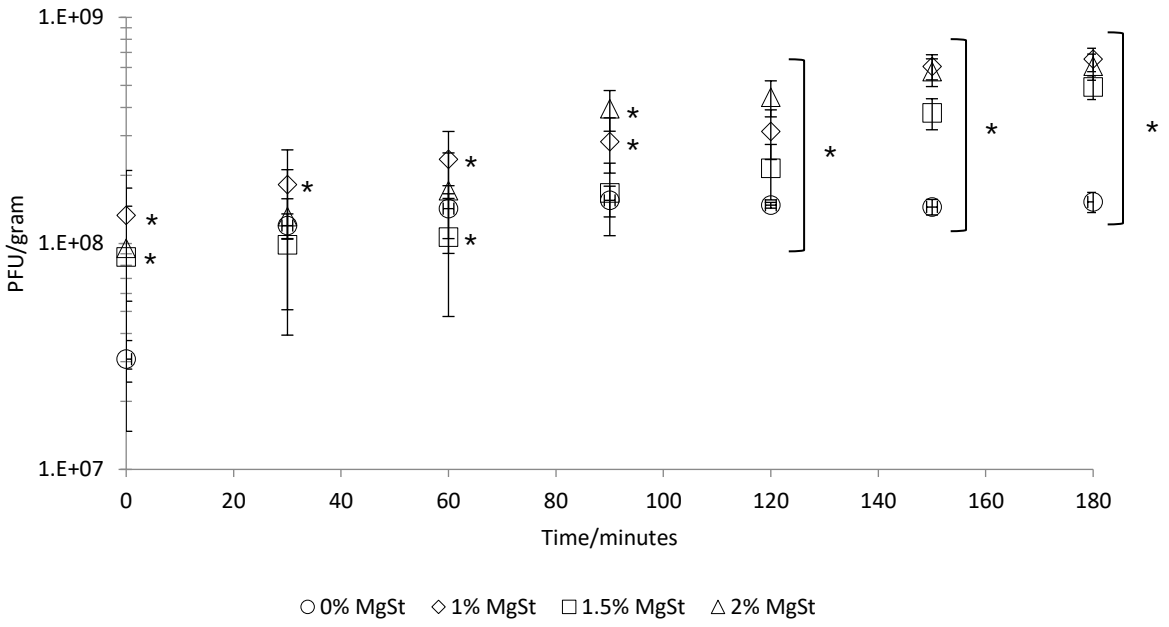

Figure 6.18. Powder release profile of 2 % (w/v) Eudragit 1 % (w/v) trehalose encapsulated phage Felix O1 using 150°C inlet temperature for spray drying with and without the addition of magnesium stearate, after 2 hours SGF exposure and subsequent release in SIF over 3 hours. *indicates a significance difference between the mean of each parameter in comparison to 0 % MgSt within each time point ($p < 0.05$) n=3.

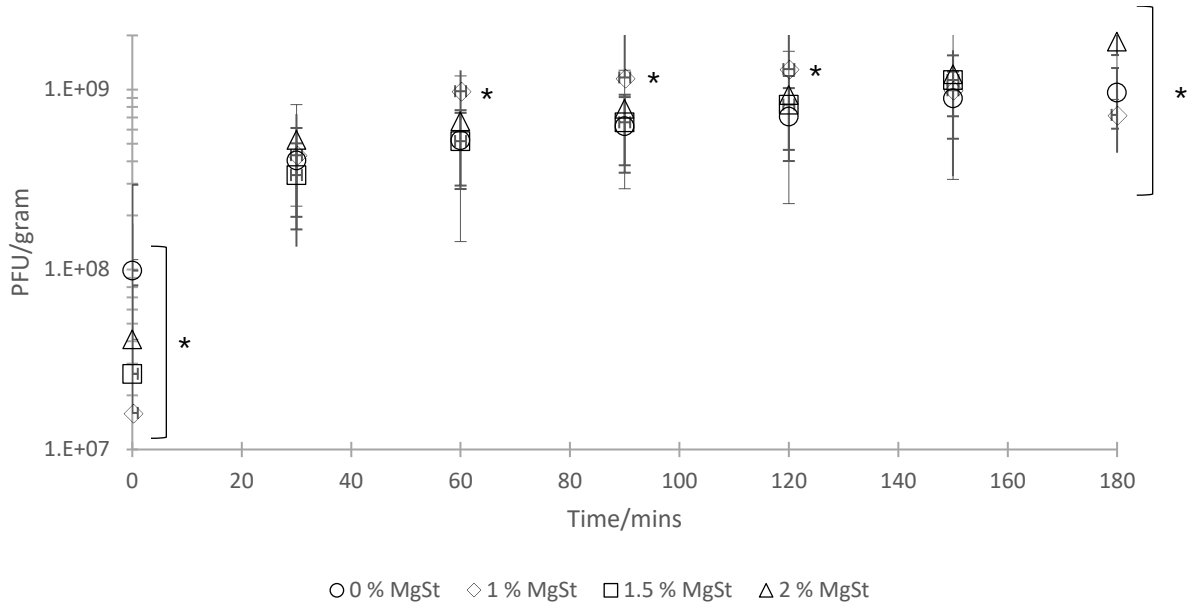

Figure 6.19. Tablet release profile of 2 % (w/v) Eudragit 1 % (w/v) trehalose encapsulated phage Felix O1 using 150°C inlet temperature for spray drying, with and without the addition of magnesium stearate, after 2 hours SGF exposure and subsequent release in SIF over 3 hours. *indicates a significance difference between the mean of each parameter in comparison to the mean of every other parameter within a timepoint ($p < 0.05$) n=3.

Tablets and powder were analysed with different concentration of magnesium stearate and exposed to SGF (pH 2) for 2 hours before release in SIF Figure 6.18 and 6.19. The titre of phage in the microparticles was 5 x10^9 PFU/gram (without SGF exposure). Release was followed for 3 hours for all samples, the release profile in all cases showed similar kinetics. A common trend was observed with an initial burst release of phage, up to 50 % phage released within minutes of SIF exposure. For all samples, the majority of the phage were released within the first hour. No influence of magnesium stearate concentration on phage yield was observed.

Release profiles of the powders at different concentrations Figure 6.18 show a gradual release of phage. Sample without magnesium stearate showed the highest loss in phage titre (1-log) after SGF exposure in comparison to the other samples. All the other samples containing various amounts of magnesium stearate showed similar release kinetics and protection against low pH. There was a notable improvement in phage titre with magnesium stearate, with losses of less than a log with final titre of the phage at 6 x 10^8 PFU/gram. For both the powder and tablet form, a further improvement on acid protection was seen after 2-hour SGF exposure and subsequent release.

Tableted phage displayed a low initial release at t=0 with a maximum of 20 % phage being unloaded. Prolonged release of phage over the 3 hours was observed for all parameters. Sample with no magnesium stearate yielded 7 x 10^8 PFU/gram phage, showing the most loss in phage viability after SGF exposure. For samples, with 1 %, 1.5 % and 2 % magnesium stearate, approximately 10^9 PFU/gram was released at the end of the 3 hours. Specifically, 1 % magnesium stearate sample release 9 x 10^9 PFU/gram which was the highest titre of phage released at the end of 3 hours.

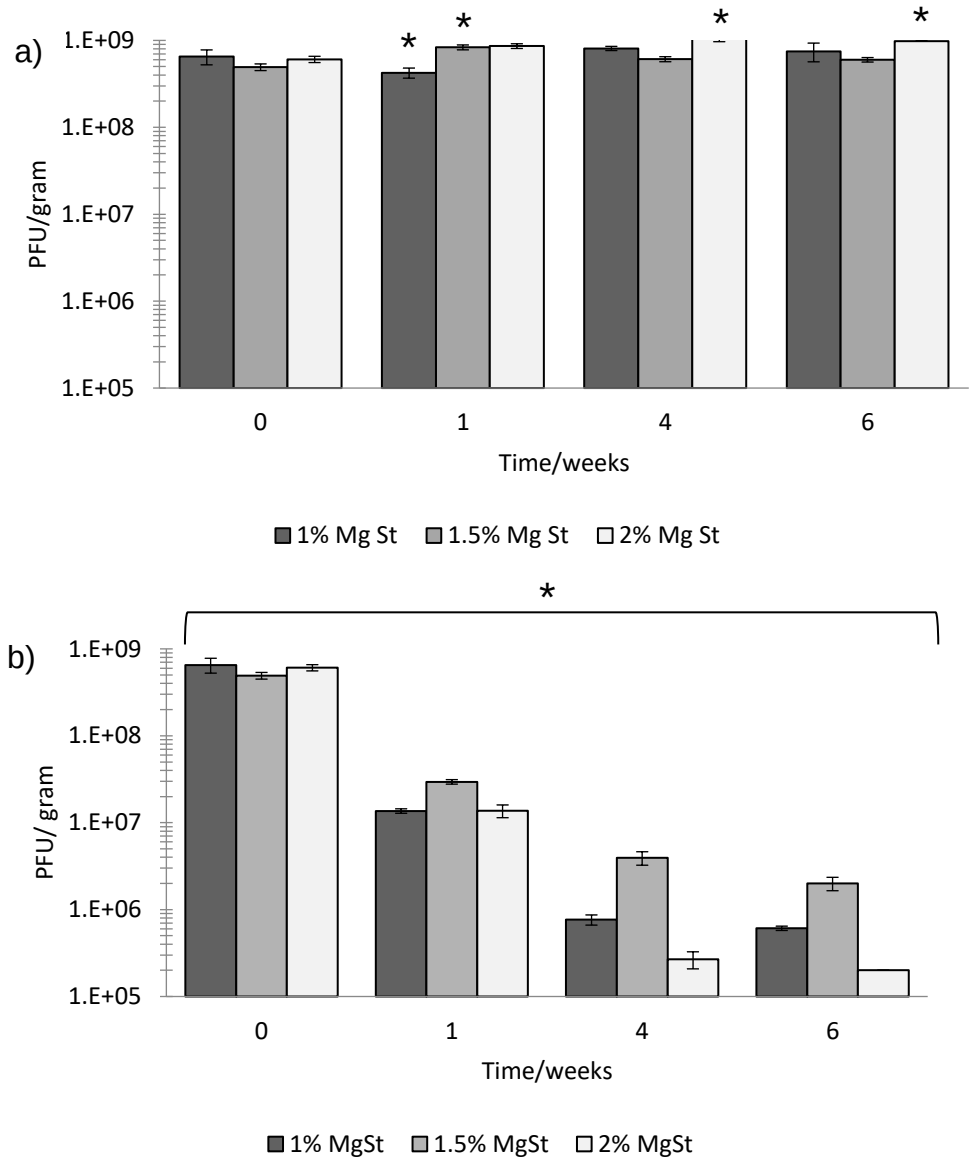

Figure 6.20. Tablet storage results with varying concentrations of magnesium stearate under a) 4°C b) 30°C, 65 % RH for 6 weeks. * indicates significance mean was compared to 0 month for all parameters tested ($p < 0.05$) using a 2-sample t-test. All measurements were done in triplicate (n = 3).

Encapsulation of phages in tablet form was further examined in terms of achieving viable phages after storage at two different conditions. Tablets were kept in glass vials with the lid finger-tight in the fridge at 4°C and at 30°C with RH of 65 %. At regular intervals of 1, 4 and 6 weeks a tablet was removed from each condition and exposed to SGF for 2 hours before releasing the phage in SIF. The results after complete release of phage are shown in Figure 6.20a and b. Approximately 1-log loss was seen for samples stored at 4°C throughout the 6-week storage, this remained the same for every sample containing a different amount of magnesium stearate. Phages were unaffected by the formulation parameters as noted in previous chapters. Phage stocks were also stored at 4°C and were stable for up to a year. A similar effect can be seen for tablets stored at 4°C since no phage loss was observed.

In contrast to the results for 4°C storage, samples stored at 30°C with 65 % RH, Figure 6.20b showed loss in phage titre over a period of 6 weeks. After just 1-week storage, with a 2-hour exposure to SGF, phage titre decreased by just under 2-logs. For the weeks following, a further 2 to 3-log reduction in phage titre was observed giving final titres around 1 x 10^5 - 1 x 10^6 PFU/gram.

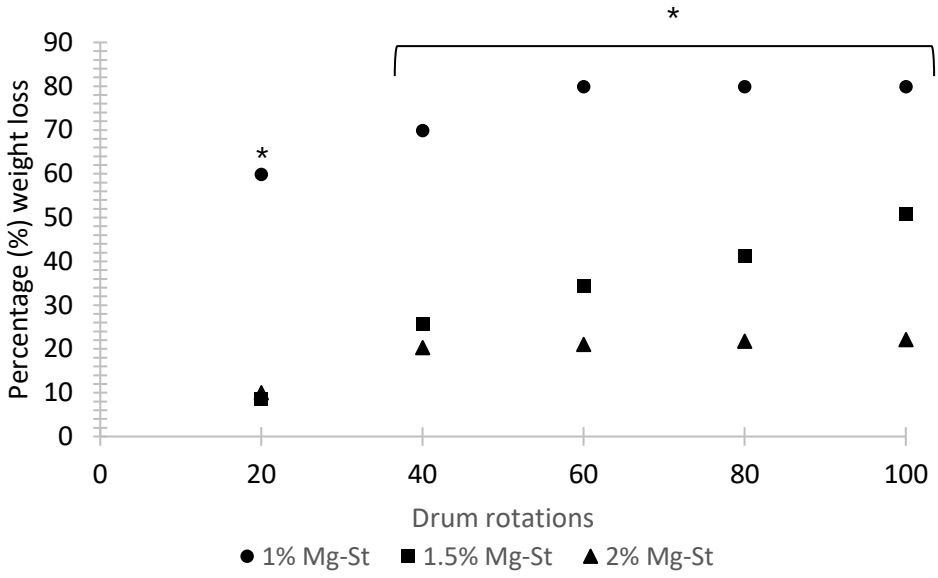

Figure 6.21. Friability of tablets produced with the addition of different magnesium stearate concentrations over 100 drum rotations. *indicates a significance difference between each parameter in comparison to the mean of every other parameter ($p < 0.05$) n=3.

Tablets were tested for robustness using a friability tester to test its compliance to British Pharmacopeia (BP) standards, 100 drum rotations were carried out and tablet weight recorded after every 20 rotations to observe loss of tablet weight. The results are shown in Figure 6.21, by 20

rotations 60 % tablet weight was lost for 1 % magnesium stearate compared with 10 % loss for 1.5 and 2 % magnesium stearate. By 100 rotations, 80 % of tablet weight was lost for 1 % magnesium stearate and 50 % and 22 % for 1.5 % and 2 % magnesium stearate respectively.

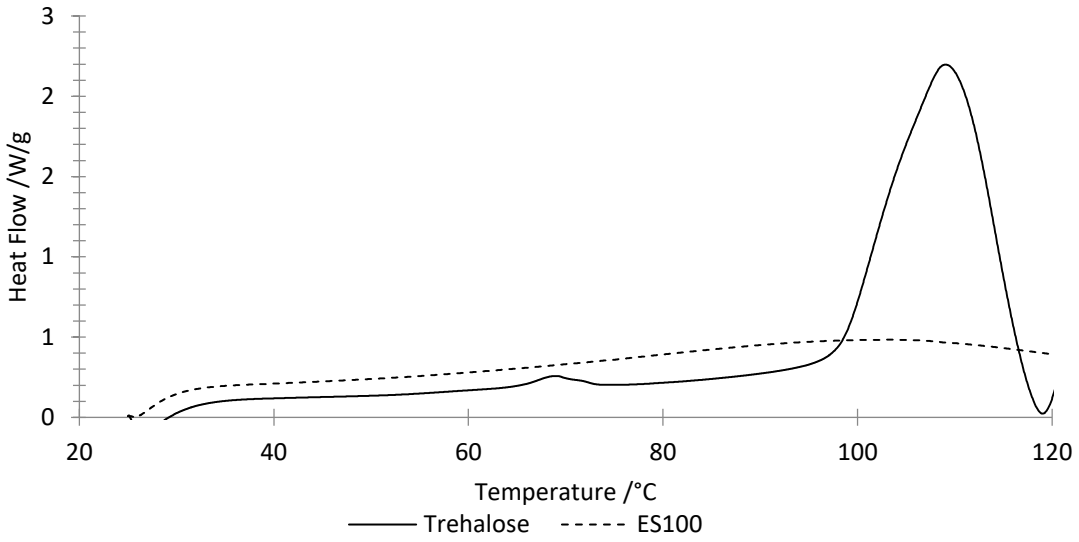

Figure 6.22. DSC thermograph of Eudragit and trehalose powder before spray drying.

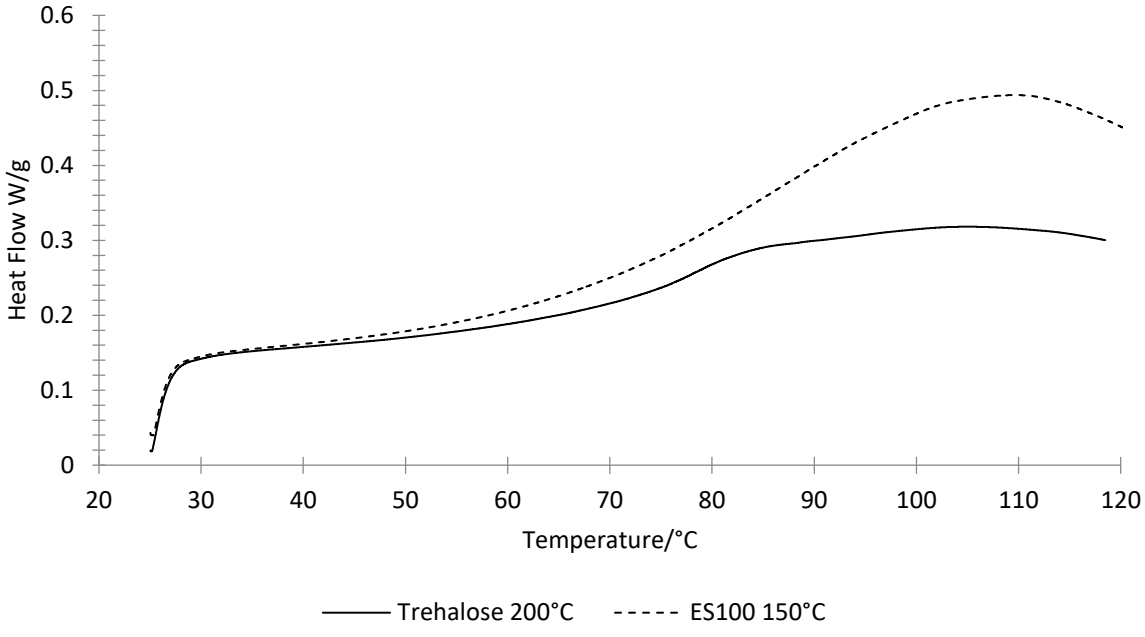

Figure 6.23. DSC thermograph of Eudragit and Trehalose after spray drying at 200°C (trehalose) and 150°C (Eudragit) inlet temperature.

Glass transition temperature was measured for Trehalose and Eudragit in the form supplied by the manufacturer (powder taken directly from the bottle). Figure 6.22 shows the DSC analysis for both

excipients, with glass transition of 55°C and 66°C respectively. Trehalose is manufactured in dihydrate form which indicates crystallisation is likely due to the presence of water molecules. However, since a glass transition temperature was recorded, this indicated that trehalose was partially crystalline. A study by Vandenheuvel *et al.*, (2014) also showed the presence of Bragg peaks demonstrating the presence of crystallinity typically found in dihydrate trehalose. A substantial exothermic peak was observed from 100°C to 120°C for trehalose where heat was released to the surroundings, demonstrating crystallisation. A smaller peak was also observed at 68°C which may be due to evaporation of residual moisture. Once trehalose was spray dried, the thermograph revealed a lower heat capacity of the initially observed peak from 2.2 to 0.3 W/g, showing a shift in the glass transition of trehalose Figure 6.23. In amorphous state, trehalose is known to exhibits a higher glass transition temperature.

DSC for Eudragit did not display a glass tranistion temperature but rather a wide peak spanning from 30°C to 120°C (Figure 6.22), although the reason for this is unclear but evaporation of residual moisture may be a reason. After spray drying Eudragit no significant difference was observed (Figure 6.23) in the thermograph, implying that since the state of Eudragit remains unchanged, it is manufactured in its amorphous form. According to the manufacturer the glass transition temperature of Eudragit S100 is 130 ± 5°C. The thermal profile of each excipient was not studied beyond 120°C due to irrelevance on storage stability of the powder.

6.4 Discussion

This study has investigated the encapsulation of phage Felix O1 using the method of spray drying. Encapsulation was carried out in different excipients or bulking agents to obtain the optimal formulation for this technique. Effect of each excipient on phage titre was investigated along with the effect of temperature. Formulation which gave SGF protection and contained stable phage after storage was carried forward for further work. Optimised conditions uncovered from investigating the phage encapsulation efficiency in the powdered form were used for tableting. Tableting required the solid dosage form to be robust enough to survive disintegration for 2 hours at SGF with subsequent dissolution. A binder was added to the tablets post spray drying of phage and the effect of binder concentration was tested. Binder was added post spray drying due to the hydrophobic nature of mageniusm stearate which does not dissolve in water. Further to this, the stability of the powder and tablet was examined for storage under different conditions. It will be discussed in this section the

findings from the study and the possible reasons why one formulation worked better than others and if spray drying and tableting is a viable way of phage encapsulation.

6.4.1 Phage encapsulation using different excipients and experimental parameters

Phage Felix O1 was used as a model phage for encapsulation using the method of spray drying which has been previously studied (Yongsheng Ma *et al*., 2008; Tang *et al.*, 2013). Based on the findings from previous chapters, Eudragit and alginate have proven to contribute towards a stable encapsulation of phage using other advanced encapsulation techniques. Spray drying is a well characterised technique; therefore, the formulation was implemented to elucidate the role of each excipient under different encapsulation conditions. Non-encapsulated Felix O1 was subjected to different temperatures representative of the outlet spray drying temperatures. Felix O1 showed resilience to temperature below 50°C however as the temperature rose to 60°C the phage titre began to drop after 60 minute exposure, correlating with the findings by Jończyk *et al.*, (2011). The ability of phage to survive elevated temperatures is a pre-requisite for high encapsulation efficiency during encapsulation via spray drying.

With the aid of trehalose as the preservative Felix O1 was found to be stable under both high and low temperatures as otherwise with outlet temperatures ranging between 80°C to 90°C, phage cannot survive the thermal stress which was found to be the case with free phage. Eudragit and alginate alone, did not provide sufficient protection from both high and low temperatures as several log reductions in the phage titre was observed. Despite the phage being resilient to temperatures up to 60°C, the added desiccation stress also has an impact. Unlike trehalose, Eudragit and alginate have different chemical properties- amorphous trehalose can interact with the phage by replacing the hydrogen bonds lost due to thermal stress and dehydration. Vitrifying phages in glass during dehydration prevents structural and conformation changes which can render them inactive (Chang *et al*., 2017b).

No phage was detectable after SGF (pH 2 for 2 hours) exposure for 3 % (w/v) Eudragit and 2 % (w/v) trehalose microparticles. Trehalose is water soluble and therefore upon exposure to aqueous solutions it readily dissolves creating pores in the composite spray dried microparticles. Phage release in SIF occurs without a drop in titre however when microparticles were exposed to SGF no phage were recovered. This was due to premature phage release and the penetration of SGF into the microparticles leading to loss in phage activity as found during free phage exposure to low pH. Hence, reconsidering the concentration of trehalose was an important step by lowering the concentration of

trehalsoe to 1 % (w/v) led to phage protection during acid exposure, further improvement to acid exposure was observed by addition of 0.5 % alginate.

Protection against SGF (pH 2) was observed with formulation, 2 % (w/v) Eudragit and 1 % (w/v) trehalose with approximately 1-log titre reduction after two-hour exposure. Addition of 0.5 % (w/v) alginate also showed SGF protection across all samples with less than 1-log reduction in phage titre. Standford *et al.,* (2010) encapsulated four *E. coli* specific phages in Eudragit (unspecified concentration) using spray drying, after 30 min pH 3 exposure 2.71 x 10^9 PFU/gram (13.6 %) of phages were recovered when compared to results from this study, 2-hour pH 2 exposure resulted in less than 1-log reduction (90 % recovery). An Initial 1-log reduction in phage titre occured during spray drying (Stanford *et al*., 2010) however only 10 % phage loss was observed when spray drying Felix O1 with Eudragit and trehalose. This suggests that by incorporating trehalose, protection against elevated outlet temperatures encountered during spray drying can be achieved preventing loss of phage viability. Incorporation of alginate showed better acid protection but loss of phage titre during spray drying meant no further work was done alginate. Formulation containing Eudragit and trehalose only were carried forward for further work.

Moisture content of the spray dried powder influences the stability of the phage during storage. Excipients such as trehalose are well known for their ability to sequester moisture, although this results in a lowering of the glass transition temperature. This prevents moisture causing conformational and activity changes of the active encapsulated agent. Spray dried Eudragit powders were found to have a high moisture content (~25 %), when spray dried with trehalose the moisture content was lowered significantly. In terms of stability during storage low moisture prevents crystalizing of trehalose which may affect phage viability. Crystallisation of trehalose may change the flowability of the powder, bonds are formed between the microparticles preventing them from dispersing easily (Chang *et al.*, 2017a). Low moisture content was seen with higher spray drying temperatures for all formulations as the driving force for drying air was higher.

Powder yield was significantly affected by the type of excipient, Eudragit showed the highest yield similar to results obtained by de Arce Velasquez *et al*., (2014) when compared to alginate and trehalose alone. When combined with Eudragit the yield was significantly increased, for blends with trehalose and alginate. Laser diffraction analysis revealed that microparticles they ranged between 1 to 20 µm. Lower temperatures 100°C and 120°C displaying some bigger particles too, between 20 µm to 100 µm. It is generally recommended to produce particles below 200 µm for oral consumption to mask the granular powder. Particles showed a smooth non-porous surface composed of Eudragit and trehalose under the SEM, typical of Eudragit particles. Low spray drying temperatures (i.e. 60°C) may

sometimes produce fractured and inflated microparticles, which was not observed in this study. SEM imaging revealed that all formulations produced spherical microparticles ranging from a few to tens of microns. The concentration of both polymer and sugar was low and despite this particle morphology did not display any cracking or blowholes. Particle merging due to a high concentration of amorphous excipients can also be an issue as observed by Leung *et al.,* (2017) with trehalose concentrations of 40 %, however this was not observed in this study.

Storage in the presence of trehalose showed that the phage titre dropped the least in comparison to Eudragit and alginate. The presence of trehalose reduced the negative effect of storage temperature and humidity from affecting the phage viability. Around 1-log reduction in phage titre was observed by Stanford *et al*., (2010) after 1 year storage of Eudragit microparticles at 20°C. In this study, a lower encapsulation efficiency of phage Felix O1 was observed however, storage results showed a similar trend in that negligible effect on phage titre was observed over 3 months. With the addition of trehalose, phage titre was preserved better as reported by Leung *et al*., (2017), only ~ 1.4 log titre drop was observed as opposed to 5.1 log without any trehalose. Similar report with Felix O1 was observed in that less than a log titre reduction was seen after 3 months storage at 4°C. Storage at 22°C showed the most reduction in phage titres across all samples, highlighting the onset of temperature and humidity fluctuations when stored at room temperature. Recrystallisation of trehalose during storage affected the phage survivability resulting in several logs drop in titre across all samples.

6.4.2 Direct compression tableting of spray dried phage

Tableting reduces the frequency of dosage by effectively increasing the localization of the active ingredient at the site of infection due to their bound conformation which ameliorates the chance of the active encapsulated agents being inactivated during transit. Incorporating, functionalised pH responsive microparticles carrying phage into tablet systems enhances their efficacy by being delivered at high titres. There are several advantages of using direct compression tableting since many processes are by-passed to avoid affecting the encapsulated phage. This study has combined the benefits of different excipients to produce powdered encapsulated phage for ease of use.

The first half of the study focused on producing powder with stable phage in excipients which provide both acid protection and sustain phage titre during storage. Tableting this powder via direct compression demonstrated the ease of use and possible scale up for producing oral dosage forms of phages. Enteric coating is usually used to coat tablets to protect active ingredients from disintegrating

in the stomach (Waddell *et al.*, 2013) and this may involve processing steps which introduce changes in temperature and expose the active ingredient to further shear. The formulation investigated here requires no further coating since the enteric element was incorporated during the spray drying process. The phages were shown to remain viable with each excipient and during the spray drying process, further investigation highlighted the powder prevents acid damage.

The effect of compression during tableting on phage viability was examined by taking six tablets for each formulation and analysing the phage titre with and without SGF exposure. Tablets as well as powder were analysed to compare the effect of tableting on phage survivability under SGF and SIF. The results revealed that there was no detrimental effect on phage during tableting since the titre showed no significant difference to powder. Similarly, exposure to SGF did not show any negative effect on phage viability and the results once again were comparable to powder. In fact, previously it was observed the use of high concentration of trehalose (2 %) resulted in 2-log titre drop after acid exposure, here equivalent results were obtained with 4 % trehalose. However, some improvement was observed with tableting with approximately a log reduction in phage titre after acid exposure. This may be explained by the structure of the tablet where only the outer layer was exposed to SGF- in the case of powder the surface area was much larger and all microparticles encounter SGF.

Pharmaceutical grade dissolution apparatus was used for SGF exposure, tablets were exposed for a period of two hours. During this time, erosion and disintegration of tablets was observed since trehalose is water soluble. To improve the tablet integrity during disintegration, magnesium stearate was added to the spray dried powder before tableting. Magnesium stearate is used in tableting to act as a lubricant or an anti-adherent to prevent powders sticking to machinery during the manufacturing process. The hydrophobic nature of magnesium stearate contributes to slow dissolution of tablet in the dissolution apparatus (Ariyasu *et al.*, 2016). It has low toxicity and is approved by the FDA in the list of pharmaceutical ingredients. Concentration of lubricants added needs to be carefully considered since too much lubricant can result in a laxative effect reducing residence times, preventing effective dissolution of the tablet at the desired site. Incorporating various concentrations of magnesium stearate to powder before tableting was to observe the effect on dissolution, tablet disintegration, effect on phage viability and friability. Higher concentrations of magnesium stearate showed improved tablet integrity with no effect on phage viability.

Phage release kinetics were examined for both powder and tablets with and without magnesium stearate after SGF exposure. Improvement in phage viability in the presence of magnesium stearate was observed for both powder and tablets, although this was more apparent in the case of powder with approximately 50 % less phage release from sample without magnesium stearate. The

hydrophobic nature of magnesium stearate shields microparticles and protects them from acid. A difference between powder and tablets also showed improved phage survival in the tablet form with approximately 70 % more phage release at the end of the 3-hour dissolution period for tablets (2.4 x 10^9 PFU/gram) in comparison to powder (6 x10^8 PFU/gram). Differences between samples with varying magnesium stearate concentration were less obvious, all samples showed similar release profiles achieving titres of 10^9 PFU/ gram for tablets.

Relative to the initial titre of phage in the microparticles, 0.3-log titre reduction was observed for tableted form (1.5 % Mg-St) and 0.9-log for powder form (1 % Mg-St) when exposed to SGF (pH 2 for 2 hours). A 13 % loss in phage titre was observed by Stanford *et al.*, (2010) after Eudragit spray dried phage was exposed to pH 3 for 30 min, showing a significant improvement in phage protection against low pH. Phage encapsulated powders have been prepared for pulmonary applications without the use of functionalised polymer for oral delivery (S. S. Y. Leung *et al*., 2017; Matinkhoo *et al*., 2011; Vandenheuvel *et al*., 2013a). However, other encapsulation techniques have been used for phage encapsulation for oral delivery by incorporating biopolymers such as alginate, whey protein and chitosan (Colom *et al*., 2017b; C Dini *et al.*, 2012; Yongsheng Ma *et al.*, 2012; Tang *et al*., 2013; Yongsheng *et al*., 2008).

Tang et al., (2014) encapsulated phage K in alginate and whey protein microsphere with additional protective agents to improve phage stability during thermal stress. Wet microspheres showed good phage viability after exposure to pH 2.5 for two hours without titre reduction for all formulations. Exposure to pH 2 however, showed phage viability was reduced across formulations, highest concentration of whey protein showing the least titre reduction. Phage viability for dried microspheres was improved which included maltose upon exposure to pH 2.5 only. The study demonstrated like the one investigated here the use of polymers with protective agents in combating the harsh gastrointestinal conditions found in the stomach. Improving the phage viability during acid exposure is a crucial factor when considering formulations for oral delivery.

Tablets were stored at two different temperatures (25°C and 4°C). The phage viability showed significant reduction for samples stored at 25°C. No reduction in phage titre was observed for tablets stored at 4°C across all samples over a period of 6 weeks. On the other hand, phage titre dropped by a log every week for the first 4 weeks losing up to 4-logs by the end of 6 weeks for samples stored at 25°C with 65 % RH. This reduction may be attributed largely to the high relative humidity (65 %) during storage. Temperature has previously shown not to influence phage since free phage stayed viable at temperatures up to 50°C. The high humidity during storage was a key factor since conditions during transit as well as delivery to low-income countries without refrigeration facilities may be required.

Hence, testing the formulation in extreme conditions to probe the ability of the formulation in protecting phage was insightful.

The role of trehalose in protecting phage from desiccation and thermal stress is widely known, however during high humidity conditions, trehalose can crystallize which can be detrimental for the phages inside the polymer matrix (Vandenheuvel *et al*., 2013a). Post spray drying, trehalose was in its amorphous state meaning the glass transition temperature was high. Upon storage under humid conditions trehalose sequesters moisture, inevitably crystallises which lowers the glass transition temperature. Phages are protected from these adverse conditions by the presence of trehalose, however once trehalose fully crystallises phage are prone to environmental stresses and damage. This was shown by storage data, demonstrating in the presence of high humidity and temperature the phage titre falls significantly. One factor which is important to consider is the optimum concentration of trehalose to avert the effect of temperature, humidity and desiccation. Studies about freeze drying with sugars have recommended concentrations of 20 % (w/w) for good freeze-drying results. At this concentration the water activity is 0.987 which does not produce osmotic stress in the freeze-drying process. Another study presented good bacterial cell protection, prolonged shelf life and stability after spray drying *L. acidophilus* in 20 % (w/v) of excipient (Pehkonen *et al.*, 2008; R. Zhao *et al.*, 2008).

6.5 Conclusions

This study demonstratesd the use of conventional spray dryer method for spray drying phage Felix O1 in pH responsive polymer Eudragit in combination with trehalose. Spray dried powder showed approximate average diameter of microparticles was 7 µm across all inlet temperatures. Encapsulated phage was sufficiently protected from SGF (pH 2 for 2 hours) with 0.5-log reduction in phage titre. Spray dried phage was then tableted where no effect of compression force was observed on phage viability. SGF (pH 2 for 2 hours) exposure showed once again less than 0.5-log reduction in phage titre. Addition of magnesium stearate improved tablet disintegration and friability. Release profile in SIF with magnesium stearate showed a prolonged phage release over a period of 3 hours. Phage storage at 4°C remained stable without loss in titre however at higher temperature and humidity the phage significantly dropped in titre. This study demonstrates the use of dry powder phage with pH responsive characteristics for enteric delivery. For ease of dosage and use, the study demonstrated that tableting is a feasible method.

Chapter 7: Electrospinning bacteriophage K in Eudragit composite fibres.

Abstract

The prevalence of multi-drug resistant (MDR) bacterial species, as seen in methicillin-resistant *Staphylococcus aureus* (MRSA) pose a serious healthcare challenge in wound infections making antibiotic-based treatment limited. Application of bacteriophages for the treatment of wound infections shows promise and is a viable alternative to the use of antibiotics. In this study, two emulsion formulations were prepared for the encapsulation of phage K in core-shell fibres using water-in-oil emulsion electrospinning. Biocompatible, pH-responsive Eudragit S100 (ES100) was used as the organic phase (forming 99% bulk of the fibre shell), and poly (vinyl alcohol) (PVA) or sodium alginate as the aqueous phase (carrying the phage). Defect-free, continuous fibres with large diameters were fabricated and their morphology was optimised to facilitate the encapsulation of phage K, serving as a proof-of-concept study for novel wound dressing applications. SEM analysis revealed that for both emulsions, fibre diameters and diameter distributions were influenced by changes to the applied voltage. Infusion rate only influenced the mean fibre diameter. Optimal electrospinning conditions for both emulsions were found to be at 15 kV and 1 ml h^{-1}. Increasing the concentration of either the organic phase or aqueous phase, which subsequently increased the viscosity and conductivity of the emulsions, had the most influence on fibre diameters. Phages were successfully encapsulated by suspending them in the aqueous phase of ES100-PVA fibres fabricated at different parameters. Phage plaque assay revealed that fibres with larger diameters and fabricated at lower applied voltages (10 and 12.5 kV) offered the best phage viability, as only a two-log reduction in phage viability was observed. Increasing the concentration of ES100 from 7 % (w/v) to 15 % (w/v) resulted in a three-log reduction in phage viability. Increasing ES100 concentration demonstrated enhanced viability compared to fibres fabricated at 15 kV applied voltage but with a lower ES100 concentration.

7.1 Introduction

7.1.1 Wound infections

Human pathogenic bacteria such as *Staphylococcus aureus* and *Pseudomonas aeruginosa* pose a serious healthcare challenge in wound infections. With the emergence of antibiotic resistance as seen in methicillin-resistant *S. aureus* (MRSA), treatment options are limited (Kelly *et al.*, 2016). Phage therapy offers a promising alternative in combating antibiotic resistance against pathogens which have already evolved resistance. Phages are protein shells, which package genetic information, they are prone to environmental stresses which can damage their structural characteristics rendering them inactive. When considering the use of phages against infectious bacteria whether that be for enteric, pulmonary or wound infections it is important to consider the dosage. Phages are prone to damage when kept under conditions outside their optimal environment, this can be in the form of thermal stress as discussed in the previous chapter 6, solvents, desiccation, humidity and low pH (Malik *et al.*, 2017). It is therefore important to address these factors during the application of phages for therapy.

Use of phages to combat bacterial contamination of food products has been well investigated and approved for use which can be used as a basis to study phage therapy for wounds. Commercially available products for such applications include EcoShield™ and SalmoFresh™ (Intralytics Ltd.). They are delivered and applied in liquid format and often require transportation under refrigeration which can be costly and may be detrimental to the stability of the phages. Maintaining phage viability whilst reducing operations/transportation cost requires alternative ways of delivering and applying phage. Dry phage products offer several advantages in addressing this issue, since the costs related to volume, shipment and storage conditions can be eradicated (Koo *et al.*, 2016). To produce dry carrier of phage with high infectivity, lypholization is often considered a viable option (Puapermpoonsiri *et al.*, 2009). It is an excellent way to preserve phage at high titres for extended periods of time, but the method remains costly and time consuming. Therefore, electrospinning phages in fibres has the potential to both reduce bacterial load in food packaging materials as well as treat infected wounds.

Global healthcare issue of wound treatment is a growing concern, acute and chronic wounds prone to infection have delayed healing due to ineffective treatment. Sizable portion of wound infections are related to diabetic ulcers which comprise 600,000 hospitalisations related specifically to diabetic foot ulcers (Sen *et al*., 2009). Commercially available wound dressings cater for various conditions, basic dressings usually protect from external biological contaminants and absorb exudates from the wound. Advanced dressings allow for air circulation, provide moisture to prevent dehydration whilst incorporating an anti-microbial agent to heal the wound (Mele, 2016).

7.1.2 Electrospinning fibres for wound dressings

Electrospinning is a growing technology which produces polymer nanofibers which can be biodegradable, biocompatible and have a high surface-to-volume ratio (A. Haider *et al.*, 2015). Ideally,

fabricated nanofibers should be uniform, continuous and bead-free; a phenomenon achieved when the experimental conditions are set to accommodate the production of ideal fibres for a specific polymer system. These conditions are classified as the electrospinning, solution and environmental parameters (A. Haider *et al*., 2015), as summarised in Table 7.1.

Table 7.1 Process conditions influencing the fabrication of electrospun nanofibers (Haider *et al*., 2015)

Electrospinning parameters	**Solution parameters**	**Environmental parameters**
Applied electric field	Solvent	Relative humidity
Distance between spinneret and collector plate	Polymer concentration	Temperature
Infusion rate	Viscosity	
Spinneret diameter	Conductivity	

Electrospun fibres have a large surface area to volume ratio which is why they form good delivery systems for surface applications (Reza Korehei & Kadla, 2014). Furthermore, they have been used for a range of applications including wound dressings (Zahedi *et al.*, 2010) and drug delivery systems (Sill & von Recum, 2008). Encapsulation of phages in electrospun fibres offers dimensional stability, improves storage and allows release of phage near the infected wound and host. Spraying phage directly onto the surface of the wound does not ensure targeted dose delivery, amount of phage delivered also depends on the spray technique and the distance from which it is sprayed. Reproducible application therefore is difficult, by ensuring phages entrapped in wound dressings and covering the infected area, one can ensure the prolonged and sustained release of phage. There is a higher chance of targeting the host bacteria if release is continuous and diffusion related, otherwise sprayed phage is prone to dehydration and therefore inactivation if host is not encountered.

Previous studies have investigated the encapsulation of phages in electrospun fibres using water soluble polymers, which show burst release of phage. M13 was encapsulated in polyvinyl pyrrolidone (PVP) by Lee & Belcher (2004) into nanofibers which showed instant release when suspended in buffer. Other phages encapsulated in water soluble PVA include T4, T7 and lambda (Salalha *et al.*, 2006) which were electrospun into nanofibers and maintained a high viability. These studies

demonstrate that encapsulating phages using electrospinning is a viable option for producing wound dressing with tailored released properties.

A drawback of encapsulation via electrospinning is that the phages would be exposed to high electric voltage which could be detrimental to the phages and therefore make it difficult to encapsulate phage at higher titres (Dai *et al.*, 2014; Drees *et al.*, 2003). Low concentration of viable phages in electrospun fibres may delay efficacy of phage therapy for wounds since the incidence of phage encountering host may lessen and the efficiency with which bacteria can be lysed be decreased. To minimise the loss of phage viability during the electrospinning process, magnesium salt has shown to be an effective additive, similarly trehalose has been shown to improve storage stability in fibres (Dai *et al.*, 2014; Koo *et al*., 2016). Other methods to improve survival of phages during electrospinning is to change the geometry of the nozzle to produce core-shell nanofibers. Co-axial electrospinning produces fibres ensuring the inner phase has minimal exposure to current and effects of dehydration (Reza Korehei & Kadla, 2014). Table 7.2 provides a summary of published research on phage encapsulation using electrospun nanofibers.

7.1.3 Formulating for electrospinning phages

So far, electrospinning for phage encapsulation has involved the use of salts, sugars, water soluble polymers and for application in food packaging polymers dissolved in solvents. Little consideration has been given to the use of stimuli responsive polymers in encapsulating phages. Encapsulation of other active agents has been well documented with the use of polymers for therapeutic applications (Mele, 2016). Fibrous wound scaffolds produced from natural polymers via electrospinning can aid wound healing through their natural anti-microbial properties. Utilisation of natural material for creating scaffolds ensures that they are biocompatible, biodegradable and are sometimes naturally anti-bacterial or anti-inflammatory. Extracellular matrix is a complex network of proteins and cells which helps maintain the natural processes of the skin. Healthy skin has an acidic pH ranging between pH 4-6; when the skin is damaged this environment changes to alkaline above pH 7 (Dargaville *et al*., 2013; Ehlers *et al.*, 2001). This is also the reason why some wounds become infected and prolong the healing process. Physiochemical changes in wounds can be exploited for preparing wound dressings which can be used to trigger release and efficiently eradicate the bacteria causing infection.

Alginate, is a natural biocompatible polysaccharide, previously utilised for wound dressings (T. Hashimoto *et al.*, 2004) and drug delivery systems (Augst *et al.*, 2006). It can effectively protect phages from harsh environmental conditions such as acidic pH without causing loss of phage viability (Colom *et al*., 2017a). Several studies have concluded its inability to form continuous fibres due to its lack of

chain entanglements without the addition of a carrier polymer, which enhances the chain elasticity of the system (Yu *et al.*, 2006). Poly(vinyl alcohol) (PVA), a non-toxic polymer, has demonstrated to provide some protection to phages during encapsulation (Salalha *et al*., 2006) but may offer enhanced protection when incorporated with different polymers and fabricated at different process conditions.

Eudragit S100 (ES100), a pH- responsive polymer has previously been electrospun to incorporate drugs targeted delivery (She *et al*., 2015). Since it is soluble at pH ≥ 7, it has the potential to enable a controlled release of phages in wounds, which become alkaline during bacterial infection, thereby making it a promising material for wound dressings. There have been no previous published studies on the encapsulation of phages for wound dressing applications using Eudragit, making it a novel material for this research

The lack of previous research on phage encapsulation in electrospun fibres for wound dressing applications means there are several combinations of polymers can be exploited. Generally, the use of organic solvent systems is ideal however, the lack of chain entanglement for continuous fibre production is a challenge. Korehei and Kalda (2014) investigated water-in-oil (w/o) emulsion electrospinning to enhance phage protection from harsh electrospinning conditions by pre-encapsulating the phages in core-shell fibres. Entrapping the phages in an aqueous core, coated with an oil-phase shell (polymer dissolved in organic water-immiscible solvent) produced a promising delivery system for phages which retained phage viability and released phages in a sustained fashion. Similarly, modifying the spinneret to produce co-axial electrospun fibres ensured the morphology of the fibres was continuous and smooth whilst minimising the exposure of phage to solvents which can affect phage viability.

Aims and objectives

In this work, two different w/o emulsion formulations were prepared for the encapsulation of phage K in core-shell fibres using emulsion electrospinning for wound dressing applications. Phage K specific against model bacterium, *Staphylococcus aureus* ATCC 6358 were used as model organisms. Biocompatible, pH responsive ES100 was used as the organic phase (forming the fibre shell) with PVA or sodium alginate as the aqueous phase (forming the fibre core) for the emulsions. Sorbitan monooleate (Span 80) was used as a non-ionic surfactant due to its low HLB value of 4.3, making it suitable for water-in-oil emulsions. This was added to the organic phase. The effects of applied voltage and infusion rate on fibre morphology were tested to determine the optimal electrospinning conditions for each emulsion formulation. Emulsion formulations were then developed by increasing

the concentration of the organic phase or aqueous phase and characterising the fibre morphology, rheology, and conductivity for each emulsion. The fabricated fibres were then screened for fibres which were continuous, defect-free and had a large mean diameter suitable for wound dressings. Phage K was encapsulated by suspension in the aqueous phase and phage viability determined by plaque assay.

Table 7.2 Summary of literature on phage encapsulation using electrospun nanofibers.

Ref	Phage	Carrier system	Encapsulation method	Additives	Target application	Fibre diameter	Advantages	Limitations
(S. W. Lee & Belcher, 2004)	M13	Polyvinyl pyrrolidine (PVP)	Wet spinning and electrospinning	Water	Biosensor	10–20 µm	Uniform PVP fibres may provide catalytic capabilities to be utilised in biomedical applications.	Viability of phages was undetermined
(Salalha et al., 2006)	T7, T4 and λ	PVA	Electrospinning	Water	Non-specific	250–400 nm	Some phage viability is retained after three months of storage at -20 and -55 °C.	Only 1% of T4 phages remained viable immediately after electrospinning, which is attributed to the rapid dehydration of the phages during fibre formation.
(R. Korehei & Kadla, 2013)	T4	Polyethylene oxide (PEO)-alginate	Emulsion and coaxial electrospinning	Chloroform	Food packaging	1 µm (emulsion) and *2* µm (coaxial)	Core-shell fibre formation (emulsion and coaxial). Coaxial electrospinning encapsulated phages with a long storage time, high	Phage activity dropped from 10^8 to 10^6 PFU ml^{-1} for emulsion electrospinning.

							loading capacity and full viability.	
(Reza Korehei & Kadla, 2014)	T4	PEO-cellulose diacetate	Coaxial electrospinning	Chloroform and methanol	Food packaging	1.35-2.48 µm	Core-shell fibre formation. PEO-CDA blends suppressed burst release of phages.	Phage activity dropped by 10^6 PFU ml^{-1} after four weeks storage.
(Koo et al., 2016)	T7	Polyvinyl pyrrolidine (PVP)	Electrospinning	Water	Various	100-200 nm	Preservation of phages in dry form, storage stability	Loss of phage viability at high humidity (33 % and 75 %)

7.2 Material and Methods

7.2.1 Materials

ES100 (M_w = 34 kDa), PVA (M_w = 13-23 kDa, partially hydrolysed 87%-89%), low viscosity sodium alginate (100-300 cP), trehalose (M_w = 378.33) and Span-80 were purchased from Sigma Aldrich Corporation. Chloroform (M_w = 119.38 Da), 1-Butanol (M_w = 74.12 Da) and calcium chloride ($CaCl_2$) were purchased from Fisher Scientific, UK. Magnesium chloride ($MgCl_2$) was purchased form Acros Ogranics, UK. BHI broth and Bacteriological Agar were obtained from Oxoid, UK. Phage K obtained from ATCC. Deionised water (DI) was obtained from the laboratory in the Department of Chemical Engineering at Loughborough University. All reagents were used as received.

7.2.2 Preparation of emulsions

The organic phase for the emulsion was prepared by dissolving a pre-weighed mass of ES100 (7, 10 or 15% w/v) and Span-80 (5% w/v) in chloroform and 1-butanol, at a ratio of 50% v/v. The solution was then sonicated for 30 minutes then stirred magnetically overnight at room temperature (16-24°C). The aqueous phase was prepared by dissolving a pre-weighed mass of PVA (5% w/v) or sodium alginate alginate (1, 3 or 5% w/v) in trehalose. The solution was then heated at 80°C and stirred, after which it was left to stir magnetically overnight at room temperature. Phage K was added to the aqueous phase the following day at a ratio of 1:1 (phage K to aqueous phase). The emulsion was prepared by adding dropwise the aqueous phase (with added phage K) to the organic phase at a ratio of 9:2 (organic to aqueous phase), at consistent intervals over the span of 12 minutes whilst simultaneously mixed at 1000 rpm using an overhead stirrer.

7.2.3 Culturing bacteria and phage K for release assay

7.2.3.1 Culturing of Staphylococcus aureus ATCC 6358

Approximately, 17.25 g BHI broth was dissolved in 500 ml of DI, autoclaved at 121˚C for 15 minutes and stored at room temperature. Double layer agar procedure was used as previously performed by Goh et al. (Goh et al., 2005) and Mahony et al. (Og, Af, Sygdomme, Henrik, & Epidemiologisk, 2009)

S. aureus strain was maintained in cryopreservation at -80˚C. Sterile 5 µl inoculation loops were used to streak the strain on a BHI agar plate. The plate was incubated for 24 hours at 37˚C. A single colony

of *S. aureus* was transferred via a sterile inoculation loop BHI broth and grown shaking at 37 ˚C overnight. The turbidity of the culture is indicative in liquid culture growth. Upon successful growth of culture, it was centrifuged at 13,000 x g (Beckham Coulter, UK) at 20˚C for 15 minutes. The supernatant was decanted, and the pellet re-suspended in 5 ml of SM buffer and stored in fridge.

7.2.3.2. Culturing of bacteriophage K

Isolated phage K can infect strain S. aureus ATCC 6358, therefore host is used to propagate phage for making stocks and analysis. Phage infection and replication was observed by plaque assays and spot tests using the double agar layer method. Phage propagation for developing stock was done in liquid culture. All work carried out was in aseptic conditions near a Bunsen flame or the laminar fume hood.

A freshly growing culture of *S. aureus* in BHI broth was checked for logarithmic growth by taking the optical density (OD_{550} nm at hourly intervals until it reached 0.2, after which (dependent on phage titre of stock) phage was added at a MOI of 0.01. The 50 ml tube was incubated shaking overnight at 37˚C for infection to occur. The following day the tube was removed and centrifuged at 4, 500 x g for 10 minutes. The supernatant was filtered using a 0.2 µm pore size filter (Millipore, USA) and a 25 ml syringe (BD Plastipak) into a new tube. The phage stock was stored at 4˚C until use.

The titre of phage stocks was determined by mixing soft agar and salt in a 50 ml tube in a 1:1 ratio and to make sloppy. Approximately, 10 µl of overnight *S. aureus* culture was mixed in 8 ml of sloppy and poured onto 1% BHI agar plates and left to set for 5 minutes under the laminar flow hood. To enumerate the phage titre, serial dilutions from 10^{-1} to 10^{-7}, 10 µl from each dilution (in triplicate) was spotted on host lawn. Dilutions were made of 90 µl of BHI broth and 10 µl of phage stock. The plates were incubated overnight at 37˚C. The following day, phage titre was determined by counting plaques and expressed as plaque forming unit PFU g^{-1}. The following equation was used to calculate the PFU g^{-1}, where P is the PFU g^{-1}, N is the number of plaques, D_f is the dilution factor and M (g) is the weight of the polymer.

$$P = \frac{N \times D_f}{M} \quad (1)$$

7.2.3.3. Phage release assay

For phage release assay, 10 µl of dissolved electrospun fibres in 10 ml SM buffer pH 7 was serially diluted in 96-well plate (as described in section 7.2.3.2) and was spotted on the gridded area on the agar in triplicate, left to evaporate and incubated at 37˚C overnight. The following day the plates were observed for clearance in form of lysis or plaques to indicate phage infection of bacteria and PFU g^{-1} calculated (equation 1).

7.2.4 Characterisation of emulsions

Rheology was characterised using the HAAKE Viscotester 550 Rotational Viscometer, equipped with a coaxial cylinder and kept at constant temperature (25 ˚C). The shear viscosity (η) was determined as a function of the shear rate (γ) from 10 to 200 s^{-1}. Conductivity of PVA and alginate were measured a using a conductivity meter (Omega CDH222) with an accuracy of (±3%) full scale.

7.2.5 Electrospinning process

Emulsions were added to 12 ml plastic syringe (Luer Lock syringe, Sigma Aldrich) and attached to a pump system (PHD ULTRA, Harvard Apparatus) in a horizontal setup. Emulsions were injected through a spinneret (inner diameter 0.5 mm) at a constant infusion rate (1-3 ml hr^{-1}) for a set duration (60 minutes) within a sealed chamber where the temperature (17-23 ˚C) and relative humidity (50-70%) were measured using a probe. A high-power voltage supply was used to generate an electric field (10-15 kV) inside the sealed chamber. Fibrous mats were collected on an oppositely charged rectangular copper plate, wrapped in aluminium foil and placed 15 cm from the spinneret tip (Figure 7.1). Three repeats were conducted for each sample fabricated. Fibre morphology was analysed using scanning electron microscopy (FEG-SEM, Zeiss 1530VP) by taking three images at different magnifications. Mean fibre diameters were calculated by measuring 30 individual fibres using NIH-ImageJ software.

7.2.6 Fourier transform infrared spectroscopy

Fourier transform infrared (FTIR) spectra of 3 samples of electrospun fibres were recorded using FTIR spectrophotometer (Model 20DXC, Nicolet Instrument Corp., Madison, WI. USA).

7.2.7 Statistical analysis

Statistical analysis was performed using a two-tailed unpaired Student's t-test (Excel, Microsoft 2010) to determine any statistical difference ($P < 0.05$) between data sets. Data was presented by giving the mean ± standard deviation.

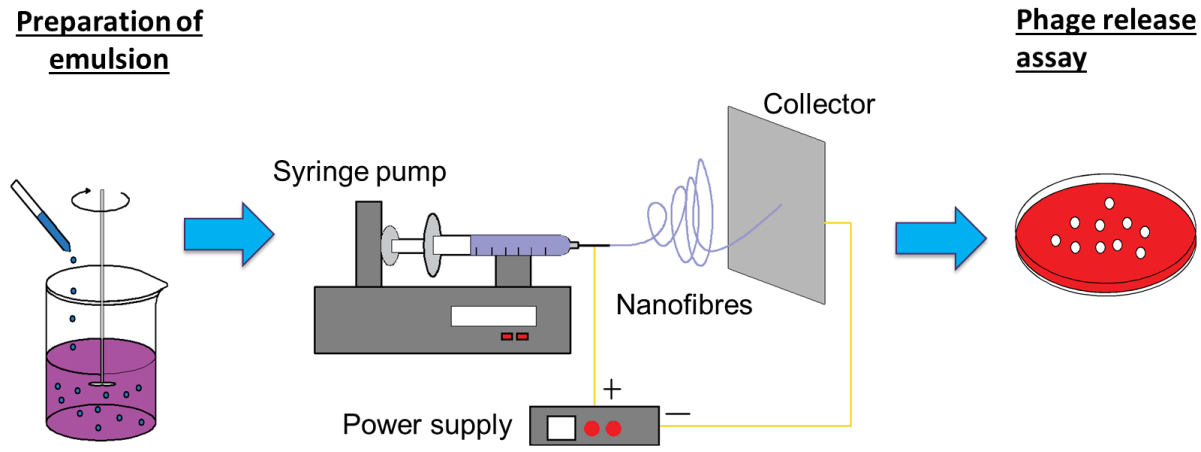

Figure 7.1 Schematic of emulsion electrospinning process for phage encapsulation.

7.3 Results

7.3.1. Determination of optimal electrospinning conditions for ES100 composite fibres

The influence of electrospinning parameters on fibre morphology have been reported for different polymer formulations. Since the fabrication of ES100-PVA and ES100-alginate fibres is novel, there were no previous reports on the influence of electrospinning parameters on the fibre morphology. Optimal conditions for producing continuous fibres was determined by testing the effect of applied voltage and infusion rate on the morphology of the fibres (Figure 7.2). The strength of the applied electric field has been reported to influence the formation of various size fibres for different polymer formulations (Sill & von Recum, 2008). Critical values for field strength varies for different polymer systems and failure in stable jet formation during electrospinning could be attributed to suboptimal field strengths (A. Haider *et al*., 2015). By increasing the voltage, the strength of the electric field at the spinneret is also increased which subsequently affects the whipping stability during electrospinning (C. Wang *et al.,* 2009). Stronger electric fields have been demonstrated to produce smaller diameter nanofibers due to increased stretching of the fibres during whipping of the charged jet in correlation with the charge repulsion within the jet (Lv *et al*., 2017).

7.3.1.1 ES100 and PVA for phage K encapsulation in electrospun fibres

Figure 7.2 shows the change in nanofiber diameter with varying voltages (10, 12.5 and 15 kV) and infusion rates (1, 2 and 3 ml hr^{-1}) for the ES100-PVA (7% w/v ES100) emulsion. The use of a two-tailed *t*-test (of 3 replicates) verifies that the difference in fibre diameter from 10 to 15 kV across all three infusion rates (1, 2 and 3 ml hr^{-1}) was significant ($P < 0.05$). Lower voltages result in larger fibre diameters, which is desirable as operating at lower voltages would decrease the likelihood of loss of phage viability. However, it was observed that electrospinning at 10 and 12.5 kV caused dripping of the polymer fluid from the spinneret tip. This was thought to be due to an insufficient voltage required to form a stabilised charged jet. Despite the increase in fibre diameter, operating at a voltage below 15 kV across all three flowrates was suboptimal, as there was significant 50 % loss of material due to partial electrospinning of the polymer solution.

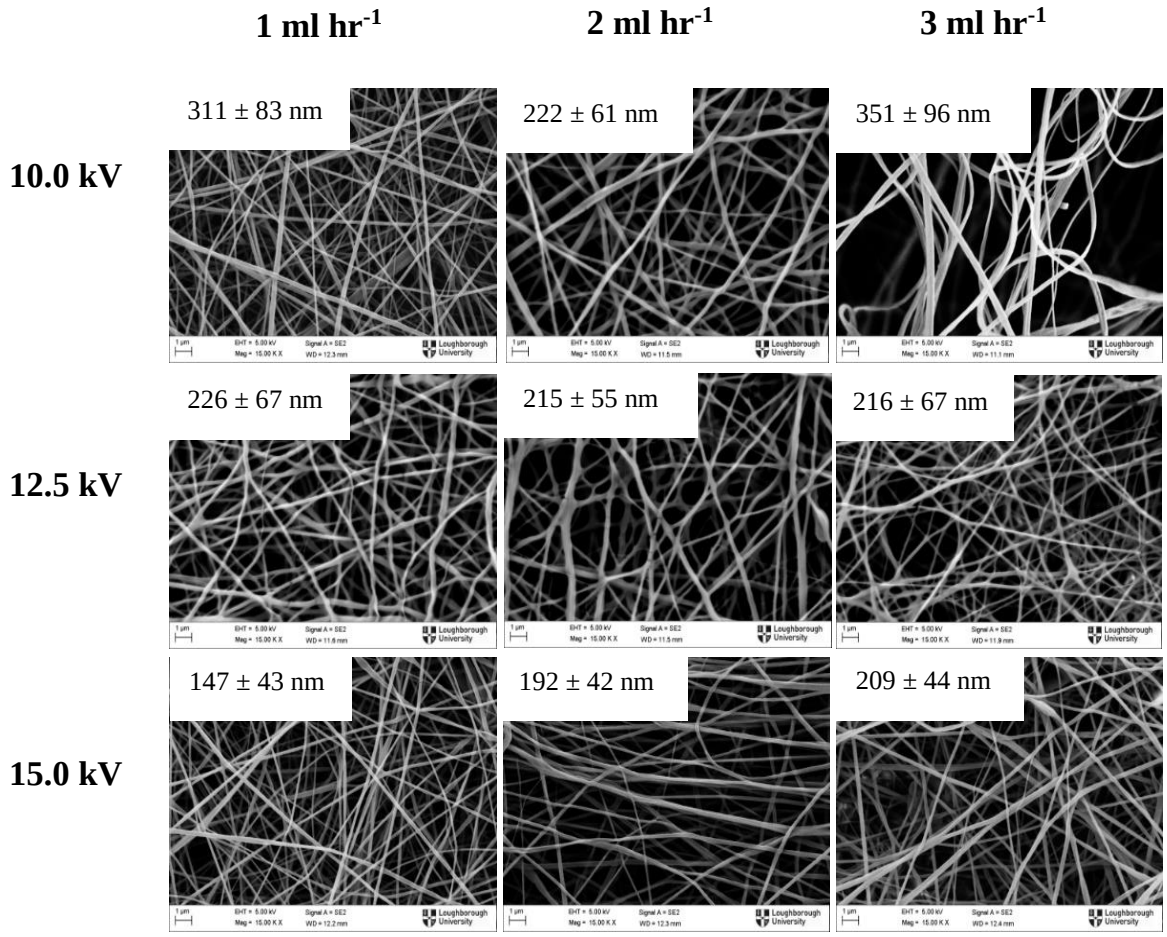

Figure 7.2 SEM micrographs of ES100-PVA (7% w/v ES100) fibres fabricated at different applied voltages (10, 12 and 15 kV) and different infusion rates (1, 2 and 3 ml hr^{-1}). Shown at magnification x15,000.

The effect of applied voltage on fibre diameter distribution was investigated for the ES100-PVA (7% w/v ES100) emulsion, (Figure 7.3). It was observed that a higher voltage produced a narrower distribution of fibre diameters across all three infusion rates (1, 2 and 3 ml hr^{-1}), which was desirable. Similar results were obtained by Huan *et al*., (2015) which could be explained by the imbalances of the three major forces influencing fibre diameter: Coulombic, surface tension and viscoelastic force. Lower applied voltages cause the surface tension to dominate over the Coulombic force, resulting in fibres with a broader diameter distribution. The three forces become balanced when the applied voltage is increased and closer to that of the optimal threshold, resulting in a narrower fibre distribution.

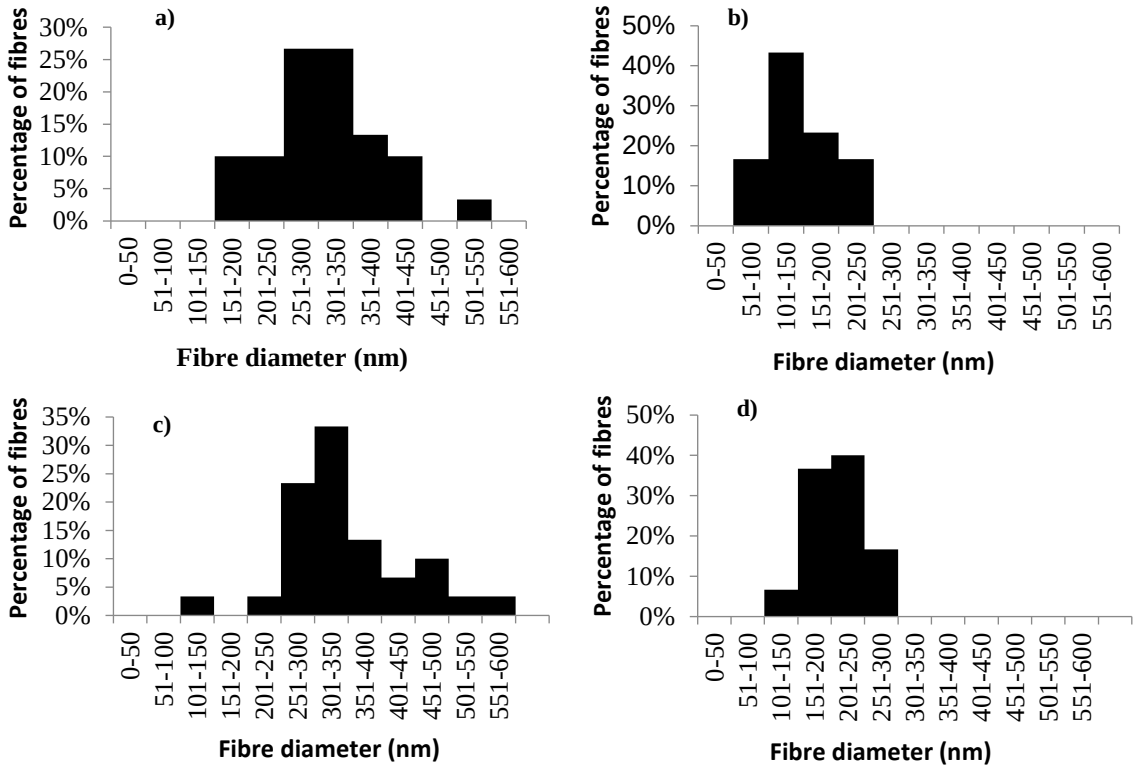

Figure 7.3 Distribution of ES100-PVA (7% w/v ES100) fibre diameters fabricated at 1 ml hr^{-1} with applied voltage of a) 10 kV and b) 15 kV. Fibres fabricated at 3 ml hr^{-1} with applied voltage of c) 10 kV and d) 15 kV.

7.3.1.2 Effect of voltage on ES100 and Alginate fibres

The effect of applied voltage on fibre diameter was investigated for the ES100-alginate (3% w/v alginate) emulsion, (Figure 7.4). Unlike the ES100-PVA fibres, the ES100-alginate fibres showed a significant ($P < 0.05$) increase in fibre diameter as the voltage was increased from 10 to 15 kV, across all three infusion rates (1,2 and 3 ml hr^{-1}). Whilst it has been discussed why an increase in voltage results in fibres with smaller diameters, it should be noted that the effect of applied voltage on fibre diameter remains unclear, with some studies reporting that an increase in voltage results in an increase in fibre diameter, for example Zhang & Yuan, (2005) showed the increase in average fibre diameter of PVA fibres with increasing voltage.

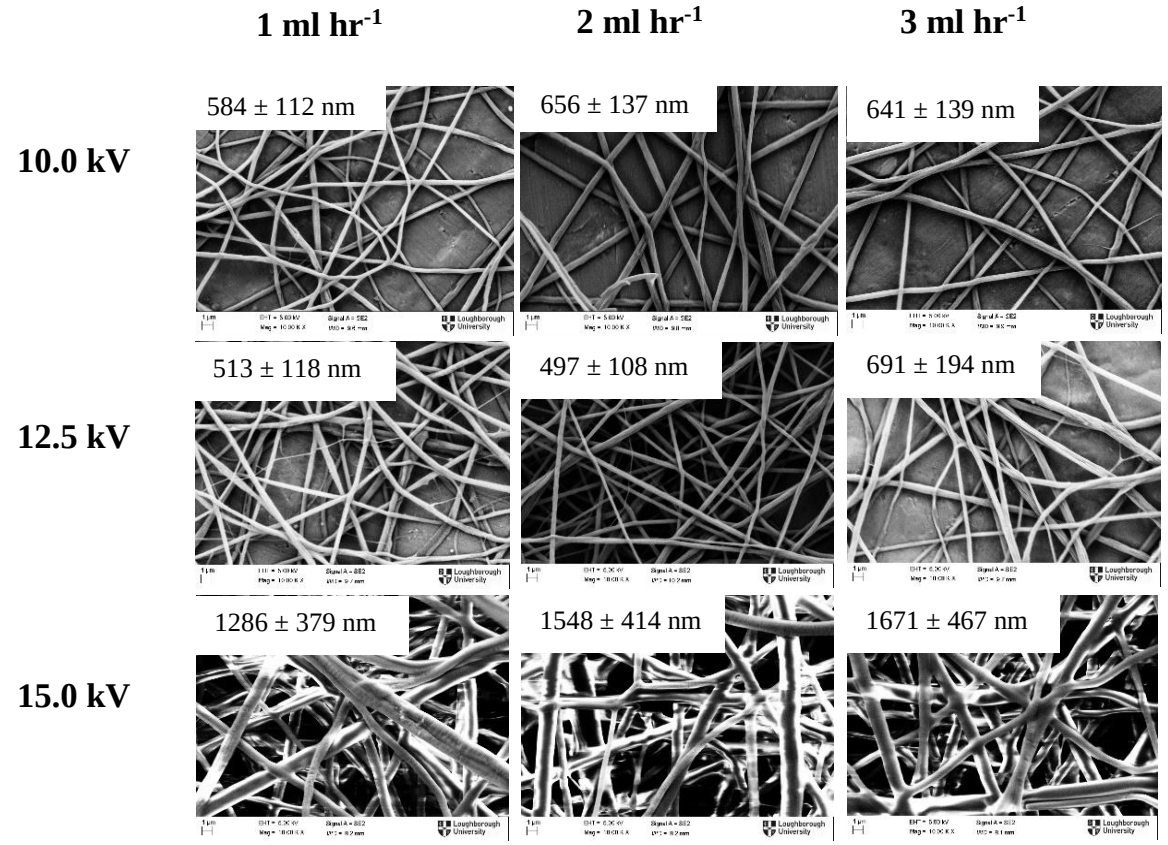

Figure 7.4 SEM micrographs of ES100-alginate (3% w/v alginate) fibres fabricated at different applied voltages (10, 12 and 15 kV) and different infusion rates (1, 2 and 3 ml hr^{-1}). Shown at magnification x10,000.

In contrast with the results obtained for the effects of applied voltage on fibre diameter distribution for the ES100-PVA fibres, it was observed that an increase in voltage resulted in a wider fibre diameter distribution for the ES100-alginate (3% w/v alginate) fibres, (Figure 7.5). Since the effect of applied voltage is determined by the three major forces, it is argued that higher applied voltages cause the

Coulombic force to dominate over the viscoelastic force. This culminates in a broader distribution of fibres, which is attributed to breakage from an over-stretched charged jet (Huan *et al*., 2015).

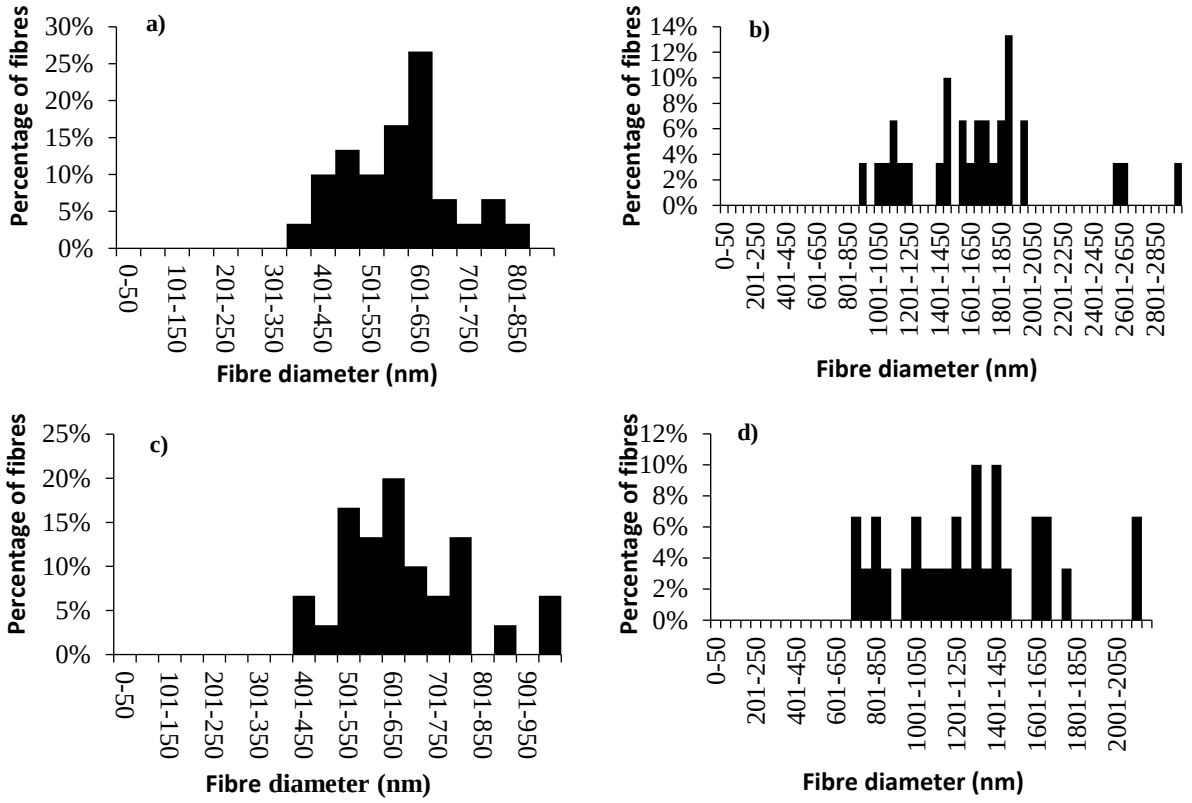

Figure 7.5 Distribution of ES100-alginate (3% w/v alginate) fibre diameters fabricated at 1 ml hr^{-1} with applied voltage of a) 10 and b) 15 kV. Fibres fabricated at 3 ml hr^{-1} with applied voltage of c) 10 kV and d) 15 kV.

Figure 7.2 illustrated that an increase in infusion rate significantly ($P < 0.05$) increases the fibre diameter for the ES100-PVA (7% w/v ES100) emulsion when operating at an applied voltage of 15 kV, but inconclusive ($P > 0.05$) when operating at 10 and 12.5 kV. It can be hypothesised that the jet was more stable when operating at 15 kV for this polymer system. This allowed for the effect of infusion rate on fibre morphology to become more apparent. It was observed that whilst operating at flowrates of 2 and 3 ml hr^{-1}, dripping of polymer fluid from the spinneret tip occurred. This may be attributed to the incomplete drying of charged jet.

The ES100-alginate (3% w/v alginate) fibres were observed to significantly increase ($P < 0.05$) in fibre diameter as the infusion rate increased from 1 ml hr^{-1} to 3 ml hr^{-1}, across all three applied voltages (10, 12.5 and 15 kV), (Figure 7.5). This indicated that the morphology of the ES100-alginate fibres was more influenced by infusion rate across a wider range of investigated applied voltages, compared to the ES100-PVA fibres. The effect of fibre diameter distribution was investigated for both polymeric emulsions, but it was concluded that the infusion rate had a minor impact on narrow fibre diameter distribution. High flowrates may cause the charged jet to become unstable and electrospray due to the pull of gravitational force, leading to a wider fibre diameter distribution (Zargham *et al.*, 2012).

Like the ES100-PVA fibres, operating at an infusion rate of 2 ml hr^{-1} or 3 ml hr^{-1} led to dripping of the polymeric fluid from the spinneret tip. This indicated that for both systems, operating at these two flowrates was suboptimal and lead to a loss of material. It was thought that a low infusion rate was generally preferred for polymer systems to sustain a balance between the withdrawing polymer fluid and the substitution of that fluid with fresh fluid during formation of the charged jet (Zeleny, 1935).

7.3.2. Development and characterisation of emulsion formulations

To observe the effects of viscosity on the production of fibres, concentrations of alginate and ES100 were changed and the effect on fibre diameter observed (Figure 7.6 and 7.7).

7.3.2.1 ES100 and alginate for phage K encapsulation in electrospun fibres

Alginate has been utilised for a range of biomedical applications and it is one of the most common materials used in microencapsulation (Colom *et al*., 2017a), making it a promising material for this work. The charge repulsions among the alginate chain debilitates the ability to electrospin pure alginate in water unless it is blended with a co-polymer such as PEO (Bhattarai *et al.*, 2006), thereby alleviating the charge repulsions and enhancing chain flexibility (Bonino et al., 2011). ES100-alginate emulsions with different concentrations of alginate (1, 3 and 5 % w/v) were electrospun to observe what effects the concentration will have on the emulsion viscosity and subsequent fibre diameter, (Figure 7.6). An increase in viscosity accompanied an increase in alginate concentration across all three concentrations. The mean fibre diameter increased from (588 ± 190 nm) (1 % w/v) to (1548 ± 414 nm) (3 % w/v), which was thought to be due to the increase in viscosity leading to an enhanced chain flexibility for electrospinning. Contrastingly, the mean fibre diameter decreases with an increasing alginate concentration from 3 % w/v (1286 ± 379 nm) to 5 % w/v (839 ± 250 nm). This may be due to the viscosity beyond the optimal threshold of the polymer system. It was observed that during

electrospinning of the 5 % w/v alginate and ES100 emulsion, the fluid started to dry at the spinneret tip, indicating that the viscosity was too high.

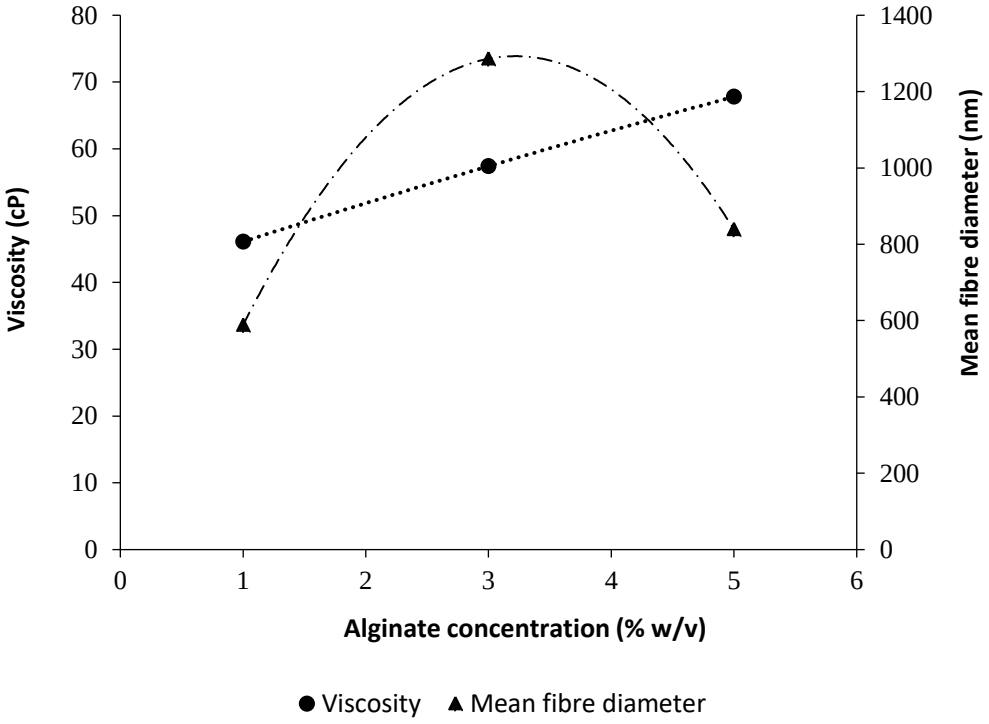

Figure 7.6 Effect of alginate concentration on viscosity and fibre diameter for ES100-alginate (3% w/v alginate) fibres fabricated at 1 ml hr^{-1} and 15 kV.

7.3.2.2 ES100 and PVA for phage K encapsulation in electrospun fibres

Similarly, the concentration of ES100 was increased to observe what effects it will have on fibre morphology. Upon increasing the ES100 concentration from 7 % w/v to 10 % w/v, the ES100-alginate emulsion (3 % w/v alginate) fails to electrospin due to the fluid drying off at the spinneret tip, suspected to be to a viscosity far exceeding the optimal threshold of the system. In contrast, the ES100-PVA fibres experience an increase in fibre diameter upon increasing ES100 concentration, (Figure 7.7). The ES100 concentration has the greatest impact on fibre diameter when compared to the effects of applied voltage and infusion rate as the fibre diameter increases almost 20-fold when increasing the ES100 concentration from 7 % w/v (147 ± 43 nm) to 15 % w/v (2914 ± 935 nm). Notably, the largest incremental increase of fibre diameter occurs from 10 % w/v (525 ± 123 nm) to 15 % w/v (2914 ± 935 nm), where the largest increase in viscosity also occurs (115 to 518.5 cP) (Figure 7.2). However, it was observed that some drying of the jet occurred at 15 % w/v ES100, once again

suspected to be because of high viscosity. This also affected the stability of the jet, as the relative standard deviation of fibre diameters was highest for the 15 % w/v ES100 emulsion, whereas the lowest relative standard deviation was for the 10 % w/v ES100 emulsion, indicating enhanced jet stability at that viscosity.

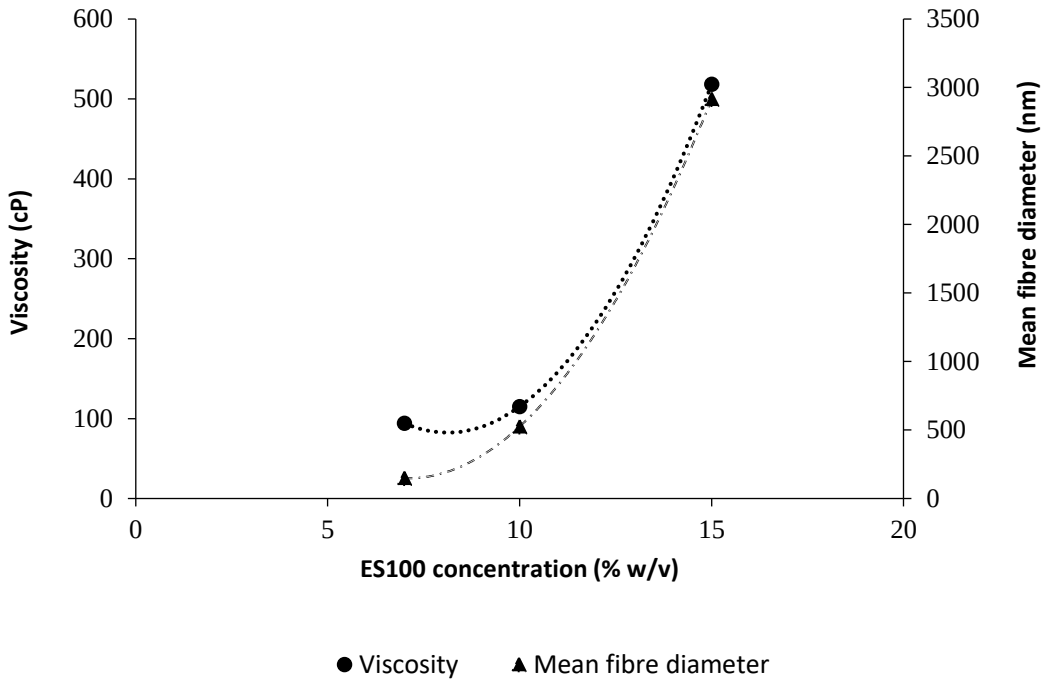

Figure 7.7 Effect of ES100 concentration on emulsion viscosity and fibre diameter for ES100-PVA fabricated at 1 ml hr^{-1} and 15 kV.

7.3.2.3 Polymer conductivity

Table 7.3 Conductivity of PVA and different alginate concentrations in DI.

Material	Concentration (% w/v)	Conductivity (mS cm^{-1})
Alginate	1	2.39 ± 0.60
	3	6.21 ± 0.60
	5	8.95 ± 0.60
PVA	5	0.37 ± 0.06

The conductivity of different alginate concentrations (1, 3 and 5 % w/v) and 5 % w/v PVA solution were compared to determine how the fibre morphology was influenced. Data in Table 7.3 illustrates that an increase in alginate concentration accompanies an increase in conductivity. Notably, the conductivity of alginate across all three concentrations was higher than PVA, which was thought to be a contributing factor to why the ES100-alginate fibres have a larger diameter than the ES100-PVA fibres. This may be because the higher conductivity expressed in the alginate solutions are closer to the optimal conductivity of the emulsion system; allowing for greater polymer surface charges for Coulombic forces to dominate leading to enhanced stretching of the fibres. This was only true to a certain extent, as when the alginate concentration was increased from 3 to 5 % w/v, the mean fibre diameter experiences a decrease, as previously shown in Figure 7.6. This could be explained by the large conductivity value at 5 % w/v (8.95 ± 0.60 mS cm^{-1}), which was hypothesised to be at a critical value which increases the surface charge on the polymer droplet to such an extent that it decreases the tangential electric field which weakens the electrostatic force on the surface of the polymer fluid (A. Haider et al., 2015). As a result, formation of the Taylor cone was affected, and thinner fibres are formed.

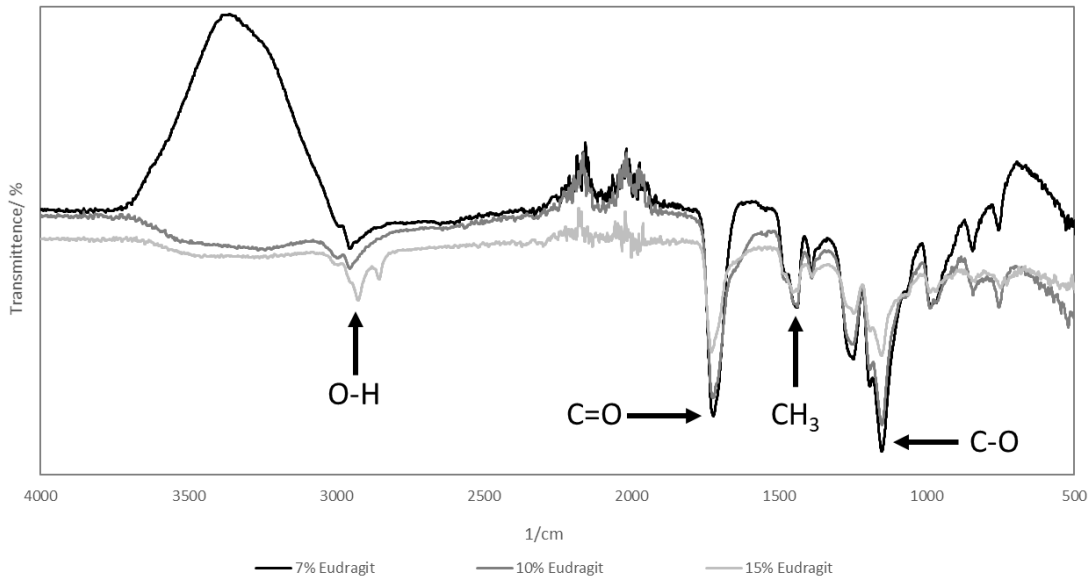

Figure 7.8 FTIR analysis of Eudragit and PVA electrospun fibres with varying Eudragit concentrations (7 %, 10 %, 15 %). Eudragit functional groups (O-H, C=O, CH_3, C-O) are labelled.

Fourier-transform infrared spectroscopy (FTIR) spectra of the ES100 and PVA fibres is presented in Figure 7.8. Due to the very low concentration of PVA in comparison to ES100, the FTIR spectrum can be attributed to the functional groups found in the ES100 structure. Fibres produced from emulsion with varying concentrations of ES100 were analysed. The spectra for all concentrations showed a similar profile confirming the presence of ES100, however the transmittance levels differ slightly which is due to higher density of polymer made with emulsion containing higher ES100 concentration. Fibres produced from the lowest ES100 concentration (7% w/v) showed a broad peak between 3000 and 3700 cm^{-1} this is explained by exchangeable protons; a compound contains many hydrogen bonds which are bonded to a different extent. Therefore, when IR absorption is acquired, varying frequencies for this bond will occur.

Peak at 2925 cm^{-1} demonstrated the presence of carboxylic acid (O-H), at 1720 cm^{-1} showed the presence of ester bond (C=O). In the fingerprint region, at 1149 cm^{-1} carbonyl group (C-O) stretch was observed as well as a methyl group bend at 1440 cm^{-1}. The FTIR analysis concluded that fibres are largely made of ES100 with concentrations of PVA being negligible and phage showing no structural impact on fibres.

7.3.3. Encapsulation and release of phage K in ES100 and PVA fibres

Having optimised the fibre morphology by testing a range of different electrospinning and developing the emulsion formulations, phage K was encapsulated in ES100-PVA fibres to determine the viability of the phages before and after electrospinning. Encapsulation of phage K was not pursued for ES100-alginate fibres for this report. This was attributed to poor reproducibility of the ES100-alginate fibres, as on occasions during repeats of the experiment, the thickness and distribution of the fibres varied significantly from the previous results.

7.3.3.1 Effect of applied voltage on phage viability during encapsulation

Phage K was encapsulated in three different ES100-PVA (7 % w/v ES100) fibrous mats, fabricated at three different electrospinning conditions. Mat 1, fabricated at 3 mlh^{-1} and 10 kV was selected for encapsulation because it produced fibres with the largest mean diameter (351 ± 96 nm), as previously shown in Figure 7.2. Mat 2 fabricated at 2 ml hr^{-1} and 12.5 kV (215 ± 44 nm) was selected to serve as an intermediate between the two extreme electrospinning parameters for comparative purposes. Mat 3, which previously produced the thinnest fibres (147 ± 43 nm) and fabricated at optimal electrospinning conditions of 1 ml hr^{-1} and 15 kV was used to compare phage viability between the thickest and thinnest fibres. Figure 7.9 shows the phage release viability for the ES100-PVA (7% w/v ES100) fibres by comparing the initial titre with the release titre after encapsulation. Mat 1 yields the highest phage viability after release, as there was only a two-log reduction in phage viability. This was likely attributed to the large diameters of the fibres offering enhanced phage protection from the harsh electrospinning conditions.

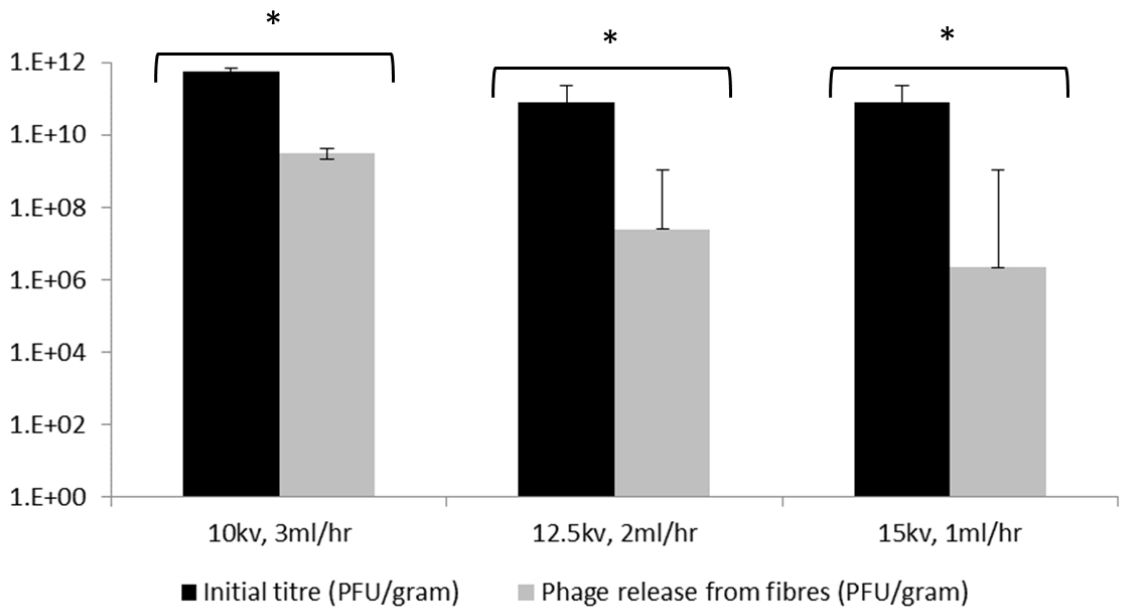

Figure 7.9 Viability of phages before and after 24 hours of encapsulation for ES100-PVA (7%w/v ES100) fibres fabricated at different electrospinning parameters. * indicates significantly different phage titres ($p < 0.05$) for a 2-sample t-test with each sample compared with initial titre released in pH 7 for each parameter.

7.3.3.2 Effect of polymer concentration on phage viability in electrospun fibres

The phage viability was assessed for ES100-PVA fibres fabricated using different ES100 concentrations (7, 10 and 15 % w/v) at optimal electrospinning conditions of 15 kV and 1 ml hr^{-1}. Figure 7.10 illustrates the phage viability for the different ES100 concentrations before and after electrospinning. Fibres fabricated using 15 % w/v ES100 (2914 ± 935 nm) yield a four-log reduction in phage viability and therefore did not offer improved phage protection when compared to fibres fabricated at 7 % w/v ES100 (147 ± 43 nm). This is thought to be attributed to the drying of the jet at the spinneret tip arising from the emulsion's high viscosity, thereby affecting the extent of successful encapsulation. The phages ability to lyse bacteria may also have been hindered at such a high viscosity. Fibres fabricated at 10% w/v ES100 (525 ± 123 nm) offered the most promising results, as it produces a three-log reduction in phage viability. This could be to an amalgamation of effects arising from the thickness of the fibres, offering improved protection, and the stability of the jet at that concentration, offering improved encapsulation. However, it does not offer improved protection compared to the ES100-PVA (7 % w/v ES100) fibres fabricated at 10 kV and 3 ml hr^{-1}, therefore inferring that the fibres' large diameters do not completely mitigate the harmful effects of a higher applied voltage on phage viability. Whilst the phage viability is not as high as the viability reported by Korehei and Kadla [18], it still offered a higher viability compared to previous work by Salalha *et al*., (2006), where 1% of phages remained viable after encapsulation.

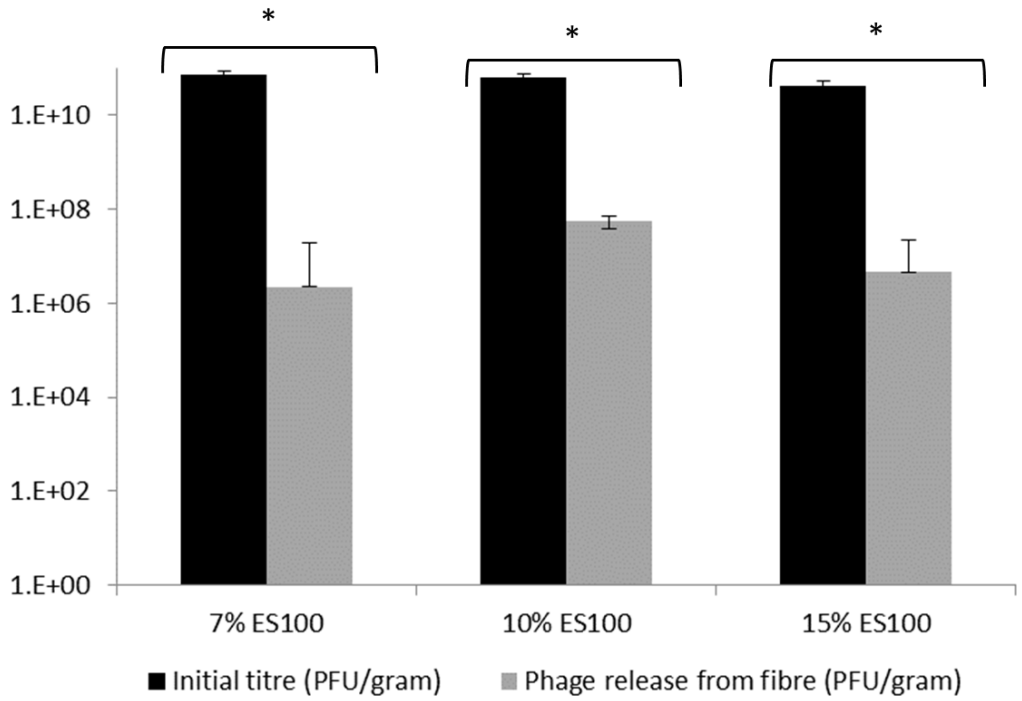

Figure 7.10 Viability of phages before and after 24 hours of encapsulation for ES100-PVA fibres fabricated at different ES100 concentrations. * indicates significantly different phage titres ($p < 0.05$) for a 2-sample t-test with each sample compared with initial titre released in pH 7 for each parameter.

7.4 Discussion

Defect-free, continuous fibres with large diameters are desired for phage encapsulation as they allow for a slower release rate of phages by hindering polymer chain unfolding and disentanglement (Reza Korehei & Kadla, 2014), thereby improving phage viability. A narrow fibre diameter distribution is also preferred as it promotes a controlled release rate of phages because each fibre would take approximately the same amount of time to dissolve. Electrospinning parameters, including applied voltage and infusion rate have been previously reported to influence electrospun nanofiber morphology. In addition to electrospinning parameters, solution parameters, including viscosity and conductivity, which are dependent on the polymeric concentration have also been reported to influence fibre morphology (Fong *et al.*, 2001). In this work, different process conditions were tested using the ES100-PVA and ES100-alginate emulsions to determine the optimal conditions to achieve defect-free, continuous fibres with large diameters to facilitate the encapsulation of phage K. After encapsulation, the release of phage K was evaluated using plaque assays.

The variations in fibre diameter could be attributed to the use of different polymer and solvent systems, which respond differently to each parameter. Baumgartner *et al.*, (1971) reported an

increase in fibre diameter with increasing voltage, which was thought to be due to a longer charged jet length. The increase in fibre diameter has also been reported to be attributed to an increase in jet velocity for the same infusion rate, due to a decrease in the size of the Taylor cone (A. Haider *et al*., 2015).

Similar to applied voltage, the infusion rate has also been reported to influence the fibre diameter and porosity of electrospun nanofibers. Megelski, (2002) reported an increase in fibre diameter with increasing flowrate, which was thought to be due to incomplete drying of the charged jet during flight to the collector plate. Wang *et al*., (2009) attributed the increase in fibre diameter with increasing infusion rate to the expansion of the Taylor cone which produced a longer and wider charged jet.

Like the ES100-PVA fibres, ES100-alginate operating at an infusion rate of 2 ml hr^{-1} or 3 ml hr^{-1} led to dripping of the polymeric fluid from the spinneret tip. This indicated that for both systems, operating at these two flowrates was suboptimal and lead to a loss of material. It was thought that a low infusion rate was generally preferred for polymer systems to sustain a balance between the withdrawing polymer fluid and the substitution of that fluid with fresh fluid during formation of the charged jet (Zeleny, 1935).

Having established the effects of the electrospinning parameters on fibre morphology, the next stage was to develop and characterise the emulsion formulations that could enhance phage K viability by changing the concentration of the organic and aqueous phase. Phage K was stored in buffer or broth which was not miscible with solvents therefore when producing an emulsion for electrospinning, phage K was added to the aqueous phase.

It has been previously reported that increasing the concentration of polymer in a polymer solution will also increase the viscosity of that system, leading to a greater number of chain entanglements in the polymer chains (A. Haider *et al*., 2015). The fabrication of defect-free, continuous fibres is determined by the number of chain entanglements in polymer systems, which are required to overcome the surface tension of the fluid. Polymer systems with dilute concentrations, low viscoelasticity or with a low molecular weight will have insufficient entanglements and therefore not meet the critical chain entanglement threshold required for the production of continuous fibres (Yu *et al*., 2006). Like the applied voltage and infusion rate, exceeding the concentration beyond a critical value could result in the fabrication of defective fibres. This is because the polymer fluid dries off at the spinneret tip, which restricts the flow of the fluid and extent of subsequent whipping (S. Haider *et al.*, 2013).

Whilst an increase in viscosity is generally preferred as it leads to thicker fibres, it has also been reported that the ability for phages to lyse bacteria declines with increasing solution viscosity (Hanlon *et al.*, 2001). Fabricating thicker fibres for phage encapsulation should therefore not rely solely on increasing the concentration of the polymer system, as the viscosity increase may hinder phage viability.

Phage encapsulation results agree with those reported by Korehei and Kadla (2014), who also reported a two-log reduction in phage viability using emulsion electrospinning. In contrast, Mat 3 exhibited a four-log reduction in phage viability, which could be attributed to smaller fibre diameters offering less phage protection. Another factor for consideration was that phages are approximately 200 nm in length from head to tail; therefore, the decrease in viability may also be attributed to the fibres being insufficient in size to accommodate the encapsulation of phages. Finally, Mat 2 yielded a three-log reduction in phage viability after release, which was expected because it was fabricated at intermediate electrospinning parameters.

7.5. Conclusions

This data serves as proof-of-concept study for the encapsulation of phage K in core-shell emulsion electrospun fibres for novel wound dressing applications. Two different w/o emulsion formulations were prepared using pH-responsive ES100 as the organic phase (forming the fibre shell) and PVA or alginate as the aqueous phase (forming the fibre core). Defect-free, continuous nanofibers with large diameters were fabricated by determining the optimal electrospinning parameters for each emulsion, followed by development and characterisation of each emulsion formulation to facilitate encapsulation and viability of phage K.

SEM micrographs revealed that changes in applied voltage and changes in infusion rate had a significant effect ($P < 0.05$) on fibre morphology for both emulsions. Higher applied voltages resulted in a wider fibre diameter distribution for the ES100-alginate fibres, and a lower distribution for the ES100-PVA fibres. Observations during the electrospinning process revealed that operating at an applied voltage below 15 kV and at an infusion rate greater than 1 ml hr^{-1} led to dripping of the polymer fluid from the spinneret tip rendering these conditions as suboptimal. Rheology and conductivity characterisation revealed that an increase in ES100 or alginate concentration resulted in a higher

viscosity and conductivity, ultimately yielding thicker fibres. Increasing the alginate concentration only increased the diameter of ES100-alginate fibres up to a critical threshold. Fabrication of ES100-alginate fibres led to poor reproducibility, therefore phage K encapsulation was done using ES100-PVA fibres.

Phage K was successfully encapsulated by suspension in the aqueous phase in different ES100-PVA fibres fabricated at a range of process conditions. Phage viability assays revealed that larger diameter fibres and lower applied voltages offered improved phage viability as reported for fibres with a mean diameter of 351 ± 96 nm (fabricated at 10 kV) which resulted in a two-log reduction in phage viability, whilst fibres with a smaller mean diameter of 147 ± 43 nm (fabricated at 15 kV) resulted in a four-log reduction in phage viability. Phage viability was improved whilst operating at 15 kV by increasing the ES100 concentration from 7 to 10% w/v, as this resulted in a three-log reduction in phage viability. The improved phage viability may be attributed to an increase in fibre diameter (525 ± 123 nm) and enhanced jet stability. However, it does not completely mitigate the harmful effects of the higher applied voltage on phage viability. Future work should focus on further optimising the ES100-alginate fibres so that good reproducibility can be established for encapsulation work.

Chapter 8: Conclusions

8.1 Key motivations

This work aimed to develop a novel formulation for the application of phage therapy. Use of phages has been active since its discovery in 1915 (Abedon et al., 2016). However, little work has been done to develop formulations and techniques which can help protect phage from biological and environmental stresses during its administration. More specifically, phage therapy against enteric pathogens remains challenging due to transit through the GI-tract to reach the small and large intestine. Several factors impact on phage survival through the digestive tract, a key one being the acidity of the stomach which can range from pH 1-2.5 depending on fed or fasted state in humans (McConnell *et al*., 2008). In animals on the other hand, the pH of the stomach is around pH 2.5 which has been the focus of many studies to date for phage encapsulation that mainly focus on biocontrol in animals.

8.1.1 Formulation development for targeted delivery of phage

This study has focused on developing a novel formulation for phage encapsulation and protection against stomach acid ranging from pH 1-2.5. A commercially available polymer, Eudragit S100 and alginate were used for their pH responsive properties and bio-compatibility. Both alginate (Colom et al., 2017b; S. Kim et al., 2015b; Yongsheng Ma et al., 2008, 2012) and Eudragit (Stanford *et al*., 2010a) have previously been used for phage encapsulation and demonstrated protection at pH 2.5 however little work has been done to study both together.

The technique used for encapsulation plays a key part in how effectively the phage is protected from acidic pH (usually below pH 3). In all studies reported so far, despite some degree of acid protection a significant loss (more than 1-log) in phage titre was observed at pH 2 (Ma *et al.*, 2008, 2012; Kim, Jo and Ahn, 2015b). Microfluidics was used for the development of uniform droplets containing phage in composite polymers blends. This technique allowed exquisite control over droplet production, by varying experimental parameters immediate change in drop diameter was observed. The resulting particles showed excellent monodispersity with CV below 1 %. Through developing this process and formulation, phage encapsulation could be fine-tuned to produce microparticles varying in size which may be targeted for specific sites of the intestines. Size can also effect the residence time in the GI-tract, where shortened transit times are observed during infection due to the onset of diarrhoea.

The combination of Eudragit and alginate was investigated further to provide phage protection at pH 1 for up to 2 hours without the aid of antacids. Here, the size of the microparticles influenced the level of acid protection which previously has not been reported. This highlighted the need for better control over particle size to provide the optimum protection against stomach acid. Smaller particles were more prone to acid attack; conventional techniques used for particle production offer little control over size which can result in a low phage yield post acid exposure. Therefore, a balance needs to be achieved between delivering a high phage dose and remaining at the site of infection long-enough to induce a positive effect.

Transferability of phage encapsulation from the in-house fabricated device to a commercial chip was demonstrated. This enables reproducibility of the system in most commercially available chips showing that the process was well-defined and controlled as opposed to dependent on mechanical processes with little control and no standardisation.

8.1.2 Scaling up phage encapsulation process

When considering phage therapy, multiple dosing (taking phage more than once), transportation, long-term storage and reproducibility are all factors which need to be considered. pH-responsive microparticles produced via microfluidic devices showed the potential use of the process in phage therapy of enteric infections. However, a key concern would be the production volume of encapsulated phage which was considerably low using microfluidic platforms. Multiple capillaries running parallel are a possible route for process scale-up. However, the material used (quartz glass) to produce these chips, can quickly add to the up-scale cost. Therefore, alternative methods were exploited, one being membrane emulsification which has the ability to produce material in litres as opposed to millilitres with capillary devices. A combination of both Eudragit and alginate were still used to produce water-in-oil droplets. A larger volume (50 ml) of encapsulated phage was produced which also presented the acid protection as seen with the microfluidic technique.

Less than 0.5-log loss in phage titre upon exposure to pH 2 and 2.5 was observed, phage release in SIF (pH 7) and pH 5 and 6 were also investigated. To date no reports have shown the release of encapsulated phage at pH lower than 7. This is an important consideration when aiming at site-specific delivery of encapsulated phage. In addition to loss in titre during exposure to stomach acid, phage is prone to release during transit through the GI-tract. Transcending through the digestive tract, pH begins to rise reaching neutral or pH 7.4 in the colon (Evans et al., 1988). At sites where the pH is 5 or 6, the pH responsive properties of polymers begin to engage, slowly dissolving due to the presence of

hydroxyl ions. This releases the phage prematurely, an important parameter which needs further investigation.

Although phage amplify in the presence of their host, they have been shown to arrest bacterial growth more effectively if the initial phage titre is high. Results demonstrated the effect of phage titre on arresting actively growing bacteria, initial low titre (10^2 PFU/ml) phages were able to catch up with bacterial killing as seen with a high titre of phage (10^8 PFU/ml). Despite this, the state of bacterial growth during infection may be different, actively growing bacteria as found *in vitro* may not necessarily translate to the *in vivo* setting. Therefore, phage-bacterium killing during various stages of bacterial growth are necessary to test the effect of encapsulation and dosing for phage therapy.

An *ex vivo* model was used to examine the three-way interaction of epithelial cells, bacteria and phage. Bacterial killing by encapsulated phage previously exposed to pH 2 for 2 hours showed growth arrest and prevented further damage to epithelial cells. The results were comparable to free phage which was used as the positive control. Complete loss of actin cytoskeleton and nuclei shrinkage was observed where no phage was added. Studying phage in the presence of epithelial cells, to observe any interaction which may prevent phage-bacterial killing or cause further distress to epithelial cells is key. Phages have previously been reported to elicit an immune response (Loc-Carrillo & Abedon, 2011) therefore evaluating its response in an *ex vivo* model is a useful tool in determining the best phage for therapy.

8.1.3 Encapsulating phage for long-term storage and ease of manufacture

A second method for scaling-up the production of encapsulated phage, commonly used in industry is spray drying. Production of dry powder phage products can be a useful tool in by-passing several downstream processing steps such as freeze drying. Phage has been reported to be spray dried in several sugar excipients aimed for pulmonary delivery (Vandenheuvel *et al.*, 2013; Leung, *et al.*, 2017). However, only one study has reported the use of Eudragit polymer for phage encapsulation (Stanford *et al.,* 2010) where Ephage was exposed to pH 3 for 20 mins. Phage encapsulation in Eudragit and alginate were investigated here with added trehalose for preservation of phage during storage. Acid exposure to pH 2 for 2 hours showed phage survival with less than 0.5-log reduction in titre.

Addition of alginate improved phage survivability during acid exposure but the increased loss during the spray drying process led to Eudragit and trehalose being used in combination only. Powder production yields during spray drying were improved with the addition of Eudragit which showed yield of 50 % on its own. For large scale production, product loss can be costly however in this case Eudragit shows promise in mass producing encapsulated phage. Trehalose provided sufficient phage protection

from desiccation and elevated temperatures encountered during spray drying. Without the addition of trehalose, phage yields were significantly low indicating there is a need to combine excipients for optimum dry powder phage production. A downside to the use of spray drying as opposed to other techniques is the need for high temperatures, which need to be tackled by careful formulation.

Powders are susceptible to environmental changes and can quickly change state depending on moisture and temperature which can damage the entrapped phage. Trehalose has a high glass transition temperature in its amorphous form, therefore it was a good excipient to use for phage encapsulation. For ease of consumption in phage therapy, tablets were produced from dry powder phage. Addition of lubricating and binding agents is common practice in tablet production therefore; magnesium stearate was added to improve tablet disintegration and friability. No effect of magnesium stearate on phage viability was observed indicating that dry powder phage products can be tableted, and blister packed for manufacture and shipment. Although further work to improve tablet friability is required, this study marked an important first-step towards designing a process for phage-tablet production. Similarly, dry powder phage may be added to animal feed to reduce bacterial loads in swine and poultry. Previously, free phage has been reported to reduce bacterial load in farm animals (R. J. Atterbury et al., 2007; Robert J. Atterbury et al., 2005) however by administering encapsulated phage a higher phage titre will be delivered to the lower GI-tract allowing for better biocontrol (Yin-hing Ma et al., 2014).

Long-term phage storage was aided by the presence of trehalose in the formulation, no loss in phage was observed for powders stored at 4°C but at 30°C with 65 % RH significant loss in phage titre was observed. Transportation of phage products to developing countries may result in exposure to elevated temperatures and humidity which can affect phage viability and dosing. To avoid significant losses in phage titre, concentration of excipients such trehalose need to be evaluated to improve survivability in more realistic conditions.

8.1.4 pH responsive delivery of phage in smart wound dressings

Use of Eudragit as a phage carrier was further probed by producing phage encapsulated fibres for wound dressings. Chronic wounds require multiple dressings to aid healing or to treat infections caused by pathogenic bacteria (Mele, 2016). Phage therapy to treat wound infections has been reported (Rose et al., 2014). Previous attempts at electrospinning phage have used polymers such as PVP and PVA which exhibit a non-specific release (Koo et al., 2016; R. Korehei & Kadla, 2013; Reza Korehei & Kadla, 2014; Salalha et al., 2006). Eudragit fibres encapsulating phage were produced in an emulsion electrospinning process using phage K.

pH-triggered release of Eudragit fibres ensures that the phage is released in the presence of infection, when the pH of infected wound changes from slightly acidic (pH 5.5) (healthy skin) to neutral or even alkaline. To ensure a high titre of phage is directly delivered in proximity to the pathogen, fibres with large diameter were produced (up to 1 µm) to improve phage encapsulation. Nano-fibres in the region of 200 nm expose phage to environmental stresses during encapsulation which can result in low phage yield. Morphology of the phage can play a crucial role in determining effective encapsulation since tailed phage equal the size of the nano-fibre diameter and cannot be effectively encapsulated.

The conventional method of directly spraying phage for biocontrol as reviewed by Hussain *et al.*, (2017) can have a limited effect. Loss of phage during spraying onto the target area can lessen the effect of phage in reducing bacterial load. Similarly, soaking scaffolds in phage suspensions before application on wounds can potentially lower phage dosing due to the random distribution of phage, leading to ineffective wound healing with possibility of bacteria developing resistance. Targeting phage close to the pathogenic bacteria in a wound can help decrease the need for changing dressings which can be costly. Phage encapsulation in Eudragit fibres is a promising step forward in exploring effective application of phage treatment in wounds.

8.1.5 Contribution to knowledge

This work has formed the first steps in engineering the effective application of phage therapy of humans and animals. The formulations explored here are transferable to diverse types of phage, although each phage needs to be tested individually for its suitability to the polymers. Encapsulation of phage using various techniques has shown the potential use of available technologies in phage encapsulation which previously had not been explored. Protection from acidic pH as low as pH 1 has been reported for the first time for a period of 2 hours; a crucial step in ensuring phage is protected during exposure to stomach pH. Consideration of particle size has been reported and its impact on phage protection and release kinetics. Additionally, Ephage-bacterial killing in the presence of epithelial cells demonstrated that encapsulation was as effective as free phage *in vitro*. This study forms the basis of several exciting future projects which can enhance the application of phage in biocontrol and therapy.

8.2 Future work

This section provides recommendations for future work based on the results obtained in the PhD research.

8.2.1 Microfluidic platforms for phage encapsulation

Further development of the formulation researched here can incorporate the encapsulation of SYBR-gold labelled phage. This can be a useful tool in studying the distribution of phage in microparticles. Release of phage from microparticles during dissolution could be followed using labelled or fluorescent phage to gain a better insight into release kinetics. Changing from a 2-phase capillary system to a 3-phase may be beneficial as the phage can be introduced through the most inner capillary whilst the polymer solutions engulfs this phase during drop formation in oil phase. This method will ensure the phage does not get exposure to any acid in the oil phase and avoid the loss of any phage viability during this process. Furthermore, phage will be entrapped within the core of the microparticle which can improve the acid protection in SGF.

To test the versatility of the process, multiple phages against different pathogenic strains can be encapsulated together. This way compatibility of each phage to the formulation can easily be tested and changed. Multi-shell microparticles can also be fabricated by producing drop-in-drop emulsions where each layer can be stripped off at various stages of the GI-tract. This is especially useful in broilers where the pH of the crop is pH 4. Therefore, to prevent dissolution, a sacrificial shell may be introduced to avoid premature release. Similarly, alternate polymer drops containing different phage may be encapsulated at the same time since each phage may behave differently to the same formulation.

8.2.2 Scale-up of phage encapsulation

To further improve and develop the current ME process, different ME systems can be used such as oscillating membrane. Using an oscillating ME system can help gain better control over droplet size by avoiding the use of paddle stirrers. Although changes to the current system can also be made by using a different metal-film membrane which can offer better surface properties and porosity that may aid in the development of monodispersed droplets. Changes to the continuous phase may also prove beneficial since the viscosity of the current oil phase is lower than the dispersed phase.

A continuous ME system may also help in controlling droplet size by shortening the exposure time to shear and wetting the membrane surface. *In situ* crosslinking of droplets can also help achieve better control over drop size by preventing the effect of shear breaking droplets further. A drop-in-drop

system can also be developed by pre-encapsulation in a primary emulsion which can then be emulsified further in a pre-mix membrane procedure. This way protection of phage from acid can further be improved since antacid can be co-encapsulated or develop a prolonged release profile by incorporating multi-shells.

8.2.3 Phage release from microparticles

Currently, pH 5, 6 and pH 7 (SIF) have been reported for phage release, this can be further studied by testing exposure of phage for various times to better understand the properties of microparticle dissolution. Similarly, pH 3, 4 can also be tested since *in vivo* there is a gradual rise in pH. Overall, a gut model with varying pH compartments in the presence of pathogenic bacteria and microflora will prove beneficial in understand the effects of phage encapsulation on phage therapy. This will offer a useful insight into further improvements needed to deliver the correct dose of phage at the correct time to effectively arrest bacterial growth.

Ex vivo models such as the one studied here, could be probed further in exploring the release of inflammatory cytokines in the presence of bacteria and phage. This will ensure there are no side effects and toxicity from both the phage and the poylymer used for encapsulation. Animal studies as the next step could be used to study the transit and deposition of these particles *in vivo*, which can provide information for further improvement in specifically targeting encapsulated phage at the site of infection. This could mean incorporating mucoadhesive properties of microparticles to help retain them at specific site for longer periods.

8.2.4 Storage of encapsulated phage

Current results show that Ephage is stable for long periods at 4˚C as opposed to elevated temperatures. Incorporation of trehalose has aided this however further investigation is required to improve storage stability of phage at higher relative humidity's. To investigate this, dry phage powder can be stored at varying degrees of temperature and humidity to identify the threshold of trehalose as a protective agent. This will enable for a better formulation development during spray drying of phage and tableting. Different types of binder could be used to improve the disintegration and friability of the tablets so as to meet he British Pharmacopeia (BP) standard or solid dosage forms.

8.2.5 Electrospinning phage

Production of defect-free Eudragit fibres encapsulating phage K was demonstrated in this work. The use of emulsion electrospinning proved to be a successful method for the production of Eudragit fibres. To further improve upon this strategy, co-axial electrospinning can be used to avoid the need for emulsion where phage is suspended in an organic solvent. Fibres produced via electrospinning offer a further advantage since the phage will be introduced in the core of the fibre, preventing exposure to high voltage.

Cryo-TEM can be a useful tool in determining the deposition of encapsulated phage in both fibres and microparticles. This enables, evaluation of the current encapsulation system which can be improved for better phage encapsulation.

Chapter 9: References

Abate, A. R., Thiele, J., & Weitz, D. a. (2011). One-step formation of multiple emulsions in microfluidics. *Lab on a Chip*, *11*(2), 253–258. https://doi.org/10.1039/c0lc00236d

Abate, a. R., & Weitz, D. a. (2009). High-order multiple emulsions formed in poly(dimethylsiloxane) microfluidics. *Small*, *5*(18), 2030–2032. https://doi.org/10.1002/smll.200900569

Abdulamir, A. S., Sabah, J., & BakarFatimah;, A. (2014). Novel approach of using a cocktail of designed bacteriophages against gut pathogenic E. coli for bacterial load biocontrol. *Annals of Clinical Microbiology and Antimicrobials*, *13*(39), 1–11.

Abedon, S. T., Kuhl, S. J., Blasdel, B. G., Kutter, E. M., Abedon, S. T., Kuhl, S. J., … Martin, E. (2016). Phage treatment of human infections, *7081*(July). https://doi.org/10.4161/bact.1.2.15845

Abuladze, T., Li, M., Menetrez, M. Y., Dean, T., Senecal, A., & Sulakvelidze, A. (2008). Bacteriophages reduce experimental contamination of hard surfaces, tomato, spinach, broccoli, and ground beef by Escherichia coli O157:H7. *Applied and Environmental Microbiology*, *74*(20), 6230–8. https://doi.org/10.1128/AEM.01465-08

Ackermann, H.-W., Tremblay, D., & Moineau, S. (2004). Long-Term Bacteriophage Preservation. *WFCC Newsletter*, *38*(January), 35–40.

Adriaenssens, E. M., van Vaerenbergh, J., Vandenheuvel, D., Dunon, V., Ceyssens, P. J., de Proft, M., … Lavigne, R. (2012). T4-related bacteriophage LIMEstone isolates for the control of soft rot on potato caused by "Dickeya solani." *PLoS ONE*, *7*(3). https://doi.org/10.1371/journal.pone.0033227

Alam, S. N., Yammine, H., Moaven, O., Ahmed, R., Moss, A. K., Biswas, B., … Biswas, R. (2012). Intestinal Alkaline Phosphotase Provents Antibiotic-Induced Susceptibility to Enteric Pathogens. *National Institute of Health*, *29*(6), 997–1003. https://doi.org/10.1016/j.biotechadv.2011.08.021.Secreted

Al Saif, N., & Brazier, J. S. (1996). The distribution of Clostridium difficile in the environment of South Wales. *Journal of Medical Microbiology*, *45*(2), 133–137. https://doi.org/10.1099/00222615-45-2-133

Albertini, B., Vitali, B., Passerini, N., Cruciani, F., Di Sabatino, M., Rodriguez, L., & Brigidi, P. (2010). Development of microparticulate systems for intestinal delivery of Lactobacillus acidophilus and Bifidobacterium lactis. *European Journal of Pharmaceutical Sciences*, *40*(4), 359–366.

https://doi.org/10.1016/j.ejps.2010.04.011

Albino, L. A. A. ., Rostagno, M. H. ., Hungaro, H. M. ., & Mendonca, R. C. S. . (2014). Isolation, characterization and application of bacteriophages for Salmonella spp. biocontrol in pigs. *Foodborne Pathogens and Disease*, *11*(8), 602–609.

Alhnan, M. A., Cosi, D., Murdan, S., & Basit, A. W. (2010). Inhibiting the gastric burst release of drugs from enteric microparticles: the influence of drug molecular mass and solubility. *Journal of Pharmaceutical Sciences*, *99*(10), 4215–4227. https://doi.org/10.1002/jps

Alisky, J., Iczkowski, K., Rapoport, a, & Troitsky, N. (1998). Bacteriophages show promise as antimicrobial agents. *The Journal of Infection*, *36*(1), 5–15. https://doi.org/10.1016/S0163-4453(98)92874-2

Ameri, M., & Maa, Y. F. (2006). Spray drying of biopharmaceuticals: Stability and process considerations. *Drying Technology*, *24*(6), 763–768. https://doi.org/10.1080/03602550600685275

Amidon, S., Brown, J. E., & Dave, V. S. (2015). Colon-Targeted Oral Drug Delivery Systems: Design Trends and Approaches. *AAPS PharmSciTech*. https://doi.org/10.1208/s12249-015-0350-9

Ananthakrishnan, A. N. (2011). Clostridium difficile infection: epidemiology, risk factors and management. *Nature Reviews. Gastroenterology & Hepatology*, *8*(1), 17–26. https://doi.org/10.1038/nrgastro.2010.190

Angelova, N., & Hunkeler, D. (1999). Rationalizing the design of polymeric biomaterials. *Trends in Biotechnology*, *17*(10), 409–421. https://doi.org/10.1016/S0167-7799(99)01356-6

Arakawa, T., & Timasheff, S. N. (1982). Stabilization of Protein Structure by Sugars. *Biochemistry*, *21*(25), 6536–6544. https://doi.org/10.1021/bi00268a033

Ariyasu, A., Hattori, Y., & Otsuka, M. (2016). Delay effect of magnesium stearate on tablet dissolution in acidic medium. *International Journal of Pharmaceutics*, *511*(2), 757–764. https://doi.org/10.1016/j.ijpharm.2016.07.034

Atterbury, R. J., Dillon, E., Swift, C., Connerton, P. L., Frost, J. a., Dodd, C. E. R., … Connerton, I. F. (2005). Correlation of Campylobacter bacteriophage with reduced presence of hosts in broiler chicken ceca. *Applied and Environmental Microbiology*, *71*(8), 4885–4887. https://doi.org/10.1128/AEM.71.8.4885-4887.2005

Atterbury, R. J., Van Bergen, M. A. P., Ortiz, F., Lovell, M. A., Harris, J. A., De Boer, A., … Barrow, P. A.

(2007). Bacteriophage therapy to reduce Salmonella colonization of broiler chickens. *Applied and Environmental Microbiology*, *73*(14), 4543–4549. https://doi.org/10.1128/AEM.00049-07

Augst, A. D., Kong, H. J., & Mooney, D. J. (2006). Alginate hydrogels as biomaterials. *Macromolecular Bioscience*, *6*(8), 623–633. https://doi.org/10.1002/mabi.200600069

Avnir, D., Braun, S., Lev, O., & Ottolenghit, M. (1994). Enzymes and Other Proteins Entrapped in Sol-Gel Materials, (12), 1605–1614.

Barea, M. J., Jenkins, M. J., Gaber, M. H., & Bridson, R. H. (2010). Evaluation of liposomes coated with a pH responsive polymer. *International Journal of Pharmaceutics*, *402*(1–2), 89–94. https://doi.org/10.1016/j.ijpharm.2010.09.028

Barrow, P., & Lovell, M. (1998). Use of Lytic Bacteriophage for Control of Experimental Escherichia coli Septicemia and Meningitis in Chickens and Calves. *Clinical and Diagnostic Laboratory Immunology*, *5*(3), 294–298.

Basit, A. W., & Ibekwe, V. C. (2007). Colonic Drug Delivery Formulation. *US Patent*, *1*(19).

Baumgarten, P. K. (1971). Electrostatic spinning of acrylic microfibers. *Journal of Colloid And Interface Science*, *36*(1), 71–79. https://doi.org/10.1016/0021-9797(71)90241-4

Bean, J. E., Alves, D. R., Laabei, M., Esteban, P. P., Thet, N. T., Enright, M. C., & Jenkins, A. T. A. (2014). Triggered Release of Bacteriophage K from Agarose / Hyaluronan Hydrogel Matrixes by Staphylococcus aureus Virulence Factors. *Chemistry of Materials*, *26*, 7201–7208.

Benita, S. (2006). Applications example 1: Microencapsulation by interfacial polycondensation. In S. Benita (Ed.), *Microencapsulation: Methods and industrial applications Second edition* (2nd ed., pp. 167–168). Israel: Taylor and Francis.

Best, E. L., Freeman, J., & Wilcox, M. H. (2012). Models for the study of Clostridium difficile infection. *Gut Microbes*, *3*(2), 145–167. https://doi.org/10.4161/gmic.19526

Betts, A., Vasse, M., Kaltz, O., & Hochberg, M. E. (2013). Back to the future: evolving bacteriophages to increase their effectiveness against the pathogen Pseudomonas aeruginosa PAO1. *Evolutionary Applications*, *6*(7), 1054–63. https://doi.org/10.1111/eva.12085

Bhattarai, N., Li, Z., Edmondson, D., & Zhang, M. (2006). Alginate-Based Nanofibrous Scaffolds: Structural, Mechanical, and Biological Properties. *Advanced Materials*, *18*(11), 1463–1467. https://doi.org/10.1002/adma.200502537

Biswas, B., Adhya, S., Washart, P., Paul, B., Trostel, A. N., Powell, B., … Merril, C. R. (2002).

Bacteriophage Therapy Rescues Mice Bacteremic from a Clinical Isolate of Vancomycin-Resistant Enterococcus faecium. *Infection and Immunity*, *70*(1), 204–210. https://doi.org/10.1128/IAI.70.1.204

Boggione, D. M. G., Batalha, L. S., Gontijo, M. T. P., Lopez, M. E. S., Teixeira, A. V. N. C., Santos, I. J. B., & Mendonça, R. C. S. (2017). Evaluation of microencapsulation of the UFV-AREG1 bacteriophage in alginate-Ca microcapsules using microfluidic devices. *Colloids and Surfaces B: Biointerfaces*, *158*, 182–189. https://doi.org/10.1016/j.colsurfb.2017.06.045

Bonino, C. A., Krebs, M. D., Saquing, C. D., Jeong, S. I., Shearer, K. L., Alsberg, E., & Khan, S. A. (2011). Electrospinning alginate-based nanofibers: From blends to crosslinked low molecular weight alginate-only systems. *Carbohydrate Polymers*, *85*(1), 111–119. https://doi.org/10.1016/j.carbpol.2011.02.002

Bouza, E. (2012). Consequences of Clostridium difficile infection: Understanding the healthcare burden. *Clinical Microbiology and Infection*, *18*(SUPPL.6), 5–12. https://doi.org/10.1111/1469-0691.12064

Briers, Y., Miroshnikov, K., Chertkov, O., Nekrasov, A., Mesyanzhinov, V., Volckaert, G., & Lavigne, R. (2008). The structural peptidoglycan hydrolase gp181 of bacteriophage phiKZ. *Biochemical and Biophysical Research Communications*, *374*(4), 747–751. https://doi.org/10.1016/j.bbrc.2008.07.102

Brouzes, E., Medkova, M., Savenelli, N., Marran, D., Twardowski, M., Hutchison, J. B., … Samuels, M. L. (2009). Droplet microfluidic technology for single-cell high-throughput screening. *Proceedings of the National Academy of Sciences of the United States of America*, *106*(34), 14195–200. https://doi.org/10.1073/pnas.0903542106

Burke, K. E., & Lamont, J. T. (2014). Clostridium difficile infection: A worldwide disease. *Gut and Liver*, *8*(1), 1–6. https://doi.org/10.5009/gnl.2014.8.1.1

Burns, K., Morris-Downes, M., Fawley, W. N., Smyth, E., Wilcox, M. H., & Fitzpatrick, F. (2010). Infection due to C. difficile ribotype 078: First report of cases in the Republic of Ireland. *Journal of Hospital Infection*, *75*(4), 287–291. https://doi.org/10.1016/j.jhin.2010.03.025

Cairns, B. J., Timms, A. R., Jansen, V. A. A., Connerton, I. F., & Payne, R. J. H. (2009). Quantitative models of in vitro bacteriophage-host dynamics and their application to phage therapy. *PLoS Pathogens*, *5*(1), 1–10. https://doi.org/10.1371/journal.ppat.1000253

Campbell, J. C., Koziol-McLain, J., Webster, D., McFarlane, J., Block, C. R., Ulrich, Y., & Glass, N.

(2006). Risk factors for femicide-suicide in abusive relationships: results from a multisite case control study. *Violence and Victims*, *21*(1), 3–21. https://doi.org/10.1891/vivi.21.1.3

Capra, M. L., Quiberoni, a, & Reinheimer, J. a. (2004). Thermal and chemical resistance of Lactobacillus casei and Lactobacillus paracasei bacteriophages. *Letters in Applied Microbiology*, *38*(6), 499–504. https://doi.org/10.1111/j.1472-765X.2004.01525.x

Carreras, N., Acuña, V., Martí, M., & Lis, M. J. (2012). Drug release system of ibuprofen in PCL-microspheres. *Colloid and Polymer Science*, *291*(1), 157–165. https://doi.org/10.1007/s00396-012-2768-x

Cartman, S. T., Heap, J. T., Kuehne, S. a., Cockayne, A., & Minton, N. P. (2010). The emergence of "hypervirulence" in Clostridium difficile. *International Journal of Medical Microbiology*, *300*(6), 387–395. https://doi.org/10.1016/j.ijmm.2010.04.008

Cerveny, K. E. ., DePaola, A. ., Duckworth, D. H. ., & Gulig, P. A. . (2002). Phage Therapy of Local and Systemic Disease Caused by Vibrio vulnificus in Iron-Dextran-Treated Mice. *Infection and Immunity*, *70*(11), 6251–6262. https://doi.org/10.1128/IAI.70.11.6251

Chang, R. Y., Wong, J., Mathai, A., Morales, S., Kutter, E., Britton, W., … Chan, H. K. (2017a). Production of highly stable spray dried phage formulations for treatment of Pseudomonas aeruginosa lung infection. *European Journal of Pharmaceutics and Biopharmaceutics*, *121*. https://doi.org/10.1016/j.ejpb.2017.09.002

Chang, R. Y., Wong, J., Mathai, A., Morales, S., Kutter, E., Britton, W., … Chan, H. K. (2017b). Production of highly stable spray dried phage formulations for treatment of Pseudomonas aeruginosa lung infection. *European Journal of Pharmaceutics and Biopharmaceutics*, *121*(September), 1–13. https://doi.org/10.1016/j.ejpb.2017.09.002

Charcosset, C. (2009). Preparation of emulsions and particles by membrane emulsification for the food processing industry. *Journal of Food Engineering*, *92*(3), 241–249. https://doi.org/10.1016/j.jfoodeng.2008.11.017

Charcosset, C., Limayem, I., & Fessi, H. (2004). The membrane emulsification process - A review. *Journal of Chemical Technology and Biotechnology*, *79*(3), 209–218. https://doi.org/10.1002/jctb.969

Chawla, A., Sharma, P., & Pawar, P. (2012). Eudragit S-100 coated sodium alginate microspheres of naproxen sodium: formulation, optimization and in vitro evaluation. *Acta Pharmaceutica (Zagreb, Croatia)*, *62*(4), 529–45. https://doi.org/10.2478/v10007-012-0034-x

Chen, S., Guo, F., Deng, T., Zhu, S., Liu, W., Zhong, H., … Deng, Z. (2016). Eudragit S100-Coated Chitosan Nanoparticles Co-loading Tat for Enhanced Oral Colon Absorption of Insulin. *AAPS PharmSciTech*. https://doi.org/10.1208/s12249-016-0594-z

Chibani-chennoufi, S., Sidoti, J., Bruttin, A., Kutter, E., Sarker, S., & Bru, H. (2004). In Vitro and In Vivo Bacteriolytic Activities of Escherichia coli Phages : Implications for Phage Therapy, *48*(7), 2558–2569. https://doi.org/10.1128/AAC.48.7.2558

Choinska-Pulit, A., Mitula, P., Sliwka, P., Choi, A., Wojciech, Ł., & Skaradzinska, A. (2015). Bacteriophage encapsulation : Trends and potential applications a. *Trends in Food Science & Technology*, *45*, 212–221. https://doi.org/10.1016/j.tifs.2015.07.001

Choonara, B. F., Choonara, Y. E., Kumar, P., Bijukumar, D., du Toit, L. C., & Pillay, V. (2014). A review of advanced oral drug delivery technologies facilitating the protection and absorption of protein and peptide molecules. *Biotechnology Advances*, *32*(7), 1269–1282. https://doi.org/10.1016/j.biotechadv.2014.07.006

Clark, W. A. (1962). Comparison of several methods for preserving bacteriophages. *Applied and Environmental Microbiology*, *10*(1951), 466–471.

Clokie, M. R. J., & Kropinski, A. M. (2009). *Bacteriophages : methods and protocols*. *Methods in molecular biology*. https://doi.org/10.1007/978-1-60327-164-6

Coco, R., Plapied, L., Pourcelle, V., Jérôme, C., Brayden, D. J., Schneider, Y. J., & Préat, V. (2013). Drug delivery to inflamed colon by nanoparticles: Comparison of different strategies. *International Journal of Pharmaceutics*, *440*(1), 3–12. https://doi.org/10.1016/j.ijpharm.2012.07.017

Collnot, E. M., Ali, H., & Lehr, C. M. (2012). Nano- and microparticulate drug carriers for targeting of the inflamed intestinal mucosa. *Journal of Controlled Release*, *161*(2), 235–246. https://doi.org/10.1016/j.jconrel.2012.01.028

Colom, J., Cano-Sarabia, M., Otero, J., Aríñez-Soriano, J., Cortés, P., Maspoch, D., & Llagostera, M. (2017a). Microencapsulation with alginate/CaCO3: A strategy for improved phage therapy. *Scientific Reports*, *7*(January), 41441. https://doi.org/10.1038/srep41441

Colom, J., Cano-Sarabia, M., Otero, J., Aríñez-Soriano, J., Cortés, P., Maspoch, D., & Llagostera, M. (2017b). Microencapsulation with alginate/CaCO 3: A strategy for improved phage therapy. *Scientific Reports*, *7*. https://doi.org/10.1038/srep41441

Colom, J., Cano-Sarabia, M., Otero, J., Cortés, P., Maspoch, D., & Llagostera, M. (2015). Liposome-Encapsulated Bacteriophages for Enhanced Oral Phage Therapy against Salmonella spp. *Applied*

and Environmental Microbiology, *81*(14), 4841–4849. https://doi.org/10.1128/AEM.00812-15

Connerton, P. L., Timms, a. R., & Connerton, I. F. (2011). Campylobacter bacteriophages and bacteriophage therapy. *Journal of Applied Microbiology*, *111*(2), 255–265. https://doi.org/10.1111/j.1365-2672.2011.05012.x

Dai, M., Senecal, A., & Nugen, S. R. (2014). Electrospun water-soluble polymer nanofibers for the dehydration and storage of sensitive reagents. *Nanotechnology*, *25*(22), 225101. https://doi.org/10.1088/0957-4484/25/22/225101

Dargaville, T. R., Farrugia, B. L., Broadbent, J. A., Pace, S., Upton, Z., & Voelcker, N. H. (2013). Biosensors and Bioelectronics Sensors and imaging for wound healing : A review. *Biosensors and Bioelectronic*, *41*, 30–42. https://doi.org/10.1016/j.bios.2012.09.029

Davies, J. D., & Kelly, M. J. (1969). The preservation of bacteriophage H1 of Corynebacterium ulcerans U103 by freeze-drying. *The Journal of Hygiene*, *67*(4), 573–583. https://doi.org/10.1017/S0022172400042030

de Arce Velasquez, A., Ferreira, L. M., Stangarlin, M. F. L., da Silva, C. D. B., Rolim, C. M. B., & Cruz, L. (2014). Novel Pullulan-Eudragit® S100 blend microparticles for oral delivery of risedronate: formulation, in vitro evaluation and tableting of blend microparticles. *Materials Science & Engineering. C, Materials for Biological Applications*, *38*, 212–7. https://doi.org/10.1016/j.msec.2014.02.003

De Arce Velasquez, A., Ferreira, L. M., Stangarlin, M. F. L., Da Silva, C. D. B., Rolim, C. M. B., & Cruz, L. (2014). Novel Pullulan-Eudragit® S100 blend microparticles for oral delivery of risedronate: Formulation, in vitro evaluation and tableting of blend microparticles. *Materials Science and Engineering C*, *38*(1), 212–217. https://doi.org/10.1016/j.msec.2014.02.003

De Menech, M., Garstecki, P., Jousse, F., & Stone, H. a. (2008). Transition from squeezing to dripping in a microfluidic T-shaped junction. *Journal of Fluid Mechanics*, *595*, 141–161. https://doi.org/10.1017/S002211200700910X

Deamer, D. W. (1985). United States Patent [19] Patent Number : 4,515,736.

Debebe Alemayehu, Casey, P. G., McAuliffe, O., Guinane, C. M., Martin, J. G., Shanahan, F., … Hill, C. (2012). Bacteriophages MR299-2 and NH-4 Can Eliminate Pseudomonas aeruginosa in the Murine Lung and on Cystic Fibrosis Lung Airway, *3*(2), 1–9. https://doi.org/10.1128/mBio.00029-12.Editor

Deitzel, J. ., Kleinmeyer, J., Harris, D., & Beck Tan, N. . (2001). The effect of processing variables on

the morphology of electrospun nanofibers and textiles. *Polymer*, *42*(1), 261–272. https://doi.org/10.1016/S0032-3861(00)00250-0

Denou, E., Bruttin, A., Barretto, C., Ngom-Bru, C., Brüssow, H., & Zuber, S. (2009). T4 phages against Escherichia coli diarrhea: Potential and problems. *Virology*, *388*(1), 21–30. https://doi.org/10.1016/j.virol.2009.03.009

Dew, M. J., Ebden, P., Kidwai, N. S., Lee, G., Evans, B. K., & Rhodes, J. (1984). Comparison of the absorption and metabolism of sulphasalazine and acrylic-coated 5-amino salicylic acid in normal subjects and patients with colitis. *British Journal of Clinical Pharmacology*, *17*(4), 474–476.

Dini, C., Islan, G. A., de Urraza, P. J., & Castro, G. R. (2012). Novel Biopolymer Matrices for Microencapsulation of Phages : Enhanced Protection Against Acidity and Protease Activity. *Macromolecular Bioscience*, *12*, 1200–1208. https://doi.org/10.1002/mabi.201200109

Dini, C., Islan, G. a, de Urraza, P. J., & Castro, G. R. (2012). Novel biopolymer matrices for microencapsulation of phages: enhanced protection against acidity and protease activity. *Macromolecular Bioscience*, *12*(9), 1200–8. https://doi.org/10.1002/mabi.201200109

Doan, T. V. P., Couet, W., & Olivier, J. C. (2011). Formulation and in vitro characterization of inhalable rifampicin-loaded PLGA microspheres for sustained lung delivery. *International Journal of Pharmaceutics*, *414*(1–2), 112–7. https://doi.org/10.1016/j.ijpharm.2011.05.007

Dobry, D. E., Settell, D. M., Baumann, J. M., Ray, R. J., Graham, L. J., & Beyerinck, R. a. (2009). A Model-Based Methodology for Spray-Drying Process Development. *Journal of Pharmaceutical Innovation*, *4*(3), 133–142. https://doi.org/10.1007/s12247-009-9064-4

Drees, K. P., Abbaszadegan, M., & Maier, R. M. (2003). Comparative electrochemical inactivation of bacteria and bacteriophage. *Water Research*, *37*(10), 2291–2300. https://doi.org/10.1016/S0043-1354(03)00009-5

Duan, H., Lü, S., Gao, C., Bai, X., Qin, H., Wei, Y., … Liu, M. (2016). Mucoadhesive microparticulates based on polysaccharide for target dual drug delivery of 5-aminosalicylic acid and curcumin to inflamed colon. *Colloids and Surfaces B: Biointerfaces*, *145*, 510–519. https://doi.org/10.1016/j.colsurfb.2016.05.038

Dubberke, E. R., Carling, P., Carrico, R., Donskey, C. J., Loo, V. G., Mcdonald, L. C., … Donskey, C. J. (2015). Control : Strategies to Prevent Clostridium dif cile Infections in Acute Care Hospitals : 2014 Update How to cite this article : Strategies to Prevent Clostridium difficile Infections in

Acute Care Hospitals : 2014 Update, (2014), 628–645. https://doi.org/10.1086/522262

Dubberke, E. R., Haslam, D. B., Lanzas, C., Bobo, L. D., Burnham, C. a D., Gröhn, Y. T., & Tarr, P. I. (2011). The ecology and pathobiology of Clostridium difficile infections: An interdisciplinary challenge. *Zoonoses and Public Health*, *58*(1), 4–20. https://doi.org/10.1111/j.1863-2378.2010.01352.x

Dubey, R., Dubey, R., Omrey, P., Vyas, S. P., & Jain, S. K. (2010). Development and characterization of colon specific drug delivery system bearing 5-ASA and Camylofine dihydrochloride for the treatment of ulcerative colitis. *Journal of Drug Targeting*, *18*(8), 589–601. https://doi.org/10.3109/10611860903572933

Egidi, E., Gasparini, G., Holdich, R. G., Vladisavljević, G. T., & Kosvintsev, S. R. (2008). Membrane emulsification using membranes of regular pore spacing: Droplet size and uniformity in the presence of surface shear. *Journal of Membrane Science*, *323*(2), 414–420. https://doi.org/10.1016/j.memsci.2008.06.047

Ehlers, C., Ivens, U. I., Senderovitz, T., & Serup, J. (2001). A study on the influence of gender , forearm site variation , right / left difference, *9*(7), 90–94.

Ekanem, E. E., Nabavi, S. A., Vladisavljevi??, G. T., & Gu, S. (2015). Structured Biodegradable Polymeric Microparticles for Drug Delivery Produced Using Flow Focusing Glass Microfluidic Devices. *ACS Applied Materials and Interfaces*, *7*(41), 23132–23143. https://doi.org/10.1021/acsami.5b06943

Engevik, M. a., Yacyshyn, M. B., Engevik, K. a., Wang, J., Darien, B., Hassett, D. J., … Worrell, R. T. (2014). Human Clostridium difficile infection: Altered mucus production and composition. *AJP: Gastrointestinal and Liver Physiology*, 510–524. https://doi.org/10.1152/ajpgi.00091.2014

Erb, R. M., Obrist, D., Chen, P. W., Studer, J., & Studart, A. R. (2011). Predicting sizes of droplets made by microfluidic flow-induced dripping. *Soft Matter*, *7*(19), 8757. https://doi.org/10.1039/c1sm06231j

Escobar-Chavez. (2006). Article Applications of thermo-reversible pluronic F-127 gels in pharmaceutical formulations Reference, *9*(3).

Evans, D. F., Pye, G., Bramley, R., Clark, a G., Dyson, T. J., & Hardcastle, J. D. (1988). Measurement of gastrointestinal pH profiles in normal ambulant human subjects. *Gut*, *29*(8), 1035–41. https://doi.org/10.1136/gut.29.8.1035

Eyre, D. W., Griffiths, D., Vaughan, A., Golubchik, T., Acharya, M., O'Connor, L., … Peto, T. E. a.

(2013). Asymptomatic Clostridium difficile colonisation and onward transmission. *PloS One*, *8*(11), e78445. https://doi.org/10.1371/journal.pone.0078445

Fawley, W. N., Freeman, J., Smith, C., Harmanus, C., Van Den Berg, R. J., Kuijper, E. J., & Wilcox, M. H. (2008). Use of highly discriminatory fingerprinting to analyze clusters of Clostridium difficile infection cases due to epidemic ribotype 027 strains. *Journal of Clinical Microbiology*, *46*(3), 954–960. https://doi.org/10.1128/JCM.01764-07

Fogg, P. C. M., Colloms, S., Rosser, S., Stark, M., & Smith, M. C. M. (2014). New applications for phage integrases. *Journal of Molecular Biology*, *426*(15), 2703–2716. https://doi.org/10.1016/j.jmb.2014.05.014

Fong, H., Liu, W., Wang, C. S., & Vaia, R. A. (2001). Generation of electrospun fibers of nylon 6 and nylon 6-montmorillonite nanocomposite. *Polymer*, *43*(3), 775–780. https://doi.org/10.1016/S0032-3861(01)00665-6

Fu, T., Wu, Y., Ma, Y., & Li, H. Z. (2012). Droplet formation and breakup dynamics in microfluidic flow-focusing devices: From dripping to jetting. *Chemical Engineering Science*, *84*, 207–217. https://doi.org/10.1016/j.ces.2012.08.039

Gal-Mor, O., Boyle, E. C., & Grassl, G. A. (2014). Same species, different diseases: How and why typhoidal and non-typhoidal Salmonella enterica serovars differ. *Frontiers in Microbiology*, *5*(AUG), 1–10. https://doi.org/10.3389/fmicb.2014.00391

Garcia-Fuentes, M., & Alonso, M. J. (2012). Chitosan-based drug nanocarriers: where do we stand? *Journal of Controlled Release : Official Journal of the Controlled Release Society*, *161*(2), 496–504. https://doi.org/10.1016/j.jconrel.2012.03.017

Gasparini, G., Kosvintsev, S. R., Stillwell, M. T., & Holdich, R. G. (2008). Preparation and characterization of PLGA particles for subcutaneous controlled drug release by membrane emulsification. *Colloids and Surfaces B: Biointerfaces*, *61*(2), 199–207. https://doi.org/10.1016/j.colsurfb.2007.08.011

George, M., & Abraham, T. E. (2006). Polyionic hydrocolloids for the intestinal delivery of protein drugs: Alginate and chitosan - a review. *Journal of Controlled Release*, *114*(1), 1–14. https://doi.org/10.1016/j.jconrel.2006.04.017

Gharsallaoui, A., Roudaut, G., Chambin, O., Voilley, A., & Saurel, R. (2007). Applications of spray-drying in microencapsulation of food ingredients: An overview. *Food Research International*, *40*(9), 1107–1121. https://doi.org/10.1016/j.foodres.2007.07.004

Ghosh, S. K. (2006). Functional Coatings and Microencapsulation : A General Perspective.

Gibson, P. R. ., Fixa, B. ., Pekarkova, B. ., Batovsky, M. ., Radford-Smith, G. ., Tibitanzl, J. ., … Greinwald, R. . (2006). Comparison of the efficacy and safety of Eudragit-L-coated mesalazine tablets with ethylcellulose-coated mesalazine tablets in patients with mild to moderately active ulcerative colitis. *Alimentary Pharmacology & Therapeutics*, *23*, 1017–1026. https://doi.org/10.1111/j.1365-2036.2006.02861.x

Gill, I., & Ballesteros, A. (2000). Bioencapsulation within synthetic polymers (Part 1): sol – gel encapsulated biologicals, *18*(JULY), 282–296.

Goh, S., Chang, B. J., & Riley, T. V. (2005). Effect of phage infection on toxin production by Clostridium difficile. *Journal of Medical Microbiology*, *54*(2), 129–135. https://doi.org/10.1099/jmm.0.45821-0

Goh, S., Hussain, H., Chang, B. J., Emmett, W., & Riley, T. V. (2013). Phage □ C2 Mediates Transduction of Tn 6215 , Encoding Erythromycin Resistance, between, *4*(6), 1–7. https://doi.org/10.1128/mBio.00840-13.Editor

Goh, S., Ong, P. F., Song, K. P., Rily, T. V., & Chang, B. J. (2007). The complete genome sequence of Clostridium difficile phage ϕC2 and comparisons to ϕCD119 and inducible prophages of CD630. *Microbiology*, *153*(3), 676–685. https://doi.org/10.1099/mic.0.2006/002436-0

Goldenberg, S. D., & French, G. L. (2011). Diagnostic testing for Clostridium difficile: A comprehensive survey of laboratories in England. *Journal of Hospital Infection*, *79*(1), 4–7. https://doi.org/10.1016/j.jhin.2011.03.030

Goudarzi, M., Seyedjavadi, S. S., Goudarzi, H., Aghdam, E. M., & Nazeri, S. (2014). Clostridium difficile Infection : Epidemiology , Pathogenesis , Risk Factors , and Therapeutic Options, *2014*.

Gouin, S. (2004). Microencapsulation: industrial appraisal of existing technologies and trends. *Trends in Food Science & Technology*, *15*(7–8), 330–347. https://doi.org/10.1016/j.tifs.2003.10.005

Govender, M., Choonara, Y. E., van Vuuren, S., Kumar, P., du Toit, L. C., & Pillay, V. (2015). A gastro-resistant ovalbumin bi-layered mini-tablet-in-tablet system for the delivery of *L actobacillus acidophilus* probiotic to simulated human intestinal and colon conditions. *Journal of Pharmacy and Pharmacology*, n/a-n/a. https://doi.org/10.1111/jphp.12389

Governal, R. a, & Gerba, C. P. (1997). Persistence of MS-2 and PRD-1 bacteriophages in an ultrapure water system. *Journal of Industrial Microbiology & Biotechnology*, *18*(5), 297–301. https://doi.org/10.1038/sj.jim.2900711

Gupta, P., & Wilkes, G. L. (2003). Some investigations on the fiber formation by utilizing a side-by-side bicomponent electrospinning approach. *Polymer*, *44*(20), 6353–6359. https://doi.org/10.1016/S0032-3861(03)00616-5

Hagens, S., & Loessner, M. J. (2007). Application of bacteriophages for detection and control of foodborne pathogens. *Applied Microbiology and Biotechnology*, *76*(3), 513–9. https://doi.org/10.1007/s00253-007-1031-8

Haider, A., Haider, S., & Kang, I. K. (2015). A comprehensive review summarizing the effect of electrospinning parameters and potential applications of nanofibers in biomedical and biotechnology. *Arabian Journal of Chemistry*. https://doi.org/10.1016/j.arabjc.2015.11.015

Haider, S., Al-Zeghayer, Y., Ahmed Ali, F. A., Haider, A., Mahmood, A., Al-Masry, W. A., … Aijaz, M. O. (2013). Highly aligned narrow diameter chitosan electrospun nanofibers. *Journal of Polymer Research*, *20*(4). https://doi.org/10.1007/s10965-013-0105-9

Han, J.-H., Koo, B.-M., Kim, J.-W., & Suh, K.-D. (2008). A facile approach to synthesize uniform hydrogel shells with controllable loading and releasing properties. *Chemical Communications (Cambridge, England)*, (8), 984–6. https://doi.org/10.1039/b715557c

Hanga, M. P., & Holdich, R. G. (2014). Membrane emulsification for the production of uniform poly-N-isopropylacrylamide-coated alginate particles using internal gelation. *Chemical Engineering Research and Design*, *92*(9), 1664–1673. https://doi.org/10.1016/j.cherd.2013.12.010

Hanlon, G. W., Denyer, S. P., Olliff, C. J., & Ibrahim, L. J. (2001). Reduction in Exopolysaccharide Viscosity as an Aid to Bacteriophage Penetration through Pseudomonas aeruginosa Biofilms. *Applied and Environmental Microbiology*, *67*(6), 2746–2753. https://doi.org/10.1128/AEM.67.6.2746-2753.2001

Hargreaves, K. R., & Clokie, M. R. J. (2014). Clostridium difficile phages: still difficult? *Frontiers in Microbiology*, *5*(April), 184. https://doi.org/10.3389/fmicb.2014.00184

Hashimoto, M., Shevkoplyas, S. S., Zasońska, B., Szymborski, T., Garstecki, P., & Whitesides, G. M. (2008). Formation of bubbles and droplets in parallel, coupled flow-focusing geometries. *Small*, *4*(10), 1795–1805. https://doi.org/10.1002/smll.200800591

Hashimoto, T., Suzuki, Y., Tanihara, M., & Kakimaru, Y. (2004). Development of alginate wound dressings linked with hybrid peptides derived from laminin and elastin, *25*, 1407–1414. https://doi.org/10.1016/j.biomaterials.2003.07.004

Hayati, I., Bailey, a, & Tadros, T. . (1987). Investigations into the mechanism of electrohydrodynamic

spraying of liquids. *Journal of Colloid and Interface Science*, *117*(1), 222–230. https://doi.org/10.1016/0021-9797(87)90186-X

He, M., Miyajima, F., Roberts, P., Ellison, L., Pickard, D. J., Melissa, J., … Kuijper, E. (2013). Europe PMC Funders Group Emergence and global spread of epidemic healthcare-associated Clostridium difficile, *45*(1), 109–113. https://doi.org/10.1038/ng.2478.Emergence

Hohmann, E. L. (2001). Nontyphoidal Salmonellosis. *Clinical Infectious Diseases*, *32*(January), 263–269.

Holdich, R. G., Dragosavac, M. M., & Vladisavljevic, G. T. (2010). Membrane Emulsification with Oscillating and Stationary Membranes, 3810–3817.

Holdich, R. G., Dragosavac, M. M., Vladisavljević, G. T., & Piacentini, E. (2013). Continuous membrane emulsification with pulsed (oscillatory) flow. *Industrial and Engineering Chemistry Research*, *52*(1), 507–515. https://doi.org/10.1021/ie3020457

Holdich, R., Kosvintsev, S., Cumming, I., & Zhdanov, S. (2006). Pore design and engineering for filters and membranes. *Philosophical Transactions of the Royal Society A: Mathematical, Physical and Engineering Sciences*, *364*(1838), 161–174. https://doi.org/10.1098/rsta.2005.1690

Holmes, A. H., Moore, L. S. P., Sundsfjord, A., Steinbakk, M., Regmi, S., Karkey, A., … Piddock, L. J. V. (2016). Understanding the mechanisms and drivers of antimicrobial resistance. *The Lancet*, *387*(10014), 176–187. https://doi.org/10.1016/S0140-6736(15)00473-0

Hooton, S. P. T., Atterbury, R. J., & Connerton, I. F. (2011). Application of a bacteriophage cocktail to reduce Salmonella Typhimurium U288 contamination on pig skin. *International Journal of Food Microbiology*, *151*(2), 157–163. https://doi.org/10.1016/j.ijfoodmicro.2011.08.015

Housby, J. N., & Mann, N. H. (2009). Phage therapy. *Drug Discovery Today*, *14*(11–12), 536–540. https://doi.org/10.1016/j.drudis.2009.03.006

Hua, S., Marks, E., Schneider, J. J., & Keely, S. (2015). Advances in oral nano-delivery systems for colon targeted drug delivery in inflammatory bowel disease: Selective targeting to diseased versus healthy tissue. *Nanomedicine: Nanotechnology, Biology and Medicine*, *11*(5), 1117–1132. https://doi.org/10.1016/j.nano.2015.02.018

Huan, S., Liu, G., Han, G., Cheng, W., Fu, Z., Wu, Q., & Wang, Q. (2015). Effect of Experimental Parameters on Morphological, Mechanical and Hydrophobic Properties of Electrospun Polystyrene Fibers. *Materials*, *8*(5), 2718–2734. https://doi.org/10.3390/ma8052718

Huanbutta, K., Sriamornsak, P., Luangtana-Anan, M., Limmatvapirat, S., Puttipipatkhachorn, S., Lim, L.-Y., … Nunthanid, J. (2013). Application of multiple stepwise spinning disk processing for the synthesis of poly(methyl acrylates) coated chitosan-diclofenac sodium nanoparticles for colonic drug delivery. *European Journal of Pharmaceutical Sciences : Official Journal of the European Federation for Pharmaceutical Sciences*, *50*(3–4), 303–11. https://doi.org/10.1016/j.ejps.2013.07.010

Huang, S., Yang, H., Lakshmanan, R. S., Johnson, M. L., Chen, I., Wan, J., … Chin, B. a. (2008). The effect of salt and phage concentrations on the binding sensitivity of magnetoelastic biosensors for Bacillus anthracis detection. *Biotechnology and Bioengineering*, *101*(5), 1014–1021. https://doi.org/10.1002/bit.21995

Huang, Y.-I., Cheng, Y.-H., Yu, C.-C., Tsai, T.-R., & Cham, T.-M. (2007). Microencapsulation of extract containing shikonin using gelatin-acacia coacervation method: a formaldehyde-free approach. *Colloids and Surfaces. B, Biointerfaces*, *58*(2), 290–7. https://doi.org/10.1016/j.colsurfb.2007.04.013

Huber, C. A., Hall, L., Foster, N. F., Gray, M., Allen, M., Richardson, L. J., … Paterson, D. L. (2014). SURVEILLANCE SNAPSHOT OF CLOSTRIDIUM DIFFICILE INFECTION IN HOSPITALS ACROSS QUEENSLAND DETECTS BINARY TOXIN PRODUCING RIBOTYPE UK 244, 279–284.

Hussain, M. A., Liu, H., Wang, Q., Zhong, F., Guo, Q., & Balamurugan, S. (2017). Use of encapsulated bacteriophages to enhance farm to fork food safety. *Critical Reviews in Food Science and Nutrition*, *57*(13). https://doi.org/10.1080/10408398.2015.1069729

Ibekwe, V. C., Fadda, H. M., McConnell, E. L., Khela, M. K., Evans, D. F., & Basit, A. W. (2008). Interplay between intestinal pH, transit time and feed status on the in vivo performance of pH responsive ileo-colonic release systems. *Pharmaceutical Research*, *25*(8), 1828–35. https://doi.org/10.1007/s11095-008-9580-9

Imamovic, L., & Muniesa, M. (2012). Characterizing RecA-independent induction of Shiga toxin2-encoding phages by EDTA treatment. *PLoS ONE*, *7*(2). https://doi.org/10.1371/journal.pone.0032393

Indra, a., Huhulescu, S., Schneeweis, M., Hasenberger, P., Kembichler, S., Fiedler, a., … Kuijper, E. J. (2008). Characterization of Clostridium difficile isolates using capillary gel electrophoresis-based PCR ribotyping. *Journal of Medical Microbiology*, *57*(11), 1377–1382. https://doi.org/10.1099/jmm.0.47714-0

Ivarsson, M. E., Leroux, J.-C., & Castagner, B. (2015). Investigational new treatments for Clostridium difficile infection. *Drug Discovery Today*, *20*(5), 602–608. https://doi.org/10.1016/j.drudis.2014.12.003

Jaeger, R., Bergshoef, M. M., Batlle, C. M. I., Schönherr, H., & Julius Vancso, G. (1998). Electrospinning of ultra-thin polymer fibers. *Macromolecular Symposia*, *127*(1), 141–150. https://doi.org/10.1002/masy.19981270119

Jain, D., Panda, A. K., & Majumdar, D. K. (2005). Eudragit S100 entrapped insulin microspheres for oral delivery. *AAPS PharmSciTech*, *6*(1), E100-7. https://doi.org/10.1208/pt060116

Jallo, L. J., Ghoroi, C., Gurumurthy, L., Patel, U., & Davé, R. N. (2012). Improvement of flow and bulk density of pharmaceutical powders using surface modification. *International Journal of Pharmaceutics*, *423*(2), 213–225. https://doi.org/10.1016/j.ijpharm.2011.12.012

Jamalludeen, N., Johnson, R. P., Shewen, P. E., & Gyles, C. L. (2009). Evaluation of bacteriophages for prevention and treatment of diarrhea due to experimental enterotoxigenic Escherichia coli O149 infection of pigs. *Veterinary Microbiology*, *136*, 135–141. https://doi.org/10.1016/j.vetmic.2008.10.021

Jeyanthi, R., Thanoo, B. C., Metha, R. C., & Deluca, P. P. (1996). Effect of solvent removal technique on the matrix characteristics of polylactide/glycolide microspheres for peptide delivery. *Journal of Controlled Release*, *38*(2–3), 235–244. https://doi.org/10.1016/0168-3659(95)00125-5

Ji, C. M., Xu, H. N., & Wu, W. (2009). Guar gum as potential film coating material for colon-specific delivery of fluorouracil. *Journal of Biomaterials Applications*, *23*(4), 311–329. https://doi.org/10.1177/0885328208089617

Jivraj, M., Martini, L. G., & Thomson, C. M. (2000). An overview of the different excipients useful for the direct compression of tablets. *Pharmaceutical Science and Technology Today*, *3*(2), 58–63. https://doi.org/10.1016/S1461-5347(99)00237-0

Jończyk, E., Kłak, M., Międzybrodzki, R., & Górski, a. (2011). The influence of external factors on bacteriophages--review. *Folia Microbiologica*, *56*(3), 191–200. https://doi.org/10.1007/s12223-011-0039-8

Jong, B. De. (1929). Coacervation. (Partial miscibility in colloid systems). (Preliminary Communication), *131*(1927).

Joscelyne, S. M., & Trägårdh, G. (2000). Membrane emulsification — a literature review. *J Memb Sci*, *169*(1999), 107–117.

Jose, S., Dhanya, K., Cinu, T., Litty, J., & Chacko, A. (2009). Colon targeted drug delivery: Different approaches. *Journal of Young Pharmacists*, *1*(1), 13. https://doi.org/10.4103/0975-1483.51869

K. Bouchemal, S. Briancon, P. Chaumont, H. F. and N. Z. (2003). Microencapsulation of dehydroepiandrosterone (DHEA) with poly(ortho ester) polymers by interfacial polycondensation. *J . A I I C ROE NCA I'S IJ I A'l'l Oh'*, *20*(5), 637–651.

Katoh, R., Asano, Y., Furuya, A., Sotoyama, K., & Tomita, M. (1996). Preparation of food emulsions using a membrane emulsification system. *Journal of Membrane Science*, *113*(1), 131–135. https://doi.org/10.1016/0376-7388(95)00227-8

Keely, S., Ryan, S., Haddleton, D. M., Limer, A., Murphy, E. P., Colgan, S. P., & Brayden, D. J. (2009). Dexamethasone-poly(dimethylamino)ethyl methacrylate (pDMAEMA) conjugates reduce inflammatory biomarkers in human intestinal epithelial monolayers. *National Institute of Health*, *29*(6), 997–1003. https://doi.org/10.1016/j.biotechadv.2011.08.021.Secreted

Kelly, R., Zoubiane, G., Walsh, D., Ward, R., & Goossens, H. (2016). Public funding for research on antibacterial resistance in the JPIAMR countries, the European Commission, and related European Union agencies: A systematic observational analysis. *The Lancet Infectious Diseases*, *16*(4), 431–440. https://doi.org/10.1016/S1473-3099(15)00350-3

Kenis, P. J. (1999). Microfabrication Inside Capillaries Using Multiphase Laminar Flow Patterning. *Science*, *285*(5424), 83–85. https://doi.org/10.1126/science.285.5424.83

Kietzmann, D., Moulari, B., Béduneau, A., Pellequer, Y., & Lamprecht, A. (2010). Colonic delivery of carboxyfluorescein by pH-sensitive microspheres in experimental colitis. *European Journal of Pharmaceutics and Biopharmaceutics : Official Journal of Arbeitsgemeinschaft Für Pharmazeutische Verfahrenstechnik e.V*, *76*(2), 290–5. https://doi.org/10.1016/j.ejpb.2010.06.013

Kim, M. D., Iskakov, R. M., Batyrbekov, E. O., Zhubanov, B. a., & Perichaud, a. (2006). Segmented polyurethane-based microparticles: Synthesis, properties, and isoniazid encapsulation and kinetics of release. *Polymer Science Series A*, *48*(12), 1257–1262. https://doi.org/10.1134/S0965545X06120054

Kim, S., Jo, A., & Ahn, J. (2015a). Application of chitosan-alginate microspheres for the sustained release of bacteriophage in simulated gastrointestinal conditions. *International Journal of Food Science and Technology*, *50*(4), 913–918. https://doi.org/10.1111/ijfs.12736

Kim, S., Jo, A., & Ahn, J. (2015b). Application of chitosan – alginate microspheres for the sustained

release of bacteriophage in simulated gastrointestinal conditions. *International Journal of Food Science and Technology*, *50*, 913–918. https://doi.org/10.1111/ijfs.12736

Kleinubing, S. A., Seraphim, D. C., Vieira, M. G. A., Canevesi, R. L. S., da Silva, E. A., César, C. L., & Mei, L. H. I. (2014). Gastro-resistant controlled release of OTC encapsulated in alginate/chitosan matrix coated with acryl-EZE® MP in fluidized bed. *Journal of Applied Polymer Science*, *131*(12), n/a-n/a. https://doi.org/10.1002/app.40444

Knezevic, P., Obreht, D., Curcin, S., Petrusic, M., Aleksic, V., Kostanjsek, R., & Petrovic, O. (2011). Phages of Pseudomonas aeruginosa: Response to environmental factors and in vitro ability to inhibit bacterial growth and biofilm formation. *Journal of Applied Microbiology*, *111*(1), 245–254. https://doi.org/10.1111/j.1365-2672.2011.05043.x

Kobašlija, M., & McQuade, D. T. (2006). Polyurea Microcapsules from Oil-in-Oil Emulsions via Interfacial Polymerization. *Macromolecules*, *39*(19), 6371–6375. https://doi.org/10.1021/ma061455x

Kong, T., Wu, J., To, M., Wai Kwok Yeung, K., Cheung Shum, H., & Wang, L. (2012). Droplet based microfluidic fabrication of designer microparticles for encapsulation applications. *Biomicrofluidics*, *6*(3). https://doi.org/10.1063/1.4738586

Koo, C. K. W., Senecal, K., Senecal, A., & Nugen, S. R. (2016). Dehydration of bacteriophages in electrospun nano fi bers : effect of excipients in polymeric solutions. *Nanotechnology*, *27*(48), 1–10. https://doi.org/10.1088/0957-4484/27/48/485102

Korehei, R., & Kadla, J. (2013). Incorporation of T4 bacteriophage in electrospun fibres. *Journal of Applied Microbiology*, *114*(5), 1425–1434. https://doi.org/10.1111/jam.12158

Korehei, R., & Kadla, J. F. (2014). Encapsulation of T4 bacteriophage in electrospun poly(ethylene oxide)/cellulose diacetate fibers. *Carbohydrate Polymers*, *100*, 150–157. https://doi.org/10.1016/j.carbpol.2013.03.079

Kosvintsev Serguei R., Gasparini Gilda, H. R. G. (2008). Membrane emulsification : droplet size and uniformity in the absence of surface shear. *Journal of Membrane Science*, *313*(1–2), 182–189.

Krasaekoopt, W., Bhandari, B., & Deeth, H. (2003). Evaluation of encapsulation techniques of probiotics for yoghurt. *International Dairy Journal*, *13*(1), 3–13. https://doi.org/10.1016/S0958-6946(02)00155-3

Kukizaki, M. (2009). Shirasu porous glass (SPG) membrane emulsification in the absence of shear flow at the membrane surface: Influence of surfactant type and concentration, viscosities of

dispersed and continuous phases, and transmembrane pressure. *Journal of Membrane Science*, *327*(1–2), 234–243. https://doi.org/10.1016/j.memsci.2008.11.026

Lalezari, D. (2012). Gastrointestinal pH profile in subjects with irritable bowel syndrome. *Annals of Gastroenterology*, *25*(4), 333–337.

Latisha Heinlen, MD1, 2 and Jimmy D. Ballard, P. (2011). Clostridium Difficile Infection, *340*(3), 247–252. https://doi.org/10.1097/MAJ.0b013e3181e939d8.Clostridium

Lee, K. T., & Mooney, D. J. (2013). Alginate : properties and biomedical applications. *Polymer Science*, *37*(1), 106–126. https://doi.org/10.1016/j.progpolymsci.2011.06.003.Alginate

Lee, S. W., & Belcher, A. M. (2004). Virus-based fabrication of micro- and nanofibers using electrospinning. *Nano Letters*, *4*(3), 387–390. https://doi.org/10.1021/nl034911t

Leibo, S. P., & Mazur, P. (1966). Effect of Osmotic Shock and Low Salt Concentration on Survival and Density of Bacteriophages T4B and T4Bo1. *Biophysical Journal*, *6*(6), 747–772. https://doi.org/10.1016/S0006-3495(66)86693-6

Lessa, F. C., Mu, Y., Bamberg, W. M., Beldavs, Z. G., Dumyati, G. K., Dunn, J. R., … McDonald, L. C. (2015). Burden of *Clostridium difficile* Infection in the United States. *New England Journal of Medicine*, *372*(9), 825–834. https://doi.org/10.1056/NEJMoa1408913

Leung, C. Y. (Joey);, & Weitz, J. S. (2016). Synergistic elimination of bacteria by phage and the immune system. *bioRxiv*. https://doi.org/10.1101/057927

Leung, S. S. Y., Parumasivam, T., Gao, F. G., Carrigy, N. B., Vehring, R., Finlay, W. H., … Chan, H.-K. (2017). Effects of storage conditions on the stability of spray dried, inhalable bacteriophage powders. *International Journal of Pharmaceutics*. https://doi.org/10.1016/j.ijpharm.2017.01.060

Leung, S. S. Y., Parumasivam, T., Gao, F. G., Carrigy, N. B., Vehring, R., Finlay, W. H., … Chan, H. K. (2016). Production of Inhalation Phage Powders Using Spray Freeze Drying and Spray Drying Techniques for Treatment of Respiratory Infections. *Pharmaceutical Research*, *33*(6), 1486–1496. https://doi.org/10.1007/s11095-016-1892-6

Leung, S. S. Y., Parumasivam, T., Gao, F. G., Carter, E. A., Carrigy, N. B., Vehring, R., … Chan, H. K. (2017). Effects of storage conditions on the stability of spray dried, inhalable bacteriophage powders. *International Journal of Pharmaceutics*, *521*(1–2), 141–149. https://doi.org/10.1016/j.ijpharm.2017.01.060

Levin, B. R., & Bull, J. J. (2004). Population and evolutionary dynamics of phage therapy. *Nature Reviews. Microbiology*. https://doi.org/10.1038/nrmicro822

Liu, X. D., Bao, D. C., Xue, W. M., Xiong, Y., Yu, W. T., Yu, X. J., … Yuan, Q. (2002). Preparation of uniform calcium alginate gel beads by membrane emulsification coupled with internal gelation. *Journal of Applied Polymer Science*, *87*(5), 848–852. https://doi.org/10.1002/app.11537

Liu, X. D., Yu, W. Y., Zhang, Y., Xue, W. M., Yu, W. T., Xiong, Y., … Yuan, Q. (2002). Characterization of structure and diffusion behaviour of Ca-alginate beads prepared with external or internal calcium sources. *Journal of Microencapsulation*, *19*(6), 775–82. https://doi.org/10.1080/0265204021000022743

Loc-Carrillo, C., & Abedon, S. (2011). Pros and cons of phage therapy. *Bacteriophage*, *1*(2), 111–114. https://doi.org/10.4161/bact.1.2.14590

Loir Yves Le, F. B. and M. G. (2003). Staphylococcus aureus and food poisoning. *Genet. Mol. Res.*, *2 (1):*, 63–76. Retrieved from http://www.funpecrp.com.br/gmr/year2003/vol1-2/sim0009_full_text.htm

Lorenzo-Lamosa, M. L., Remuñán-López, C., Vila-Jato, J. L., & Alonso, M. J. (1998). Design of microencapsulated chitosan microspheres for colonic drug delivery. *Journal of Controlled Release*, *52*(1–2), 109–118. https://doi.org/10.1016/S0168-3659(97)00203-4

Lu, T. K., & Koeris, M. S. (2011). The next generation of bacteriophage therapy. *Current Opinion in Microbiology*, *14*(5), 524–31. https://doi.org/10.1016/j.mib.2011.07.028

Lv, J., Yin, X., Zeng, Q., Dong, W., Liu, H., & Zhu, L. (2017). Preparation of carboxymethyl chitosan nanofibers through electrospinning the ball-milled nanopowders with poly (lactic acid) and the blood compatibility of the electrospun NCMC/PLA mats. *Journal of Polymer Research*, *24*(4), 60. https://doi.org/10.1007/s10965-017-1224-5

Lyerly, D. M., Krivan, H. C., & Wilkins, T. D. (1988). Clostridium-Difficile its Disease and Toxins. *Clinical Microbiology Reviews*, *1*(1), 1–18. https://doi.org/10.1128/CMR.1.1.1.Updated

Ma, Y., Islam, G. S., Wu, Y., Sabour, P. M., Chambers, J. R., Wang, Q., … Griffiths, M. W. (2014). Temporal distribution of encapsulated bacteriophages during passage through the chick gastrointestinal tract.

Ma, Y., Pacan, J. C., Wang, Q., Sabour, P. M., Huang, X., & Xu, Y. (2012). Enhanced alginate microspheres as means of oral delivery of bacteriophage for reducing Staphylococcus aureus intestinal carriage. *Food Hydrocolloids*, *26*(2), 434–440.

https://doi.org/10.1016/j.foodhyd.2010.11.017

Ma, Y., Pacan, J. C., Wang, Q., Xu, Y., Huang, X., Korenevsky, A., & Sabour, P. M. (2008). Microencapsulation of bacteriophage felix O1 into chitosan-alginate microspheres for oral delivery. *Applied and Environmental Microbiology*, *74*(15), 4799–805. https://doi.org/10.1128/AEM.00246-08

Macfarlane, G. T., Macfarlane, S., & Gibson, G. R. (1998). Validation of a three-stage compound continuous culture system for investigating the effect of retention time on the ecology and metabolism of bacteria in the human colon. *Microbial Ecology*, *35*(2), 180–187. https://doi.org/10.1007/s002489900072

Madene, A., Jacquot, M., Scher, J., & Desobry, S. (2006). Flavour encapsulation and controlled release - a review. *International Journal of Food Science and Technology*, *41*(1), 1–21. https://doi.org/10.1111/j.1365-2621.2005.00980.x

Mahony, D. E., Bell, P. D., & Easterbrook, K. B. (1985). Two Bacteriophages of Clostridium difficile. *Journal of Clinical Microbiology*, *21*(2), 251–254. https://doi.org/10.1016/j.disamonth.2009.04.010

Malik, D. J., Sokolov, I. J., Vinner, G. K., Mancuso, F., Cinquerrui, S., Vladisavljevic, G. T., … Kirpichnikova, A. (2017). Formulation, stabilisation and encapsulation of bacteriophage for phage therapy. *Advances in Colloid and Interface Science*. https://doi.org/10.1016/j.cis.2017.05.014

Martins, S., Sarmento, B., Souto, E. B., & Ferreira, D. C. (2007). Insulin-loaded alginate microspheres for oral delivery – Effect of polysaccharide reinforcement on physicochemical properties and release profile. *Carbohydrate Polymers*, *69*(4), 725–731. https://doi.org/10.1016/j.carbpol.2007.02.012

Marwaha, M., Sandhu, D., & Marwaha, R. K. (2010). Coprocessing of Excipients: A Review On Excipient Development For Improved Tabletting Performance. *International Journal of Applied Pharmaceutics*, *2*(3), 41–47. Retrieved from http://www.ijaponline.org/Vol2Issue3/108.pdf

Matinkhoo, S., Lynch, K. H., Dennis, J. J., Finlay, W. H., & Vehring, R. (2011). Spray-dried Respirable Powders Containing Bacteriophages for the Treatment of Pulmonary Infections. *Journal of Pharmaceutical Sciences*, *100*(12), 5197–5205. https://doi.org/10.1002/jps.22715

Matsubara, T., Emoto, W., & Kawashiro, K. (2007). A simple two-transition model for loss of infectivity of phages on exposure to organic solvent. *Biomolecular Engineering*, *24*(2), 269–271.

https://doi.org/10.1016/j.bioeng.2007.02.002

McConnell, E. L., Fadda, H. M., & Basit, A. W. (2008). Gut instincts: explorations in intestinal physiology and drug delivery. *International Journal of Pharmaceutics*, *364*(2), 213–26. https://doi.org/10.1016/j.ijpharm.2008.05.012

Meader, E., Mayer, M. J., Gasson, M. J., Steverding, D., Carding, S. R., & Narbad, A. (2010). Bacteriophage treatment significantly reduces viable Clostridium difficile and prevents toxin production in an in vitro model system. *Anaerobe*, *16*(6), 549–554. https://doi.org/10.1016/j.anaerobe.2010.08.006

Meader, E., Mayer, M. J., Steverding, D., Carding, S. R., & Narbad, A. (2013). Evaluation of bacteriophage therapy to control Clostridium difficile and toxin production in an in vitro human colon model system. *Anaerobe*, *22*, 25–30. https://doi.org/10.1016/j.anaerobe.2013.05.001

Meechaisue, C., Dubin, R., Supaphol, P., Hoven, V. P., & Kohn, J. (2006). Electrospun mat of tyrosine-derived polycarbonate fibers for potential use as tissue scaffolding material. *Journal of Biomaterials Science, Polymer Edition*, *17*(9), 1039–1056. https://doi.org/10.1163/156856206778365988

Megelski, S. (2002). Micro and nanostructured surface morphology on electrospun polymer fibers. *Macromolecules*, *35*(22), 8456–66.

Mele, E. (2016). Electrospinning of natural polymers for advanced wound care: towards responsive and adaptive dressings. *J. Mater. Chem. B*, *4*(4), 4801–4812. https://doi.org/10.1039/c6tb00804f

Merabishvili, M., Vervaet, C., Pirnay, J. P., de Vos, D., Verbeken, G., Mast, J., … Vaneechoutte, M. (2013). Stability of Staphylococcus aureus Phage ISP after Freeze-Drying (Lyophilization). *PLoS ONE*, *8*(7). https://doi.org/10.1371/journal.pone.0068797

Merril, C. R., Scholl, D., & Adhya, S. L. (2003). The prospect for bacteriophage therapy in Western medicine, *2*(June), 1–10.

Miller, D. P., & de Pablo, J. J. (2000). Calorimetric solution properties of simple saccharides and their significance for the stabilization of biological structure and function. *Journal of Physical Chemistry B*, *104*(37), 8876–8883. https://doi.org/Doi 10.1021/Jp000807d

Mirzaei, M. K., Haileselassie, Y., Navis, M., Cooper, C., & Nilsson, A. S. (2016). Morphologically Distinct Escherichia coli Bacteriophages Differ in Their Efficacy and Ability to Stimulate Cytokine Release In Vitro, *7*(March), 1–7. https://doi.org/10.3389/fmicb.2016.00437

Monk, a. B., Rees, C. D., Barrow, P., Hagens, S., & Harper, D. R. (2010). Bacteriophage applications: Where are we now? *Letters in Applied Microbiology*, *51*(4), 363–369. https://doi.org/10.1111/j.1472-765X.2010.02916.x

Morelli, S., Holdich, R. G., & Dragosavac, M. M. (2017). Microparticles for cell encapsulation and colonic delivery produced by membrane emulsi fi cation. *Journal of Membrane Science*, *524*(November 2016), 377–388. https://doi.org/10.1016/j.memsci.2016.11.058

Mountzouris, K. C., Tsirtsikos, P., Kalamara, E., Nitsch, S., Schatzmayr, G., & Fegeros, K. (2007). Evaluation of the efficacy of a probiotic containing Lactobacillus, Bifidobacterium, Enterococcus, and Pediococcus strains in promoting broiler performance and modulating cecal microflora composition and metabolic activities. *Poultry Science*, *86*(2), 309–317. https://doi.org/86/2/309 [pii]

Müller-Merbach, M., Rauscher, T., & Hinrichs, J. (2005). Inactivation of bacteriophages by thermal and high-pressure treatment. *International Dairy Journal*, *15*(6–9), 777–784. https://doi.org/10.1016/j.idairyj.2004.08.019

Nakashima, T., Shimizu, M., & Kukizaki, M. (2000). Particle control of emulsion by membrane emulsification and its applications. *Advanced Drug Delivery Reviews*, *45*(1), 47–56. https://doi.org/10.1016/S0169-409X(00)00099-5

Nale, J., Redgwell, T., Millard, A., & Clokie, M. (2018). Efficacy of an Optimised Bacteriophage Cocktail to Clear Clostridium difficile in a Batch Fermentation Model. *Antibiotics*, *7*(1), 13. https://doi.org/10.3390/antibiotics7010013

Nale, J. Y., Chutia, M., Carr, P., Hickenbotham, P. T., & Clokie, M. R. J. (2016). "Get in Early"; Biofilm and Wax Moth (Galleria mellonella) Models Reveal New Insights into the Therapeutic Potential of Clostridium difficile Bacteriophages. *Frontiers in Microbiology*, *7*(August), 1–16. https://doi.org/10.3389/fmicb.2016.01383

Nale, J. Y., Shan, J., Hickenbotham, P. T., Fawley, W. N., Wilcox, M. H., & Clokie, M. R. J. (2012). Diverse temperate bacteriophage carriage in Clostridium difficile 027 strains. *PLoS ONE*, *7*(5), 1–9. https://doi.org/10.1371/journal.pone.0037263

Nale, J. Y., Spencer, J., Hargreaves, K. R., Buckley, A. M., Trzepin, P., & Douce, G. R. (2016). Bacteriophage Combinations Significantly Reduce Clostridium difficile Growth In Vitro and Proliferation In Vivo, *60*(2), 968–981. https://doi.org/10.1128/AAC.01774-15.Address

Nataro, J. P., & Kaper, J. B. (1998). Diarrheagenic Escherichia coli. *Clinical Microbiology Reviews*,

11(1), 142–201. https://doi.org/file://Z:\References\Text Files\00000004472.txt

Navaneethan, U., & Giannella, R. a. (2009). Thinking beyond the colon-small bowel involvement in clostridium difficile infection. *Gut Pathogens*, *1*(1), 7. https://doi.org/10.1186/1757-4749-1-7

Nazir, A., Schroën, K., & Boom, R. (2010). Premix emulsification: A review. *Journal of Membrane Science*, *362*(1–2), 1–11. https://doi.org/10.1016/j.memsci.2010.06.044

Nguyen, D. a., & Fogler, H. S. (2005). Facilitated diffusion in the dissolution of carboxylic polymers. *AIChE Journal*, *51*(2), 415–425. https://doi.org/10.1002/aic.10329

Nicholson, J. K., Holmes, E., Kinross, J., Burcelin, R., Gibson, G., Jia, W., & Pettersson, S. (2012). Metabolic Interactions, *108*(June), 1262–1268.

Nie, Z., Xu, S., Seo, M., Lewis, P. C., & Kumacheva, E. (2005). Polymer particles with various shapes and morphologies produced in continuous microfluidic reactors. *Journal of the American Chemical Society*, *127*(22), 8058–8063. https://doi.org/10.1021/ja042494w

Nieth, A., Verseux, C., Barnert, S., Süss, R., & Römer, W. (2015). A first step toward liposome-mediated intracellular bacteriophage therapy. *Expert Opinion on Drug Delivery*, (May 2015), 1–14. https://doi.org/10.1517/17425247.2015.1043125

Nii, T., & Ishii, F. (2005). Encapsulation efficiency of water-soluble and insoluble drugs in liposomes prepared by the microencapsulation vesicle method. *International Journal of Pharmaceutics*, *298*(1), 198–205. https://doi.org/10.1016/j.ijpharm.2005.04.029

Niyogi, S. K. (2005). Shigellosis. *Journal of Microbiology*, *43*(2), 133–143. https://doi.org/file://Z:\References\Text Files\00000004522.txt

Nobrega, F. L., Costa, A. R., Kluskens, L. D., & Azeredo, J. (2015). Revisiting phage therapy: new applications for old resources. *Trends in Microbiology*, *23*(4), 185–191. https://doi.org/10.1016/j.tim.2015.01.006

Noren, T. (2010). *Clostridium dificille Method and Protocols*.

Og, G., Af, F., Sygdomme, S., Henrik, P., & Epidemiologisk, A. (2009). Clostridium difficile, *21*(2), 251–254.

Patil, P., Chavanke, D., & Wagh, M. (2012). A REVIEW ON IONOTROPIC GELATION METHOD : NOVEL APPROACH FOR CONTROLLED GASTRORETENTIVE GELISPHERES. *International Journal of Pharmacy and Pharmaceutical Sciences*, *4*.

Payne, R. J. H., & Jansen, V. (2001). Understanding Bacteriophage Therapy as a Density-dependent Kinetic Process. *Journal of Theoretical Biology*, *208*, 37–48. https://doi.org/10.1006/jtbi.2000.2198

Pehkonen, K. S., Roos, Y. H., Miao, S., Ross, R. P., & Stanton, C. (2008). State transitions and physicochemical aspects of cryoprotection and stabilization in freeze-drying of Lactobacillus rhamnosus GG (LGG). *Journal of Applied Microbiology*, *104*(6), 1732–1743. https://doi.org/10.1111/j.1365-2672.2007.03719.x

Peng, S. J., & Williams, R. A. (1998). Controlled production of emulsions using a crossflow membrane. Part I: Droplet formation from a single pore. *Chemical Engineering Research and Design*, *76*(A8), 894–901. https://doi.org/10.1205/026387698525694

Philip, A., & Philip, B. (2010). Colon Targeted Drug Delivery Systems: A Review on Primary and Novel Approaches. *Oman Medical Journal*, *25*(2), 70–78. https://doi.org/10.5001/omj.2010.24

Pillay, V., Seedat, A., Choonara, Y. E., du Toit, L. C., Kumar, P., & Ndesendo, V. M. K. (2013). A review of polymeric refabrication techniques to modify polymer properties for biomedical and drug delivery applications. *AAPS PharmSciTech*, *14*(2), 692–711. https://doi.org/10.1208/s12249-013-9955-z

Puapermpoonsiri, U., Spencer, J., & van der Walle, C. F. (2009). A freeze-dried formulation of bacteriophage encapsulated in biodegradable microspheres. *European Journal of Pharmaceutics and Biopharmaceutics*, *72*(1), 26–33. https://doi.org/10.1016/j.ejpb.2008.12.001

Rahman Yueh-Erh, Elizabeth, A. (1976). United States Patent 3,993,754.

Ramesh, V., Fralick, J. A., & Rolfe, R. D. (1999). Prevention of Clostridium difficile -induced ileocecitis with Bacteriophage.

Rashid, S., Barylski, J., Hargreaves, K., Millard, A., Vinner, G., & Clokie, M. (2016). Two Novel Myoviruses from the North of Iraq Reveal Insights into Clostridium difficile Phage Diversity and Biology. *Viruses*, *8*(11), 310. https://doi.org/10.3390/v8110310

Rea, M. C., Alemayehu, D., Ross, R. P., & Hill, C. (2013). Gut solutions to a gut problem: bacteriocins, probiotics and bacteriophage for control of Clostridium difficile infection. *Journal of Medical Microbiology*, *62*(Pt 9), 1369–78. https://doi.org/10.1099/jmm.0.058933-0

Ríos, Á., & Zougagh, M. (2015). Trends in Analytical Chemistry Modern qualitative analysis by miniaturized and microfluidic systems. *Trends in Analytical Chemistry*, *69*, 105–113.

https://doi.org/10.1016/j.trac.2015.04.003

Roca, I., Akova, M., Baquero, F., Carlet, J., Cavaleri, M., Coenen, S., … Vila, J. (2015). The global threat of antimicrobial resistance: Science for intervention. *New Microbes and New Infections*, *6*(February 2015), 22–29. https://doi.org/10.1016/j.nmni.2015.02.007

Rose, T., Verbeken, G., Vos, D. De, Merabishvili, M., Vaneechoutte, M., Jennes, S., … Pirnay, J. (2014). Experimental phage therapy of burn wound infection : difficult first steps. *Int J Burn Trauma*, *4*(2), 66–73.

Rotimi, V. O., Jamal, W. Y., Mokaddas, E. M., Brazier, J. S., Johny, M., & Duerden, B. I. (2003). Prevalent PCR ribotypes of clinical and environmental strains of Clostridium difficile isolated from intensive-therapy unit patients in Kuwait, 705–709. https://doi.org/10.1099/jmm.0.05207-0

Rupnik, M., Wilcox, M. H., & Gerding, D. N. (2009). Clostridium difficile infection: new developments in epidemiology and pathogenesis. *Nature Reviews. Microbiology*, *7*(7), 526–536. https://doi.org/10.1038/nrmicro2164

Sadeghifard, N., Gürtler, V., Beer, M., & Seviour, R. J. (2006). The mosaic nature of intergenic 16S-23S rRNA spacer regions suggests rRNA operon copy number variation in Clostridium difficile strains. *Applied and Environmental Microbiology*, *72*(11), 7311–7323. https://doi.org/10.1128/AEM.01179-06

Saez, A. C. ., Zhang, J. ., Rostagno, M. H. ., & Ebner, P. D. . (2011). Direct feeding of microencapsulated bacteriophages to reduce salmonella colonization in pigs. *Foodborne Pathogens and Disease*, *8*(12), 1269–1274.

Sağlam, D., Venema, P., de Vries, R., Sagis, L. M. C., & van der Linden, E. (2011). Preparation of high protein micro-particles using two-step emulsification. *Food Hydrocolloids*, *25*(5), 1139–1148. https://doi.org/10.1016/j.foodhyd.2010.10.011

Salalha, W., Kuhn, J., Dror, Y., & Zussman, E. (2006). Encapsulation of bacteria and viruses in electrospun nanofibres. *Nanotechnology*, *17*(18), 4675–4681. https://doi.org/10.1088/0957-4484/17/18/025

Samtlebe, M., Ergin, F., Wagner, N., Neve, H., Küçükçetin, A., Franz, C. M. a. P., … Atamer, Z. (2016). Carrier systems for bacteriophages to supplement food systems: Encapsulation and controlled release to modulate the human gut microbiota. *LWT - Food Science and Technology*, *68*, 334–340. https://doi.org/10.1016/j.lwt.2015.12.039

Sandborn, W. J., Kamm, M. a, Lichtenstein, G. R., Lyne, a, Butler, T., & Joseph, R. E. (2007). MMX Multi Matrix System mesalazine for the induction of remission in patients with mild-to-moderate ulcerative colitis: a combined analysis of two randomized, double-blind, placebo-controlled trials. *Alimentary Pharmacology & Therapeutics*, *26*(2), 205–215. https://doi.org/10.1111/j.1365-2036.2007.03361.x

Sarker, S. A., Sultana, S., Reuteler, G., Moine, D., Descombes, P., Charton, F., … Brüssow, H. (2016). Oral Phage Therapy of Acute Bacterial Diarrhea With Two Coliphage Preparations: A Randomized Trial in Children From Bangladesh. *EBioMedicine*, *4*, 124–137. https://doi.org/10.1016/j.ebiom.2015.12.023

Scallan, E., Hoekstra, R. M., Angulo, F. J., Tauxe, R. V, Widdowson, M., Roy, S. L., … Griffin, P. M. (2011). Foodborne Illness Acquired in the United States — Major Pathogens. *Emerging Infectious Diseases*, *17*(1), 7–15. https://doi.org/10.3201/eid1701.P11101

Schmelcher, M., & Loessner, M. J. (2014). Application of bacteriophages for detection of foodborne pathogens. *Bacteriophage*, *4*(1), e28137. https://doi.org/10.4161/bact.28137

Scholl, D., Adhya, S., & Merril, C. (2005). Escherichia coli K1 ' s Capsule Is a Barrier to Bacteriophage T7. *Applied and Environmental Microbiology*, *71*(8), 4872–4874. https://doi.org/10.1128/AEM.71.8.4872

Scholl, D., & Merril, C. (2005). The genome of bacteriophage K1F, a T7-like phage that has acquired the ability to replicate on K1 strains of Escherichia coli. *Journal of Bacteriology*, *187*(24), 8499–8503. https://doi.org/10.1128/JB.187.24.8499-8503.2005

Sekirov, I., Russell, S., & Antunes, L. (2010). Gut microbiota in health and disease. *Physiological Reviews*, *90*(3), 859–904. https://doi.org/10.1152/physrev.00045.2009.

Sen, C. K., Gordillo, G. M., Roy, S., Kirsner, R., Lambert, L., Hunt, T. K., … Longaker, M. T. (2009). Human skin wounds: A major and snowballing threat to public health and the economy: PERSPECTIVE ARTICLE. *Wound Repair and Regeneration*, *17*(6), 763–771. https://doi.org/10.1111/j.1524-475X.2009.00543.x

Senuma, Y., Lowe, C., Zweifel, Y., Hilborn, J. G., & Marison, I. (2000). Alginate hydrogel microspheres and microcapsules prepared by spinning disk atomization. *Biotechnology and Bioengineering*, *67*(5), 616–22. Retrieved from http://www.ncbi.nlm.nih.gov/pubmed/10649236

Seo, M., Paquet, C., Nie, Z., Xu, S., & Kumacheva, E. (2007). Microfluidic consecutive flow-focusing droplet generators. *Soft Matter*, *3*(8), 986. https://doi.org/10.1039/b700687j

Shan, J., Ramachandran, A., Thanki, A. M., Vukusic, F. B. I., Barylski, J., & Clokie, M. R. J. (2018). Bacteriophages are more virulent to bacteria with human cells than they are in bacterial culture; insights from HT-29 cells. *Scientific Reports*, *8*(1), 5091. https://doi.org/10.1038/s41598-018-23418-y

Sharma, M. (2013). Lytic bacteriophages: Potential interventions against enteric bacterial pathogens on produce. *Bacteriophage*, *3*(2), e25518. https://doi.org/10.4161/bact.25518

She, X., Chen, L., Velleman, L., Li, C., Zhu, H., He, C., … Kong, L. (2015). Fabrication of high specificity hollow mesoporous silica nanoparticles assisted by Eudragit for targeted drug delivery. *Journal of Colloid and Interface Science*, *445*, 151–160. https://doi.org/10.1016/j.jcis.2014.12.053

Shi, L. E., Zheng, W., Zhang, Y., & Tang, Z. X. (2016). Milk-alginate microspheres: Protection and delivery of Enterococcus faecalis HZNU P2. *LWT - Food Science and Technology*, *65*, 840–844. https://doi.org/10.1016/j.lwt.2015.08.071

Sill, T. J., & von Recum, H. A. (2008). Electrospinning: Applications in drug delivery and tissue engineering. *Biomaterials*, *29*(13), 1989–2006. https://doi.org/10.1016/j.biomaterials.2008.01.011

Silva, C. M., Ribeiro, A. J., Ferreira, D., & Veiga, F. (2006). Insulin encapsulation in reinforced alginate microspheres prepared by internal gelation. *European Journal of Pharmaceutical Sciences : Official Journal of the European Federation for Pharmaceutical Sciences*, *29*(2), 148–59. https://doi.org/10.1016/j.ejps.2006.06.008

Silva, P. S., Dragosavac, M. M., Vladisavljevic, G. T., Bandulasena, H. C. H., & Holdich, R. G. (2015). Droplet microfluidics on a planar surface. *American Institute of Chemical Engineers AIChE J, 51: 415–425, 2005*, *61*(504), 3–194. https://doi.org/10.1002/aic

Singla, S., Harjai, K., Katare, O. P., & Chhibber, S. (2016). Encapsulation of Bacteriophage in Liposome Accentuates Its Entry in to Macrophage and Shields It from Neutralizing Antibodies. *Plos One*, *11*(4), e0153777. https://doi.org/10.1371/journal.pone.0153777

Singla, S., Harjai, K., Raza, K., Wadhwa, S., Katare, O. P., & Chhibber, S. (2016). Phospholipid vesicles encapsulated bacteriophage: A novel approach to enhance phage biodistribution. *Journal of Virological Methods*. https://doi.org/10.1016/j.jviromet.2016.07.002

Sinha, V. R., & Kumria, R. (2001). Polysaccharides in colon-specific drug delivery. *International Journal of Pharmaceutics*, *224*(1–2), 19–38. https://doi.org/10.1016/S0378-5173(01)00720-7

Siqueira, R. S. De, Dodd, C. E. R., & Rees, C. E. D. (2006). Evaluation of the natural virucidal activity of

teas for use in the phage amplification assay, *111*, 259–262. https://doi.org/10.1016/j.ijfoodmicro.2006.04.047

Sirard, S., Valiquette, L., & Fortier, L. C. (2011). Lack of association between clinical outcome of Clostridium difficile infections, strain type, and virulence-associated phenotypes. *Journal of Clinical Microbiology*, *49*(12), 4040–4046. https://doi.org/10.1128/JCM.05053-11

Smith, Williams; Huggins, Michael B.; Shaw, K. M. ; (1987). The Control of Experimental Escherichia coli Diarrhoea in Calves by Means of Bacteriophages. *Journal of General Microbiology*, *133*, 1111–1126.

Smith, H. W., Huggins, M. B., & Shaw, K. M. (1987). The control of experimental Escherichia coli diarrhoea in calves by means of bacteriophages. *Journal of General Microbiology*, *133*(5), 1111–26. https://doi.org/10.1099/00221287-133-5-1111

Smits, W. (2013). Hype or hypervirulence. A reflection on problematic C. difficile strains. *Virulence*, *4*(7), 592–596. https://doi.org/10.4161/viru.26297

Sookkasem, A., Chatpun, S., Yuenyongsawad, S., & Wiwattanapatapee, R. (2015). Alginate beads for colon specific delivery of self-emulsifying curcumin. *Journal of Drug Delivery Science and Technology*, *29*, 159–166. https://doi.org/10.1016/j.jddst.2015.07.005

Soto, M. J. ., Retamales, J. ., Palza, H. ., & Bastias, R. . (2018). Encapsulation of specific Salmonella Enteritidis phage f3αSE on alginate-spheres as a method for protection and dosification. *Electronic Journal of Biotechnology*, *31*, 57–60.

Souza, D. F. De, Goebel, K., & Andreazza, I. F. (2013). Development of enteric coated sustained release minitablets containing mesalamine, *49*.

Spyropoulos, F., Lloyd, D. M., Hancocks, R. D., & Pawlik, A. K. (2014). Advances in membrane emulsification. Part A: Recent developments in processing aspects and microstructural design approaches. *Journal of the Science of Food and Agriculture*, *94*(4), 613–627. https://doi.org/10.1002/jsfa.6444

Spyropoulosa, F., Hancocks, R. D., & Norton, I. T. (2011). Food-grade emulsions prepared by membrane emulsification techniques. *Procedia Food Science*, *1*, 920–926. https://doi.org/10.1016/j.profoo.2011.09.139

Stanford, K., Niu, Y. D., & Johnson, R. (2010a). Oral delivery systems for encapsulated bacteriophages targeted at Escherichia coli O157 : H7 in feedlot cattle. *Journal of Food Protection*, *73*(7), 1304–1312.

Stanford, K., Niu, Y. D., & Johnson, R. (2010b). Oral delivery systems for encapsulated bacteriophages targeted at Escherichia coli O157 : H7 in feedlot cattle . *Journal of Food Protection*, (June 2015).

Stillwell, M. T., Holdich, R. G., Kosvintsev, S. R., Gasparini, G., & Cumming, I. W. (2007). Stirred cell membrane emulsification and factors influencing dispersion drop size and uniformity. *Industrial and Engineering Chemistry Research*, *46*(3), 965–972. https://doi.org/10.1021/ie0611094

Sulakvelidze, A., & Alavidze, Z. (2001). MINIREVIEW Bacteriophage Therapy, *45*(3), 649–659. https://doi.org/10.1128/AAC.45.3.649

Sutter, R., Tschudin-Sutter, S., Grize, L., Fuhr, P., Bonten, M. J. M., Widmer, A. F., … Rüegg, S. (2012). Associations between infections and clinical outcome parameters in status epilepticus: A retrospective 5-year cohort study. *Epilepsia*, *53*(9), 1489–1497. https://doi.org/10.1111/j.1528-1167.2012.03576.x

Tang, Z., Huang, X., Baxi, S., Chambers, J. R., Sabour, P. M., & Wang, Q. (2013). Whey protein improves survival and release characteristics of bacteriophage Felix O1 encapsulated in alginate microspheres. *Food Research International*, *52*(2), 460–466. https://doi.org/10.1016/j.foodres.2012.12.037

Tang, Z., Huang, X., Sabour, P. M., Chambers, J. R., & Wang, Q. (2014). Preparation and characterization of dry powder bacteriophage K for intestinal delivery through oral administration. *LWT - Food Science and Technology*, *60*(1), 263–270. https://doi.org/10.1016/j.lwt.2014.08.012

Tang, Z., Huang, X., Sabour, P. M., Chambers, J. R., & Wang, Q. (2015). Preparation and characterization of dry powder bacteriophage K for intestinal delivery through oral administration. *LWT - Food Science and Technology*, *60*(1), 263–270. https://doi.org/10.1016/j.lwt.2014.08.012

Tanji, Y., Shimada, T., Fukudomi, H., Miyanaga, K., Nakai, Y., & Unno, H. (2005). Therapeutic use of phage cocktail for controlling Escherichia coli O157:H7 in gastrointestinal tract of mice. *Journal of Bioscience and Bioengineering*, *100*(3), 280–7. https://doi.org/10.1263/jbb.100.280

Tanji, Y., Shimada, T., Yoichi, M., Miyanaga, K., Hori, K., & Unno, H. (2004). Toward rational control of Escherichia coli O157:H7 by a phage cocktail. *Applied Microbiology and Biotechnology*, *64*(2), 270–274. https://doi.org/10.1007/s00253-003-1438-9

Taylor, G. (1969). Electrically Driven Jets. *Proceedings of the Royal Society A: Mathematical, Physical and Engineering Sciences*, *313*(1515), 453–475. https://doi.org/10.1098/rspa.1969.0205

Thomas E. Waddell, Roger Johnson, A. M. (2013, October 15). Methods and compositions for controlled release of bioactive compounds. Retrieved from http://www.google.com/patents/CA2463827C?cl=en

Thorsen, T., Roberts, R. W., Arnold, F. H., & Quake, S. R. (2001). Dynamic pattern formation in a vesicle-generating microfluidic device. *Physical Review Letters*, *86*(18), 4163–4166. https://doi.org/10.1103/PhysRevLett.86.4163

Tiwari Ruchi; Kuldeep Dhama; Sandip Chakraborty; Amit Kumar; Anu Rahal; kapoor Snajay. (2014). Bacteriophae Therapy for safeguarding animal and human health a review.pdf.

Un, S. A. M., & Lements, D. J. U. M. C. C. (2007). Preparation and Characterization of Water / Oil and Water / Oil / Water Emulsions Containing Biopolymer-Gelled Water Droplets.

Utada, A. S., Fernandez-Nieves, A., Stone, H. a., & Weitz, D. a. (2007). Dripping to jetting transitions in coflowing liquid streams. *Physical Review Letters*, *99*(9), 1–4. https://doi.org/10.1103/PhysRevLett.99.094502

Van Citters, G. W., & Lin, H. C. (2006). Ileal brake: Neuropeptidergic control of intestinal transit. *Current Gastroenterology Reports*, *8*(5), 367–373. https://doi.org/10.1007/s11894-006-0021-9

Van Den Beld, M. J. C., & Reubsaet, F. A. G. (2012). Differentiation between Shigella, enteroinvasive Escherichia coli (EIEC) and noninvasive Escherichia coli. *European Journal of Clinical Microbiology and Infectious Diseases*, *31*(6), 899–904. https://doi.org/10.1007/s10096-011-1395-7

Van Der Graaf, S., Schroën, C. G. P. H., & Boom, R. M. (2005). Preparation of double emulsions by membrane emulsification - A review. *Journal of Membrane Science*, *251*(1–2), 7–15. https://doi.org/10.1016/j.memsci.2004.12.013

Vandamme, T. F., Lenourry, a., Charrueau, C., & Chaumeil, J. C. (2002). The use of polysaccharides to target drugs to the colon. *Carbohydrate Polymers*, *48*(3), 219–231. https://doi.org/10.1016/S0144-8617(01)00263-6

Vandenheuvel, D., Meeus, J., Lavigne, R., & Van Den Mooter, G. (2014). Instability of bacteriophages in spray-dried trehalose powders is caused by crystallization of the matrix. *International Journal of Pharmaceutics*, *472*(1–2), 202–205. https://doi.org/10.1016/j.ijpharm.2014.06.026

Vandenheuvel, D., Singh, A., Vandersteegen, K., Klumpp, J., Lavigne, R., & Van Den Mooter, G. (2013a). Feasibility of spray drying bacteriophages into respirable powders to combat pulmonary bacterial infections. *European Journal of Pharmaceutics and Biopharmaceutics*,

84(3). https://doi.org/10.1016/j.ejpb.2012.12.022

Vandenheuvel, D., Singh, A., Vandersteegen, K., Klumpp, J., Lavigne, R., & Van Den Mooter, G. (2013b). Feasibility of spray drying bacteriophages into respirable powders to combat pulmonary bacterial infections. *European Journal of Pharmaceutics and Biopharmaceutics*, *84*(3), 578–582. https://doi.org/10.1016/j.ejpb.2012.12.022

Vandenheuvel, D., Singh, A., Vandersteegen, K., Klumpp, J., Lavigne, R., & Van Den Mooter, G. (2013c). Feasibility of spray drying bacteriophages into respirable powders to combat pulmonary bacterial infections. *European Journal of Pharmaceutics and Biopharmaceutics*, *84*(3), 578–582. https://doi.org/10.1016/j.ejpb.2012.12.022

Vardakas, K. Z., Polyzos, K. a., Patouni, K., Rafailidis, P. I., Samonis, G., & Falagas, M. E. (2012). Treatment failure and recurrence of Clostridium difficile infection following treatment with vancomycin or metronidazole: A systematic review of the evidence. *International Journal of Antimicrobial Agents*, *40*(1), 1–8. https://doi.org/10.1016/j.ijantimicag.2012.01.004

Velge, P., Wiedemann, A., Rosselin, M., Abed, N., Boumart, Z., Chaussé, A. M., … Virlogeux-Payant, I. (2012). Multiplicity of Salmonella entry mechanisms, a new paradigm for Salmonella pathogenesis. *MicrobiologyOpen*, *1*(3), 243–258. https://doi.org/10.1002/mbo3.28

Vemula, S. K., Veerareddy, P. R., & Devadasu, V. R. (2015). Pharmacokinetics of colon-specific pH and time-dependent flurbiprofen tablets. *European Journal of Drug Metabolism and Pharmacokinetics*, *40*(3), 301–311. https://doi.org/10.1007/s13318-014-0210-0

Vinner, G. K., Vladisavljević, G. T., Clokie, M. R. J., & Malik, D. J. (2017). Microencapsulation of Clostridium difficile specific bacteriophages using microfluidic glass capillary devices for colon delivery using pH triggered release. *PLoS ONE*, *12*(10), 0–27. https://doi.org/10.1371/journal.pone.0186239

Viswanathan, V. K., Hodges, K., & Hecht, G. (2009). Enteric infection meets intestinal function: how bacterial pathogens cause diarrhoea. *Nat Rev Microbiol*, *7*(2), 110–119. https://doi.org/10.1038/nrmicro2053

Vladisavljevic, G. T. (2015). Structured microparticles with tailored properties produced by membrane emulsification. *Advances in Colloid and Interface Science*, *225*, 53–87. https://doi.org/10.1016/j.cis.2015.07.013

Vladisavljević, G. T., Duncanson, W. J., Shum, H. C., & Weitz, D. a. (2012). Emulsion templating of poly(lactic acid) particles: Droplet formation behavior. *Langmuir*, *28*(36), 12948–12954.

https://doi.org/10.1021/la302092f

Vladisavljević, G. T., Kobayashi, I., & Nakajima, M. (2012). Production of uniform droplets using membrane, microchannel and microfluidic emulsification devices. *Microfluidics and Nanofluidics*, *13*(1), 151–178. https://doi.org/10.1007/s10404-012-0948-0

Vladisavljević, G. T., Shimizu, M., & Nakashima, T. (2006). Production of multiple emulsions for drug delivery systems by repeated SPG membrane homogenization: Influence of mean pore size, interfacial tension and continuous phase viscosity. *Journal of Membrane Science*, *284*(1–2), 373–383. https://doi.org/10.1016/j.memsci.2006.08.003

Voth, D., & Ballard, J. (2005). Clostridium difficile toxins: mechanism of action and role in disease. *Clinical Microbiology Reviews*, *18*(2), 247–263. https://doi.org/10.1128/CMR.18.2.247

Waddell, T. E., Johnson, R., & Mazzocco, A. (2013). Methods and compositions for controlled release of bioactive compounds Publication type. *Patent CA2463827*, (11).

Wagdare, N. A., Marcelis, A. T. M., Ho, O. B., Boom, R. M., & van Rijn, C. J. M. (2010). High throughput vegetable oil-in-water emulsification with a high porosity micro-engineered membrane. *Journal of Membrane Science*, *347*(1–2), 1–7. https://doi.org/10.1016/j.memsci.2009.09.057

Walker, A. S., Eyre, D. W., Wyllie, D. H., Dingle, K. E., Harding, R. M., Connor, O., … Peto, T. E. A. (2012). Characterisation of Clostridium difficile Hospital Ward – Based Transmission Using Extensive Epidemiological Data and Molecular Typing, *9*(2). https://doi.org/10.1371/journal.pmed.1001172

Wall, S. K., Zhang, J., Rostagno, M. H., & Ebner, P. D. (2010). Phage therapy to reduce preprocessing Salmonella infections in market-weight swine. *Applied and Environmental Microbiology*, *76*(1), 48–53. https://doi.org/10.1128/AEM.00785-09

Walters, R. H., Bhatnagar, B., Tchessalov, S., Izutsu, K.-I., Tsumoto, K., & Ohtake, S. (2014). Next generation drying technologies for pharmaceutical applications. *Journal of Pharmaceutical Sciences*, *103*(9), 2673–95. https://doi.org/10.1002/jps.23998

Wang, C., Chien, H. S., Yan, K. W., Hung, C. L., Hung, K. L., Tsai, S. J., & Jhang, H. J. (2009). Correlation between processing parameters and microstructure of electrospun poly(D,l-lactic acid) nanofibers. *Polymer*, *50*(25), 6100–6110. https://doi.org/10.1016/j.polymer.2009.10.025

Wang, Y., Li, P., Peng, Z., She, F. H., & Kong, L. X. (2013). Microencapsulation of nanoparticles with enhanced drug loading for pH-sensitive oral drug delivery for the treatment of colon cancer.

Journal of Applied Polymer Science, *129*(2), 714–720. https://doi.org/10.1002/app.38582

Watanabe, R., Matsumoto, T., Sano, G., Ishii, Y., Tateda, K., Sumiyama, Y., … Yamaguchi, K. (2007). Efficacy of bacteriophage therapy against gut-derived sepsis caused by Pseudomonas aeruginosa in mice. *Antimicrobial Agents and Chemotherapy*, *51*(2), 446–452. https://doi.org/10.1128/AAC.00635-06

WHO. (2014). Antimicrobial resistance. Global report on surveillance. *World Health Organization*, *61*(3), 383–394. https://doi.org/10.1007/s13312-014-0374-3

Wikswo, M. E., Kambhampati, A., Shioda, K., Walsh, K. A., Bowen, A., & Hall, A. J. (2015). Outbreaks of Acute Gastroenteritis Transmitted by Person-to-Person Contact, Environmental Contamination, and Unknown Modes of Transmission — United States, 2009–2013. *MMWR. Surveillance Summaries*, *64*(12), 1–16. https://doi.org/10.15585/mmwr.mm6412a1

Wilcox, M. H. (2011). Laboratory diagnosis of Clostridium difficile infection: In a state of transition or confusion or both? *Journal of Hospital Infection*, *79*(1), 1–3. https://doi.org/10.1016/j.jhin.2011.05.010

Wilcox, M. H., Shetty, N., Fawley, W. N., Shemko, M., Coen, P., Birtles, a., … Wren, M. W. D. (2012). Changing epidemiology of clostridium difficile infection following the introduction of a national ribotyping-based surveillance scheme in England. *Clinical Infectious Diseases*, *55*(8), 1056–1063. https://doi.org/10.1093/cid/cis614

Wilcox, M. H., & Smyth, E. T. M. (1998). Incidence and impact of Clostridium difficile infection in the UK, 1993-1996. *Journal of Hospital Infection*, *39*(3), 181–187. https://doi.org/10.1016/S0195-6701(98)90256-0

Williams, R. A., & Vladisavljevic, G. T. (2005). Recent developments in manufacturing emulsions and particulate products using membranes, *113*, 1–20. https://doi.org/10.1016/j.cis.2004.10.002

Wills, Q. F., Kerrigan, C., & Soothill, J. S. (2005). Experimental Bacteriophage Protection against Staphylococcus aureus Abscesses in a Rabbit Model Experimental Bacteriophage Protection against Staphylococcus aureus Abscesses in a Rabbit Model. *Antimicrobial Agents and Chemotherapy*, *49*(3), 1220–1221. https://doi.org/10.1128/AAC.49.3.1220

Wittaya-areekul, S., Kruenate, J., & Prahsarn, C. (2006). Preparation and in vitro evaluation of mucoadhesive properties of alginate / chitosan microparticles containing prednisolone. *Int. J. Pharm.*, *312*, 113–118. https://doi.org/10.1016/j.ijpharm.2006.01.003

Xiao, B., Laroui, H., Ayyadurai, S., Viennois, E., Charania, M. A., Zhang, Y., & Merlin, D. (2012).

Mannosylated bioreducible nanoparticle-mediated macrophage specific TNF-alpha RNA interference for IBD therapy. *Changes*, *29*(6), 997–1003. https://doi.org/10.1016/j.biotechadv.2011.08.021.Secreted

Xu, J. H., Li, S. W., Tan, J., & Luo, G. S. (2008). Correlations of droplet formation in T-junction microfluidic devices: From squeezing to dripping. *Microfluidics and Nanofluidics*, *5*(6), 711–717. https://doi.org/10.1007/s10404-008-0306-4

Xu, Q., & Nakajima, M. (2004). The generation of highly monodisperse droplets through the breakup of hydrodynamically focused microthread in a microfluidic device. *Applied Physics Letters*, *85*(17), 3726–3728. https://doi.org/10.1063/1.1812380

Yadav, D., Survase, S., & Kumar, N. (2011). Dual coating of swellable and rupturable polymers on glipizide loaded MCC pellets for pulsatile delivery: formulation design and in vitro evaluation. *International Journal of Pharmaceutics*, *419*(1–2), 121–30. https://doi.org/10.1016/j.ijpharm.2011.07.026

Yang, M., Yamamoto, H., Kurashima, H., Takeuchi, H., Yokoyama, T., Tsujimoto, H., & Kawashima, Y. (2012). Design and evaluation of inhalable chitosan-modified poly (DL-lactic-co-glycolic acid) nanocomposite particles. *European Journal of Pharmaceutical Sciences : Official Journal of the European Federation for Pharmaceutical Sciences*, *47*(1), 235–43. https://doi.org/10.1016/j.ejps.2012.05.016

Yarin, A. L., Koombhongse, S., & Reneker, D. H. (2001). Bending instability in electrospinning of nanofibers. *Journal of Applied Physics*, *89*(5), 3018–3026. https://doi.org/10.1063/1.1333035

Yen, M., Cairns, L. S., Camilli, A., Zuckerman, J. N., Rombo, L., Fisch, A., … Camilli, A. (2017). A cocktail of three virulent bacteriophages prevents Vibrio cholerae infection in animal models. *Nature Communications*, *8*, 14187. https://doi.org/10.1038/ncomms14187

Yin, X., & Sto, H. D. H. (2003). Hydrogel Microspheres Formed by Complex Coacervation of Partially MPEG-Grafted Poly (styrene- alt -maleic anhydride) with PDADMAC and Cross-Linking with Polyamines, 8773–8779.

Yongsheng, M., Pacan, J. C., Wang, Q., Xu, Y., Huang, X., Korenevsky, A., & Sabour, P. M. (2008). Microencapsulation of bacteriophage felix o1 into chitosan-alginate microspheres for oral delivery. *Applied and Environmental Microbiology*, *74*(15), 4799–4805. https://doi.org/10.1128/AEM.00246-08

Young, R., & Gill, J. J. (2015). Phage therapy redux — What is to be done? *Science*, *350*(6265), 1163–

64. https://doi.org/10.1126/science.aad8222

Yu, J. H., Fridrikh, S. V, & Rutledge, G. C. (2006). The role of elasticity in the formation of electrospun fibers, *47*, 4789–4797. https://doi.org/10.1016/j.polymer.2006.04.050

Zahedi, P., Rezaeian, I., Ranaei-Siadat, S. O., Jafari, S. H., & Supaphol, P. (2010). A review on wound dressings with an emphasis on electrospun nanofibrous polymeric bandages. *Polymers for Advanced Technologies*, *21*(2), 77–95. https://doi.org/10.1002/pat.1625

Zargham, S., Bazgir, S., Tavakoli, A., Rashidi, A. S., & Damerchely, R. (2012). The Effect of Flow Rate on Morphology and Deposition Area of Electrospun Nylon 6 Nanofiber. *Journal of Engineered Fibers and Fabrics*, *7*(4), 42–49.

Zeleny, J. (1935). The role of surface instability in electrical discharges from drops of alcohol and water in air at atmospheric pressure. *Journal of the Franklin Institute*, *219*(6). https://doi.org/http://dx.doi.org/10.1016/S0016-0032(35)91985-8

Zhang, C., & Yuan, X. (2005). EUROPEAN POLYMER Study on morphology of electrospun poly (vinyl alcohol) mats, *41*, 423–432. https://doi.org/10.1016/j.eurpolymj.2004.10.027

Zhang, S., Luo, Y., Zeng, H., Wang, Q., Tian, F., Song, J., & Cheng, W. H. (2011). Encapsulation of selenium in chitosan nanoparticles improves selenium availability and protects cells from selenium-induced DNA damage response. *Journal of Nutritional Biochemistry*, *22*(12), 1137–1142. https://doi.org/10.1016/j.jnutbio.2010.09.014

Zhang, Y. Z., Wang, X., Feng, Y., Li, J., Lim, C. T., & Ramakrishna, S. (2006). Coaxial electrospinning of (fluorescein isothiocyanate-conjugated bovine serum albumin)-encapsulated poly(ε-caprolactone) nanofibers for sustained release. *Biomacromolecules*, *7*(4), 1049–1057. https://doi.org/10.1021/bm050743i

Zhao, C.-X. (2013). Multiphase flow microfluidics for the production of single or multiple emulsions for drug delivery. *Advanced Drug Delivery Reviews*, *65*(11–12), 1420–46. https://doi.org/10.1016/j.addr.2013.05.009

Zhao, R., Sun, J., Torley, P., Wang, D., & Niu, S. (2008). Measurement of particle diameter of Lactobacillus acidophilus microcapsule by spray drying and analysis on its microstructure. *World Journal of Microbiology and Biotechnology*, *24*(8), 1349–1354. https://doi.org/10.1007/s11274-007-9615-0

Chapter 10: Appendix

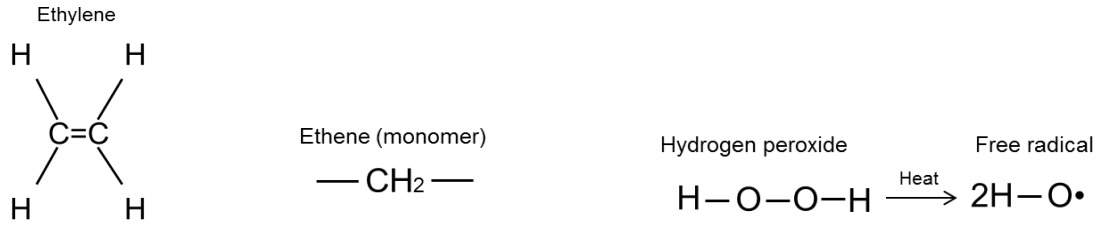

a) Initiation

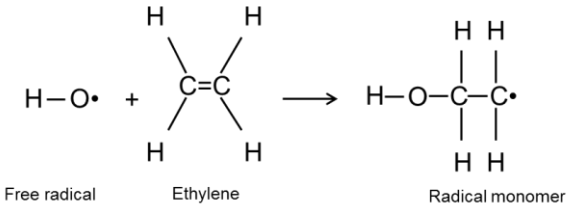

b) Propagation

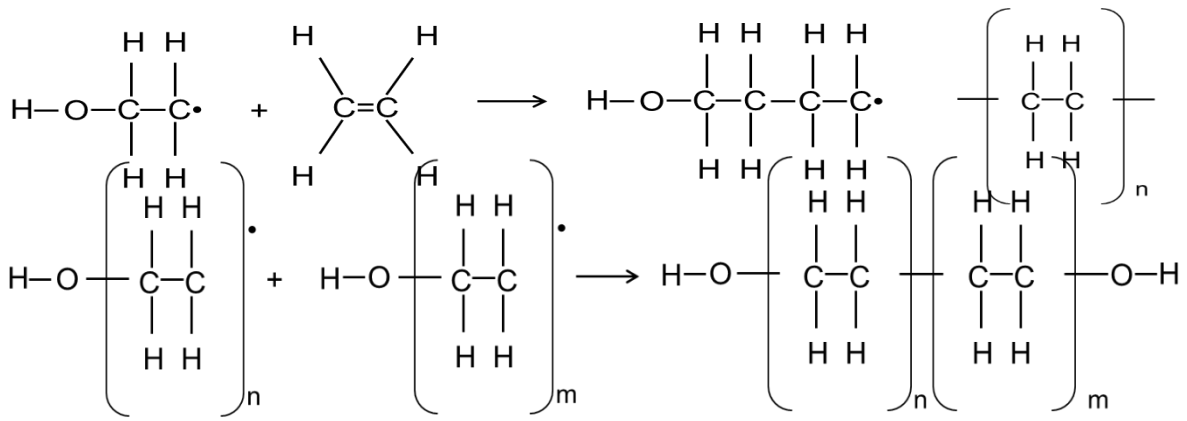

c) Or Termination

Figure 9.1. Chemical reactions that occur during formation of polymer, polyethylene. During initiation (a) a hydrogen peroxide free radical activated a monomer (ethane) by opening the double bond between two carbons. This triggers the propagating step (b) an unstable monomer activates other monomers forming a chain of saturated polymer. Termination is when the reaction stops (c) by coming together of two unstable monomers. The two radicals react with each other and form a stable subunit and no further reaction takes place.

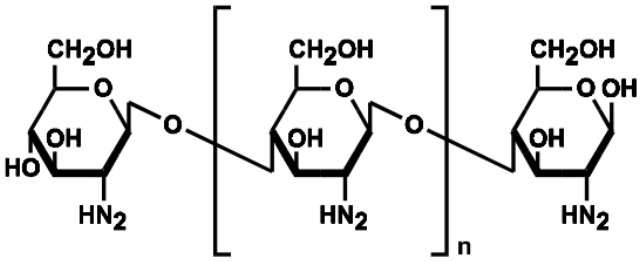

Figure 9.2. Chitosan chemical structure

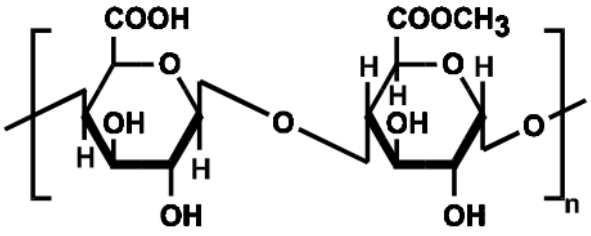

Figure 9.3. Pectin chemical structure

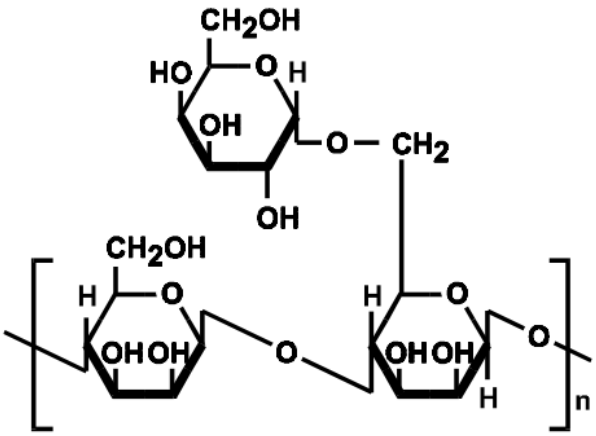

Figure 9.4 Guar gum chemical structure

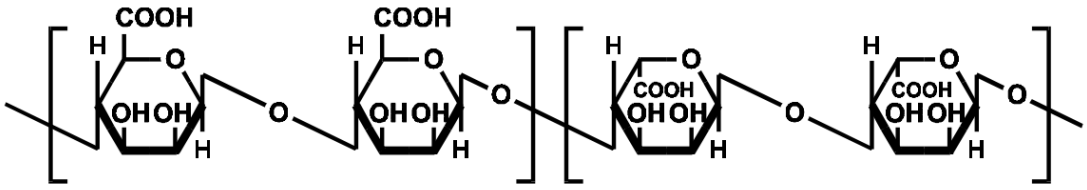

Figure 9.5 Alginate chemical structure

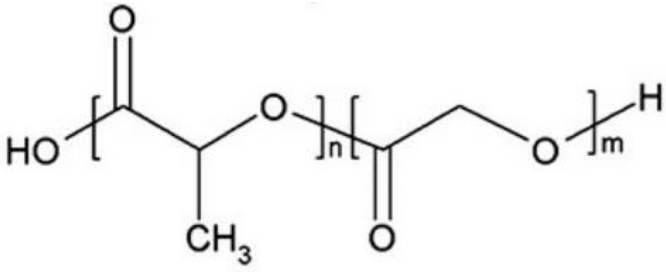

Figure 9.6 Poly lactic-co-glycolic acid chemical structure

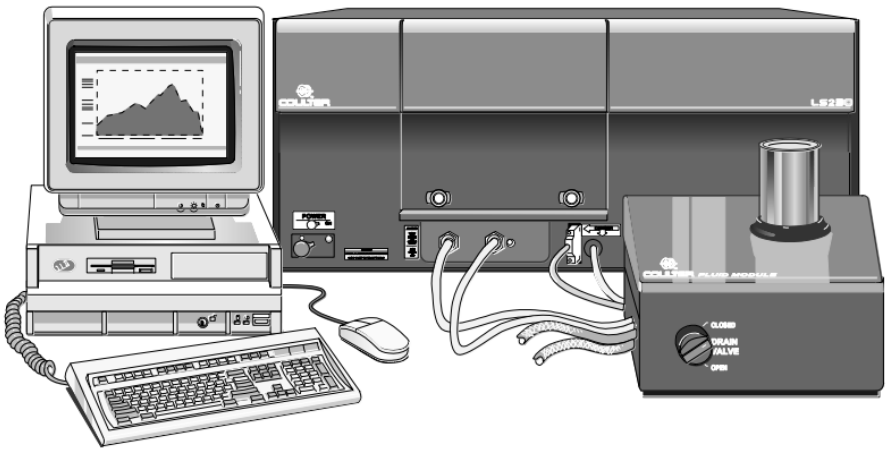

Figure 9.7 Coulter LS series instrument set up

Method 9.1 FAS Coating

Procedure
(Using chloroform as solvent)
“FAS coating solution”
To prepare this solution prior to start clean procedure in order to give time for the diffusion of FAS.
To add 1 mL of FAS in 114 mL of chloroform. 10^{-2} M FAS
Clean the membrane according to the following steps:
1. Alkali clean (4M NaOH), 1 minutes in US bath with 5 minutes soak
2. Tap water rinse, place into distilled water, 1 minute in US bath
3. Acid clean (10% HCl), 1 minutes in US bath with 5 minutes soak
4. Tap water rinse, place into distilled water, 1 minute in US bath
5. Dry
Coating the membrane according to the following steps:
1. To put about 40 mL of FAS solution into a beaker of 100 mL.
2. To place the cleaned membrane into the beaker. (Check if there are no air bubbles, at the membrane surface).
3. A total soaking of at least 2 days is recommended plus 3 minutes initially in the US bath.
4. Seal the beakers with (kitchen) plastic film.
5. Dry and then ready to use.
(It was observed that is possible to reuse the FAS solution at least 1 time)
The FAS used is: 1H, 1H, 2H, 2H-Perfluorodecyltriethoxysilane. This chemical was purchased from Fluorochem®.
Procedure
(Using undecane as solvent)
“FAS coating solution”
To prepare this solution prior to start clean procedure in order to give time for the diffusion of FAS.
To add 1 mL of FAS in 114 mL of undecane. 10^{-2} M FAS
Clean the membrane according to the following steps:
1. Alkali clean (4M NaOH), 1 minutes in US bath with 5 minutes soak
2. Tap water rinse, place into distilled water, 1 minute in US bath
3. Acid clean (10% HCl), 1 minutes in US bath with 5 minutes soak

4. Tap water rinse, place into distilled water, 1 minute in US bath
5. Dry
Coating the membrane according to the following steps:
1. To put about 40 mL of FAS solution into a beaker of 100 mL.
2. To place the cleaned membrane into the beaker. (Check if there is no air bubbles, at the membrane surface).
3. Seal the beakers with (kitchen) plastic film.
4. Ultra-sonication for (min) 3 minutes.
5. Place the beaker in a bath at 45 degrees for at least 16 hours.
6. Rinse the membrane with acetone.
7. Dry and then ready to use.
(It was observed that is possible to reuse the FAS solution at least 2 times)
The FAS used is: 1H, 1H, 2H, 2H-Perfluorodecyltriethoxysilane. This chemical was purchased from Fluorochem®.

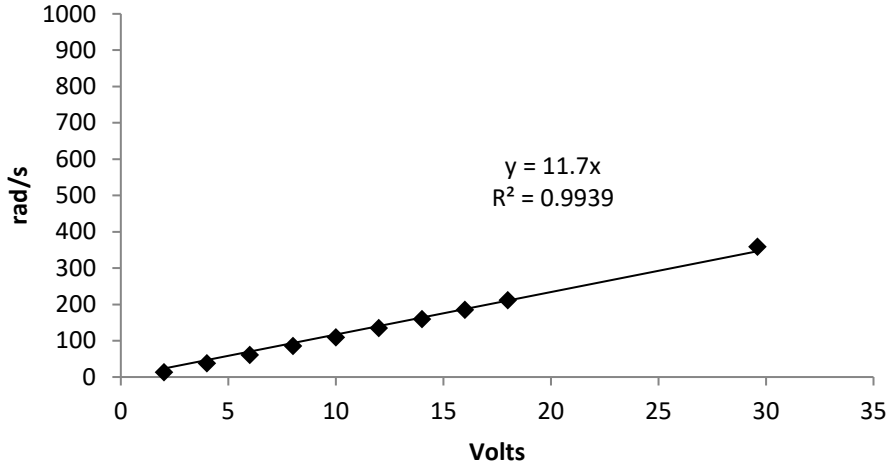

Figure 9.8 Conversion from volts to rad s^{-1} for paddle stirrer in dispersion cell obtained using Tachometer readings.

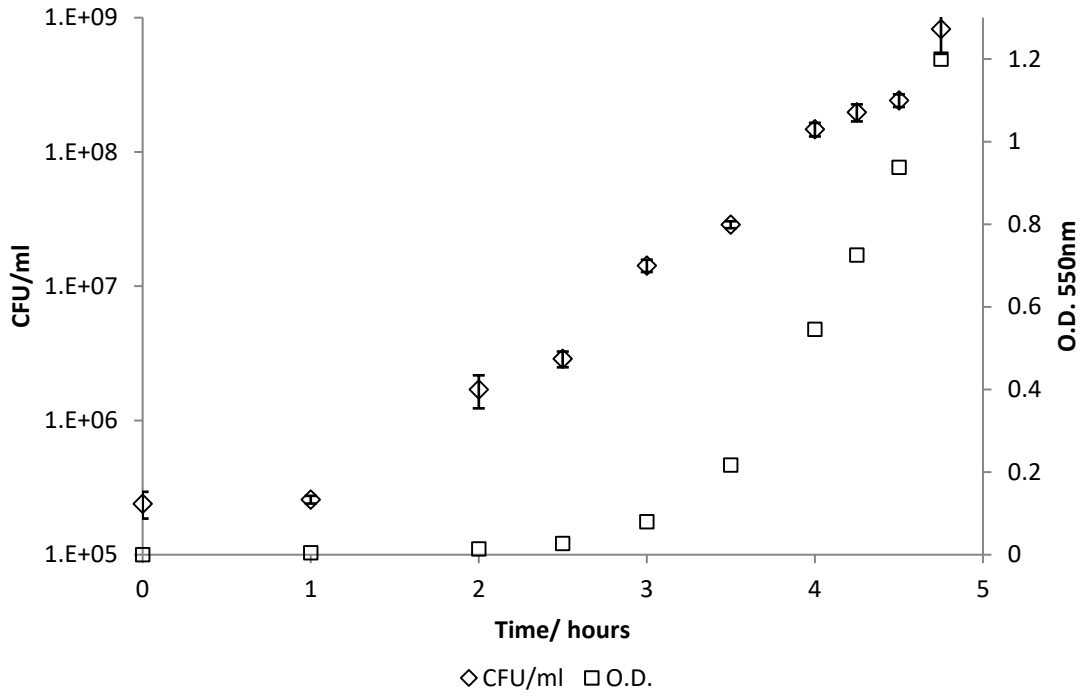

Figure 9.9 Salmonella enteric ATCC 19585 growth curve.

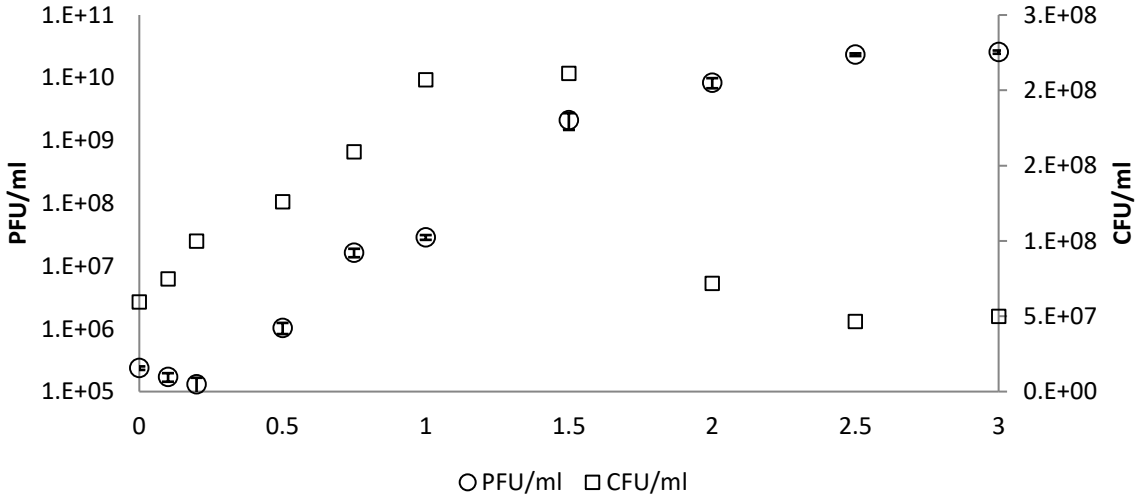

Figure 9.10 Phage growth curve with CFU counts (file name- 2 Felix 01 adsorption for 8 hours with CFU counts 14th Nov 16)

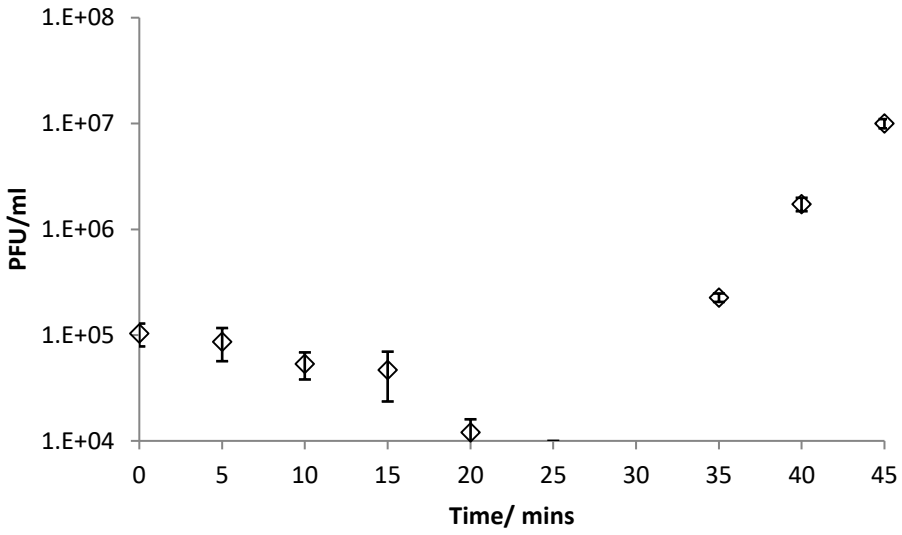

Figure. 9.11 Felix 01 phage adsorption assay

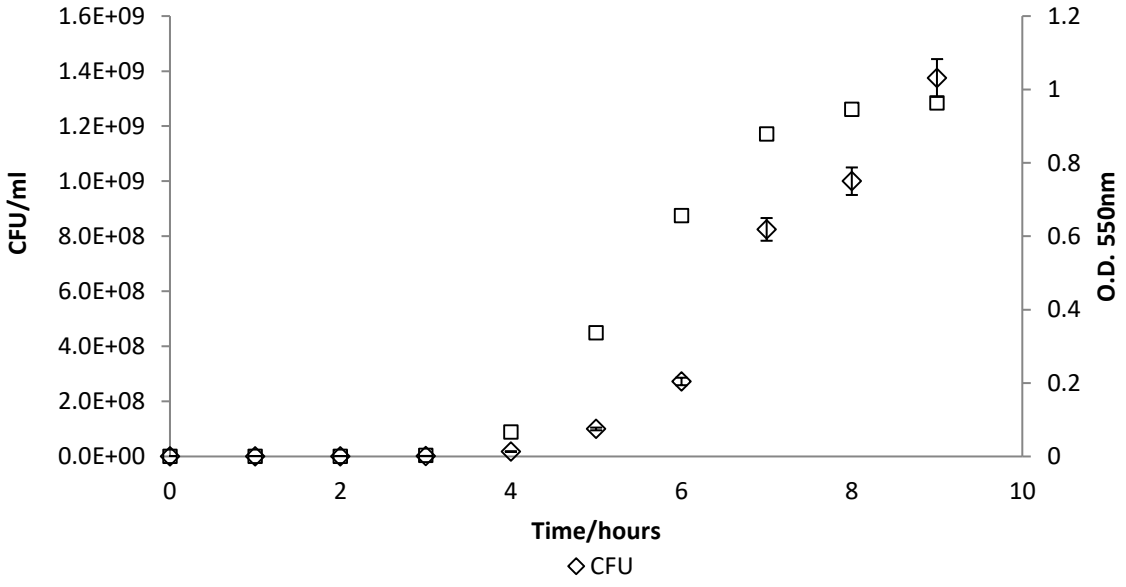

Figure 9.12 EV36 growth curve, OD and CFU counts over 9 hours.

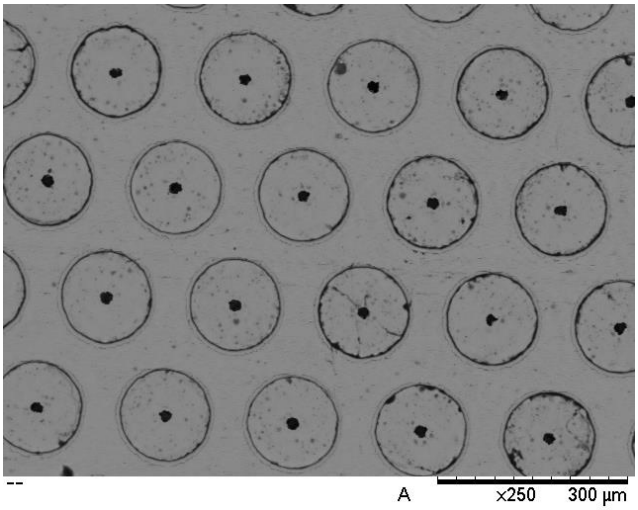

Figure 9.13 SEM of nickel 20 µm pore size membrane.

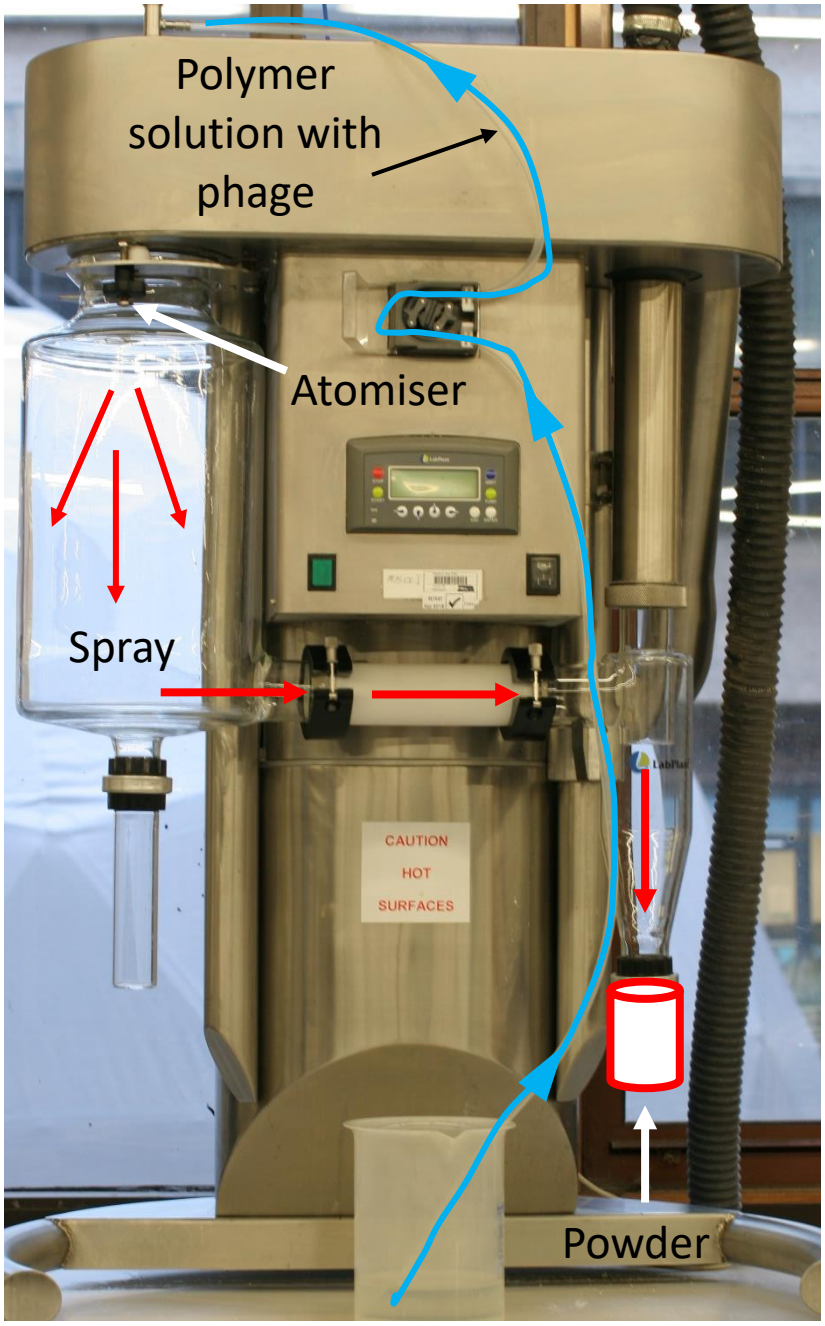

Figure 9.14 Spray drying equipment for Felix O1 encapsulation in different excipients. The polymer solution with phage is delivered from the container via a peristaltic pump to an inlet at the top of the spray dryer (blue arrows). The liquid feed travelled through a small diameter nozzle which was surrounded by an outer tube delivering compressed air causing the liquid feed to be atomised into the drying chamber. The liquid evaporates, leaving powder which is flown (red arrows) by the cyclone and collected in a bottle.

Table 9.1. Summary of p-values (2-sample t-test for means) for free phage K1F exposure to different pH

Time / hrs	**pH2.5**	**pH3**	**pH4**	**pH5**	**pH6**
0	0.007	0.012*	0.667	0.139	0.338
0.5	-	0.034*	0.184	0.116	0.111
1	-	0.004*	0.007*	0.646	0.219
3	-	0.022*	0.070	1.000	1.000
6	-	0.026*	0.070	0.800	1.000
24	-	0.021*	0.114	0.159	1.000

Notes: * indicates reported mean values at time point are different compared with pH7 sample are different $p < 0.05$ indicates rejection of null hypothesis;

Figure 9.15 Minipress MII for tableting spray dried powder.

Figure 9.16 Erweka tablet disintegration system.

Figure 9.17 Erweka tablet friability tester